QUARTERLY JOURNAL
OF THE
ROYAL METEOROLOGICAL SOCIETY

Editor: J. S. SAWYER

Vol. 87 APRIL 1961 No. 372

CONTENTS

PAGE

R. J. MURGATROYD and F. SINGLETON—Possible meridional circulations in the stratosphere and mesosphere 125

M. A. ESTOQUE—A theoretical investigation of the sea breeze 136

G. B. TUCKER—Precipitation over the North Atlantic Ocean 147

J. L. MONTEITH and G. SZEICZ—The radiation balance of bare soil and vegetation .. 159

J. L. MONTEITH—The long-wave radiation balance of the British Isles 171

F. B. SMITH—An analysis of vertical wind fluctuations at heights between 500 and 5,000 ft 180

A. G. DAVENPORT—The spectrum of horizontal gustiness near the ground in high winds 194

B. J. MASON and R. EMIG—Calculations of the ascent of a saturated buoyant parcel with mixing 212

B. M. HERMAN and L. J. BATTAN—Calculations of Mie back-scattering of microwaves from ice spheres 223

K. J. BIGNELL—Heat balance measurements from an earth satellite – an analysis of possibilities 231

Shorter Contribution—

L. WARTENA and A. J. W. BORGHORST—The energy balance of an evaporation pan and the measurement of the reflectivity of its bottom 245

Notice—

G. A. BULL—Note on universal decimal classification 250

Discussions—

J. T. HOUGHTON and J. S. SEELEY—Spectroscopic observations of the water-vapour content of the stratosphere (*Q.J.*, **86**, p. 358) 251

F. R. BARCLAY, M. J. W. ELLIOTT, P. GOLDSMITH and J. V. JELLEY—A direct measurement of the humidity in the stratosphere using a cooled-vapour trap (*Q.J.*, **86**, p. 259) 252

K. H. STEWART—Some recent changes in atmospheric electricity and their cause (*Q.J.*, **86**, p. 399) 253

H. A. PANOFSKY, A. K. BLACKADAR and G. E. MCVEHIL—The diabatic wind profile (*Q.J.*, **86**, p. 390) 254

J. S. A. GREEN—A problem in baroclinic stability (*Q.J.*, **86**, p. 237) 255

Proceedings at meetings of the Society 256

Reviews—

The atmosphere and the sea in motion, (Ed.) B. Bolin (R.C.S.); *Physics of the upper atmosphere*, (Ed.) J. A. Ratcliffe (R.F.); *The scientific papers of Sir Geoffrey Ingram Taylor*, (Ed.) G. K. Batchelor (P.A.S.); *Atlantic hurricanes*, G. E. Dunn and B. I. Miller (I.J.W.P.); *Proceedings of the International Clean Air Conference*, Nat. Soc. for Clean Air (R.G.V.); *Theorie der Meersswellen*, W. W. Schulejkin (J.D.); *Quellentexte zur Witterungsgeschichte Europas von der Zeitwende bis zum Jahre 1850*, C. Weikinn (G.M.); *The Green Flash and other low sun phenomena*, D. J. K. O'Connell (B.C.V.O.); *Cumulus dynamics*, Proceedings of conference on cumulus convection (F.H.L.) 259

PUBLISHED AND SOLD BY THE
ROYAL METEOROLOGICAL SOCIETY
49 CROMWELL ROAD, LONDON, S.W.7
PRICE THIRTY SHILLINGS ($4.50)
ANNUAL SUBSCRIPTION £5 - 4 - 0 ($16), POST FREE

ROYAL METEOROLOGICAL SOCIETY

Founded on 3 April 1850, for the advancement of meteorological science. The Society was incorporated by Royal Charter in 1866.

MEMBERSHIP

Membership is open to all persons genuinely interested in meteorology. The annual subscription is as follows :

Fellows	£4-4-0	(Entrance fee, 1 guinea)
Foreign Members ..	£4-4-0	„ „
Students	£1-10-0	
Corporate Members..	£21-0-0	

All Members receive free the regular publications of the Society, including the monthly publication *Weather* (annual subscription to non-members 24s. plus 2s. 6d. postage).

The Descriptive Account of the Society and an application form will be sent on request to the Assistant Secretary.

Quarterly Journal

EDITING COMMITTEE

J. S. Sawyer — *Editor and Chairman*

A. G. Forsdyke	R. F. Jones	J. S. Marshall	B. J. Mason
R. J. Murgatroyd	F. Pasquill	R. C. Rainey	R. S. Scorer

The primary purpose of the *Quarterly Journal* is to publish results of original research and reports of the Society's scientific meetings. Papers intended for the *Journal* **should be submitted in accordance with standards laid down by the Council in the Society's memorandum** ' Preparation of Papers for the *Quarterly Journal*' which is available on request. Failure to conform with these standards involves the Society's officers and staff in much needless work and the Society in unnecessary expense. **Manuscripts will therefore not be considered for publication unless they conform reasonably closely with the procedure laid down.** The attention of authors is drawn particularly to the requirements in regard to mathematics and diagrams and the Assistant Secretary will be pleased to advise authors on their special problems of illustration before papers are formally submitted. Diagrams should, if possible, be submitted flat, not rolled, and a duplicate rough set for refereeing purposes should be included. Where rulings on a diagram are desirable the closest acceptable spacing is approximately 1 cm and this may be done on **blue-lined** graph paper by thickening the centimeter rulings. Manuscripts may be submitted in duplicate to expedite refereeing, but authors must retain complete copies in their possession.

Price to non-members is £5-4-0 (post free) per annum and £1-10-0 for single issues (postage extra).

PUBLICATIONS

Copies of the publications *Centenary Proceedings of the Royal Meteorological Society*, 1950 (£1. 1s.) and *Proceedings Toronto Meteorological Conference* 1953 (£1. 10s.) are still available.

Reprints of papers recently published in the *Quarterly Journal* are generally available, the prices being as follows (postage extra): 8 pp., 1s. 2d.; 16 pp., 1s. 10d.; 20 pp., 2s. 2d.

Weather Lore. Fourth edition of the late Richard Inwards's unique compilation, revised, augmented and edited for the Society by E. L. Hawke. Published in 1950. 4s. 6d., postage 1s.

Rainfall Atlas of the British Isles. Published in 1926. Price to Members, 15s. post free.

Collected Scientific Papers of William Henry Dines, F.R.S. This memorial volume contains reproductions of nearly sixty papers and other original communications by W. H. Dines. 15s., postage 1s.

Cloud study : a pictorial guide. By F. H. Ludlam and R. S. Scorer. 75 photographs. Published in 1957 under the auspices of the Society by John Murray. 12s. 6d. (11s. to Members), postage 1s.

Cloud photographs. A new series of 24 postcards reproduced from the unique Clarke and Cave Collection. Complete set, 7s. 6d., postage 6d.

THE SOCIETY'S OFFICES

Assistant Secretary — Col. J. H. Willink, C.B.E.

49 Cromwell Road, London, S.W.7.

(*Telephone :* KENsington 0730)

The offices and library of the Society are open daily (Monday to Friday) from 10 a.m. to 5 p.m. All enquiries and correspondence concerning the Society and its publications should be addressed to the Assistant Secretary.

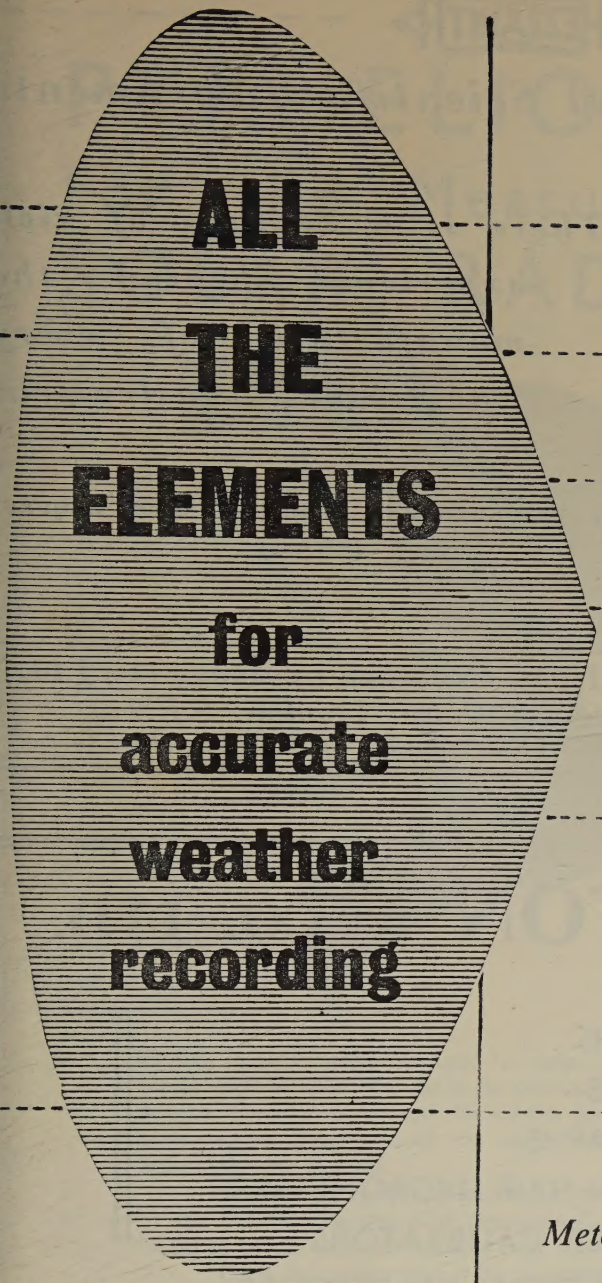

Thermometers

Hygrometers

Barometers

Rain Gauges

Sunshine Recorders

Wind Direction and Velocity Indicators, etc.

Meteorological Instruments by

NEGRETTI & ZAMBRA LTD

Manufacturers of instruments for the indication, recording, controlling of :— Temperature, pressure, liquid level. volume, specific gravity, humidity, etc.

122, REGENT STREET, LONDON, W.1
'Phone: REGent 3406. 'Grams: Negretti, Piccy, London
Branches : Birmingham, Cardiff, Glasgow, Leeds, Manchester, Nottingham.
Agents or Subsidiaries in most countries.

TRADE HEZZANITH MARK

Meteorological and Scientific Instruments

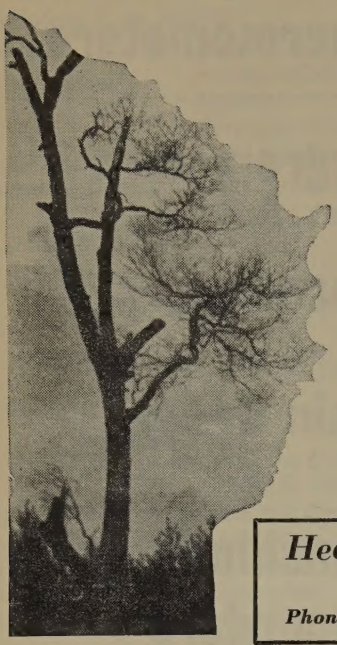

There is a century of rich experience behind the manufacture of every "HEZZANITH" Instrument

CATALOGUES ARE AVAILABLE UPON REQUEST (RMS.A1)

Heath, Hicks & Perken (THERMOMETERS) *Ltd.*
New Eltham, London, S.E.9
Phone : ELTHAM 3836. Grams : "OPTIMUS," Souphone, London

F. DARTON & CO. LTD.

Makers of :

THERMOGRAPHS
BAROGRAPHS
HYGROGRAPHS
PRECISION HAIR HYGROMETERS
ALTIMETER CALIBRATORS
KEW PATTERN BAROMETERS
FORTIN'S PRINCIPLE BAROMETERS
GRASS & SOLAR THERMOMETERS
RAIN GAUGES, etc.

All enquiries to :

Established 1834

WATFORD FIELDS, WATFORD, HERTS

Tel. : WATFORD 26019 & 26010

PYRHELIOMETER

For the Measurement of SOLAR RADIATION

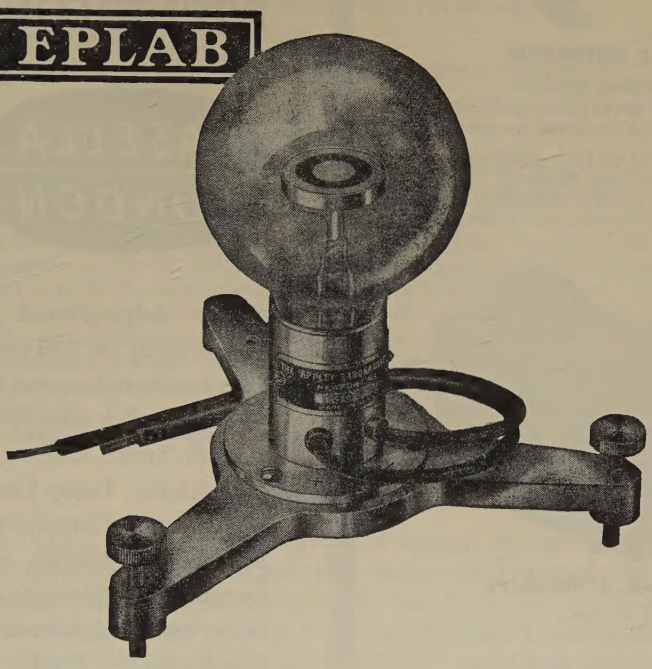

Eppley Pyrheliometers are used for solar radiation measurements at ninety-eight weather stations in the continental United States, Canada, Alaska, Greenland, Iceland, Caribbean Sea, and the Pacific Ocean. Sixty-two of these stations are under the direction of the United States Weather Bureau.

The Eppley Pyrheliometer was adopted as standard equipment by the Weather Bureau after considerable experimentation. It was found to be the best instrument so far tested by the Bureau.

Used in conjunction with a suitable recorder, the Eppley Pyrheliometer will provide an accurate and reliable record of total solar and sky radiation on a horizontal surface.

Bulletin No. 2 on Request

THE EPPLEY LABORATORY INC.

Scientific Instruments

20 Sheffield Avenue Newport, Rhode Island, U.S.A.

PORTABLE ANEMOMETER

Incorporating synthetic sapphire jewel bearings having a very low frictional torque.

In spite of its high sensitivity it has the large range of 25/5,000 feet per minute.

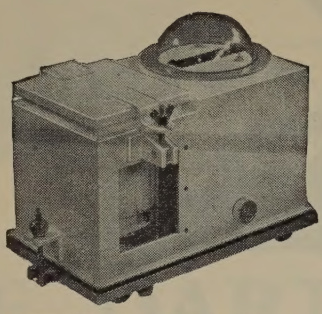

BIMETALLIC ACTINOGRAPH

Designed by the British Meteorological Office

This instrument records the short wave radiation received from the sun and sky on a horizontal surface.

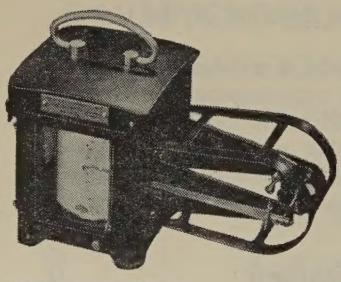

THE THERMOGRAPH

An accurate, reliable and robust instrument. It incorporates a bimetallic coil which gives rapid response to temperature changes and very accurate recording. Supplied with daily or weekly charts to a wide variety of ranges.

150 Years of Service to Meteorology

CASELLA LONDON

As the " helping hand " of Meteorology for 150 years Casella have numbered among their customers such famous names as Darwin, Speke, Galton and Livingstone. Today Casella serve Synoptic and Climatological Stations, Universities, Schools, Geographical Societies and Government departments throughout the World.

Wherever meteorological phenomena have to be recorded, *wind, pressure, temperature, humidity, precipitation, evaporation, rainfall or sunshine etc.*, Casella can provide " quality first" instruments of optimum accuracy and reliability. *Send for your copy of the Casella Meteorological Instruments Catalogue.*

C. F. CASELLA & CO. LTD.

(Dept. RMS) Regent House, Fitzroy Square
LONDON W.1 *EUSton 3944/5/6/7*

Members Scientific Instrument Manufacturers' Association of Great Britain and the British Scientific Instrument Research Association.

QUARTERLY JOURNAL
OF THE
ROYAL METEOROLOGICAL SOCIETY

Vol. 87 APRIL 1961 No. 372

551.513.1

Possible meridional circulations in the stratosphere and mesosphere

By R. J. MURGATROYD and F. SINGLETON
Meteorological Research Flight, Farnborough

(Manuscript received 14 September 1960; in revised form 13 December 1960)

SUMMARY

A calculation has been made of the meridional circulation sufficient to transport heat between the radiational sources and sinks in the stratosphere (15-55 km) and mesosphere (55-80 km). Assuming that the principal heat sources are in the region of the equatorial tropopause and in the mesosphere over the summer pole, with the corresponding heat sinks near the polar tropopause and over the winter pole in the mesosphere, the main circulation patterns are found. Below 30 km there is rising air over the equator with outflow towards both poles and descent towards the tropopause in high latitudes in both hemispheres. At higher levels there is ascent over the summer pole and descent over the winter pole with a well defined flow towards the winter pole above 50 km and a more indeterminate flow pattern between 30 and 50 km. The order of magnitude of the speed of these circulations is m sec^{-1} horizontally and cm sec^{-1} vertically.

The calculations were made for the solstices, equinoxes and mid-times between them and several particle trajectories were determined. The results are in agreement with many of the observed physical features of the stratosphere and mesosphere, particularly the distribution of tracer elements.

1. INTRODUCTION

During recent years, studies of the balance of energy, angular momentum and water of the atmospheric circulation in the troposphere have tended to emphasize the importance of transport by horizontal eddies compared with that by purely meridional circulations. It has also been established that, during the polar night at least, horizontal eddies are an extremely important feature of the circulation up to at least 30 km. Nevertheless, the presence of a direct Hadley cell in the tropics and subtropics can hardly be questioned while, at the present time, the transport of tracers such as water vapour, ozone and atomic debris in the stratosphere is most generally discussed in terms of meridional circulations (e.g., Ramanathan and Kulkarni 1960; Machta 1960; Brewer 1949). Inferences drawn from observations of tracer distributions are, however, largely qualitative and a first attempt has been made to specify more definitely the possible magnitudes of meridional circulations, both in the stratosphere and in the mesosphere. Vertical and meridional motions sufficient to transport the heat between radiative sources and sinks as given by Murgatroyd and Goody (1958) and Ohring (1958) have been calculated. The model used is a meridional cross-section only and it is assumed that all the heat is transported by motion in meridional planes, the horizontal and vertical velocities being calculated from the equations of heat transport and mass continuity. Possible contributions to heat transport of horizontal eddies are neglected as they cannot yet be assessed with the observational data available. There is some partial justification for this as much of the region considered is very stable and the results when compared with tracer observations suggest that this assumption is not very serious. Nevertheless, their neglect leads to considerable difficulties when angular momentum balance is considered. The sphericity of the earth is taken into account in the form of the continuity equation used. Molecular conduction is also neglected, which appears to be a reasonable assumption from the work of Davies (1959). The other major assumption made in this model is that the meridional velocity is zero at both poles.

2. The equations of heat and continuity

The total rate of change of temperature dT/dt of a moving particle can be expressed as

$$\frac{dT}{dt} = \left(\frac{\partial T}{\partial t} + \mathbf{V}.\nabla_p T + \omega \frac{\partial T}{\partial p}\right) = \frac{R}{C_p}\frac{T}{p}\omega + \left(\frac{dT}{dt}\right)_R \quad . \quad . \quad (1)$$

where T is temperature, t time, $\mathbf{V}$ horizontal wind vector, $\nabla_p T$ temperature gradient in a constant pressure surface p, ω vertical velocity in pressure coordinates, R gas constant, C_p specific heat of air at constant pressure, and $(dT/dt)_R$ rate of radiative heating. The latter is the resultant sum of the solar and terrestrial heating and is usually expressed in degrees per day.

From Eq. (1), with zonal advection zero on a meridional cross-section it readily follows that

$$\left(\frac{dT}{dt}\right)_R = \frac{\partial T}{\partial t} + v\left(\frac{\partial T}{\partial y}\right)_p + \omega S T \quad . \quad . \quad . \quad (2)$$

where v is the velocity along the meridional direction y and S $(= 1/\theta\ \partial\theta/\partial p)$, the static stability, where θ is the potential temperature. Since eddy transports are neglected, each term on the right-hand side is a mean value round a latitude circle at a given pressure.

The continuity equation, allowing for the sphericity of the earth and also applied similarly to a mean meridional cross-section is

$$\frac{\partial v}{\partial \phi} - v \tan\phi = -E\frac{\partial \omega}{\partial p} \quad . \quad . \quad . \quad . \quad (3)$$

where ϕ is latitude and E the distance from the centre of the earth to the point considered.

Integrating between two latitudes ϕ_0 and ϕ

$$v\cos\phi - v_0\cos\phi_0 = -\int_{\phi_0}^{\phi} E\cos\phi\frac{\partial\omega}{\partial p}\,d\phi \quad . \quad . \quad . \quad (4)$$

In the model used, (i.e., a meridional plane through both hemispheres extending from pole to pole), it is necessary to postulate that v tends to zero near both poles at all levels, i.e. as $\phi \to \pi/2$ and $\phi_0 \to -\pi/2$

$$\int_{\phi_0}^{\phi} E\cos\phi\frac{\partial\omega}{\partial p}\,d\phi \to 0 \quad . \quad . \quad . \quad . \quad (5)$$

and that this integral is zero when $\phi = \pi/2$ and $\phi_0 = -\pi/2$ (see Section 4).

3. The data

Murgatroyd and Goody (1958) have presented estimates of the sources and sinks of radiative energy, in degrees per day, between 30 and 100 km at the solstices, by calculating the differences between direct heating by absorption of solar radiation by ozone and molecular oxygen and the long-wave cooling by carbon dioxide and ozone. Their results have uncertainties at the upper boundary due to the failure of Kirchhoff's law in this region, and around 30 km due to the neglect of line overlap in the calculations of absorption by carbon dioxide and also to the neglect of a possible contribution due to water vapour. Their results were therefore used between 35 and 80 km.

Ohring (1958) has presented results of a similar type expressed as absorption of solar radiation minus emission of infra-red radiation in langleys per minute throughout the year, separately for the height ranges tropopause to 55 km and 21-55 km. These latter calculations included the effect of carbon dioxide, ozone and water vapour although

the amount of the latter above the lower stratosphere is still uncertain. In order to obtain a unified set of data throughout the whole range tropopause to 80 km, the resultant heating rates of Murgatroyd and Goody (1958) for the height range 35-55 km were converted to langleys per minute and subtracted from Ohring's values to give the remaining absorption in the 21-35 km interval. Mean values of heating rates in the range tropopause to 21 km were also found by subtraction. Using these different values and extrapolating downwards from 35 km, an estimate was then made for the solstices throughout both hemispheres of the distribution of the net radiative heating at all levels from the tropopause upwards. The shapes of the curves of radiational temperature change rates against height so obtained were in reasonable agreement with those given by Ohring for selected latitudes and seasons in the range tropopause to 55 km. It is considered that, although the assumptions and methods of Murgatroyd and Goody and those of Ohring, both as regards the solar heating and infra-red cooling calculations, are very different, a reasonably consistent picture of the overall distribution of radiational sources and sinks has emerged. The principal feature of both papers, i.e., probable heat transfer from summer pole to winter pole in the upper stratosphere and mesosphere and from equator to both poles in the lower stratosphere and their approximate magnitudes have been retained.

Temperatures and pressure heights between 20 and 100 km as presented by Murgatroyd (1957), and extrapolated as necessary, were used to calculate potential temperatures, stabilities, and horizontal temperature gradients as functions of latitude and height. From the tropopause to 20 km, mean values supplied by the Upper-Air Climatology Division, Meteorological Office, were used.

As data for the solstices only were available above about 30 km, it was decided to form the data at other seasons by fitting a curve of the form $a + b \cos t$ to the above quantities. This involves the assumption that both radiational heating and temperature are mutually in phase with the sun. Some indications that this assumption as regards temperature is not greatly in error are given by the radiosonde observations to about 40 km of Arnold and Lowenthal (1959). This assumption does not take into account the sudden warming of the polar night.

4. Computational procedure

The calculations were carried out for 10-degrees latitude bands from pole to pole, i.e., at points 85°, 75° to 5°, − 5° to − 75°, − 85° at six-weekly intervals commencing at the solstice. The summer solstice in the northern hemisphere was regarded as occurring on the same cross-section as the winter solstice in the southern hemisphere and therefore four cross-sections gave conditions throughout the year. The heights used were 16, 21, 28, 34, 40, 50, 60, 70 and 80 km.

Potential temperatures were first calculated and from them stabilities; $\partial\theta/\partial p$ was formed by centred differences except at 16 km, at which level it was assumed that

$$\left(\frac{\partial\theta}{\partial p}\right)_{16} + \left(\frac{\partial\theta}{\partial p}\right)_{21} = \overline{2\left(\frac{\partial\theta}{\partial p}\right)_{16,21}} = \frac{2(\theta_{21} - \theta_{16})}{p_{21} - p_{16}} \quad . \quad . \quad (6)$$

and at 80 km, where a similar procedure was adopted.

The general scheme of the computation was firstly to calculate approximate values of ω from Eq. (2) assuming that $v = 0$ everywhere. Next, using Eq. (4) with the boundary conditions $v = 0$ at all heights at one pole ($\phi = \pi/2$) and forming vertical gradients from the computed values of ω (in a similar manner to that described above for θ), a set of values of v was computed. These values were then fed back into Eq. (2) to obtain a second approximation to ω, the process then being repeated until successive sets of v and ω showed negligible change. In practice, three or four iterations were sufficient. In general, however, at this stage it was found that v did not tend to zero near the other pole ($\phi = -\pi/2$).

There were then two possibilities :

(a) accepting that it was not possible to obtain zero values of v near both poles, to attempt some minimizing procedure for v at high latitudes;

(b) make adjustments to the original data so that Eq. (5) was satisfied.

Attempts to follow course (a) were not satisfactory, it being found impossible to obtain values of v less than 100-1,000 cm sec^{-1} at 85° latitude (owing to division by $\cos\phi$ for values of ϕ near 90°; see Eq. (4)). Course (b) is only justifiable when any adjustments required do not result in significant changes in the original data. A failure here would probably mean that the original assumption as regards the mode of the heat transfer processes is unrealistic, or alternatively, the original data are grossly in error. A trial computation showed that it was possible to adjust the original data to satisfy Eq. (5) by relatively small changes in the radiational heating rates. The correction procedure adopted was as follows :

Let ϵ at any level be the correction required at all latitudes to the original values of $\partial\omega/\partial p$ to obtain final values $(\partial\omega/\partial p)'$.

Then
$$\int_{-\frac{\pi}{2}}^{\frac{\pi}{2}} E\cos\phi\left(\frac{\partial\omega}{\partial p}\right)' d\phi = 0 = \int_{-\frac{\pi}{2}}^{\frac{\pi}{2}} E\cos\phi\left(\frac{\partial\omega}{\partial p}+\epsilon\right) d\phi \quad . \quad . \quad (7)$$

The computation therefore included the intermediate step of calculating

$$\epsilon = -\frac{\int_{-\frac{\pi}{2}}^{\frac{\pi}{2}} \cos\phi\left(\frac{\partial\omega}{\partial p}\right) d\phi}{\int_{-\frac{\pi}{2}}^{\frac{\pi}{2}} \cos\phi\, d\phi} \quad . \quad . \quad . \quad (8)$$

for each level and hence in Eq. (4) setting $v_{-\frac{\pi}{2}} = 0$

$$v\cos\phi = -\int_{-\frac{\pi}{2}}^{\phi} E\cos\phi\left(\frac{\partial\omega}{\partial p}+\epsilon\right) d\phi \quad . \quad . \quad . \quad (9)$$

This must also satisfy the condition $v \to 0$ as $\phi \to \pi/2$.

The correction $\Delta\omega$ to ω corresponding to the values of ϵ then followed from the finite-difference equation for $\partial\omega/\partial p$. The conversion from ω mb sec^{-1} to w cm sec^{-1} vertical velocity was made at this stage by writing

$$\frac{\partial\omega}{\partial p} = \frac{\partial w}{\partial z} + \frac{w}{\rho}\frac{\partial\rho}{\partial z} \quad . \quad . \quad . \quad . \quad (10)$$

Finally, the corrections to the radiation term followed directly from Eq. (2) using the corrected values for ω and known values of all the other quantities. The resulting radiational heating terms are shown in Fig. 1. This figure may be compared with the corresponding diagram of sources and sinks of radiative heat energy in Murgatroyd and Goody's (1958) paper. It will be seen that the positions of the sources and sinks and their approximate magnitudes are substantially unchanged but that the position of the zero line between heating and cooling is slightly shifted. Below 35 km where Ohring's (1958) values were used the corrections are also small.

5. Results

The results are summarized in Fig. 2 in four pairs of diagrams referring to the solstices, equinoxes, and the mid-periods between them. Each pair consists of a cross-section from pole to pole of meridional and vertical velocities between altitudes of 15 and 80 km.

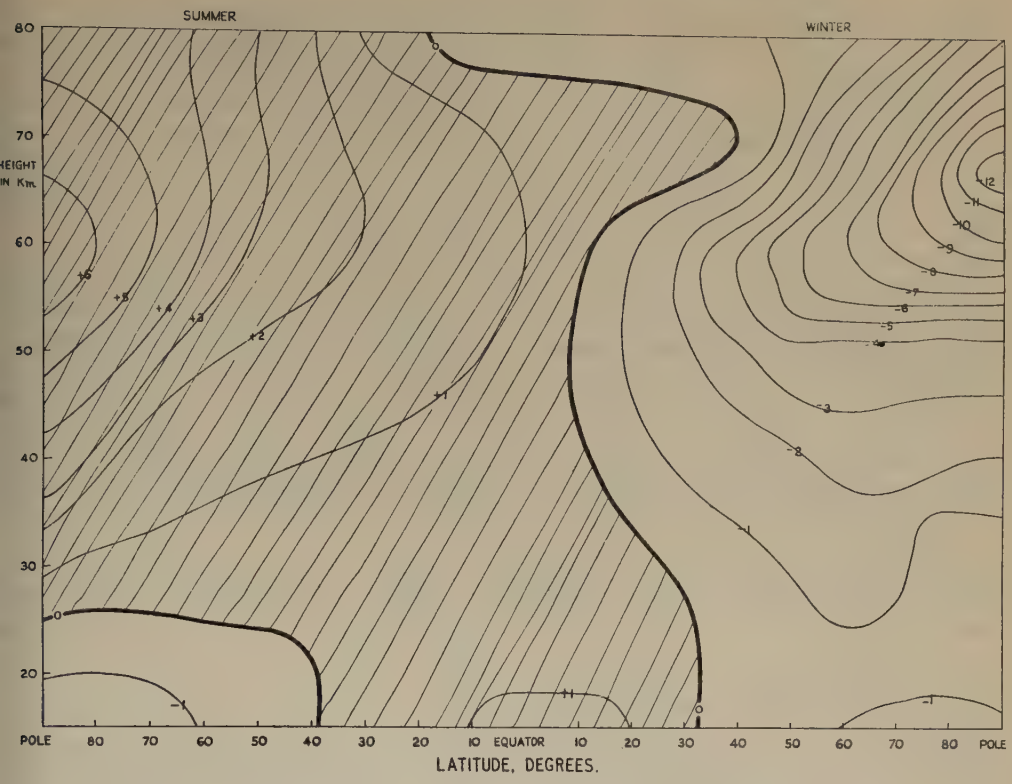

Figure 1. Radiative heating and cooling °K day^{-1}. Regions of heating are shaded.

The former have magnitudes up to a few m sec^{-1}, and the latter two or three orders less. Following the sequence of change throughout the year :

(a) In midsummer in the lower stratosphere there is a region of upwards motion near the equator of magnitude of about 0·1 cm sec^{-1} extending to about 30° latitude and, further polewards, descending air of comparable speed. Correspondingly, at all latitudes the air is moving polewards with a speed up to about 70 cm sec^{-1}. In the corresponding winter hemisphere conditions are broadly similar but the speed of the horizontal motions reaches about 100 cm sec^{-1} in middle latitudes.

In the summer hemisphere there is an equatorwards flow between 30 and 45 km with a polewards flow between 45 and 50 km both about 20 cm sec^{-1}. In the winter, apart from a small region of light equatorwards flow near the pole at 30 km, there is a general region of polewards motion of about 50 cm sec^{-1} up to 50 km. Above 50 km to 80 km, or higher, the horizontal component of motion is from summer to winter pole with speeds up to 5 or 6 m sec^{-1}. There is a continuous region of upwards motion throughout the summer hemisphere (except in the lower polar stratosphere) and downwards motion throughout most of the winter hemisphere. The maximum upwards velocity is about 1·7 cm sec^{-1} at 70 km near the summer pole, and the maximum downwards velocity 1·5 cm sec^{-1} at the same altitude and 65° latitude in the winter hemisphere.

(b) Six weeks later the general pattern has not changed except for the disappearance of the regions of polewards motion near 50 km in the summer and equatorwards motion near 30 km in the winter. The maximum speed towards the winter pole is about 4·5 m sec^{-1}. Correspondingly the maximum upwards speed over the summer pole is 0·9 cm sec^{-1} and the maximum downwards speed in the winter hemisphere is 1·3 cm sec^{-1} and somewhat nearer the pole.

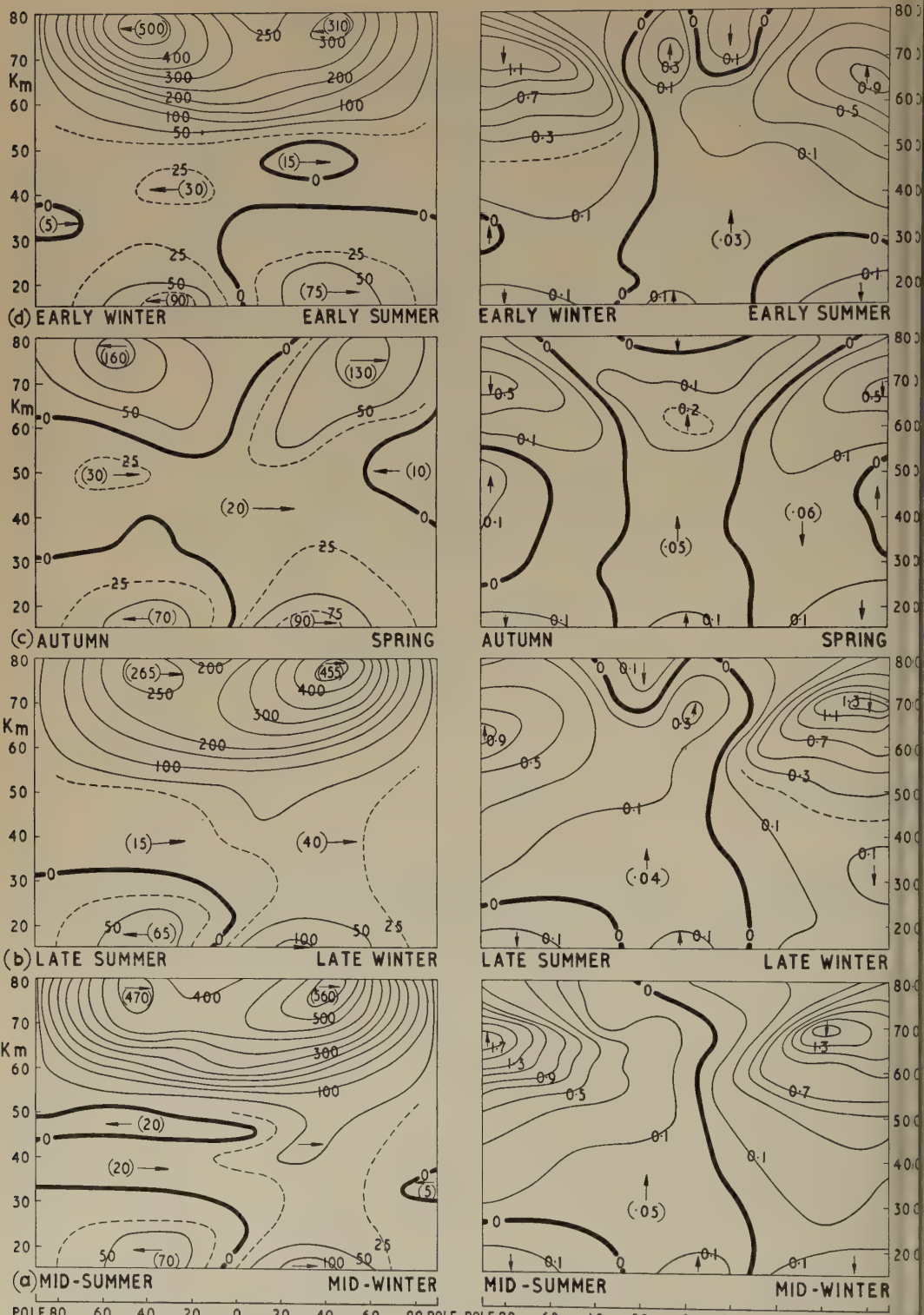

Figure 2. Cross-sections of meridional and vertical velocities (cm sec^{-1}) from pole to pole at different times of the year.

(c) At the equinoxes below 30 km there is little change, with upwards motion at the equator and downwards at both poles of about the same magnitude.

Above 30 km, however, a considerable change of pattern has taken place. The main flow above 60 km has broken up into two parts with meridional motion towards the pole in both hemispheres. A new feature is the appearance of equatorwards motion in the spring at 40 to 50 km. The horizontal motions are comparatively weak with maximum meridional speeds of 1·3 to 1·6 m sec^{-1} at 75 km.

The corresponding vertical motions are upwards in the upper stratosphere at both poles, with maxima of about 0·1 cm sec^{-1} at 45 km, and downwards, with maxima of about 0·5 cm sec^{-1}, in the mesosphere near 70 km at the poles. There is a large region of upwards motion of about 0·2 cm sec^{-1} centred at 60 km above the equator. The mechanism of change from the previous diagram appears to be the introduction of a region of ascending air in the upper stratosphere in spring and descending air near the mesopause in the autumn.

(d) Finally, as the next solstice is approached very little change is evidenced in the lower stratosphere whilst at higher levels the general pattern is tending towards the mirror image of the case (a).

It will be noted that the sequences described above are not symmetrical about the equinoxes, a result which is due to the use of the form $a + b \cos t$ to describe the seasonal variations of temperature and radiational heating.

6. Air trajectories

In order to illustrate the motion of air particles to be expected from this model a selection of trajectories has been computed and the results are shown in Fig. 3. The method was to back-track the motion in steps of three weeks, starting at selected positions in spring and autumn respectively, to examine the displacement during the preceding winter and summer half-years. In a few cases (shown dotted) the air motion was traced for a further six months. The end points were as follows :

At 20 km – 75, 60, 45 and 15 degrees of latitude
35 km – 60 and 30 degrees
50 km – 60 and 30 degrees
65 km – 60 and 30 degrees

The main features shown by this diagram are as follows :

(1) The air reaching the lower stratosphere in both spring and autumn between the equator and at least 50° latitude is always of recent tropospheric origin. Further towards the pole the air reaching the lower stratosphere in spring has descended from about 30 to 40 km during the winter. The air reaching this region during the autumn has, however, only been at heights of 20 to 28 km during the preceding summer. In both cases the continuation of the trajectories back for a further period indicates that most of the air in the lower stratosphere is of originally tropospheric origin but may have taken about 1 to 2 years to reach the lower polar stratosphere.

(2) Tropospheric air only ascends into the high atmosphere from very near the equator; descent from the high atmosphere to the lower stratosphere is confined to very high latitudes during the polar night.

(3) There is little or no transference of air between the hemispheres in the lower stratosphere.

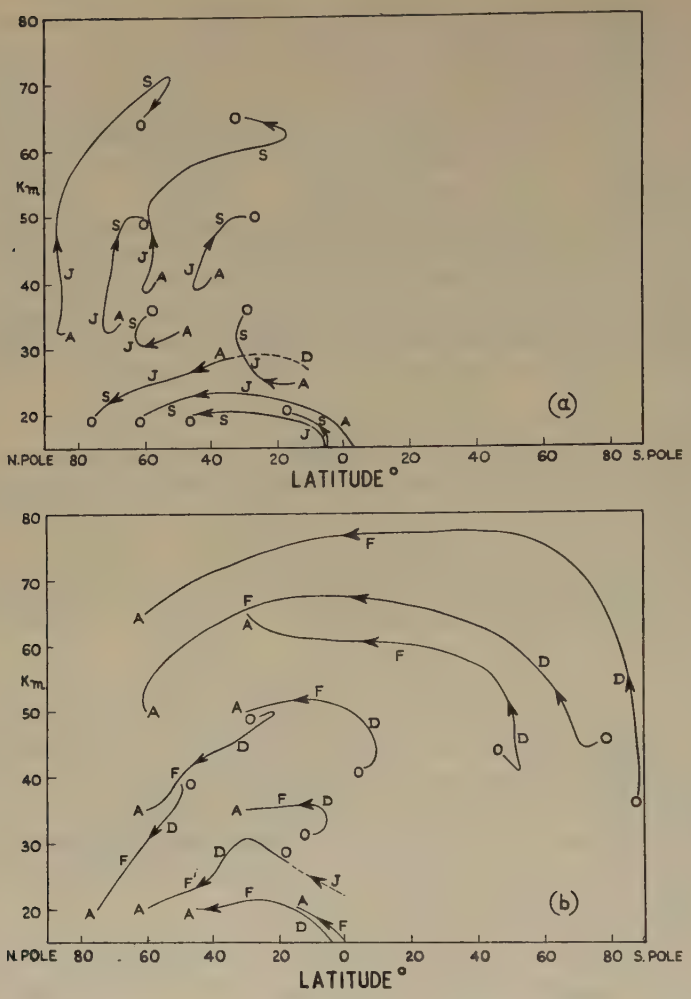

Figure 3. Selected air trajectories over six-monthly periods. Upper diagram shows trajectories ending in autumn, lower in spring in northern hemisphere. Dashed lines indicate movement in preceding six months. F denotes February position, A April, J July, S September, O October, D December.

(4) In the mesosphere, in spring, much of the air has originated in the other hemisphere and crossed the equator during the previous six months, whilst in autumn the air has generally come from lower levels in the same hemisphere.

7. Discussion

Although this model is not a very realistic representation of conditions in the atmosphere (in that it does not take into account eddy transfer processes and therefore, without further elaboration, could not be expected to be consistent with the observed mean zonal wind fields), it is, however, qualitatively in agreement with many of the other observed physical features of the stratosphere and mesophere. The idea that there was general meridional motion towards the winter pole in the mesodecline followed by subsidence in that region was put forward by Kellogg and Schilling (1951) to explain the observations of high temperatures around 65 km during the polar night. Since they could not be due to radiative effects, advection and subsidence appeared to be their main causes. Similarly,

to account for the region of low temperature around 80 km over the summer pole, several writers have proposed general ascent in that region. It is possible that this could lead to the formation of noctilucent clouds if these are water (Hzostikov 1952). Alternatively, if these are not water or ice clouds but dust (Ludlam 1957), the upwards currents of order 1 cm sec^{-1} proposed above could probably support particles up to 10^{-2} μ radius and lead to dust concentrations near 80 km in the region of the summer pole. From considerations of polarization Witt (1960) deduced particle sizes of about 10^{-1} μ. Nearer the equator, in the summer, the vertical speeds are considerably less and therefore would be less likely to support dust particles of the required size or initiate condensation. In the winter hemisphere the vertical currents are downwards and hence noctilucent clouds would not be expected.

In the lower stratosphere the scheme of circulations proposed is broadly similar to that inferred from observations of water vapour, ozone and radioactive debris. It appears from the trajectory calculations that most of the air in the stratosphere, up to 25 km at least, must have passed through the equatorial tropopause region within the last year or so. Since the latter is at a temperature of about $-80°C$ it would be expected that the frost point throughout the lower stratosphere would be around this value. This is in agreement with the many measurements by the Meteorological Research Flight in temperate latitudes; no data as yet have been obtained for the equatorial lower stratosphere. Recently there have been indications (e.g., Barclay *et al.* 1960) that the humidity mixing ratio may increase above 25 km. This is not necessarily inconsistent with the results described above as it was pointed out that there seems to be little interchange of air between the upper and lower stratosphere except very near the equator and very near the winter pole. The principal features of the observed seasonal and latitudinal distribution of ozone in the lower stratosphere are low values in low latitudes and higher values in temperate and high latitudes, where the maximum occurs during the late winter and spring. This latter observation has been shown to be due to an increase of ozone content in the lower stratosphere near the poles in these seasons. It cannot be explained by photo-chemical processes but is due rather to horizontal advection and subsidence. The trajectory calculations above suggest that these motions are largely from equator to pole with maximum heights between 30 and 40 km for air reaching the lower polar stratosphere in the spring but lower altitudes (and therefore regions of less ozone content) for air reaching the lower polar stratosphere in the autumn.

In general, air from the regions of maximum ozone content, i.e., 25-35 km tends to be transported upwards in the summer and downwards in the winter. In the former case, as it moves to regions of less ozone content as determined by the photochemical processes, ozone will tend to be destroyed. In the latter case, as the air descends the ozone content of the lower stratosphere will be increased.

The distribution of atomic debris after explosions in the lower stratosphere is such that it appears generally to move polewards, (see e.g., Hagemann *et al.* 1959; Pierson *et al.* 1960) and thereafter to have maximum concentrations in spring and minimum in autumn in the lower stratosphere. There also appears to be little transfer between hemispheres. Such motions are consistent with the circulation scheme given above with air movements tending to transport the dust upwards above aircraft sampling levels in the summer and transport it downwards again during the winter and spring.

The phenomenon of the ' sudden warming ' of the stratosphere in late winter at high latitudes is not considered to be inconsistent with the ideas given above. The evidence is that (Teweles and Finger 1958) this is mainly due to large-scale subsidence and it appears likely (Stroud *et al.* 1960) that it occurs through the mesosphere as well as the stratosphere. In the large-scale meridional movements in the mesosphere suggested above, there will be continued subsidence (at a rate dependent on the radiative conditions) throughout the winter into the top of the cold polar vortex around 30 km. Whether this slow subsidence creates a general build up of warm air that finally causes the more rapid subsidence which terminates the winter regime, or whether it is some combination of this process with smaller

effects linked with tropospheric conditions that finally causes the ' sudden warming,' will require further investigation. The radiative conditions and hence the rates of subsidence may be different in the two hemispheres.

It must be emphasized that these ideas are tentative and only a first attempt at providing a meridional circulation scheme for the mesosphere and stratosphere as simple as that given by Ferrel or Hadley for the troposphere. Clearly systems on the scale of cyclones and anticyclones, and possibly also, diffusion, must play a large part in the movement of the tracer elements discussed above and the model can be no more than a resultant mean effect. It is likely for instance that the filling of the lower stratosphere with ozone-rich air in the late winter will be a combination of the ' sudden warming ' associated with the breakdown of large-scale cyclonic systems in conditions provided by the meridional circulations for the ozone-rich air to be available for downward transport.

This model, in company with all models which deduce meridional circulations from tracer observations, does not provide conditions for balance of angular momentum. Some of the trajectories shown, particularly at the higher levels, involve meridional displacements of tens of degrees of latitude within a few months. If angular momentum were conserved, a polewards-moving particle would be expected to acquire a large increase of westerly component, and an equatorwards-moving particle, a similar increase of easterly component. The non-conservation of angular momentum implies the existence of eddy processes which are likely to be of importance in the heat balance as well as in the momentum balance. Failure to deal fully with this point is a defect of the present model and probably the next step should be to design a further more elaborate model to attempt to resolve this difficulty. In general, the problem is more severe in the mesosphere (although when there is transference across the equator there will be cancellation effects) than in the stratosphere where the meridional velocities are considerably slower. Near the tropopause there is reasonably good agreement between the vertical and horizontal velocities and those computed from direct observations at 200 mb (Tucker 1959) and it seems that in this region at least the difficulty as regards angular momentum is not serious. Between 25 and 50 km the computed meridional velocities are in qualitative agreement with observed zonal momentum changes. It is known that between 60 and 80 km there are considerable eddy motions which probably govern the transport of angular momentum at these levels.

Finally, since the calculated circulations are supported by the tracer observations, this also provides some confirmation of the radiation data on which they are based. It is probably to be expected that the summer pole near 50 km will be a source of radiative heat due to the large direct absorption of solar radiation by the ozone layer and similarly, that at corresponding, or somewhat greater, heights in the polar night there will be a sink of energy due to lack of solar radiation. The probability of source regions near the mesopause at the summer pole and the tropopause at the equator is not so obvious. These are both very cold regions with infra-red convergence probably providing the energy source at the mesopause (Murgatroyd and Goody 1958). This suggestion seems quite plausible for the tropopause also (Brooks 1958) and has received some support by a few balloon-borne measurements (e.g., Gergen 1957). It is more difficult, however, to accept the result that the sink regions near the tropopause at the summer and winter poles are of approximately equal magnitude. Although the dispositions of the sources and sinks near the polar tropopause are probably correct the tracer observations indicate that it is likely that the winter sink is larger and of greater magnitude than that in summer.

Acknowledgments

Acknowledgments are made to the Director-General of the Meteorological Office for permission to publish this paper, to Mr. J. S. Sawyer for his valuable constructive criticism, to Mathematical Services Division, Royal Aircraft Establishment, Farnborough, whose Mercury Computer was used in this work and to Mr. J. F. Keers for assistance in the computations and production of the diagrams.

References

Arnold, A. and Lowenthal, M. J.	1959	*J. Met.*, **16**, p. 626.
Barclay, F. R., Elliott, M. J. W., Goldsmith, P. and Jelley, J. V.	1960	*Quart. J. R. Met. Soc.*, **86**, p. 259.
Brewer, A. W.	1949	*Ibid.*, **75**, p. 351.
Brooks, D. L.	1958	*J. Met.*, **15**, p. 210.
Davies, T. V.	1959	*J. Fluid Mech.*, **5**, p. 593.
Gergen, J. L.	1957	*J. Met.*, **14**, p. 495.
Hagemann, F., Gray, J. Jr., Machta, L. and Turkevich, A.	1959	*Science*, **130**, p. 542.
Hzostikov, I. A.	1952	*Priroda*, Moscow, **5**, p. 49.
Kellogg, W. W. and Schilling, G. F.	1951	*J. Met.*, **8**, p. 222.
Ludlam, F. H.	1957	*Tellus*, **9**, p. 341.
Machta, L.	1960	*W.M.O. Bull.*, **9**, p. 64.
Murgatroyd, R. J.	1957	*Quart. J. R. Met. Soc.*, **83**, p. 417.
Murgatroyd, R. J. and Goody, R. M.	1958	*Ibid.*, **84**, p. 225.
Ohring, G.	1958	*J. Met.*, **15**, p. 440.
Pierson, D. H., Crooks, R. N. and Fisher, E. M. R.	1960	*Nature*, **186**, p. 224.
Ramanathan, K. R. and Kulkarni, R. N.	1960	*Quart. J. R. Met. Soc.*, **86**, p. 144.
Stroud, W. G., Nordberg, W., Bandeen, W. R., Bartman, F. L. and Titus, P.	1960	Inst. Aeronaut. Sci., Paper No. 60-47.
Teweles, S. and Finger, F. G.	1958	*Mon. Weath. Rev.*, **86**, p. 23.
Tucker, G. B.	1959	*Quart. J. R. Met. Soc.*, **85**, p. 209.
Witt, G.	1960	*J. Geophys. Res.*, **65**, p. 925.

551.511 : 551.553.11

A theoretical investigation of the sea breeze

By M. A. ESTOQUE
*Geophysics Research Directorate, Bedford, Massachusetts**

(Manuscript received 8 August 1960)

Summary

A primitive equation model is formulated and integrated numerically to study the sea breeze. The formulation is an extension of an atmospheric boundary-layer model previously developed for a homogeneous terrain. External gravity-wave type solutions are suppressed by a modelling assumption involving the equation of continuity. The results of an integration showing the evolution of the sea breeze under conditions of no large-scale synoptic motion are presented.

1. Introduction

The phenomena of sea breezes provide an interesting yet simple framework for studying the transfer of heat energy from the earth's surface to the atmosphere and its eventual transformation into kinetic energy of air motions. The sea breeze has been studied with linearized models by Haurwitz (1947), Pierson (1950), Defant (1951) and others. These models explain some of the observed features of sea-breeze circulations, e.g., the local wind variations at the coast. Linear models, however, are not capable of treating many of the interesting characteristics of the sea breeze which are obviously due to non-linear processes.

One of the first efforts to integrate a nonlinear model is due to Pearce (1955). His model prescribes a somewhat artificial heating mechanism of the atmosphere. Using a similar approach, Fisher (1959a) introduced a different heating mechanism. Both mechanisms imply vertical heat transfers which do not depend directly on the existing temperature and velocity fields; under actual conditions these factors are closely coupled.

The intensity, duration, and dimensions of the sea breeze must be governed largely by the amount of heat supplied by the ground to the atmosphere and also of the prevailing large-scale synoptic conditions. A more realistic treatment of these factors is, therefore, desirable. The modelling approach to be presented is an attempt in this direction.

2. Observed characteristics of the sea breeze

Although the sea breeze is a relatively common phenomenon, it is quite surprising to find no detailed quantitative description of the wind and temperature fields during different stages of its life cycle. Qualitative descriptions of land and sea breezes have been written by Wexler (1947) and Defant (1951). A brief summary based mainly on their articles follows.

When the prevailing large-scale wind is light, the sea breeze develops as a small circulation in the immediate vicinity of the shore. The circulation gradually increases in depth and horizontal extent, both landward and seaward. The existence of a large-scale wind blowing from land to sea results in an initial development out at sea. The sea breeze advances more slowly landward and reaches the coast much later in the afternoon like a cold front with its characteristic wind shift.

* Present affiliation : *University of Hawaii, Honolulu.*

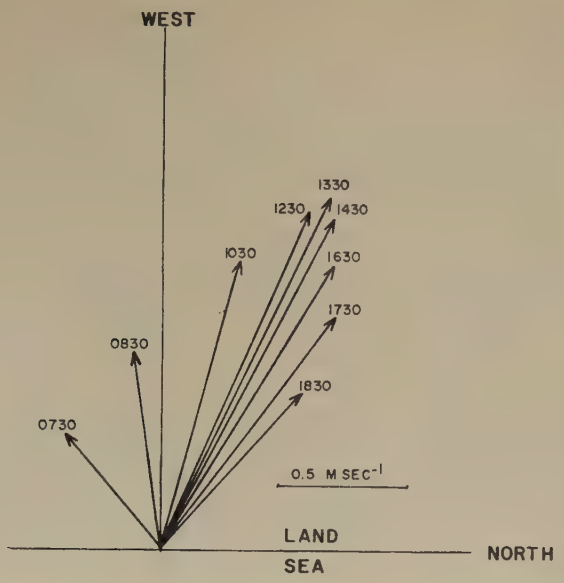

Figure 1. Mean winds during sea-breeze periods at Boston, Massachusetts (after Defant).

The circulation system consists of a landward current adjacent to the earth's surface and a much weaker but deeper return flow above. The top of the landward current ranges from a few hundred metres near large lakes and temperate latitude sea coasts to approximately two kilometres in the tropics. The landward penetration of the sea breeze varies with the land-sea temperature contrasts and the prevailing synoptic situation. Under ideal conditions the sea breeze is frequently observed as far as 30 to 50 km from the seashore in middle latitudes. In tropical regions, the sea breeze sometimes reaches 100 to 200 km inland.

Maximum wind speeds are as high as a few tens of metres per second while the vertical velocities are about two orders of magnitude smaller. The daily maximum winds generally occur shortly after the temperature maximum (Fig. 1). In the Northern Hemisphere, the wind shifts to the right owing to the Coriolis effect. The land breeze which subsequently develops is much weaker in intensity and smaller in dimensions. In places where the sea temperature is sufficiently low, the land breeze is entirely suppressed.

The only available wind and temperature measurements of a sea breeze cross-section have been made by Fisher (1959b) under somewhat unsteady large-scale synoptic conditions. Figs. 2-4 represent the velocity components on a plane normal to the shoreline; the temperature distribution at 1330 LCT is shown in Fig. 5. A maximum landward component may be seen at an elevation of about 300 m. The return flow aloft and the local clockwise rotation of the wind are not evident owing to complications introduced by the prevailing large-scale flow pattern and irregularities in the shoreline. Note also the disturbing influence in the temperature field by the offshore island.

3. The theoretical model

We shall investigate the sea breeze over a straight shoreline using a rectangular co-ordinate system (Fig. 6) whose x-axis is normal to the shoreline and z-axis is along the vertical. No variation in the sea breeze along the shore-line (y-axis) is assumed. The vertical cross-section of the atmosphere to be considered is bounded at the bottom by the earth's surface and at the top by the level, $z = H$. The lateral boundaries are located

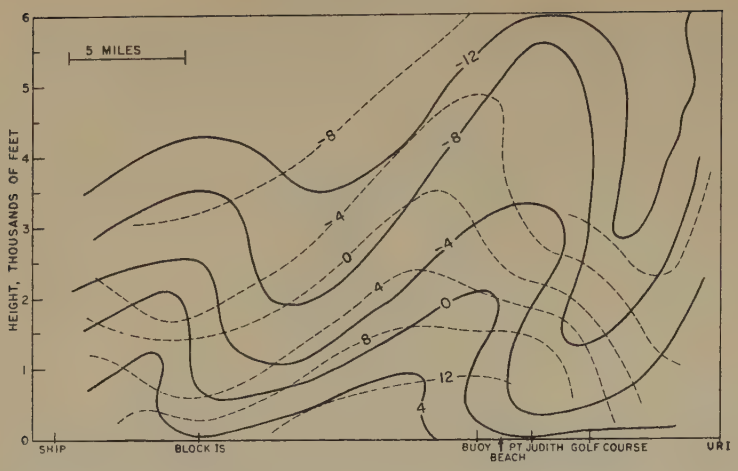

Figure 2. Vertical cross-section of the wind field (m sec^{-1}) in a sea breeze at 1200 EST, 5 August 1958.

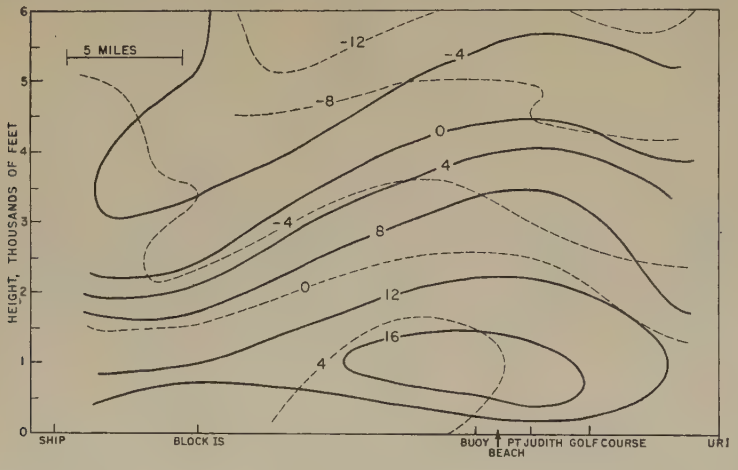

Figure 3. Vertical cross-section of the wind field (m sec^{-1}) in a sea breeze at 1500 EST, 5 August 1958.

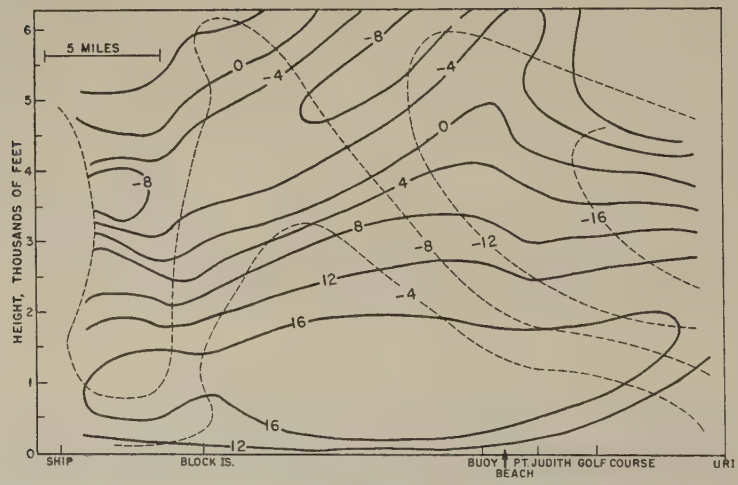

Figure 4. Vertical cross-section of the wind field (m sec^{-1}) in a sea breeze at 1800 EST, 5 August 1958.

Solid lines indicate component normal to shoreline, positive landward; dashed lines indicate component parallel to shore, positive into the paper (after Fisher).

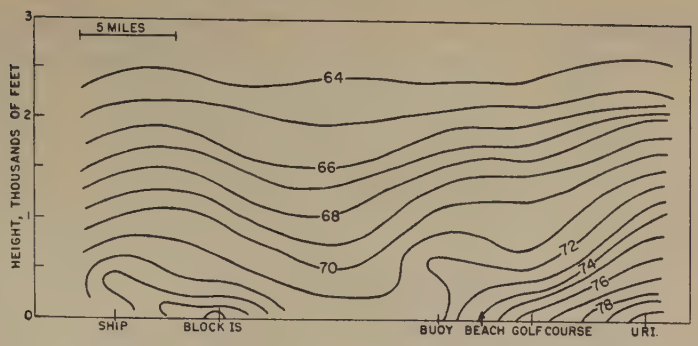

Figure 5. Vertical cross-section of the temperature field, °F, at 1330 EST, 5 August 1958 (after Fisher).

at $x = \pm D$. The magnitude of H and D are chosen to be sufficiently large so that the velocity and temperature changes associated with the sea breeze at these boundaries may be neglected. Actual observations suggest a practical value of at least 2 km for H and about one hundred times greater for D.

Following an earlier work (Estoque 1959) we shall divide the entire region into two horizontal sublayers : a relatively thin stratum, $0 \leqslant z \leqslant h \approx 50$ m, characterized by the constancy with height of the vertical eddy fluxes of heat and momentum and an overlying transition sublayer, $h \leqslant z \leqslant H \approx 2$ km, where the effect of eddy fluxes decreases with elevation.

Accordingly, the wind and temperature profiles in the lower sublayer are expressed by :

$$\frac{\partial}{\partial z}\left(K\frac{\partial U}{\partial z}\right) = 0 \qquad . \quad . \quad . \quad . \quad (1)$$

$$\frac{\partial}{\partial z}\left(K\frac{\partial \theta}{\partial z}\right) = 0 \qquad . \quad . \quad . \quad . \quad (2)$$

and the eddy diffusivity, K, by :

$$K = [k_0 (z + z_0)(1 + \alpha Ri)]^2 \frac{\partial U}{\partial z}, \qquad Ri \geqslant (Ri)_c \approx -\cdot 03 \; . \quad . \quad (3)$$

$$K = \lambda z^2 \left(\frac{g}{T}\left|\frac{\partial \theta}{\partial z}\right|\right)^{\frac{1}{2}}, \qquad Ri < (Ri)_c \quad . \quad . \quad . \quad (4)$$

where $\alpha \approx -3$ and $\lambda \approx 0{\cdot}9$ are empirical constants; the rest of the notation is standard. The first expression for eddy diffusivity was used previously by Estoque (1959) while the second expression has been suggested by Priestley (1959) for the free convection regime, $Ri < (Ri)_c \approx -\cdot 03$.

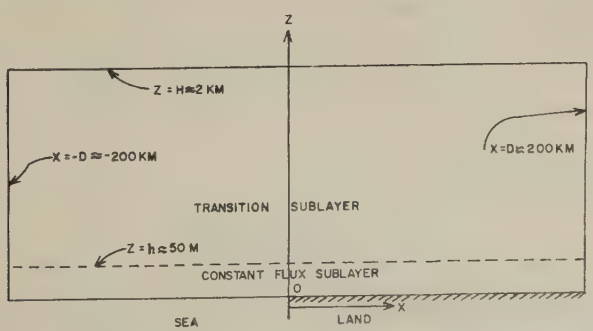

Figure 6. The co-ordinate system.

The equations for the upper sublayer, $h \leqslant z \leqslant H$, will be derived using the following equations :

$$\frac{d\mathbf{V}}{dt} = -\frac{RT}{p}\nabla p - f\mathbf{k} \times \mathbf{V} + \frac{\partial}{\partial z}\left(K\frac{\partial \mathbf{V}}{\partial z}\right) \quad . \quad . \quad . \quad (5)$$

$$\frac{\partial p}{\partial z} = -\frac{pg}{RT} \quad . \quad . \quad . \quad . \quad . \quad (6)$$

$$\frac{d\theta}{dt} = \frac{\partial}{\partial z}\left(K\frac{\partial \theta}{\partial z}\right) \quad . \quad . \quad . \quad . \quad . \quad (7)$$

$$\frac{1}{\rho}\frac{d\rho}{dt} = -\nabla \cdot \mathbf{V} - \frac{\partial w}{\partial z} \quad . \quad . \quad . \quad . \quad (8)$$

where $\mathbf{V} = \mathbf{i}u + \mathbf{j}v$ is the horizontal wind vector and $\nabla = \mathbf{i}\,\partial/\partial x + \mathbf{j}\,\partial/\partial y$; the other symbols have their customary meaning. The eddy diffusivity in the upper sublayer is assumed to be linear with height, starting with a value equal to that of the lower sublayer at $z = h$ (Eqs. (4) and (5)) and then decreasing to zero at $z = H$.

Let us represent each dependent variable as the sum of a given large-scale synoptic component (subscript L) and a disturbance (primed quantity) due to effects of friction and differential heating. Thus,

$$\mathbf{V} = \mathbf{V}_L + \mathbf{V}'; \quad \theta = \theta_L + \theta'; \quad \text{etc.} \quad . \quad . \quad . \quad (9)$$

Furthermore, let us assume that the large-scale components are governed by the following equations :

$$\frac{\partial \mathbf{V}_L}{\partial t} + \mathbf{V}_L \cdot \nabla \mathbf{V}_L + w_L\frac{\partial \mathbf{V}_L}{\partial z} = -\frac{RT_L}{p_L}\nabla p_L - f\mathbf{k} \times \mathbf{V}_L \quad . \quad . \quad (10)$$

$$\frac{\partial \theta_L}{\partial t} + \mathbf{V}_L \cdot \nabla\theta_L + w_L\frac{\partial \theta_L}{\partial z} = 0 \quad . \quad . \quad . \quad (11)$$

$$\nabla \cdot \mathbf{V}_L + \frac{\partial w_L}{\partial z} = 0 \quad . \quad . \quad . \quad . \quad (12)$$

$$\frac{\partial p_L}{\partial z} = -\frac{p_L g}{RT_L} \quad . \quad . \quad . \quad . \quad . \quad (13)$$

Subtracting Eq. (10) from Eq. (5) and noting that $RT_L \nabla p_L/p_L \approx RT\,\nabla p_L/p$, one gets the prediction equation for the sea breeze wind in terms of the given large-scale parameters. Thus

$$\frac{\partial \mathbf{V}'}{\partial t} = -\mathbf{V}' \cdot \nabla \mathbf{V}_L - \mathbf{V} \cdot \nabla \mathbf{V}' - w'\frac{\partial \mathbf{V}_L}{\partial z} - w\frac{\partial \mathbf{V}'}{\partial z} - \frac{RT}{p}\nabla p' - f\mathbf{k} \times \mathbf{V}' + \frac{\partial}{\partial z}\left(K\frac{\partial \mathbf{V}}{\partial z}\right) \quad . \quad (14)$$

A similar operation yields the temperature equation :

$$\frac{\partial \theta'}{\partial t} = -\mathbf{V}' \cdot \nabla\theta_L - \mathbf{V} \cdot \nabla\theta' - w'\frac{\partial \theta_L}{\partial z} - w\frac{\partial \theta'}{\partial z} + \frac{\partial}{\partial z}\left(K\frac{\partial \theta}{\partial z}\right) \quad . \quad (15)$$

and the hydrostatic equation :

$$\frac{\partial p'}{\partial z} = -\frac{gp}{RT} + \frac{gp_L}{RT_L} \quad . \quad . \quad . \quad . \quad (16)$$

The numerical integration of the basic dynamical equations is rather impractical owing to the small forward time-increments required for computational stability. In designing models one generally introduces some assumptions to achieve greater stability

in the calculations. In the present formulation, we shall do this by differentiating Eq. (8) with respect to height and assuming that the term involving compressibility is negligible. Thus

$$\frac{\partial^2 w}{\partial z^2} + \frac{\partial}{\partial z}(\nabla \cdot \mathbf{V}) = -\frac{\partial}{\partial z}\left(\frac{1}{\rho}\frac{d\rho}{dt}\right) \approx 0$$

Using the above equation with Eq. (12), one may derive the equation of continuity

$$\frac{\partial^2 w'}{\partial z^2} = -\frac{\partial}{\partial z}\left(\frac{\partial u'}{\partial x}\right) \quad . \quad . \quad . \quad . \quad (17)$$

The vertical velocity will be assumed to vanish at $z = 0$ and $z = H$.

Eqs. (14) to (17), together with Eq. (9) and the definition of θ constitute a set of equations in $\mathbf{V}'$, w', θ', T', and p' which can be integrated if the synoptic-scale wind and temperature fields are given or predicted with a large-scale prediction model. The set is filtered with respect to sound and external gravity waves. No theoretical justification for the filtering assumption concerning the equation of continuity will be presented. The assumption will distort, to a certain degree, the calculated velocity and temperature fields. However, the initial integrations indicate that the distortions are not serious.

4. Initial and boundary conditions

The initial conditions to be prescribed are the distributions of the wind, $\mathbf{V}'(x, z, o)$, and the temperature, $T'(x, z, o)$, in the region, $-D \leqslant x \leqslant D$, $h < z < H$.

The external boundary conditions are the statements of horizontal homogeneity at the lateral extremities :

$$x = \pm D : \quad \frac{\partial}{\partial x}(\mathbf{V}', p', \theta') = w' = 0$$

vanishing of the disturbance at the top :

$$z = H : \qquad p' = w' = \mathbf{V}' = T' = \theta' = 0$$

vanishing velocities at the earth's surface :

$$z = 0 : \qquad \mathbf{V} = w = 0$$

and the heating of the earth's surface :

$$z = 0 : \qquad \theta = \theta(x, t)$$

The solutions for both sublayers are matched by imposing certain conditions on $\mathbf{V}$ and θ at the internal boundary, $z = h$. For the case $Ri \geqslant -\cdot 03$, continuity in both $\mathbf{V}$ and θ and their vertical derivatives is used in conjunction with Eq. (1), (2) and (3). The matching equations are derived in the paper mentioned earlier (Estoque 1959).

For $Ri < -\cdot 03$, a rather crude matching scheme may be derived by introducing the following assumptions :

(a) the constancy of heat and momentum fluxes extends up to $z = h + \Delta z$

(b) the temperature gradient at $z = h$ is approximated by the expression

$$\frac{\partial \theta}{\partial z} = \beta \frac{[\theta(x, h + \Delta z, t) - \theta(x, 0, t)]}{h + \Delta z}$$

where β is an empirical constant of proportionality; a corresponding relationship holds between the velocity and its gradient. The value of β has not been evaluated owing to

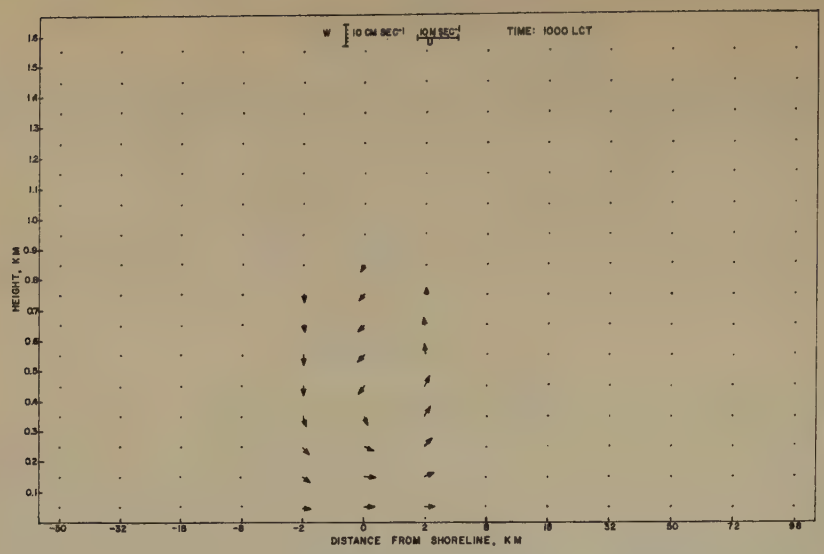

Figure 7. The computed normal and vertical velocity components at 1000 LCT.

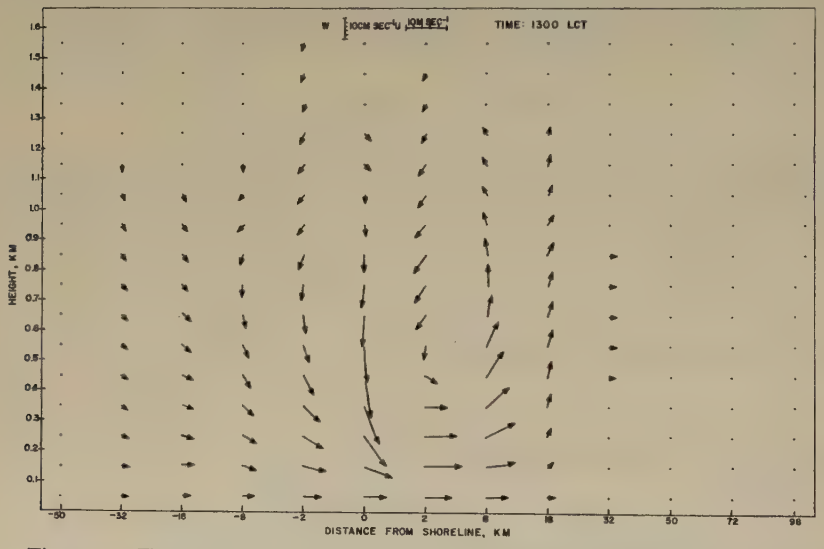

Figure 8. The computed normal and vertical velocity components at 1300 LCT.

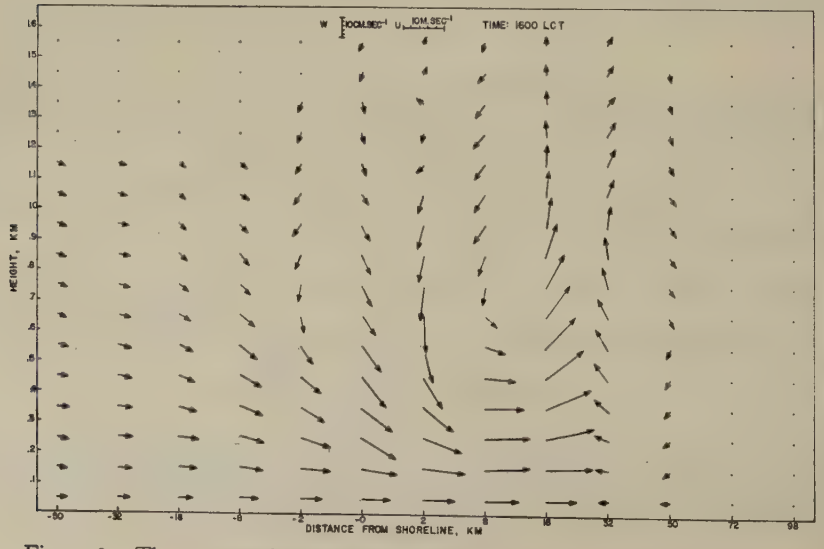

Figure 9. The computed normal and vertical velocity components at 1600 LCT.

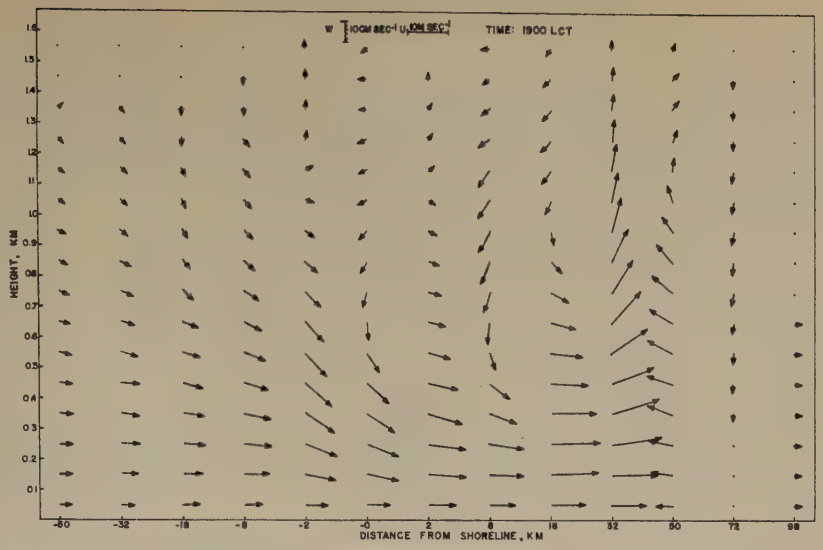

Figure 10. The computed normal and vertical velocity components at 1900 LCT.

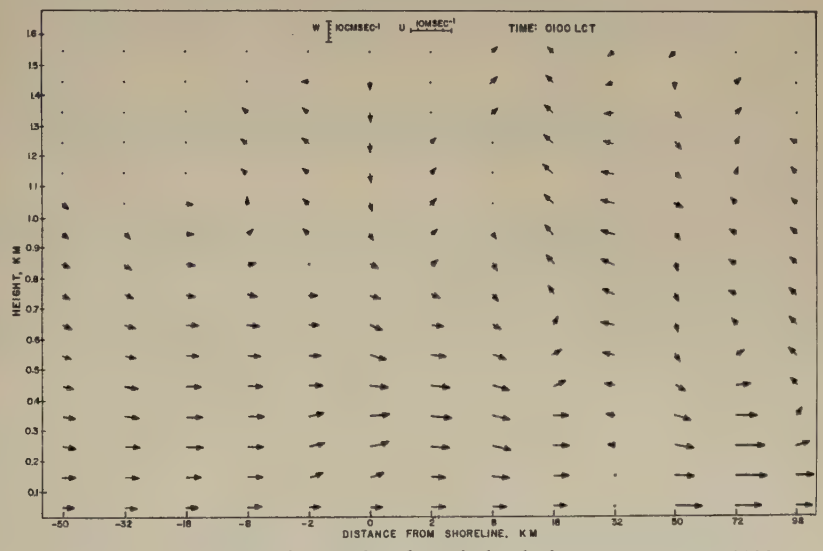

Figure 11. The computed normal and vertical velocity components at 0100 LCT.

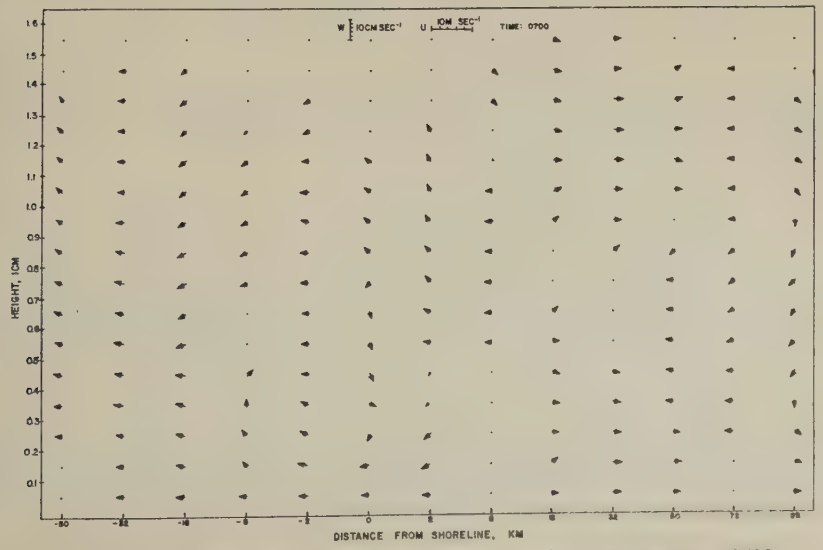

Figure 12. The computed normal and vertical velocity components at 0700 LCT.

lack of observations; in the integrations a value of unity was used. Using these assumptions together with Eqs. (1), (2) and (4), one may derive the matching equations :

$$\theta(x, h, t) = \frac{3\beta h^{4/3}\,[\theta(x, h + \Delta z, t) - \theta(x, 0, t)]\,[(h + \Delta z)^{-1/3} - h^{-1/3}]}{h + \Delta z} + \theta(x, h + \Delta z, t)$$

$$\mathbf{V}(x, h, t) = \frac{3\beta h^{4/3}\,[\mathbf{V}(x, h + \Delta z, t)]\,[(h + \Delta z)^{-1/3} - h^{-1/3}]}{h + \Delta z} + \mathbf{V}(x, h + \Delta z, t)$$

$$K(x, h, t) = \lambda \left(\frac{g\beta}{\bar{\theta}}\right)^{1/2} \left|\frac{\theta(x, h + \Delta z, t) - \theta(x, 0, t)}{h + \Delta z}\right|^{1/2} h^2$$

where $\bar{\theta}$ is the average value in the lower sublayer and Δz is the distance between the lowest gridpoint in the upper sublayer and $z = h$.

5. Numerical integration procedure

The numerical integration is performed only within the upper sublayer. The steps are as follows :

(a) Using the prescribed initial values of T' and $\mathbf{V}'$ at the lowest gridpoint ($z = h + \Delta z$) of the upper sublayer and the boundary value for temperature at the ground, compute the values of $\mathbf{V}'$, θ', and K at $z = h$ using the equations discussed in the preceding section.

(b) Compute the initial pressure distribution by integrating Eq. (16) and using the prescribed values of T', T_L, and p_L. The integration proceeds downward from $z = H$ where the value of p' is zero.

(c) Compute the initial values of w' using Eq. (17) and the initial u' distribution.

(d) Compute $\partial \mathbf{V}'/\partial t$ and $\partial \theta'/\partial t$ using Eqs. (14) and (15).

(e) Extrapolate $\mathbf{V}'$ and θ' for a short time interval to obtain the $\mathbf{V}'$ and θ' forecasts. Using the latter, compute the corresponding T'.

(f) Repeat steps (a) to (e), using the predicted $\mathbf{V}'$ and T' in place of the prescribed initial distributions to obtain the next forecasts. The cyclic procedure is repeated until the summation of the short time intervals is equal to the desired period of the forecast.

6. Results of an integration

The model has been applied to study the evolution of the sea breeze, starting with zero wind in the morning, in response to a prescribed differential heating of the earth's surface given by

$$T = 283 + 10 \sin(15\,t + 240°) \qquad x > 0$$

$$T = 283 \qquad x < 0$$

$$T = 1/2\,[T(x > 0) + T(x < 0)] \qquad x = 0$$

where t is the number of hours after midnight. A set of simple initial conditions were specified at $t = 8$. These are : $u' = v' = T' = 0$. During the entire period of integration, the large-scale velocity and temperature fields were held constant with time such that

$$\mathbf{V}_L(x, z, t) = 0; \quad T_L(x, z, t) = 283 - 8\,z \times 10^{-5}$$

A 19 by 20 grid system with equal spacing of 100 metres along the vertical was used. The horizontal grid spacing starts with a value of 2 km at the shoreline and increases with distance from this point to a maximum spacing of 34 km at the lateral boundaries.

Figs. 7-12 show the distributions of the wind component normal to the shoreline and the vertical velocities. One can see the initial formation of the circulation over the beach, its intensification, the movement of the whole pattern inland, and its subsequent decay. The velocity and temperature fields near the time of maximum development are shown in greater detail in Figs. 13 and 14. The wind component normal to the shoreline attains a maximum speed of about 10 m sec^{-1} near an altitude of 250 m.

There is a weak return flow aloft. The negative values of v in regions of positive u, and vice versa, show the extent to which the wind vector has rotated clockwise with time. Near the region of maxima for both components, the wind at this time makes an angle of arctan 4/10 or about 20° to the right of a line directed inland normal to the shoreline.

An interesting feature of the circulation is the formation of a zone of low-level convergence at the leading edge of the landward current in the afternoon. The zone appears to have many characteristics of a cold front – upward motions, wind shift, and cold air pushing warmer air. The front, which is located between 18 and 32 km at 1600 LCT, advances slowly inland. It is presumed that the lines of cumulus which are often observed parallel to shorelines in the afternoons are a manifestation of this feature.

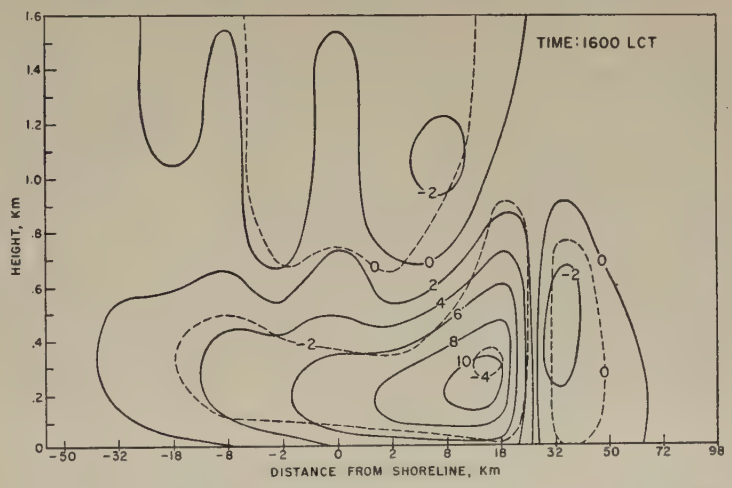

Figure 13. The computed distributions of velocity components in m sec^{-1} normal (solid lines) and parallel (dashed lines) to the shoreline at 1600 LCT.

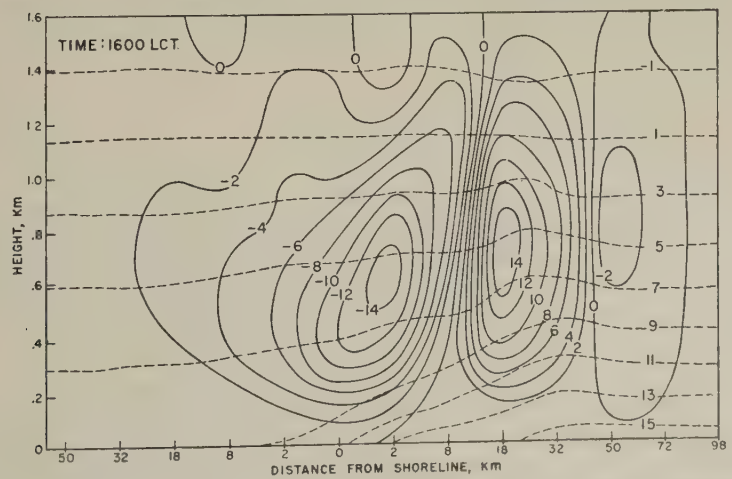

Figure 14. The computed distributions of the vertical velocity in cm sec^{-1} (solid lines) and temperature in °C (dashed lines) at 1600 LCT.

An unexpected characteristic of the calculated velocity field is the increase in the wind speed at night farther inland as indicated by the 0100 LCT distributions (Fig. 11). This peculiarity may be explained in terms of the horizontal differences in the vertical heat transfer mechanisms. During the daytime, the atmosphere over land is heated more or less uniformly along the horizontal by free convection and turbulent mixing. As soon as a temperature inversion forms in the evening, however, free convection ceases and the only effective heat transfer process is turbulent mixing. This operates mainly near the shore where the sea breeze has not dissipated, thereby cooling the atmosphere by transferring heat from the lower layers to the ground. Farther inland, the winds are much lighter so that turbulent heat flux to the ground is negligible. Thus the air here remains warmer compared to that nearer the coast. The resulting horizontal temperature distribution produces a pressure gradient force in the surface layers which accelerates the air towards the interior regions. Whether this peculiarity in the calculations actually occurs in nature cannot be verified by available observations.

7. Conclusions

Additional integrations are being done to examine the effects of varying the boundary and initial conditions and to determine the optimum values of the model constants. The influences of the strength and direction of the prevailing wind and the thermal stratification of the air mass on the development of the sea breeze are being studied.

This study may be considered as an initial attempt to predict quantitatively the evolution of a larger-scale atmospheric circulation pattern resulting from heat transfer processes between the ground and the atmosphere by small-scale eddies. Whilst one must not attach too much significance to the results of a single integration, the successful application of the model to the sea breeze is encouraging. Using the same approach for studying the development of cyclones over warm water surfaces is an interesting possibility. Furthermore, the feasibility of using an improved version to make local wind and temperature forecasts in conjunction with an independent prediction of the large-scale synoptic situation is worth exploring.

Acknowledgments

The author wishes to thank Miss Joan Dwyer for assistance in the analysis, Mr. Vincent Mazzio for programming the computations, and his colleagues in the Boundary Layer Branch, Geophysical Research Directorate, U.S.A.F., for stimulating discussions.

References

Defant, F. 1951 *Compendium of meteorology*, Amer. Met. Soc., p. 658.

Estoque, M. A. 1959 'A preliminary report on a boundary-layer experiment,' *GRD Res. Notes*, **20**, AFCRC, Bedford, Mass.

Fisher, E. L. 1959a 'The sea breeze project,' *Quart. Progress Rep.*, **2**, Contract No. DA-36-039-SC-78091, NYU, New York.

1959b 'The sea breeze project,' *Final Rep.*, Contract No. DA-36-039-SC-78091, NYU, New York.

Haurwitz, B. 1947 *J. Met.*, **4**, p. 1.

Pearce, R. P. 1955 *Quart. J. R. Met. Soc.*, **81**, p. 353.

Pierson, W. J. Jr. 1950 'The effects of eddy viscosity, Coriolis deflection, and temperature fluctuation on the sea breeze as a function of time and height,' *Met. Paps.*, **2**, NYU, New York.

Priestley, C. H. B. 1959 *Turbulent transfer in the lower atmosphere*, Chigaco Univ. Press, p. 41.

Wexler, R. 1946 *Bull. Amer. Met. Soc.*, **27**, p. 272.

551.501.42 : 551.577.2 (261)

Precipitation over the North Atlantic Ocean

By G. B. TUCKER
Meteorological Office, Bracknell, Berks.

(Manuscript received 7 September 1960)

Summary

The frequency of various types of ' present-weather ' observations are analysed and a method is derived using these to obtain estimates of mean monthly precipitation. The method is applied to observations from ocean weather ships in the North Atlantic Ocean to obtain the mean monthly, seasonal and annual precipitation over the ocean during the five-year period 1953 to 1957. The results are then compared with previous estimates.

1. Introduction

Climatological values of precipitation over the oceans are of fundamental importance in general circulation studies. The difference between precipitation and evaporation determines a large part of the energy exchange between ocean and atmosphere. This precipitation/evaporation difference also provides a check on charts of the horizontal flux of water vapour and hence of latent heat; when integrated from the bottom to the top of the atmosphere, any net horizontal divergence or convergence of water vapour must be balanced by a corresponding excess or deficit of evaporation over precipitation.

A comparison between precipitation over sea and over land on a large scale was previously attempted by Brooks and Hunt (1929), but perhaps the most careful and thorough attempt to assess the seasonal precipitation over the oceans was made by Jacobs (1950, 1951), whose method and its inherent limitations are described briefly below.

Jacobs used Wust's (1936) mean latitude values of annual precipitation over the oceans together with the chart of mean annual precipitation in the *Great Soviet World Atlas* (1937). Wust's values were based on an analysis of ocean-surface salinities as a function of the latitudinal differences between evaporation and precipitation. The mean annual precipitation chart was drawn to the values of Meinardus (1934) and Schott (1926; 1935) which are in turn based solely on extrapolation from coastal and island rainfall stations. Comparing mean zonal values taken from the precipitation chart with those of Wust, Jacobs found that they could be reconciled by the application of a simpler linear scaling factor of 0·75 for the Atlantic, 0·70 for the Indian Ocean and 0·55 for the Pacific Ocean. He then drew up a new mean annual precipitation chart accepting Wust's latitudinal values as being qualitatively correct and the *Soviet Atlas* as giving the correct areal distribution. From this Jacobs constructed seasonal precipitation charts by assessing the relative seasonal precipitation amounts in each 10° square from published charts (U.S. Weather Bureau 1938) showing the seasonal frequency of precipitation according to several rough classifications, e.g., ' drizzle,' ' steady rain,' ' passing showers. '

This original method has produced plausible seasonal precipitation charts, but it is, however, open to three criticisms :

(a) The charts of Meinardus and Schott, as well as the more recent chart in the *Morskoi Atlas* (Moscow 1953) are based on extrapolation from coastal and island stations with no reference to oceanic observations of any kind. The area distribution which is the feature of these charts used by Jacobs, cannot therefore be very reliable.

(b) The latitudinal profiles of precipitation prepared by Wust are based on the difference between two derived quantities. The inaccuracies involved in the estimation of mean zonal evaporation and salinity must result in a certain amount of uncertainty in the final precipitation values which were used as the quantitative basis for Jacobs's charts.

(c) The coarse classification of precipitation types in the U.S. Weather Bureau charts, notwithstanding the ingenious way in which they were handled by Jacobs, must give rise to further uncertainties in the seasonal distribution of precipitation.

There are, therefore, sources of considerable error in magnitude, spatial distribution and temporal distribution of precipitation in Jacobs's charts which at the time of their construction were unavoidable. Since 1947 the several ocean weather ships stationed in the North Atlantic provide a means of determining more accurately the seasonal values of precipitation at their locations.

The difficulties of recording precipitation on board ship are obvious, and the problem has been discussed in detail elsewhere (Frith 1954; Roll 1958). Spinnangr (1958) has discussed experimental attempts to measure precipitation at ship *M* and concludes that the measured values are too low. Ocean weather ships do not make routine measurements of precipitation, but ' present weather ' reports from these ships can be analysed in such a way as to yield a fairly reliable quantitative estimate of the seasonal distribution of precipitation which is not subject to the inaccuracies involved in Jacobs's method.

2. Method

Three-hourly surface observations since 1 January 1951 at all reporting Atlantic Ocean weather ships, except *M* and *K*, are available on punched cards at the Meteorological Office, and *M* and *K* are available on microfilm. The present-weather code reserves the numbers from 50 to 99 to indicate various types of precipitation at the time of observation, and the numbers from 20 to 29 to indicate precipitation, fog or a thunderstorm at the station in the past hour but not at the time of observation.

The crudest way to use these observations to estimate the amount of precipitation falling over a given period of about one month is perhaps to attempt to relate the precipitation over a land station to the number of times *any* of the 60 present-weather code numbers representing precipitation is reported. This factor could then be applied to the number of reports at the weather ships.

The most laborious method is to allocate 60 constants to these 60 code numbers, then, from the frequency of occurrence of each parameter in the month at a land station and the recorded rainfall, 60 different equations could be formed to solve for the constants. This elaborate method cannot be justified in practice because some present-weather reports occur very rarely, and in an analysis of this type a parameter must occur quite frequently if the inaccuracies involved in applying numbers to the subjective estimates of different observers are to be reduced to a minimum.

A compromise solution was adopted by using three parameters x, y and z and making an approximate assessment of the present-weather code numbers from 50 to 99 in terms of these, while neglecting the contribution of 20 to 29. The neglect of 20-29 implies that three-hourly samples of precipitation intensity are sufficient to estimate the total precipitation over a long period to within a reasonable degree of accuracy.

The assessment of present-weather code numbers in terms of x, y and z is given in Table 1. x is associated with light continuous rain, y with moderate continuous rain and z with heavy continuous rain.

TABLE 1. Assessment of present weather code numbers in terms of x, y and z

	0	1	2	3	4	5	6	7	8	9
5	0	$x/2$	$x/2$	x	y	$2y$	$x/2$	$y/2$	$x/2$	$y/2$
6	$x/2$	x	$y/2$	y	$z/2$	z	x	$\frac{y+z}{2}$	x	$\frac{y+z}{2}$
7	$x/2$	x	$y/2$	y	$z/2$	z	0	0	0	0
8	$x/2$	$y/2$	$z/2$	$x/2$	$\frac{y+z}{4}$	$x/2$	$\frac{y+z}{4}$	$x/2$	$\frac{y+z}{2}$	$x/2$
9	$\frac{y+z}{2}$	x	$\frac{y+z}{2}$	x	$\frac{y+z}{2}$	$\frac{x+y}{2}$	$\frac{x+y}{2}$	z	0	z

The above assessments are extremely subjective and independent assessors would doubtless arrive at a different table. Particularly difficult to verify are the assumed relations between the rates intermittent and continuous, rain and snow, showers and more prolonged precipitation. Some confidence in this classification is obtained when the assessment for certain code numbers are compared with the average precipitation associated with selected code numbers in a note by Sawyer (1952). Sawyer analysed the reports of drizzle and rain made by observers in the United Kingdom and compared them with rates of rainfall estimated from the amount of rainfall in the hour preceding the observation. These rates are compared with the present subjective assessment in Table 2.

TABLE 2. COMPARISON OF SUBJECTIVE ASSESSMENT AND AVERAGE RAINFALL RATE (Sawyer 1952) ASSOCIATED WITH SELECTED PRESENT-WEATHER CODE NUMBERS

Present-weather code	Average rainfall rate (mm hr^{-1})	Assessment	Present-weather code	Average rainfall rate (mm hr^{-1})	Assessment
20	0·1	0	59	1·0	$y/2$
21	0·2	0	60	0·2	$x/2$
50	0·1	0	61	0·7	x
51	0·3	$x/2$	62	1·0	$y/2$
52	0·4	$x/2$	63	1·6	y
53	0·6	x	65	2·4	z
58	0·3	$x/2$			

Provided the classification is physically plausible, the final justification will be reflected in the errors produced between estimated and actual precipitation at the land stations used to determine x, y and z. For this classification to be realistic (cf. Table 2), the derived values of x, y and z should satisfy the following criteria :

(i) $y = nx$ where $1 < n < 5$

(ii) $z = my$ where $1 < m < 3$

(iii) $z \simeq 10$ mm (in 3 hr)

The last condition gives the correct order of magnitude necessary for physical plausibility, and all three conditions correspond to the definitions of light, moderate and heavy continuous rainfall given in the *Observers' Handbook*, (H.M.S.O., 1956).

A further condition for the method to have any utility is that the r.m.s. error in estimating monthly rainfall is less than about 50 per cent of the average.

3. DETERMINATION OF x, y AND z

When determining the values of x, y and z, it is desirable that the frequency distributions of present-weather code numbers at the land stations used shall be roughly comparable with those at the weather ships where the values will be applied. However, it would be interesting to know whether or not this distribution is a critical factor in the method. Accordingly, twelve stations in the British Isles were chosen ; six *A* stations on the West Coast whose rainfall is as little affected by orographic effects as possible, and six *B* stations whose rainfall might be expected to be affected by orography (Fig. 1).

A station		*B* station	
Ballykelly	St. Mawgam	Aberporth	Plymouth
Benbecula	Tiree	Blackbushe	Renfrew
Ronaldsway	Valley	Mildenhall	Silloth

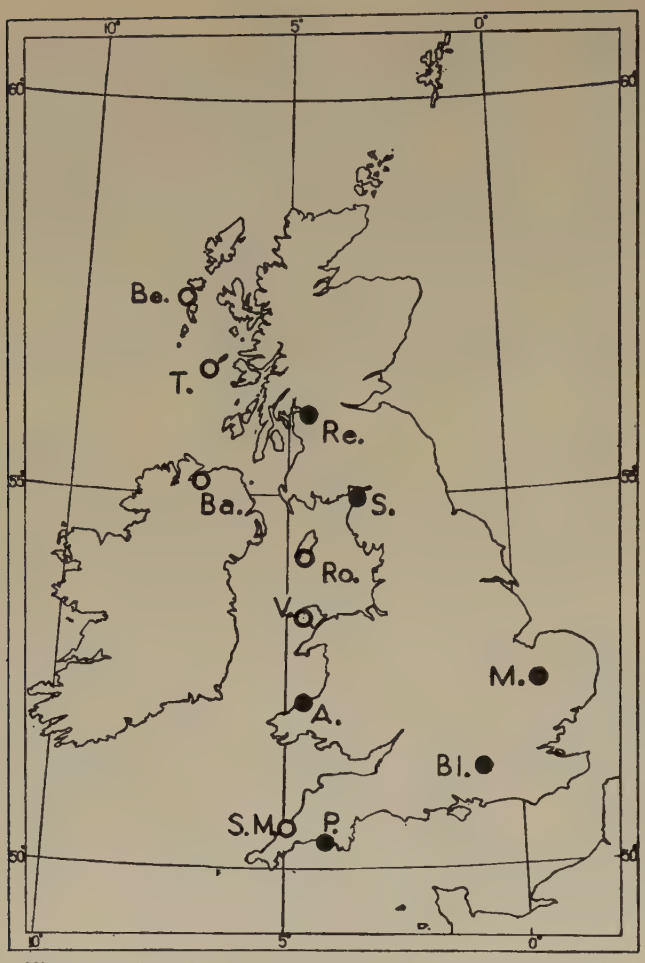

Figure 1. Location of rainfall stations used in the analysis.

○ A stations ● B stations

Ba	Ballykelly	Ro	Ronaldsway	Re	Renfrew	P	Plymouth
Be	Benbecula	V	Valley	S	Silloth	Bl	Blackbushe
T	Tiree	SM	St. Mawgan	A	Aberporth	M	Mildenhall

Punched cards for surface observations at land stations in Britain exist only from January 1957. All the months available for the above stations were used. The total number of months was 105 for the *A* stations and 144 for the *B* stations. The values of the parameters giving the least r.m.s. error in estimates of monthly rainfall were computed for both groups of six stations and for the twelve stations combined. They are given below in Table 3.

It is interesting to compare these values with those which can be evaluated from Sawyer's limited data which are $x = 1{\cdot}9$, $y = 6{\cdot}9$, $z = 7{\cdot}2$.

TABLE 3. VALUES OF x, y, z, n AND m

	A stations	B stations	All stations combined
x	1·85	1·75	1·83
y	5·66	5·61	5·33
z	8·13	9·95	10·17
n	3·2	3·4	3·1
m	1·4	1·8	1·9

Each of the sets of values in Table 3 were used to estimate the precipitation at each of the twelve stations for every month. The r.m.s. error (i.e., difference between observed and estimated precipitation) for each station over the period considered is given for each set of values in Table 4 as a percentage of the average monthly precipitation for the period.

TABLE 4. ROOT-MEAN-SQUARE ERROR OF THE MONTHLY RAINFALL ESTIMATES AS A PERCENTAGE OF THE AVERAGE MONTHLY RAINFALL FOR THE PERIOD

	r.m.s. error obtained from values of x, y, z as determined for			
A stations	A stations	B stations	All stations	Period (months)
Ballykelly	29·7	30·0	29·2	22
Benbecula	32·8	34·4	33·2	21
Ronaldsway	23·5	24·0	23·1	19
St. Mawgam	22·5	21·3	20·7	19
Tiree	16·4	17·4	17·3	12
Valley	28·4	29·1	29·5	12
B stations				
Aberporth	32·7	32·5	32·3	24
Blackbushe	39·4	39·9	40·1	24
Mildenhall	39·0	38·0	37·8	24
Plymouth	29·7	29·5	29·9	24
Renfrew	27·7	27·6	27·9	24
Silloth	27·7	26·9	27·3	24

The values in Table 4 suggest that the similarity of frequency distribution of present weather coded reports is not a critical feature since the errors at Tiree (the station with the smallest errors) and at Blackbushe (the station with the largest errors) are not significantly altered by using any of the sets of values of x, y and z. Another important feature is that the stations which can be assumed to have the least orographic effect contributing to their rainfall are the stations with the smallest error. This method therefore appears to be particularly applicable to such stations and, similarly, to ocean weather ships. Details of the estimated and measured precipitation at Valley and Tiree for each month in 1957 are given in Table 5. The values of x, y and z obtained from the analysis of the west coast stations give slightly smaller errors in the rainfall estimates for these stations than do the other values. They have been used in Table 5 and will be adopted throughout the rest of this investigation, i.e., $x = 1{\cdot}85$, $y = 5{\cdot}66$, $z = 8{\cdot}13$.

TABLE 5. ESTIMATED AND MEASURED MONTHLY PRECIPITATION (mm) AT TIREE AND VALLEY FOR 1957

	VALLEY			TIREE		
	Estimated	Measured	Error	Estimated	Measured	Error
January	99·6	91·6	+ 8	137·2	148·0	− 11
February	73·4	99·2	− 27	70·1	81·5	− 11
March	88·2	72·0	+ 16	154·5	119·2	+ 35
April	22·3	12·3	+ 10	48·3	45·2	+ 3
May	86·6	76·6	+ 10	83·4	70·1	+ 13
June	33·6	46·6	− 13	51·7	60·2	− 8
July	59·8	113·9	− 54	127·1	128·6	− 1
August	73·2	115·8	− 43	73·6	93·8	− 20
September	132·7	146·6	− 14	70·4	74·7	− 5
October	118·8	98·4	+ 20	111·5	125·1	− 14
November	48·4	53·7	− 5	83·3	59·9	+ 23
December	105·4	102·5	+ 3	138·2	140·2	− 2

The errors shown in Table 5 suggest an annual variation. The spring months of March, April and May show positive errors for both stations, whereas the summer months of June, July and August and also September show negative errors. An annual variation in error is also a feature of both the A and B groups of stations. For each group, the mean observed precipitation for each calendar month of the period considered has been calculated, together with the mean error (i.e., the average of the differences between measured and estimated precipitation for each month) and are given in Table 6. The annual variation is evident. Also included in Table 6 are the corresponding values for Goose Bay (over the two years 1957-58) which was the only east coast Canadian station for which 3-hourly present weather observations were readily available. The Goose Bay rainfall is probably heavily influenced by orography, but the figures emphasize that this annual variation in error is a feature of the method. The r.m.s. difference between the measured and estimated precipitation in the 24 months considered at Goose Bay was 32·7 per cent of the average monthly precipitation. There is a greater tendency to underestimate the precipitation here than in groups A and B; this is possibly due to a difference between the subjective estimates of rainfall rates of Canadian and U.K. observers. For example, in the two years 1957 and 1958, only slight showers were reported at Goose Bay (code figures 80, 85 and 87); apparently no showers of moderate or heavy intensity were considered to have occurred.

TABLE 6. MEAN MONTHLY MEASURED PRECIPITATION (M) AND THE AVERAGE ERROR (E) IN ITS ESTIMATION. A POSITIVE ERROR IMPLIES AN EXCESS OF ESTIMATED OVER MEASURED PRECIPITATION (UNITS – mm)

		Jan.	Feb.	Mar.	Apr.	May	June	July	Aug.	Sept.	Oct.	Nov.	Dec.	Annual
Group A stations	M	123	95	101	46	76	63	77	81	92	98	68	111	1,026
	E	+ 3	− 5	+ 27	+ 13	+ 6	0	− 6	− 14	− 12	− 15	+ 6	− 8	− 2
Group B stations	M	87	101	73	33	60	58	77	69	83	70	48	85	844
	E	+ 6	+ 10	+ 21	+ 13	0	− 7	− 15	− 13	− 20	− 6	− 4	− 7	− 22
Goose Bay	M	40	70	80	110	60	110	100	125	130	70	65	45	1,005
	E	+ 11	− 8	+ 1	− 23	+ 19	− 30	− 37	− 50	− 47	− 9	+ 19	+ 23	− 131

To attempt to correct for the annual variation in accuracy shown in Table 5, a correction factor was applied to the precipitation estimates. Since the observations at ocean weather ships were being used to estimate precipitation, these factors were obtained from the A group of stations which have the least orographic increment. The correction factor applied to the estimated value for each month was $M/(M + E)$, where M is the measured precipitation and E is the difference between estimated and measured values. The factors are :

Jan.	Feb.	Mar.	April	May	June	July	Aug.	Sept.	Oct.	Nov.	Dec.	Annual
0·98	1·06	0·79	0·78	0·92	1·01	1·08	1·21	1·15	1·18	0·92	1·08	1·00

The application of this factor reduces the overall percentage error at the A group of stations to 22·6 per cent of the average monthly value. 30 per cent, therefore, appears to be a reasonable assessment of the r.m.s. percentage error involved in estimating monthly rainfall at ocean weather ships using this method. The error for mean monthly, seasonal and annual rainfall over a five-year period will then be 13 per cent, 8 per cent and 4 per cent, if the errors can be assumed to be normally distributed and the frequency distribution of present-weather reports is similar to that for the land stations in group A.

4. Limitations of the Method

The derived values of x, y and z can now be applied to the present-weather frequencies at the ocean weather ships to estimate precipitation. This was done, but before presenting the results, it is appropriate to mention the limitations of the method. Criticisms fall into three main groups :

(a) The values of x, y and z are derived for the particular type of frequency distribution of present weather represented by the six land stations used. Although these were selected to be as representative as possible of weather ships, the frequency pattern of present-weather reports from these ships may be sufficiently different to render the results inaccurate. The statistical procedure used to determine x, y and z was a least square solution of a series of equations of the type $\alpha_i x + \beta_i y + \gamma_i z = \delta_i$ where α, β and γ are the total coefficients of x, y and z rainfall reported during a month, and δ is the measured precipitation. i is the serial number of the month, and varies from 1 to 105. If the ratios of the coefficients in these equations (i.e., the ratios of the frequencies of x, y and z precipitation) were nearly constant, the values of x, y and z might give a satisfactory fit but be poorly determined – especially if applied to rainfall regimes with markedly different ratios. However, the ratios α_i/β_i and β_i/γ_i showed a large variation; the maximum, minimum and average ratios for both the A group of stations and the ocean weather ships are shown in Table 7.

TABLE 7. Ratios of percentage frequencies of x, y and z type precipitation

	Maximum	Minimum	Mean	Maximum	Minimum	Mean
Group A stations	∞	0·8	3·1	∞	0·5	5·2
Ocean weather ships	∞	1·8	9·6	∞	1·7	8·5

It will be seen that the ocean weather ship ratios fall within the range found at the land stations from which x, y and z were determined. The larger average value of α_i/β_i over the sea shows that a greater percentage frequency of precipitation falls as light rain or showers over the oceans; the same is true of the β_i/γ_i ratio but to a less extent.

TABLE 8. Percentage frequency of present-weather reports between 50 and 99 at Ocean Weather Ship *A*. Frequencies given to 0·1 per cent, values less then 0·1 are omitted

	0	1	2	3	4	5	6	7	8	9
January 1955-December 1957 (British)										
5	2.2	2·1	–	0·2	–	–	–	–	0·5	–
6	3·0	5·8	0·2	2·0	–	0·1	–	–	0·5	0·2
7	0·3	0·3	0·1	0·1	–	–	–	0·1	–	–
8	2·2	0·3	–	0·3	0·1	1·5	0·6	0·5	0·1	–
9	0·1	–	–	–	–	–	–	–	–	–
January 1953-December 1954 (U.S.A.)										
5	0·9	2·1	0·2	0·3	–	0·1	–	–	–	–
6	1·5	7·2	0·1	1·3	–	0·1	–	–	0·4	–
7	0·5	1·9	0·1	0·7	–	0·3	–	–	–	–
8	2·8	0·3	–	0·2	–	6·1	0·4	0·4	0·1	–
9	–	–	–	–	–	–	–	–	–	–

(b) If we can assume that the standard of present-weather reporting is uniform among British observers, is this standard similar to that of foreign observers? The Goose Bay result given in Table 6 suggests that apart from one aspect, the standards are similar; this conclusion is strengthened by considering the reports at Ocean Weather Ship 'A.' For the period January 1953 to December 1954 this was a United States ship, and for the remainder of the period considered, it was a British ship. Although the present weather experienced in each period could have been dissimilar, nevertheless a comparison of the percentage frequencies will at least serve to show up any large differences if they occur.

These frequency patterns (Table 8) are quite similar, the only striking difference being that the American observers reported 85 (snow showers, slight) more frequently than the British.

(c) Ocean weather ships were sometimes off station, and no report was available. The ratio of the number of observations received to those possible is given for the five-year period for each ship in Table 9. This suggests that the errors due to this are probably quite small.

TABLE 9. PERCENTAGE RATIO OF THE NUMBER OF OBSERVATIONS AVAILABLE TO THE NUMBER POSSIBLE DURING THE FIVE-YEAR PERIOD JANUARY 1953-DECEMBER 1957

Ocean weather ships							
A	*B*	*C*	*D*	*E*	*I*	*J*	*K*
93·0	97·6	97·6	97·8	96·5	94·5	96·9	93·5

5. RESULTS

Results are given as charts of mean seasonal and mean annual rainfall over the North Atlantic (Figs. 2 to 6), together with the mean monthly and annual values for each ocean weather ship (Table 10).

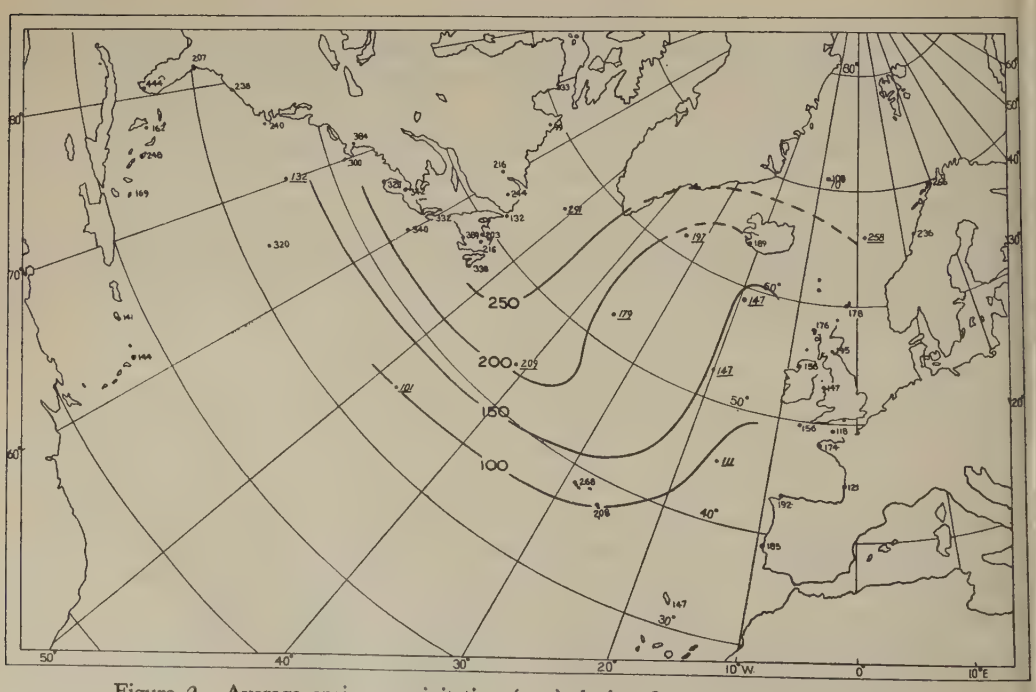

Figure 2. Average spring precipitation (mm) during five-year period 1953-1957.

On the rainfall charts the values deduced for the weather ships are underlined, and isopleths have been drawn at 100 mm intervals on the mean annual chart and at 50 mm intervals on the seasonal charts. Some coastal station values have been included for comparison.

The most noticeable result is the large difference between the rainfall over islands

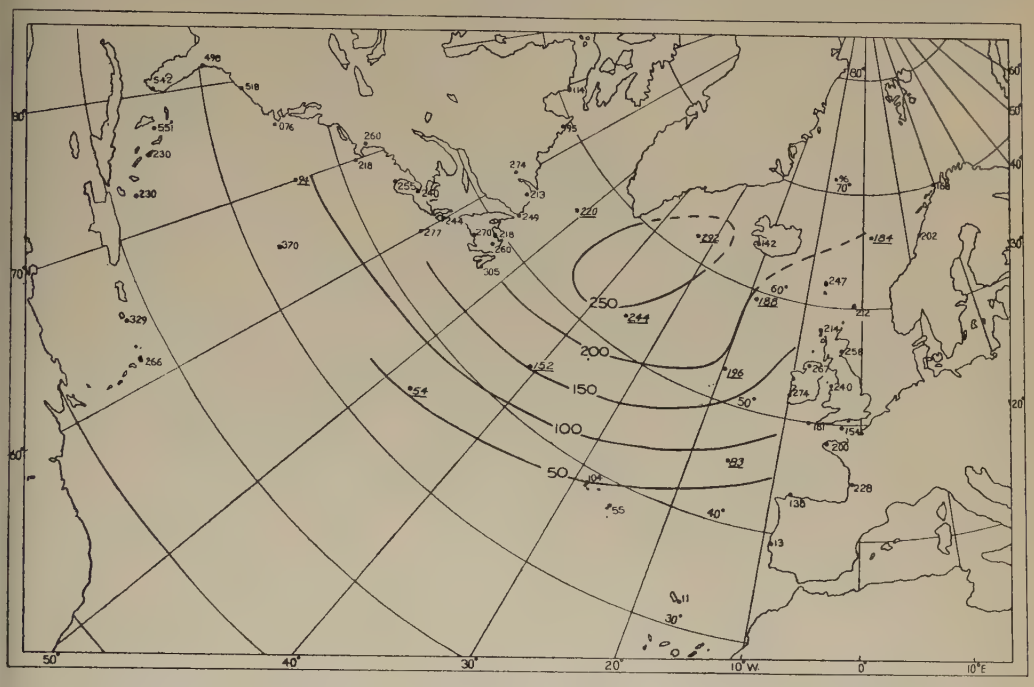

Figure 3. Average summer precipitation (mm) during five-year period 1953-1957.

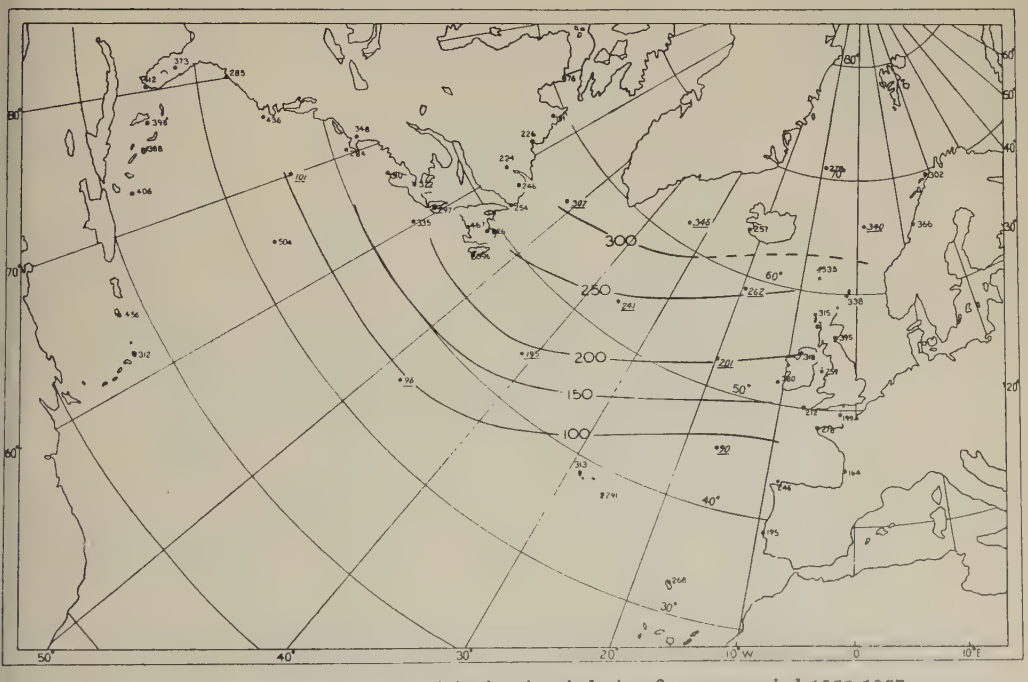

Figure 4. Average autumn precipitation (mm) during five-year period 1953-1957.

and coasts with on-shore prevailing winds and the rainfall over neighbouring sea areas. In general, the difference increases southwards, and in south-western Europe there appears to be a marked discontinuity of rainfall in the vicinity of the coastline. However, the rainfall over the coast of Labrador, over Reykjavik and over the northern half of the Norwegian coast appears to be less than that over the adjacent sea areas as given by ships *B*, *A* and

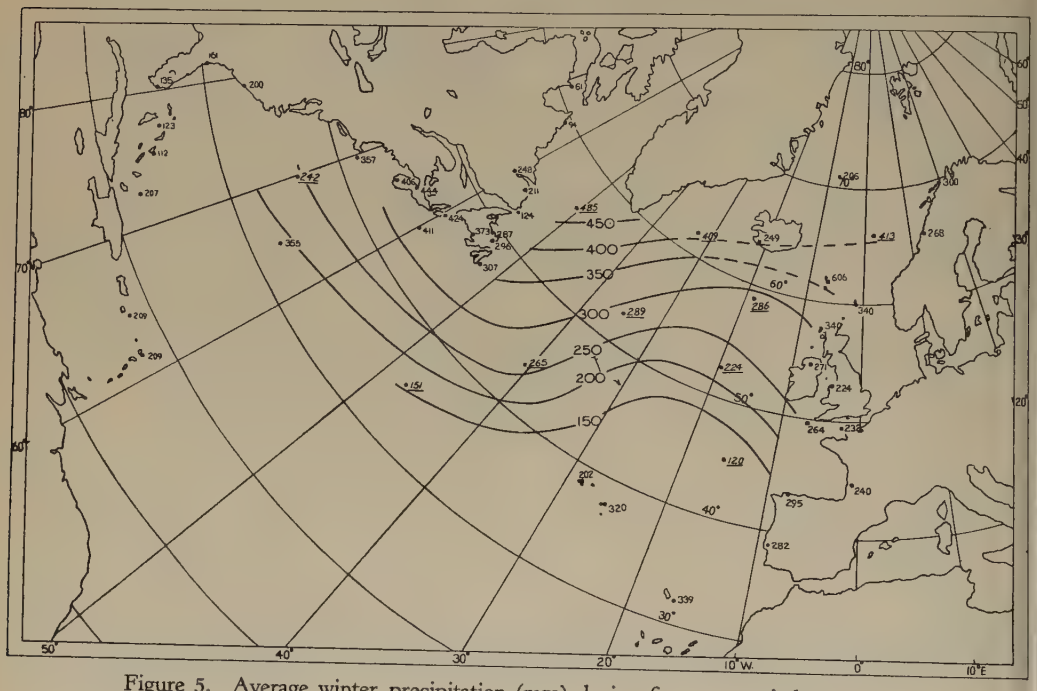

Figure 5. Average winter precipitation (mm) during five-year period 1953-1957.

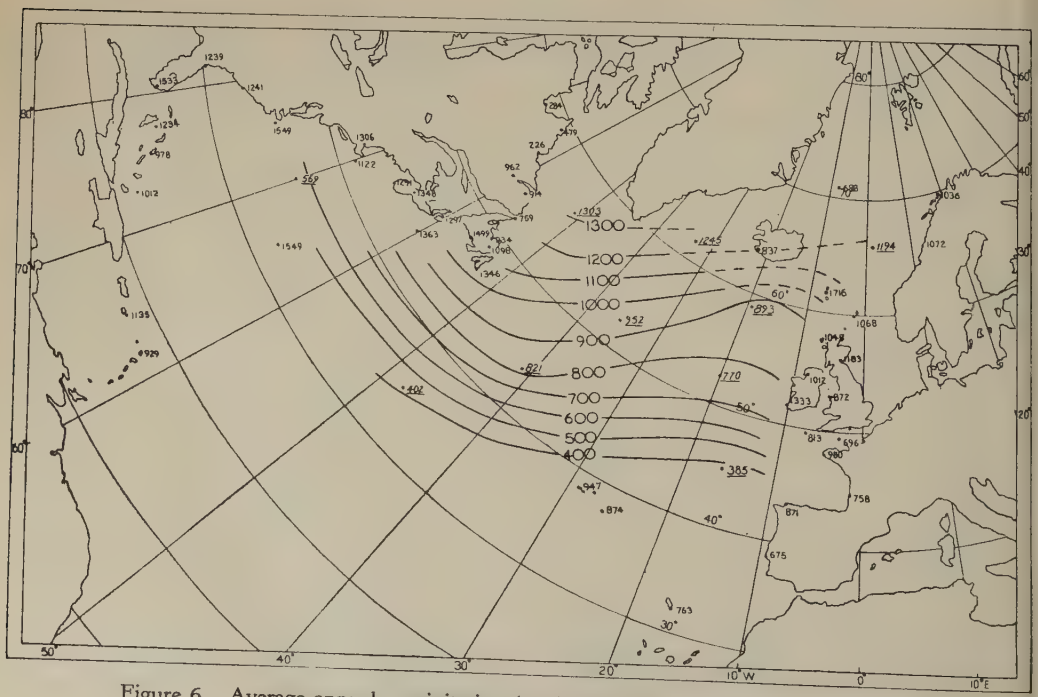

Figure 6. Average annual precipitation (mm) during five-year period 1953-1957.

M. This is less easy to explain, particularly since the totals at Thorshaven and Lerwick appear to be larger than over the surrounding sea areas. Because of this uncertainty the isopleths have been continued as dashed lines in areas north of 60°N.

It is obvious from the charts that rainfall over island and coastal stations cannot be regarded in any way as being representative of that over the open sea. Consequently the present mean rainfall maps over the oceans (Jacobs 1951; *Morskoi Atlas* 1953) must be inaccurate. The charts of the mean annual precipitation from the *Morskoi Atlas* and that obtained by Jacobs are reproduced in Fig. 7 (a) and (b). Compared with Fig. 6, both

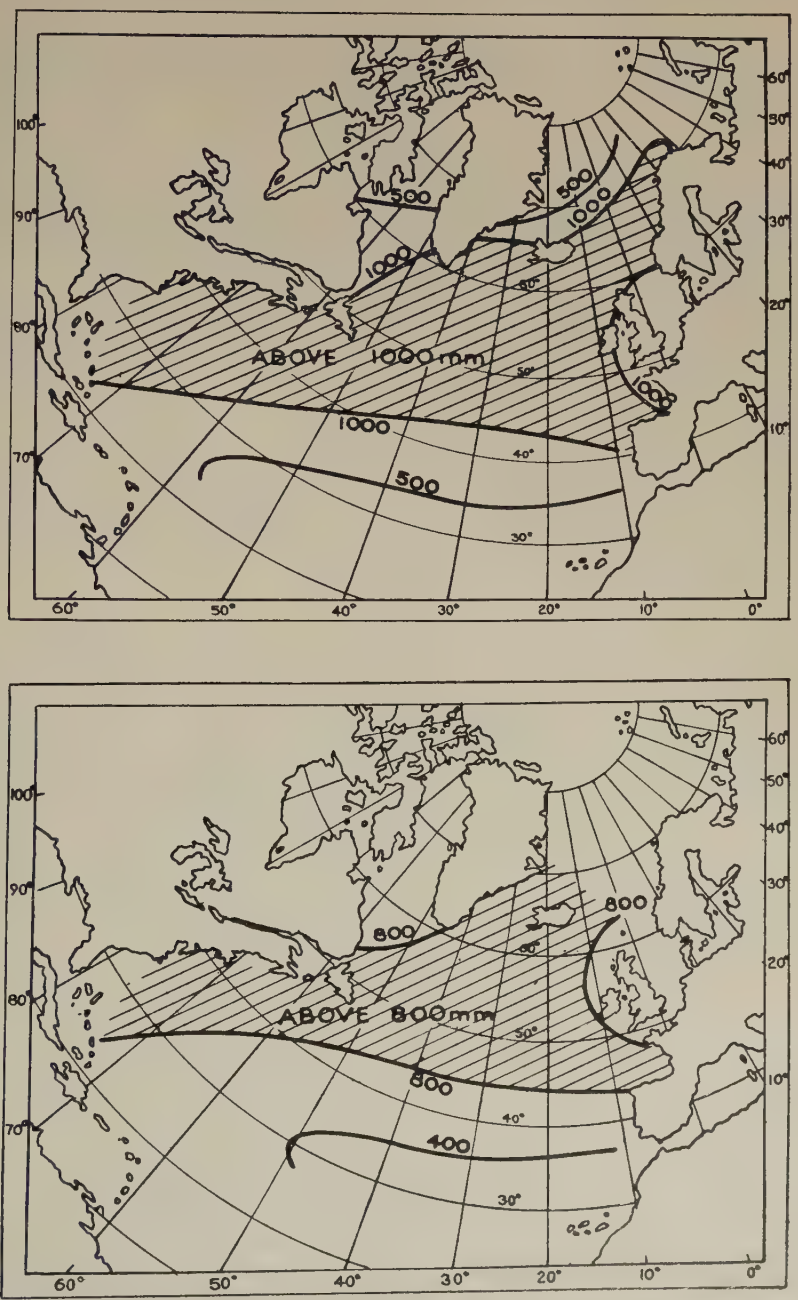

Figure 7. (a) Mean annual precipitation (*Morskoi Atlas* 1953) and (b) mean annual precipitation (Jacobs 1951).

TABLE 10. MEAN MONTHLY AND MEAN ANNUAL PRECIPITATION (mm) OVER ATLANTIC OCEAN WEATHER SHIPS DURING THE FIVE-YEAR PERIOD JANUARY 1953-DECEMBER 1957

Ocean weather ship	Jan.	Feb.	Mar.	Apr.	May	June	July	Aug.	Sept.	Oct.	Nov.	Dec.	Annual
A	120	148	77	69	51	71	95	127	107	138	101	141	1,245
B	146	169	123	93	75	68	59	93	97	105	105	170	1,303
C	108	78	61	54	65	76	72	95	85	80	76	102	952
D	75	77	76	67	66	65	38	49	65	73	57	113	821
E	61	52	51	20	30	24	15	15	33	39	24	38	402
I	97	86	50	42	55	65	61	72	92	92	78	103	893
J	78	55	49	43	55	64	56	77	69	68	64	92	770
K	35	47	52	24	35	26	20	29	28	27	28	34	385
M	142	146	88	92	78	73	59	52	102	121	116	125	1,194
H (2 years)	97	99	59	36	37	37	25	32	23	52	26	46	569

these charts show lower values of the precipitation in the north-west Atlantic (Ocean weather ship *B* area) and higher values in the east (Ocean weather ships *I*, *J* and *K*). The latter discrepancy is particularly true of the Jacobs charts for spring where ship *J* is allocated a value in the 200-300 mm range whereas the estimate for *J* using the above technique is 147 mm. Perhaps the most noticeable features of the result are the very low values computed for *K* compared with the previous estimates.

These inaccuracies must also lead to large errors in the charts of precipitation minus evaporation and hence in any studies of the water balance of the general circulation.

ACKNOWLEDGMENTS

This paper is published by permission of the Director-General of the Meteorological Office. My thanks are due to Miss J. A. Edey who performed many of the computations in this analysis. I am also grateful to the Director of the Canadian Meteorological Service for providing in manuscript form the Goose Bay data.

REFERENCES

Brooks, C. E. P. and Hunt, T. 1929 'The zonal distribution of rainfall over the earth,' *Mem. R. Met. Soc.*, III, No. 28.

Frith, R. 1954 'The measurement of rainfall at sea,' *Air Ministry, Met. Res. Cttee., M.R.P.* No. 880.

Jacobs, W. C. 1950 'The distribution and some effects of the seasonal quantities of E-P (evaporation minus precipitation) over the North Atlantic and North Pacific,' *Arch. Met. Geophys. Biokl.*, A, **11**, p. 1.

1951 'The energy exchange between sea and atmosphere and some of its consequences,' B. Scripps Inst. Ocean., Univ. California, **6**, No. 2, p. 27.

Meinardus, W. 1934 *Eine neue Niederschallag Kart der Erde*, Petermanns Mitt., Gotha, **80**, pp. 1-4.

Moscow 1953 *Morskoi (Marine) Atlas*, Navy Ministry, **11**, Map 48 (b).

Roll, H. V. 1958 *Zur Niederschlagsmessung auf see : Ergebnisse von Vergleichsmessungen auf Feuerschiffen und benach barten Inseln*, No. 16, Deutsch, Wett. See.

Sawyer, J. S. 1952 'The estimation of rainfall amounts from observations of present weather,' Met. Office Orders, C5/1952, Met. Office, London.

Schott, G. 1926 *Geographie des Atlantischen Ozeans*, Boysen, Hamburg.

1935 *Geographie des Indische und Stillen Ozeans*, Boysen, Hamburg.

Spinnangr, F. 1958 'Some remarks on precipitation measurements at sea,' *Met. Ann.*, Oslo, Bd. **4**. No. 7, p. 123.

U.S. Weather Bureau 1938 *Atlas of climatic charts of the Oceans*, No. 1247, Washington.

Wust, G. 1936 *Oberflachensalzgehalt, Verdunstung, und Niederschlag auf dern Weltmeene*, Landerkundliche Forschung, Festschrift Norbent Krebs, Stuttgart, p. 347.

551.521 : 551.584.32 : 551.584.42

The radiation balance of bare soil and vegetation

By J. L. MONTEITH and G. SZEICZ
Rothamsted Experimental Station, Harpenden, Herts.

(Manuscript received 12 July 1960; in revised form 22 November 1960)

Summary

Incoming short-wave radiation S, reflected short-wave radiation αS and net radiation R were measured over bare soil and crops from 1957 to 1959, and net long-wave radiation (L) was deduced from

$$R = (1 - \alpha) S + L$$

For grass, α increased from 0·23 at solar elevation 60° to 0·28 at 20° with daily mean 0·26. For bare soil, the corresponding increase was from 0·16 to 0·19 with mean 0·17. In mid-June, L for bare soil decreased from $-$ 0·1 cal cm^{-2} min^{-1} during the night to $-$ 0·4 cal cm^{-2} min^{-1} in the early afternoon. For long grass, in August, the corresponding change was from $-$ 0·05 to $-$ 0·22 cal cm^{-2} min^{-1}. Under clear skies the incoming long-wave component varied much less than the outgoing component, and net flux L was closely related to surface temperature.

With a ' heating coefficient ' $\beta = -dL/dR$, the observed linear dependence of R on S in the absence of cloud may be expressed as

$$R = S(1 - \alpha)/(1 + \beta) + L_0$$

where, formally, $R = L_0$ when $S = 0$. For grass, sugar beet and potatoes, β lay between 0·15 and 0·22 with a variation which may depend on wind speed rather than on crop. The value for dry bare soil was higher (0·41) because there was greater surface heating.

Measurements under clear skies and over grass at Cambridge and Kew agree well with Rothamsted values ($\beta = 0{\cdot}22$, $L_0 = -$ 5·9 cal cm^{-2} hr^{-1}). Over Nebraska prairie, $\beta = 0{\cdot}25$, $L_0 = -$ 4·5 cal cm^{-2} hr^{-1} from selected observations during Projects Great Plains and Prairie grass.

1. Introduction

In many problems of surface-heat balance, an important meteorological variable is the net radiation absorbed by the surface in the wave-length range 0·3 to 30 μ. Serious interest in the measurement of net radiation is comparatively recent, and there are no climatological records comparable with those for short-wave radiation alone (0·3 to 3 μ). In agricultural meteorology, the importance of net radiation in determining crop evaporation was emphasized by Penman (1948); and Pasquill (1950) suggested that in the climate of the British Isles annual latent heat of evaporation from short grass is equal to annual net radiation. Measurements by House, Rider and Tugwell (1960) and the preliminary analysis of three years' records at Rothamsted show that there is often close agreement between *daily* totals of latent heat and net radiation. For future exploitation of this useful relationship, the dependence of net on short-wave radiation under clear skies has been examined for grass, sugar beet, wheat, and bare soil.

2. Instruments and crops

Incoming short-wave radiation was measured on the laboratory roof with a Kipp solarimeter installed in 1955 after calibration at Kew Observatory, and subsequently recalibrated both at Kew and at the National Institute of Agricultural Engineering, Silsoe. From May 1955 until June 1958, output was fed to a single-point recording potentiometer giving a continuous record on an 18 cm wide chart with a sensitivity of 0·09 cal cm^{-2} min^{-1} per cm, and radiation totals were obtained by planimetry. In June 1958, a more elaborate potentiometer with mechanical integrator was installed to give radiation totals on a counter reading directly in cal cm^{-2}. The chart width is 25 cm and the sensitivity 0·06 cal cm^{-2} min^{-1} per cm.

A small solarimeter (Monteith 1959a) was built to measure short-wave radiation in the field. Measurements began in 1958 using two receivers set to face the sky and the ground and giving spot measurements of reflection coefficient when read alternately. In 1959, downward-facing solarimeters gave a continuous record of reflected radiation on a potentiometer. Net radiation was measured with a Gier and Dunkle ventilated radiometer similar to that described by McDowall (1955). Calibrated at Kew Observatory in 1956, it was subsequently repainted but not re-calibrated after each season. Evidence for the stability of the calibration is presented in Table 4. The radiometer was mounted on a wooden tripod about 1·5 m above the ground and output was recorded on a multi-point potentiometer.

The experimental site adjoining the meteorological enclosure is approximately 50×50 m and its surroundings were described by Penman and Long (1960). Table 1 gives a crop time-table in which an approximate date for the establishment of ' complete ground cover ' was estimated from records of evaporation and reflection coefficient rather than from more arbitrary visual observations.

TABLE 1. Crop timetable

Year	Crop	Sown	Complete cover	Harvest or cut
1957	Spring wheat (Koga II)	21 March	24 May	26 August
1958	Sugar beet (Klein E)	11 April	15 July	17 November
1959	Grass (40 per cent S.51 Timothy) (60 per cent S.214 Meadow Fescue)	4 May	1 August	28 August

3. Symbols

The following were chosen to represent terms in surface radiation balance :

S – incoming short-wave radiation from sun and sky

α – reflection coefficient for short-wave radiation

L_d – downward long-wave radiation from the atmosphere

L_u – upward long-wave radiation from the surface $= \epsilon \sigma T_0^4 + (1 - \epsilon) L_d$

T_0 – radiative temperature of surface (°K)

σ – Stefan-Boltzman constant $= 8{\cdot}13 \cdot 10^{-11}$ cal cm^{-2} °K^{-4} min^{-1}

ϵ – long-wave emissivity of surface

L – net incoming long-wave radiation

R – net radiation for all wave-lengths

From these definitions it follows that

$$L = L_d - L_u \quad . \quad . \quad . \quad . \quad . \quad (1)$$

and

$$R = (1 - \alpha) S + L \, . \quad . \quad . \quad . \quad . \quad (2)$$

The unit of radiation is g cal cm^{-2} per minute, hour or day.

4. Cloudless days 1959

(a) *Diurnal variation of radiation balance*

In June 1959, the grass in the experimental plot was still struggling to survive after late sowing and scanty rainfall, and measurements both of reflection and of evaporation show that the surface was behaving meteorologically like bare soil. The diurnal variation in radiation components on a cloudless June day is shown in Fig. 1 (a) where S, αS and R are all measured quantities. The diurnal variation in the net long-wave term L was calculated by difference from Eq. (2) and therefore shows small irregularities not present in the other components. At mid-day, the heat loss by long-wave exchange was three times its nocturnal value and twice the contemporary loss by short-wave reflection. Similar variation of L was reported by Ayzenstat and Zuev (1952) : over dry steppe near Tashkent the mean long-wave loss on clear days increased from 0·09 cal cm^{-2} min^{-1} before dawn to 0·35 cal cm^{-2} min^{-1} shortly after noon when maximum solar radiation was 1·2 cal cm^{-2} min^{-1}.

Two months later, evaporation from a thick stand of grass 40 cm high reduced the diurnal variation of surface temperature and hence of long-wave radiation (Fig. 1 (b)). From 0700 to 1500 GMT, more radiation was lost by short-wave reflection (maximum 0·25 cal cm^{-2} min^{-1}) than by long-wave exchange (maximum 0·21 cal cm^{-2} min^{-1}), and displacement of this maximum to 1400 GMT illustrates an important dependence of long-wave exchange on surface temperature, to be discussed in the next section.

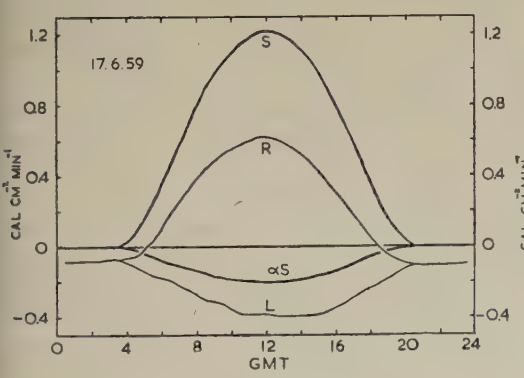

(a) bare soil, 17 June

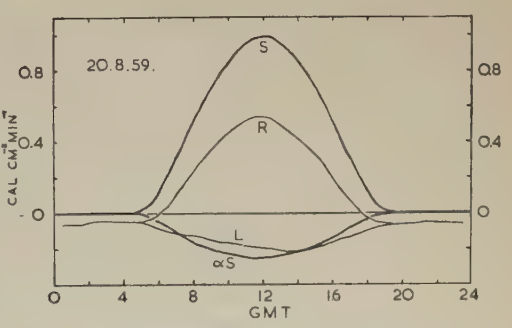

(b) long grass (40 cm high), 20 August

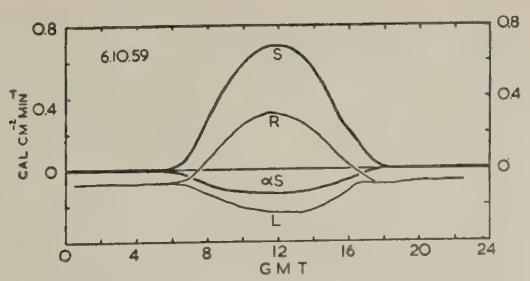

(c) short grass (10 cm high after cutting), 6 October.

Figure 1. (a) (b) (c). Diurnal variation of radiation balance components over experimental site, 1959.

The grass was cut to a height of 10 cm at the end of August; with no rain during September, re-growth was very slow; and even at the beginning of October, evaporation from the crop was still only 40 per cent of the potential rate for a freely transpiring green cover. On 6 October (Fig. 1 (c)), long-wave exchange reached $-0{\cdot}25$ cal cm^{-2} min^{-1}, although maximum solar radiation was only $0{\cdot}70$ cal cm^{-2} min^{-1}. Comparison with Figs. 1 (a) and (b) suggests that there was strong surface heating of dry soil.

(*b*) *Long-wave exchange*

To examine the diurnal variation in long-wave exchange in more detail, the complete radiation balance was calculated for 1100 on each of the three days and for 2300 on previous nights. At these times, a radiosonde ascent at Crawley, 50 mi south of Rothamsted, provided temperature and humidity data from which incoming long-wave radiation could be estimated on a Kew radiation chart (Robinson 1950).

Outgoing radiation L_u was then calculated by combining Eqs. (1) and (2) to give

$$L_u = L_d + (1 - \alpha)\, S - R$$

Assuming an error of $\pm 0{\cdot}01$ cal cm^{-2} min^{-1} in the chart determination, and of $\pm 0{\cdot}02$ cal cm^{-2} min^{-1} in each of the three measured components, the error in L_u was $\pm 0{\cdot}02$ cal cm^{-2} min^{-1} at night and $\pm 0{\cdot}04$ cal cm^{-2} min^{-1} during the day. Effective radiative temperature of the surface could therefore be determined to ± 3°C at night and ± 5°C during the day, assuming an emissivity of 1·0 for grass (Gates and Tantraporn 1952) and 0·9 for bare soil (Brooks 1959). For comparison, there are measurements of soil surface and leaf temperature kindly provided by Mr. I. F. Long, whose thermometers are nickel resistance elements 0·8 mm in diameter and 5 mm in length (Long 1957). These were inserted in the leaf sheath or rested horizontally on the soil with the upper half of the element exposed to the air. Treating the radiative surface as bare soil in June and October, and as grass in August, differences between temperature measured directly (but at one point only), and calculated from the radiation balance agree well in the two later months (Table 2 where comparable temperatures are marked *). In June, however, radiative temperature is 12°C *above* measured soil temperature at 1100 hr and 8°C *below* it at 2300 hr. The size and sign of the day-time discrepancy is consistent with the existence of a very steep temperature gradient in the soil at the surface. The average over the first 10 mm was $-0{\cdot}8$°C mm^{-1} as measured and might well have been ten times as great in the first 1 mm of dry soil particles in which the 'surface' thermometer was lying. At night, as the measured temperature gradient was only $\pm 0{\cdot}3$°C mm^{-1}, it is most unlikely that the 'surface' thermometer was 8°C above surface radiative temperature. An alternative source of error is the undetected presence of high cloud leading to under-estimation of L_d and hence of L_u and T_0.

TABLE 2. RADIATION BALANCE AND SURFACE TEMPERATURE
(Unit: cal cm^{-2} min^{-1})

Time (GMT)	16 June 2300	17 June 1100	19 Aug. 2300	20 Aug. 1100	5 Oct. 2300	6 Oct. 1100
S	0·00	0·99	0·00	0·70	0·00	0·49
R	− 0·08	0·59	− 0·08	0·58	− 0·08	0·30
L	− 0·08	− 0·40	− 0·08	− 0·20	− 0·08	− 0·19
L_d (Kew Chart)	0·39	0·44	0·47	0·52	0·45	0·42
T_0 (°K) $\epsilon = 1{\cdot}0$	276	319	287*	307*	284	294
$\epsilon = 0{\cdot}9$	277*	323	287	309	284*	296*
T_0 (leaf)			288*	301*	283*	294
T_0 (soil)	285*	311*	289	297	284*	296*

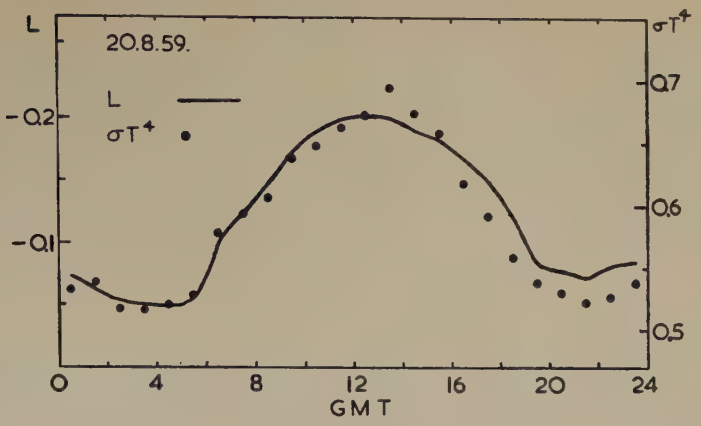

Figure 2. Diurnal variation of net long-wave loss L and black body radiation at leaf temperature σT_0^4, 20 August 1959, with axes adjusted to make $\sigma T_0^4 + L = 0{\cdot}47$ (Unit : cal cm^{-2} min^{-1}).

Table 2 shows that diurnal changes were much greater in the outgoing than in the incoming component of long-wave radiation. During the October day-time, incoming radiation even decreased with increasing surface temperature when relatively stagnant moist air of Mediterranean origin was replaced during the night by the dry polar air of an anti-cyclone over Norway. Fig. 2 shows how closely the changes in net long-wave exchange followed changes in the outgoing component calculated from leaf-surface temperature, implying that incoming long-wave radiation was relatively constant throughout the day.

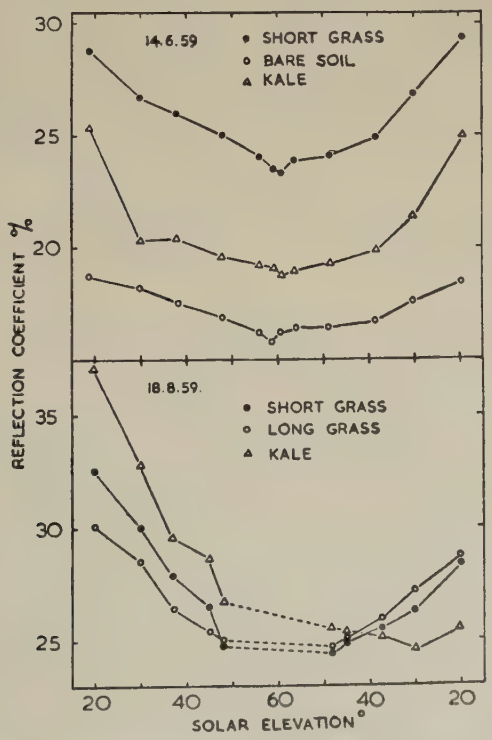

Figure 3. Diurnal variation of reflection coefficient on 14 June and 18 August 1959 as function of solar elevation.

(c) *Reflection coefficient*

Diurnal variation of reflection coefficients is shown in Fig. 3 by ' bare soil ' and ' long grass ' points for the experimental plot, by ' short grass ' points for the adjacent meteorological enclosure (mown weekly to a height of 1 cm), and for a nearby field of kale.

In June, reflection by short grass and bare soil was least at mid-day, and increased almost linearly with decreasing solar elevation, more rapidly over grass than over soil. The kale plants were only 30 cm high, and with rows 60 cm apart, cover was far from complete. When solar elevation exceeded 30°, the coefficient for the kale field was 0·19 to 0·20, slightly greater than for bare soil; but below 30°, reflection increased sharply with decreasing elevation.

Records for August 18 show enhanced reflection after a dewy night. Reflection coefficients of long and short grass were almost identical when leaves were dry; when wet there was consistently greater reflection from short grass. There was more reflection from the wet kale than from either of the grasses, consistent with the observation that dew-drops were larger and persisted longer on this crop. In the afternoon, reflection from both grass surfaces followed the pattern of 14 June but it is not known why the coefficient for kale failed to increase towards sunset.

Table 3 shows a mean reflection coefficient, obtained by dividing daily totals of reflected and incoming radiation. For all three crops, there is little departure from the figure of 0·26, previously given as a mean from spot readings over a wide range of crops with solar elevation exceeding 40° (Monteith 1959b). This useful agreement follows from heavy weighting of the daily mean coefficient by the large amounts of energy received when the sun is high.

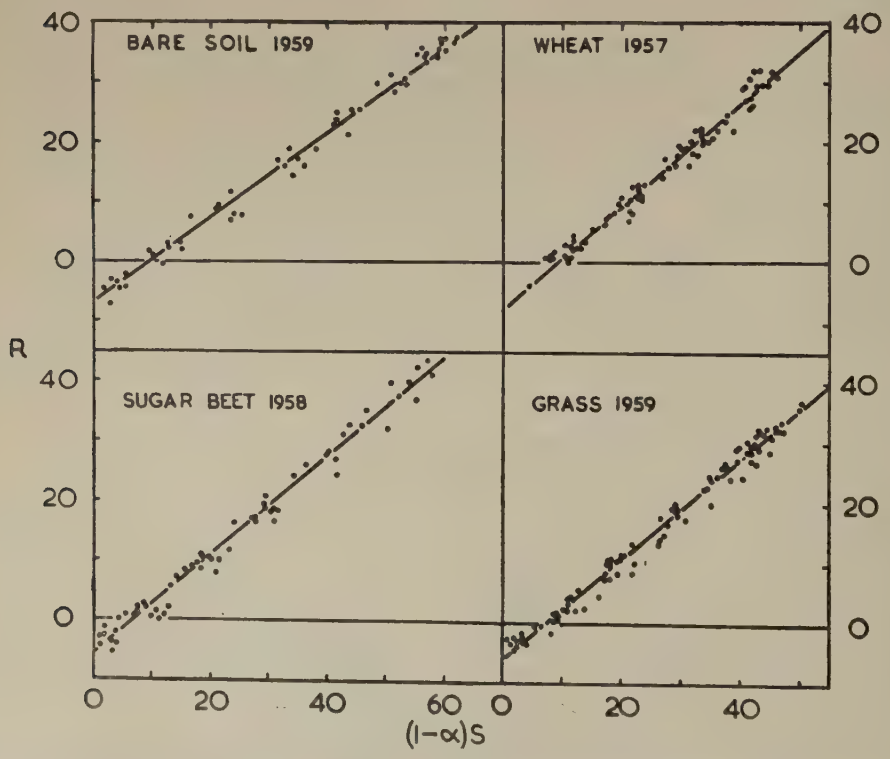

Figure 4. Variation of hourly totals of net radiation R with net short-wave radiation $(1 - \alpha)\, S$ in the absence of cloud (Unit : cal cm^{-2} hr^{-1}).

TABLE 3. MEAN REFLECTION COEFFICIENTS (CLEAR DAYS)

Date	Short grass (Met. enclosure)	Bare soil	Long grass	Kale
14 June 1959	0·25	0·17	–	0·19
18 August 1959	0·27	–	0·26	0·28
25 August 1959	0·25	–	0·26	0·25

6. CLOUDLESS HOURS 1957-1959

The correlation between solar and net radiation for 532 cloudless hours in the summers of 1957-1959 is in Fig. 4. The only data purposely omitted from this diagram are for short-wave intensities above 60 cal cm^{-2} hr^{-1} between 11 and 17 June 1957, when the radiometer was not raised during very rapid growth. Anomalously high net radiation was recorded during the middle of the day, probably because reflected radiation was not properly received by the under-side of the plate.

The constants of the regression formula

$$R = a(1 - \alpha) S + b \quad . \quad . \quad . \quad . \quad (3)$$

are in Table 4 with values of wind speed u, the correlation coefficient r^2 and a parameter β defined in Section 8.

TABLE 4. SUMMARY OF DATA FOR CLOUDLESS DAYS

		u^*	a	b	β	r^2
Spring wheat	25 May-27 July 1957	3·2	0·87	− 7·9	0·15	0·98
Sugar beet	3 July-27 Sept. 1958	1·3	0·83	− 5·8	0·21	0·94
Grass	23 July-27 August 1959	1·4	0·82	− 5·9	0·22	0·97
Bare soil	14 April-30 April 1957	2·4	0·74	− 4·5	0·35	0·97
Bare soil	1 May-18 June 1958	1·1	0·72	− 5·2	0·39	0·90
Bare soil	13 June-20 June 1959	2·8	0·71	− 6·8	0·41	0·97
Bare soil	7 Sept.-20 Sept. 1959	1·2	0·73	− 5·9	0·37	0·93

* u is mean wind speed in m sec^{-1} on relevant days, at 2 m over short grass in meteorological enclosure

As a check on the stability of the radiometer calibration during the three years, Table 4 gives values of a, nominally over ' bare soil ' but including measurements until one month before complete crop cover. Data for September 1959 are given in this category too because the field was sparsely covered during the rainless period which followed cutting on 28 August. Year-to-year differences in the ' bare soil ' value of a are small and may well be real. Further support for the data of Table 4 was given by measurements in 1960 when long-wave flux was measured directly with a Linke Feussner radiometer. From one day's data only (June 2), values of a calculated from solarimeter records and spot readings with the Linke Feussner were : wheat, 0·90; short grass, 0·80; bare soil, 0·76.

The scatter of points in Fig. 4 conceals a noteworthy daily cycle. For equal short-wave radiation intensities, the net radiation was always smaller in the afternoon than in the morning because of higher afternoon surface temperatures. The cycle was most pronounced over bare soil for which a typical daily cycle is given in Fig. 5.

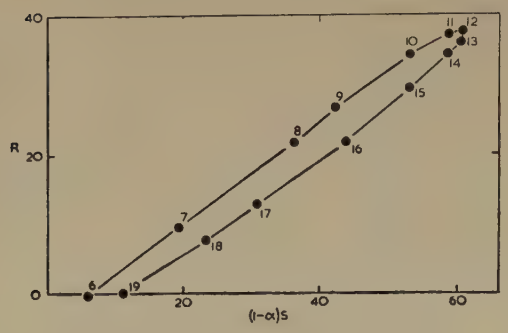

Figure 5. Variation of hourly totals of R and $(1 - \alpha)\,S$ over bare soil on a cloudless day, 2 June 1959, for hours ending at time shown (GMT) (Unit : cal cm^{-2} hr^{-1}).

8. A GENERAL RADIATION-BALANCE EQUATION

The empirical equation for the dependence of net radiation on short-wave radiation under clear skies

$$R = a\,(1 - \alpha)\,S + b \qquad . \quad . \quad . \quad . \quad (3)$$

can satisfy

$$R = (1 - \alpha)\,S + L \qquad . \quad . \quad . \quad . \quad (2)$$

only when L is a linear function of R having the form

$$L = b/a - R\,(1 - a)/a$$

$$= b/a - \beta R \quad \text{say,}$$

so defining β as given in Table 4. Because L is negative, β is the increase of net long-wave loss per unit increase of net radiation income. As an increase of net radiation is associated with an increase in surface temperature to which the net long-wave loss is very closely related (Fig. 2), β may be regarded as a heating coefficient. With the formal assumption that when $S = 0$, L has the value $L_0\,(= b)$ then

$$R = S\,(1 - \alpha)/(1 + \beta) + L_0 \qquad . \quad . \quad . \quad (4)$$

Table 4 shows that the heating coefficient is greater for dry bare soil than for vegetation, which is consistent with known differences in the diurnal variation of radiation balance for these contrasting surfaces. The smaller value of β for wheat than for sugar beet or grass implies a smaller diurnal variation of surface temperature for given radiation income and this difference is consistent with the higher wind speed prevailing during the wheat observations (Table 4). The simplest hypothesis is that β depends on wind but is the same for all freely transpiring crops exposed to the same weather. Further study is needed to show whether β is sensitive to differences in crop structure. For example, the normal spacing of a cereal allows free air movement below the crop canopy and in given weather the effective surface temperature of a cereal (and hence β) may be less than for a densely growing crop of sugar beet or grass exposed to the same weather.

Attempts to use Eq. (4) to calculate daily totals of net radiation have so far failed because of difficulty in specifying L_0. The formal definition of L_0 as net long-wave radiation in the absence of short-wave radiation has clear statistical significance (Fig. 4), but for the grass data the points near the origin lie above the mean line fitting all the data. Thus the statistical value of L_0 for grass in August ($= b$ in Table 4) is $-5{\cdot}9$ cal cm^{-2} hr^{-1} whereas on a typical clear night (Fig. 2) the mean net long-wave flux is about -4 cal cm^{-2} hr^{-1}.

Daily totals of net radiation over short grass on a clear day can be found directly from Eq. (2), given measurements of incoming short-wave radiation reflection coefficient, and an estimate of long-wave exchange from an empirical formula derived from radiation records at Kew (Monteith 1961). Because this formula contains a correction for the difference between mean air temperature and mean surface radiative temperature, it is not accurate for surfaces which differ from short grass in radiative temperature. The development of a climatological formula for calculating net radiation absorbed by surfaces other than short grass awaits analysis of the dependence of β and L_0 on wind speed, on surface properties and on season.

9. Examination of other data for grass

Eq. (4) can be used to find the clear-sky relationship between net and short-wave radiation for any crop and climate given reflection and heating coefficients and the value of L_0. If L_0 and β are unknown the equation can still be used to check the internal consistency of radiation measurements, because when R is plotted against S or $(1 - \alpha)\, S$, points should lie close to a straight line. Four sets of data will be examined.

(*a*) *Cambridge and Kew*

Radiation measurements by Pasquill (1959) were made over ' patchy grass, mainly 2 cm high, with occasional tufts up to 5 to 7 cm,' at Cambridge; and by Rider and Robinson (1951) over level grass kept mown to an average height of 1 to 2 cm at Kew. Their observations for cloudless weather (Fig. 6) are in good agreement with the straight line correlating net and short-wave radiation under clear skies at Rothamsted (Fig. 4), where the grass grew up to 40 cm high. This suggests that the radiation balance of grass is virtually independent of height or management.

(*b*) *Nebraska, Project Great Plains*

As part of the Great Plains Turbulence Field Programme, solar and net radiation were measured at O'Neill, Nebraska with instruments provided by several co-operating institutions and described by Suomi, Davis, and Brooks (Lettau and Davidson 1957).

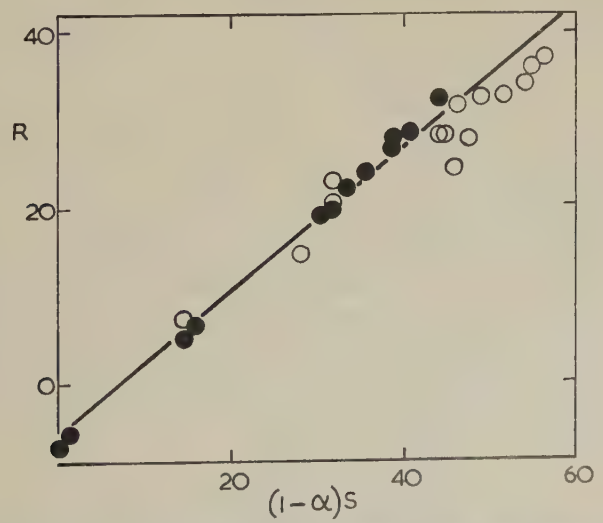

Figure 6. Variation of R and $(1 - \alpha)\, S$ over short grass at Kew (○) and over rough pasture near Cambridge (●) with Rothamsted regression $R = 0{\cdot}82\ (1 - \alpha)\, S - 5{\cdot}9$ (Unit : cal $cm^{-2}\ hr^{-1}$).

Eppley solarimeters recorded incoming and reflected solar radiation. Gier and Dunkle type radiometers gave net radiation : Johns Hopkins University (JH) used a commercial model, accepting the maker's calibration; the University of Wisconsin (UW) used the improved model described by Suomi *et al.* (1954); the University of Texas (UT) model

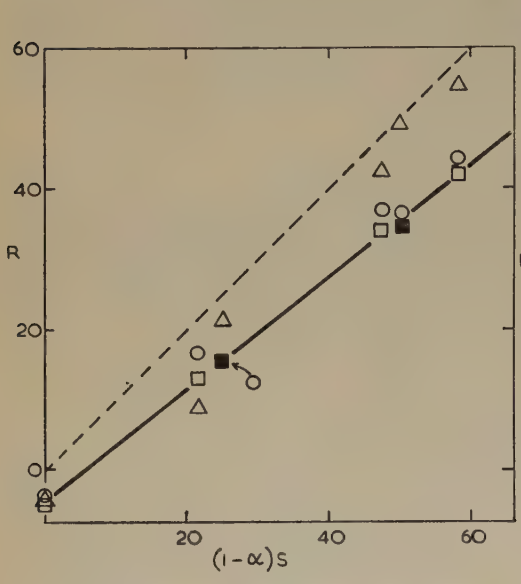

(a) 7 September 1953 Project Great Plains

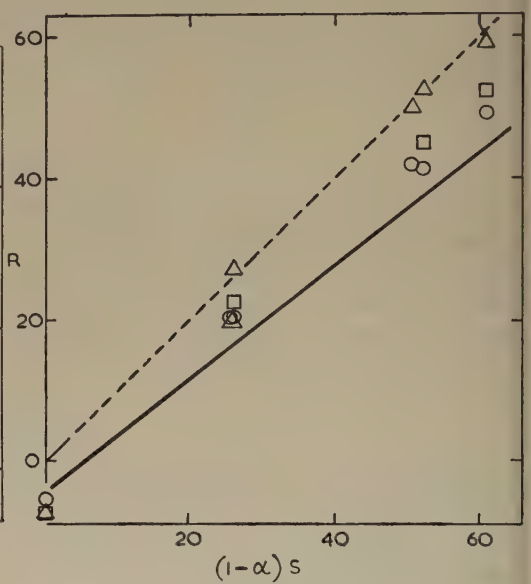

(b) 25 August 1953 Project Great Plains

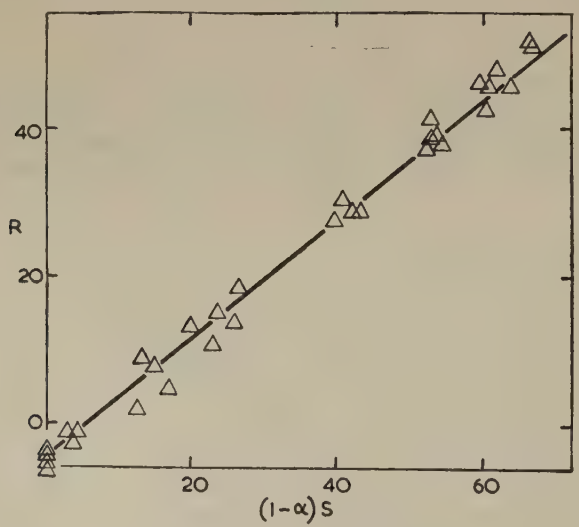

(c) Project Prairie Grass.

Figure 7 (a) (b) (c). Variation of hourly totals of R and $(1 - \alpha)\,S$ over prairie at O'Neill, Nebraska (Unit : cal $cm^{-2}\,hr^{-1}$).

△ University of Texas
○ Johns Hopkins University
□ University of Wisconsin
■ University of Wisconsin calibration points
——— $R = 0{\cdot}80\ (1 - \alpha)\,S - 4{\cdot}5$
- - - - $R = (1 - \alpha)\,S$

is unspecified. Outputs were recorded on electronic potentiometers (UT, UW) or on a milliameter after amplification (JH).

All the radiometers were exposed at 1 m above 'thick clumps of grass scrub surrounded by relatively thin patches with small (approximately 10 cm diameter) patches of bare ground distributed randomly throughout the field.' The mean grass height was about 6 cm. The tabulation of α by Davis provides mean hourly values for the period 5-7 September now used in analysis of solar and net radiation data for the two cloudless days 25 August and 7 September. Fig. 7 (a) shows R from each of the radiometers on September 7 plotted against $(1 - \alpha)\ S$ from one solarimeter (Geophysics Research Directorate). It is immediately obvious that the UT points (triangles) are inconsistent with the other sets; they imply that the net loss of long-wave radiation L is close to zero (i.e., $R \simeq (1 - \alpha)\ S$) and will not be given further discussion. There are two UW calibration points (full squares) obtained by shading both the net radiometer and a solarimeter from direct solar radiation. With a further four points (open squares) these define a straight line with $\beta = 0{\cdot}25$, $L_0 = -4{\cdot}5$ cal cm^{-2} hr^{-1}. The mean wind speed at 2 m was 8-9 m sec^{-1} (cf. 2·8 m sec^{-1} during observations at Rothamsted) and had soil moisture been adequate, rapid transpiration should have reduced the heating coefficient below the Rothamsted value ($\beta = 0{\cdot}22$). Halstead's (1954) analysis shows that evaporation was checked by shortage of soil moisture, and surface heating should therefore have been greater than for freely transpiring vegetation exposed to the same weather. Fortuitously, the combination of high wind and low evaporation gave almost the same surface heating per unit net radiation as measured at Rothamsted.

The JH net radiation values are on average 9 per cent higher than the UW data and points are more scattered. A 10 per cent discrepancy in the same sense between the short-wave measurements of JH (not used here), and those of the Geophysics Research Directorate (used to calculate $(1 - \alpha)\ S$) suggests a systematic error in the calibration of the JH radiation equipment.

Observations for 25 August are plotted in Fig. 7(b) where agreement with expectation is less obvious. The UT points are again regarded as inconsistent and the UW points do not now define a straight line. The JH points, reduced by 10 per cent, define a line with slope close to $\beta = 0{\cdot}25$. Confirmation for this value of β comes from soil temperature measurements : the diurnal range at $-0{\cdot}5$ cm was about 23°C on 25 August. Assuming the same change in effective surface radiative temperature and no change in incoming long-wave radiation, the calculated change in net flux is about 0·2 cal cm^{-2} min^{-1}. With R (max) = 0·75 cal cm^{-2} min^{-1} (JH reduced value), $\beta = 0{\cdot}26$.

(c) *Nebraska, Project Prairie Grass*

The University of Texas was responsible for radiation measurements at O'Neill during a programme of diffusion measurements sponsored by the Geophysical Research Directorate and known as Project Prairie Grass. There are published data (Barad 1958) for hourly totals of incoming and reflected solar radiation (Eppley solarimeter) and for net radiation (Gier and Dunkle radiometer manufactured by Messrs. Beckman and Whitley). Net radiation was plotted against net short-wave radiation for cloudless hours during three days in July and August 1956. Fig. 7 (c) shows a good distribution of points about the 'best' line obtained by the University of Wisconsin in 1953 ($\beta = 0{\cdot}25$, $L_0 = -4{\cdot}5$ cal cm^{-2} hr^{-1}), (Fig. 7 (a)). These observations provide further support for the validity of Eq. (4) and for criticism of the published radiation data from Project Great Plains.

Acknowledgments

We are grateful to Dr. H. L. Penman for suggesting improvements to the original draft of this paper and to Mr. I. F. Long for temperature records.

References

Ayzenstat, B. A. and Zuev, M. B.	1952	*Leningrad, Glav. Geof. Obs. T.*, **6**, p. 7.
Barad, M. L.	1958	*Geophys. Res. Pap.* No. 59, U.S. Geophysical Research Directorate, Massachusetts.
Brooks, F. A.	1959	*An introduction to physical microclimatology*, California University.
Gates, D. M. and Tantraporn, W.	1952	*Science*, **115**, p. 613.
Halstead, M. H.	1954	*Publications in climatology*, Johns Hopkins University, **7**, p. 326.
House, G. J., Rider, N. E. and Tugwell, C. P.	1960	*Quart. J. R. Met. Soc.*, **86**, p. 215.
Lettau, H. H. and Davidson, B.	1957	*Exploring the atmosphere's first mile*, Pergamon Press, London.
Long, I. F.	1957	*Quart. J. R. Met. Soc.*, **83**, p. 202.
MacDowall, J. M.	1955	*Met. Mag.*, London, **84**, p. 65.
Monteith, J. L.	1959a	*J. Sci. Instr.*, **36**, p. 341.
	1959b	*Quart. J. R. Met. Soc.*, **85**, p. 286.
	1961	*Ibid*, **87**, p. 171.
Pasquill, F.	1949	*Proc. Roy. Soc.*, A, **198**, p. 116.
	1950	*Air Ministry, Met. Res. Cttee., M.R.P.* No. 579.
Penman, H. L.	1948	*Proc. Roy. Soc.*, A, **193**, p. 120
Penman, H. L. and Long, I. F.	1960	*Quart. J. R. Met. Soc.*, **86**, p. 16.
Robinson, G. D.	1950	*Ibid.*, **76**, p. 37.
Rider, N. E. and Robinson, G. D.	1951	*Ibid.*, **77**, p. 375.
Suomi, V. E., Franssila, M. and Islitzer, N. F.	1954	*J. Met.*, **11**, p. 276.

551.521.32

An empirical method for estimating long-wave radiation exchanges in the British Isles

By J. L. MONTEITH
Rothamsted Experimental Station, Harpenden

(Manuscript received 12 July 1960; in revised form 23 November 1960)

SUMMARY

From radiation measurements at Kew Observatory (tabulated by Lönnqvist), the effective emissivity of the atmosphere ϵ, defined as the ratio of incoming long-wave radiation to black-body radiation at screen temperature, can be related to optical path m (cm) by

$$\epsilon = 0{\cdot}70 + 0{\cdot}22 \log m$$

with standard deviation $\pm$ 0·018. The relation between m and surface vapour pressure e (mb) found from Belasco's (1952) air mass analysis is

$$\log m = 0{\cdot}29 \sqrt{e} - 0{\cdot}80$$

giving

$$\epsilon = 0{\cdot}53 + 0{\cdot}065 \sqrt{e}$$

almost the same as Brunt's equation from Benson data.

Net long-wave radiation L over short grass can be calculated from

$$L = (1 - c)(\epsilon - 1)\sigma T_A^4 + c\Delta L_1 - \Delta L_2$$

where c is fractional cloudiness; σT_A^4 is black-body radiation at screen temperature; ΔL_1 is a correction for the difference between T_A and cloud-base temperature; and ΔL_2 for the difference between T_A and surface radiative temperature. From Roach's Kew data, $\Delta L_1 = -18$ cal cm^{-2} day^{-1} and ΔL_2 varies with season from -12 cal cm^{-2} day^{-1} (December) to $+20$ cal cm^{-2} day^{-1} (June). Throughout the British Isles, annual mean L with $c = 0$ is close to -200 cal cm^{-2} day^{-1}, and for real values of c,

$$L = 178\,c - 200 \text{ cal cm}^{-2} \text{ day}^{-1}$$

Estimated annual net (total) radiation is 29 k cal cm^{-2} with little variation over the British Isles.

1. INTRODUCTION

Many different formulae have been proposed for the flux of long-wave radiation at the earth's surface. The most theoretical are derived from the emission spectra of radiating gases, and can be used only when vertical distributions of temperature and humidity to a height of about 7 km are known from radiosonde ascents. The most empirical are statistical summaries of the correlation between observed radiation and such surface parameters as air temperature and humidity at screen height. Lönnqvist's (1954) comparison of more than 20 procedures shows that the accuracy of a radiation formula bears little relation to the amount of pure theory underlying its derivation. For example, the empirical formulae of Brunt (1932) and Ångström (1916) fit radiation observations by Robinson at Kew Observatory better than values given by the chart methods of Raethjen, Möller, and Elsasser, and the statement that ' neither expression compares in accuracy with individual estimates made with the aid of a radiation-flux chart ' (Sutton, 1953) requires qualification. It is true that an empirical formula established for one particular station cannot be used elsewhere with the same confidence as a theoretical method based on fundamental principles; but it can provide material for climatological studies of radiation *over the region for which it is valid* with much less effort than any chart method and with comparable accuracy.

The purpose of this note is to re-determine the constants of the Brunt formula by a new method which establishes its validity throughout the year for the whole of the British Isles; and to estimate the seasonal variation in net long-wave loss with clear and cloudy skies.

2. Derivation of emissivity formula

Atmospheric water in any form, natural gases and pollutants contribute to the downward flux of long-wave radiation at the earth's surface. Measurements by Robinson (1950) and others, show that the emissivity of an isothermal layer of water vapour increases with the logarithm of its optical depth m within the normal atmospheric range 0·3 to 3 cm precipitable water. From Robinson's data for clear skies at Kew, the minimum emissivity for water vapour and carbon dioxide together was

$$\epsilon = 0{\cdot}725 + 0{\cdot}17 \log m \quad . \quad . \quad . \quad . \quad . \quad (1)$$

but there was often an additional component of radiation, attributed to atmospheric pollution or to unobserved cloud, which increased emissivity by about 0·02 on average.

To find a similar relationship for real (non-isothermal) air masses, the ratio of incoming long-wave radiation with clear skies, L_d', to black-body radiation at screen temperature, σT_A^4 was correlated with optical path for 38 Kew observations tabulated by Lönnqvist. The effective emissivity was

$$\epsilon = L_d'/\sigma T_A^4 = 0{\cdot}70_4 + 0{\cdot}22_0 \log m \quad . \quad . \quad . \quad (2)$$

with a standard deviation of $\pm$ 0·018. By inference from Robinson's 'isothermal' data, effective emissivity in the absence of 'additional radiation' will be 0·02 less than the value from Eq. (2).

To derive a Brunt-type formula from Eq. (2), optical path and surface vapour pressure were correlated for 30 characteristic air masses which cross the British Isles. Corresponding values of surface vapour pressure at Kew Observatory (e mb) and total atmospheric water content were obtained from Belasco's (1952) analysis and the usual square root pressure correction was used to find the effective optical path. From inspection of Fig. 1, the variation of total water content with surface vapour pressure is greater in winter than in summer; but when the data from both seasons are combined, the line of best fit is

$$\log m = 0{\cdot}29_5 \sqrt{e} - 0{\cdot}80_3 \quad . \quad . \quad . \quad . \quad (3)$$

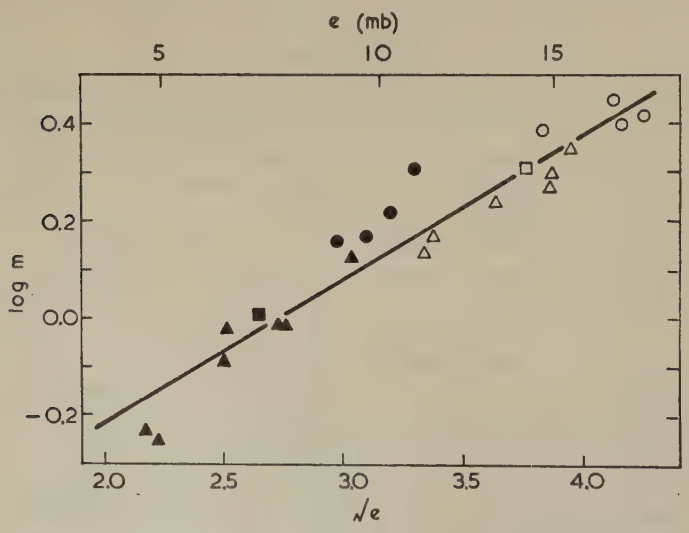

Figure 1. Correlation of log m (m = optical path in cm for characteristic air masses over British Isles) anb $\sqrt{e}$ (e = mean surface vapour pressure at Kew Observatory in mb).

	Jan. and Feb.	July and Aug.
Polar air masses	▲	△
Tropical air masses	●	○
Anticyclonic air masses	■	□

Combination of Eqs. (2) and (3) then gives

$$\epsilon = 0{\cdot}53 + 0{\cdot}065\sqrt{e} \quad . \quad . \quad . \quad . \quad (4)$$

which agrees well with Brunt's original formula derived from radiation measurements by Dines and Dines (1932) at Benson, and vapour pressure at Kew, viz.:

$$\epsilon = 0{\cdot}52 + 0{\cdot}065\sqrt{e} \quad . \quad . \quad . \quad . \quad (5)$$

Fig. 2 compares observed values of ϵ with values calculated from Eq. (4) using Kew screen data tabulated by Lönnqvist. The standard deviation for an individual determination of ϵ was $\pm$ 0·022, or $\pm$ 0·020 when one anomalous observation was rejected. *Random* error in estimating instantaneous radiative flux from surface data is therefore $\pm$ 13 cal cm^{-2} day^{-1} at 0°C and $\pm$ 20 cal cm^{-2} day^{-1} at 30°C (cf. $\pm$ 12 cal cm^{-2} day^{-1} for the Kew chart). The error in weekly or monthly means should be much smaller. Possible sources of *systematic* error when Eq. (4) is used at stations other than Kew are :

(i) a difference in the relationship between surface vapour pressures and optical path, unimportant within the British Isles where monthly mean vapour pressures are normally within $\pm$ 10 per cent of the contemporary value at Kew;

(ii) a difference in the relationship between effective emissivity and optical path. With the arbitrary assumption that local atmospheric pollution was responsible for half the 'additional' radiation observed by Robinson, Eq. (4) will overestimate emissivity at rural stations by about 0·01.

Differences in the constants of Brunt-type formulae derived from observations in other parts of the world can be attributed either to major differences in the distribution of atmospheric water vapour with height or to experimental error. The formula most frequently quoted in text-books.

$$\epsilon = 0{\cdot}44 + 0{\cdot}080\sqrt{e} \quad . \quad . \quad . \quad . \quad (6)$$

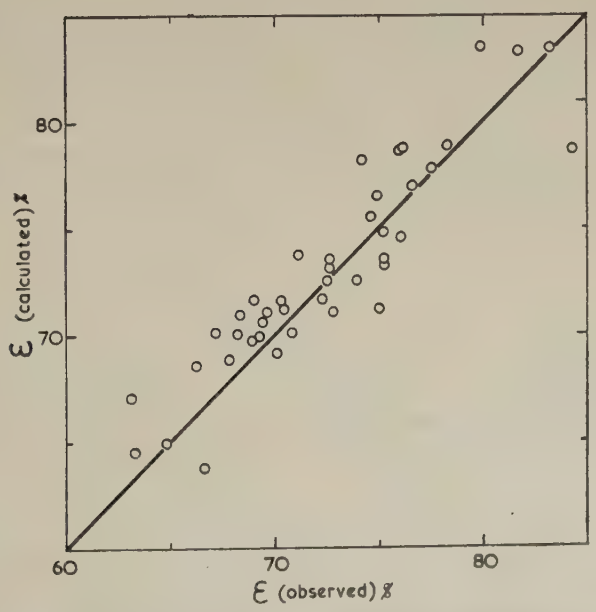

Figure 2. Comparison of observed and calculated effective emissivity with line of unit slope.

ϵ (observed) $= L_d'/\sigma T_A^4$

ϵ (calculated) $= 0{\cdot}53 + 0{\cdot}065\sqrt{e}$

is a world mean for six stations including Benson (Brunt 1939) and is distorted by anomalous data from Robitzsch whose technique was adversely criticised by Raman (1935). It is unlikely to be valid anywhere; and when used in the British Isles will under-estimate incoming radiation by 6 per cent and overestimate net long-wave loss by 16 per cent (comparing Eqs. (4) and (6) at $e = 9$ mb).

3. Radiation from cloudy skies

Making the usual assumption that downward long-wave radiation from cloud is full black-body radiation at cloud-base temperature T_c and ignoring its absorption by water vapour and carbon dioxide between cloud and surface, Roach (1955) calculated the total downward flux at the surface when a fraction c of the sky is covered from

$$L_d = (1 - c)\, L_d' + c\, \sigma T_c^4 \qquad (7)$$

where $\sigma = 1{\cdot}17 \times 10^{-7}$ cal cm^{-2} K^{-4} day^{-1}

and where radiation in the absence of cloud is distinguished by a primed symbol. For climatological work, the usefulness of Eq. (7) is limited by the difficulty of obtaining mean cloud-base temperatures from upper-air data. If cloud-base temperature and screen temperature were equal, the equation could be written in the simpler form

$$L_d = \{\epsilon + c\,(1 - \epsilon)\}\, \sigma T_A^4 \qquad (8)$$

and in Fig. 3 monthly means of L_d calculated from Eq. (8) for the period May 1953 to April 1954 are compared with determinations by Roach. (Roach used available net radiometer records covering 50 per cent of all hours, but when rain fell the radiometer was not exposed, and long-wave radiation was found from a Kew radiation chart and Eq. (7)). The mean difference between calculated and 'observed' values is only + 12 cal cm^{-2} day^{-1}, or less than 2 per cent, with mean cloud cover 68 per cent. This difference corresponds to overestimation of cloud-base temperature by 1·7°C at 10°C surface temperature, equivalent to a difference between black-body radiation at cloud and screen temperatures of $\Delta L_1 = -18$ cal cm^{-2} day^{-1}. Assuming no seasonal change of ΔL_1, Eq. (8) can now be corrected to

$$L_d = \{\epsilon + c\,(1 - \epsilon)\}\, \sigma T_A^4 + c\, \Delta L_1 \qquad (9)$$

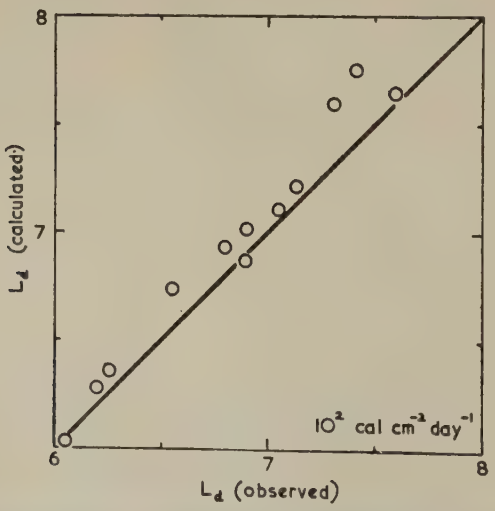

Figure 3. Comparison of observed and calculated incoming long-wave radiation at Kew Observatory for each month from May 1953-April 1954 with line of unit slope.

Bolz's (1949) cloudiness formula

$$L_d/L_d' = 1 + 2{\cdot}2\, c^{2{\cdot}5}$$

gives poor agreement with Roach's data, underestimating L_d by 40 to 110 cal cm^{-2} day^{-1} in individual months with a mean difference for the year of $-$ 80 cal cm^{-2} day^{-1}.

4. Net long-wave radiation

(*a*) *With clear skies*

The mean effective radiative temperature of a short grass surface (T_0), assumed a perfect black body, is given by the mean temperature of a grass minimum thermometer with an accuracy of $\pm$ 0·6°C (Robinson 1950) equivalent to about $\pm$ 6 cal cm^{-2} day^{-1}. Without any temperature records, an *approximate* value for outgoing long-wave radiation is given by $L_u = \sigma T_A^4$ but greater accuracy requires correcting for the difference between mean screen and surface temperatures. Roach gave monthly values for σT_0^4, calculated from the readings of a thermocouple inserted in a grass minimum thermometer, which may be compared with corresponding values of σT_A^4, where T_A is the *mean* of daily maximum and minimum screen temperatures published in the *Monthly Weather Report*. Table 2 (Appendix) shows the seasonal change in $\sigma(T_0^4 - T_A^4)$ with a maximum in June at 20 cal cm^{-2} day^{-1} (about 12 per cent of net long-wave flux on a clear day) and a minimum in December at $-$ 11 cal cm^{-2} day^{-1}. Graphical smoothing gives values of the correction ΔL_2 (fourth column, Table 2) appropriate to average cloudiness, which will be used to find mean monthly values of net long-wave radiation. As an intermediate step, the bold assumption that ΔL_2 will be the same on a cloudless day as on a day of average cloudiness gives

$$L_u' = \sigma T_A^4 + \Delta L_2$$

and hence

$$L' = L_d' - L_u' = (\epsilon - 1)\,\sigma T_A^4 - \Delta L_2 \quad . \quad . \quad (10)$$

Net long-wave radiation on cloudless days was computed from Eq. (10) for the years 1950 to 1959 at Rothamsted using mean screen temperature and screen vapour pressure at 0900 (the diurnal variation of vapour pressure is sufficiently small for this approximation to be adequate.) The data, plotted in Fig. 4, show an annual amplitude of $\pm$ 80 cal cm^{-2} day^{-1} in both outgoing and incoming radiation, but only $\pm$ 12 cal cm^{-2} day^{-1} in net radiation, with minima in January and August. In all months, the maximum year-to-year variation in each of the upward and downward components is about $\pm$ 25 cal cm^{-2} day^{-1}.

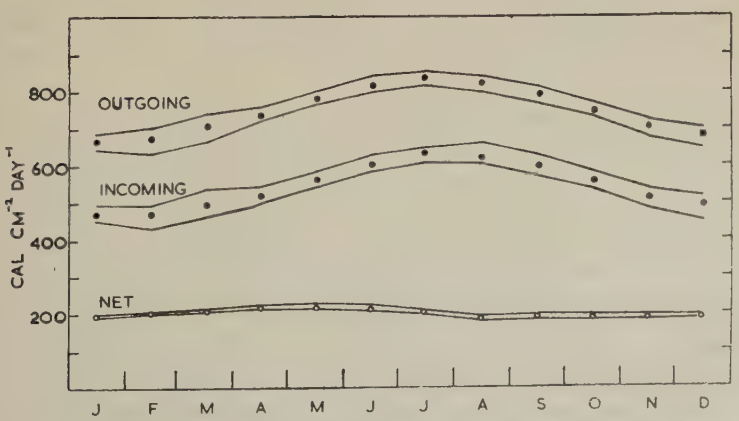

Figure 4. Annual variation of long-wave radiation components at Rothamsted showing maximum, minimum and mean monthly values for 1950/59 (as absolute magnitudes).

The mean variation of *net* flux is only $\pm$ 6 cal cm^{-2} day^{-1} because temperature and vapour pressure anomalies are so correlated that an increase of outgoing radiation with higher temperature is compensated by an almost equal increase of incoming radiation with higher atmospheric water content.

Mean fluxes calculated for Rothamsted are given in Table 3 (Appendix) for comparison with the mean of five years' observations from 1922-1926 by Dines and Dines (1932). Agreement is good except for June and July when Rothamsted figures exceed those for Benson by more than 10 per cent. (Dines and Dines used $\sigma = 1{\cdot}11 \times 10^{-7}$ cal cm^{-2} K^{-4} day^{-1} when calibrating their radiometer, and for consistency with the value used here their fluxes were increased by 5·6 per cent before making this comparison).

Net flux was evaluated for five widely separated stations (Table 4, Appendix), using normals of temperature and humidity published by the Meteorological Office, and assuming the Kew surface temperature correction to be valid everywhere. The maximum difference between stations in monthly net flux is $\pm$ 6 cal cm^{-2} day^{-1} or $\pm$ 3 per cent, and annual totals differ by only $\pm$ 2 cal cm^{-2} day.

(*b*) *With cloudy skies*

Net long-wave radiation with cloudy skies can be written

$$L = (1 - c)(\epsilon - 1)\sigma T_A^4 + c\,\Delta L_1 - \Delta L_2$$
$$= (1 - c)\,L' + c\,(\Delta L_1 - \Delta L_2) \quad . \quad . \quad . \quad (11)$$

where ΔL_2 is now the appropriate correction with average cloudiness.

Eq. (11) is more sensitive to realised differences in cloud amount than in surface parameters, and assuming that Kew values of ΔL_1 and ΔL_2 are valid throughout the British Isles, the geographical variation of L is much greater than the corresponding variation of L' (Table 5, Appendix).

Averaging Eq. (11) over a year and assuming that at all stations

$$\overline{L'} = -200 \text{ cal cm}^{-2} \text{ day}^{-1} \text{ (Table 4)}$$
$$\overline{\Delta L_1} = -18 \text{ cal cm}^{-2} \text{ day}^{-1}$$
$$\overline{\Delta L_2} = 4 \text{ cal cm}^{-2} \text{ day}^{-1} \text{ (Table 2)}$$

it follows that

$$\overline{L} = 178\,c - 200 \quad . \quad . \quad . \quad . \quad . \quad (12)$$

Fig. 5 shows that this simple formula will give the annual value of L as accurately as the much longer calculation from monthly mean temperature and humidity data at each individual station.

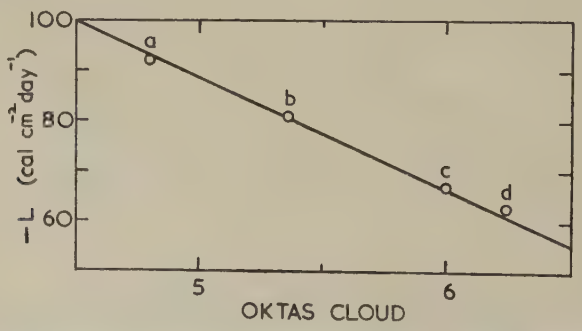

Figure 5. Annual total of net long-wave radiation at five stations plotted against mean annual cloud, using Eq. (11) with monthly mean values of vapour pressure and temperature at each station.

(a) Falmouth (b) Birmingham and London
(c) Lerwick (d) Glasgow

The straight line is Eq. (12) $L = 178\,c - 200$.

The formula for net long-wave loss proposed by Ångstrom (1919)

$$L/L' = 1 - 0{\cdot}9\,c \quad . \quad . \quad . \quad . \quad . \quad (13)$$

is a special case of Eq. (11) with

$$\overline{\Delta L_1} - \overline{\Delta L_2} = 0{\cdot}1\,\bar{L}$$

For

$$\bar{L}' = -200 \text{ cal cm}^{-2} \text{ day}^{-1}$$

$$\overline{\Delta L_1} - \overline{\Delta L_2} = -\ 20 \text{ cal cm}^{-2} \text{ day}^{-1}$$

The value from Roach's data is -22 cal cm^{-2} day^{-1} and although such close agreement is fortuitous, the consistency of two formulae obtained by different methods from observations in Scandinavia and Southern England increases the confidence with which either may be used at other Western European stations.

The transformation of Ångström's formula proposed by Penman (1948)

$$L/L' = 0{\cdot}1 + 0{\cdot}9\,n/N \quad . \quad . \quad . \quad . \quad (14)$$

(where n is hours of sunshine from a Campbell-Stokes recorder and N is maximum possible sunshine) is also in excellent agreement with Roach's Kew data when Eq. (4) is used to find L'.

7. Annual radiation balance

The annual radiation balance of a short grass surface can be computed from Eq. (11) and from observations of solar radiation (published in the *Monthly Weather Report* since 1956) assuming a mean reflection coefficient of 0·25.

TABLE 1. Annual radiation for grass at Kew, Eskdalemuir and Lerwick from mean solar radiation, screen air temperature and cloudiness 1956-1959 (unit : k cal cm^{-2})

		Kew	Eskdalemuir	Lerwick
Short-wave (0·3-2 μ)	Incoming	78	72	67
	Reflected	20	18	17
	Net	58	54	50
Long-wave (3-100 μ)	Incoming	249	239	241
	Outgoing	278	264	263
	Net	− 29	− 25	− 22
Net total radiation		29	29	28

Table 1 shows that changes in net solar radiation with cloud and latitude are of the same size and sign as changes in net long-wave loss with cloud alone, and on balance there is little difference in net total radiation between stations. Direct observations are needed to show whether this result is generally valid, whether it is peculiar to the choice of stations or years, or whether it is a consequence of the assumptions behind Eq. (11). Accepting 29 k cal cm^{-2} as annual net radiation throughout the British Isles, there are important consequences for the complete heat balance of vegetation, assumed to have the same radiative properties as grass. Penman (1950) gave figures for the annual evaporation from catchments (calculated as rainfall minus run-off with an uncertainty of about ± 1 in.). Values ranged from 20 in. in south-east England to 14 in. in the north of Scotland. Combining the equivalent latent heat flux with the data in Table 1 and assuming no net storage of heat in the soil, the annual transfer of sensible heat from surface to atmosphere is $0 \pm 1{\cdot}5$ k cal cm^{-2} in south-east England and $8 \pm 1{\cdot}5$ k cal cm^{-2} in north Scotland.

Acknowledgment

I am grateful to Dr. H. L. Penman for constructive criticism of the original manuscript.

References

Ångström, A.	1916	*Met. Z.*, **36**, p. 529.
	1919	*Ibid.*, **39**, p. 257.
Belasco, J. E.	1952	*Geophys. Mem., Met. Off.*, No. 87.
Bolz, H. M.	1949	*Z. Met.*, **3**, p, 201.
Brunt, D.	1932	*Quart. J. R. Met. Soc.*, **58**, p. 389.
	1939	*Physical and dynamical meteorology*, Cambridge Univ. Press.
Dines, W. H. and Dines, L. H. G.	1932	*Mem. R. Met. Soc.*, **2**, No. 11.
Lönnqvist, O.	1954	*Ark. Geofys.*, **2**, p. 245.
Penman, H. L.	1948	*Proc. Roy. Soc.*, A, **193**, p. 120.
	1950	*Quart. J. R. Met. Soc.*, **76**, p. 372.
Raman, P. K.	1935	*Proc. Indian Acad. Sci.*, **1**, p. 815.
Roach, W. T.	1955	*Air Ministry Met. Res. Cttee. M.R.P.* No. 936.
Robinson, G. D.	1950	*Quart. J. R. Met. Soc.*, **76**, p. 37.
Sutton, O. G.	1953	*Micrometeorology*, McGraw-Hill, London.

Appendix

TABLE 2. Black-body radiation at mean surface and screen temperature (cal cm^{-2} day^{-1}); Kew Observatory May 1953 to April 1954 (from Roach 1955 and *Monthly Weather Report*).

	σT_0^4	σT_A^4	$\sigma (T_0^4 - T_A^4)$	ΔL_2
May	809	789	20	+ 17
June	824	806	18	+ 20
July	834	821	13	+ 16
August	843	835	8	+ 7
September	799	802	− 3	0
October	758	762	− 4	− 4
November	737	740	− 3	− 8
December	719	730	− 11	− 12
January	673	683	− 10	− 8
February	681	681	0	− 1
March	721	716	5	+ 5
April	739	730	9	+ 10
Year				+ 4

When $T_0 - T_A = 1°C$, $\Delta L_2 \simeq +10$ cal cm^{-2} day^{-1}

TABLE 3. Long-wave radiation components with clear sky measured at Benson from 1922-1926 (Dines and Dines 1932) and computed from Eq. (10) using Rothamsted temperature and humidity data for 1950-59 with standard deviation from 10-yr mean

(Unit : cal cm^{-2} day^{-1})

	Incoming		Outgoing		Net	
	Benson	Rothamsted	Benson	Rothamsted	Benson	Rothamsted
January	480	471 ± 11	662	667 ± 13	− 182	− 196 ± 2
February	497	472 ± 18	701	676 ± 20	− 204	− 204 ± 2
March	496	496 ± 24	715	705 ± 22	− 219	− 209 ± 4
April	543	520 ± 15	763	737 ± 12	− 220	− 217 ± 5
May	596	562 ± 13	803	781 ± 9	− 207	− 219 ± 4
June	627	604 ± 13	815	817 ± 12	− 188	− 213 ± 3
July	661	633 ± 12	845	835 ± 11	− 184	− 202 ± 3
August	622	633 ± 16	803	821 ± 15	− 181	− 188 ± 4
September	599	601 ± 18	793	789 ± 14	− 194	− 187 ± 5
October	553	557 ± 16	753	747 ± 12	− 200	− 190 ± 4
November	495	511 ± 14	682	702 ± 12	− 187	− 191 ± 3
December	487	491 ± 19	678	681 ± 17	− 191	− 190 ± 3

TABLE 4. NET LONG-WAVE RADIATION WITH CLEAR SKIES (L') AND WITH AVERAGE CLOUDINESS (L) AT FIVE STATIONS IN BRITISH ISLES

(Unit : cal cm^{-2} day^{-1})

	Lerwick		Glasgow		Birmingham		London*		Falmouth	
	L'	L	L'	L	L'	L	L'	L	L'	L
January	194	53	191	41	196	62	196	58	195	71
February	202	57	204	51	204	73	204	69	205	81
March	207	66	212	70	214	88	209	83	208	84
April	213	78	217	77	217	96	217	94	212	117
May	217	86	222	89	222	101	219	106	211	119
June	215	82	213	85	211	99	213	101	204	113
July	206	73	205	73	203	86	202	91	197	108
August	191	63	195	59	193	85	188	81	187	101
September	191	82	191	84	187	86	187	89	181	91
October	195	59	197	52	191	74	190	76	190	83
November	191	56	193	43	191	64	191	64	190	74
December	189	53	190	37	190	55	190	54	186	64
Year	200	67	201	63	201	81	200	81	197	92

* Vapour pressure and temperature data from Rothamsted; cloudiness data for London Airport.

551.551.25 : 551.551.5 : 551.551.8

An analysis of vertical wind-fluctuations at heights between 500 and 5,000 ft

By F. B. SMITH
Meteorological Office and C.D.E.E., Porton Down, Wilts.

(Manuscript received 10 May 1960; in revised form 11 Oct. 1960)

SUMMARY

A series of records, totalling over 120 hr showing the vertical fluctuations of high-response wind-vanes positioned on a captive balloon cable, are analysed to give statistical information on turbulence at heights between 500 and 5,000 ft, for an eddy frequency range 0·003-12 cycles min^{-1}. The use of specially designed filter and smoothing circuits facilitates the determination of the angular standard deviation of the inclination of the vane, as a function of run of wind, and of spectra, length-scales and other parameters of turbulence. 18 spectra are given which show well-defined peaks. Except in very stable conditions, the high wave-number forms of the spectra are generally consistent with the existence of an inertial sub-range. Estimates of the length-scale, again excluding very stable conditions, do not apparently vary with height and average about 300 m. Intensity is found to depend on stability and to decrease in a very marked way with increasing wind speed, a result peculiar to these heights. This variation, applicable to specified meteorological conditions, is shown to have value in the determination of the spread of both continuous-source plumes and clusters of particles according to recent treatments.

1. INTRODUCTION

Statistical predictions of the diffusion of particles within the atmosphere require an adequate amount of data on the characteristics of turbulence for various atmospheric conditions and heights above ground. Much has been done in this respect on turbulence near the ground (for example, see Panofsky and Deland (1959)), but rather less at heights of the order of 1,000 ft. To remedy this, records of vertical gustiness have been obtained using high-response wind-vanes attached to the cable of a captive balloon at the Balloon Development Establishment (B.D.E.) Cardington (Jones and Butler 1958). An analysis of early records has been carried out by R. A. Jones (1957, 1958), who describes and uses Tukey's method (1950) to obtain power spectra in the frequency range 0·3-10 cycles min^{-1}.

More recently, filter circuits have been designed (Jones and Pasquill 1959) to facilitate the collection and analysis of large quantities of data on the properties of atmospheric turbulence. This paper describes a detailed analysis of 17 periods of observation and a simpler analysis of sixty others, a total of over 120 hr. The detailed results are presented as curves of standard deviation of the angular fluctuations of the vane plotted against run of wind. From these are deduced energy spectra, and corresponding length and time scales. The data provide a means of estimating diffusion in the atmosphere in terms of wind speed and stability.

2. DATA

Three wind-vanes were mounted on a balloon cable at heights varying from 500 ft to 5,000 ft. The electrical output, proportional to the angular deviation of the vane from the horizontal, was brought to ground by lightweight cables, and fed into the filter circuits mentioned above. The outputs from the top and bottom vanes were each reduced to a low-pass trace (a low-frequency output equivalent to a running average over 30 sec intervals) and a complementary high-pass trace (a high-frequency output rectified and smoothed, and equivalent to the standard deviation of the full trace within running samples of 30 sec duration). The output from the middle vane went through the same process, except that in addition, two further high-pass traces were obtained, equivalent to sampling durations of 5 sec and 3 min. The wind speed was given by small pulses recorded on the low-pass trace at fixed intervals of run of wind.

17 sets of records obtained from the middle vane, when its height was either 500, 1,000 or 2,000 ft, were analysed in detail. The majority of these periods came from two months, May and June 1959, and the results may be partially biased on this account. To clarify this, 60 periods were analysed in less detail, and as far as could be deduced, no marked differences existed between the two groups. This simpler analysis consisted of reading off the extreme range of the low-pass trace, excluding for reasons of statistical accuracy the greatest single positive peak and the greatest single negative trough. In each case, the intensity, i, defined as the r.m.s. angular fluctuation of the vane, was estimated by dividing this range by an empirical constant equal to 4·6. This value was determined by comparing the range and the true intensity in the 17 cases of detailed analysis.

Another and more definite form of bias exists as a result of the conditions under which the traces were recorded, for no traces were recorded

(i) when the wind speed fell below 1·5 m sec^{-1}, because of poor vane response;

(ii) when the wind speed rose above 10 m sec^{-1}, because induced oscillations of the balloon cable would then be seriously recorded by the vanes;

(iii) when there existed a risk of lightning;

(iv) when precipitation was heavy;

(v) when the atmosphere was very stable with immeasurable turbulence.

The possible implications of this bias will be discussed in § 6. During operations the vane was out of cloud in all periods except in 4 of the 60 cases of limited analysis. The presence of cloud is believed not to affect the validity of the traces provided heavy precipitation is absent.

3. Variations in the level of turbulence

A field of turbulence is said to be stationary if the values of each of its statistics has equal expectation at all times. Whilst such a state does not preclude a significant degree of variation in the instantaneous values, it is necessary that such deviations from the mean should be random and unbiased. An extreme form of this kind of variation was noted by Townsend (1950) for a turbulent wake surrounded by undisturbed fluid. The flow at certain positions alternated irregularly between typically turbulent flow and laminar flow. This phenomenon was termed 'intermittency.' Since all fields of turbulence, stationary or otherwise, are characterized by random variations in velocity, the term 'intermittency' may be used more generally to describe the moment-to-moment random variations in the energy level associated with any band of wave-numbers in the spectrum of turbulence. It follows that the average properties of the turbulence can be found only from a sample long enough to eliminate the effects of intermittency.

Additional variations in the turbulence occur when the conditions for a stationary state no longer hold. These variations result from changes in the external phenomena generating the turbulence, and may be of varying magnitude and rapidity; they affect the whole spectrum and generally the energy density changes in the same sense at all wave-numbers. The turbulence is then said to be non-stationary. Over any short period, however, there is no objective method of distinguishing between the two types of variation, and this leads to difficulties which are not yet fully resolved.

It appears unlikely that any of the practical results are adversely affected by these difficulties to any significant degree, but the precise details of the analysis partially depend on the two types of variation. One such detail concerns the type of averaging employed in forming the mean values of the angular standard deviation $\Theta(\tau)$ for samples of duration τ over the whole period of record; another concerns the interpretation of small fluctuations in the curve of $\Theta(\tau)$ at large τ. These will be discussed briefly in turn.

One of the primary applications of the results of this kind of analysis is in the field of particle diffusion. As discussed in § 7, the average spread of a plume of particles, at a distance x downwind of a continuous source, sampled for a time τ in a wind U, is linearly proportional to a standard deviation of wind fluctuations which have been averaged (i.e., smoothed) over times $x/4U$ and sampled over the time τ. Such values had to be found from the recorded outputs of the filter circuits. But in practice, the outputs of the high-pass filter circuits were rectified and smoothed to give traces which were in the form of mean deviations rather than standard deviations. *A priori*, when varying degrees of intermittency and non-stationary trends are admitted, it is difficult to assess the validity of any constant relationship such as the $\sqrt{(\pi/2)}$ ratio associated with a Gaussian distribution. Jones and Pasquill (1959), in their paper describing the system for recording the traces, gave the results of actual comparisons between the two deviations which indicate that the form factors (the ratio of linear-average standard deviation to average mean deviation) fluctuate considerably for *individual* samples of duration τ but are much less variable for longer samples of duration 10 τ. The results shown in their Table 4, in which averaging times of 5 sec and sampling durations τ of 3 min were used, give form factors, derived from 30-min means, between 1·21 and 1·26. An average value of 1·25 was recommended. A further check on the adequacy of this empirical relation between the two deviations has come from comparing the values of standard deviation for $\tau = 3$ min derived by two methods. One value was determined directly from the 180 sec high-pass trace, the other from the combined use of the low-pass trace and the 30 sec high-pass trace by the method described in the next section. Linear averaging as opposed to r.m.s. averaging was used, or implied, throughout. Generally, the two values were very similar, the difference never exceeding 5 per cent.

A consequence of the non-stationary character of the turbulence is that, for the larger sampling periods at least, the estimates of the standard deviation depend on the positioning of the sub-sections, within the whole, relative to any significant changes in the level of turbulence. For example, a rapid change in the turbulence may occur *within* a sub-section and hence give a large value of standard deviation; alternatively it may occur across the boundary between two consecutive sub-sections and hence give much smaller standard deviations. As a result of this, average values of standard deviations for two sampling periods τ_1 and τ_2 ($\tau_2 > \tau_1$) may, in extreme cases, and when τ_1 and τ_2 are not greatly different, be such that the one for τ_2 is less than that for τ_1. Non-stationary turbulence therefore introduces anomalies of fluctuating magnitude in the values of standard deviation. To minimize these, when significant changes in the level of turbulence were indicated, as many points as could reasonably be obtained were plotted as a function of sampling time and a smooth curve drawn by eye through the scatter of points (see, for example, as an extreme case, the curve for 7 May 1959, Fig. 3). These changes in level were of limited duration because only periods displaying an overall uniformity were selected for analysis.

4. The Standard deviation $\Theta(\tau)$, as a function of sampling duration

The values of the standard deviation $\Theta(\tau)$ for sampling times of 5, 30 and 180 sec were obtained by visually averaging the high-pass traces to the nearest half-degree over consecutive periods of one minute and then calculating their average value over the total period under consideration. Values of standard deviation at other sampling times (> 30 sec) were determined by the additional use of the low-pass trace. Instantaneous values were read off the low-pass trace at intervals of $\frac{1}{8}$ min, this being the smallest practical interval. Standard deviations were then evaluated over consecutive periods τ, and linearly averaged over the whole period of the trace to give the overall value Θ_τ'. The full value of the standard deviation Θ_τ, for sampling duration τ, was then calculated by including the contribution of energy Θ_{30}^2 lost by the filtering process $\Theta_\tau^2 = (\Theta_\tau')^2 + \Theta_{30}^2$

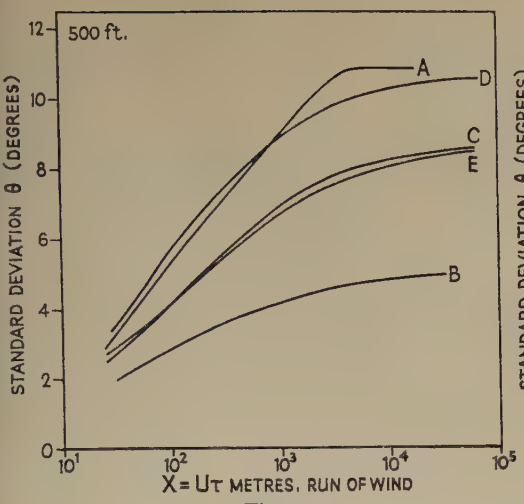

Figure 1.

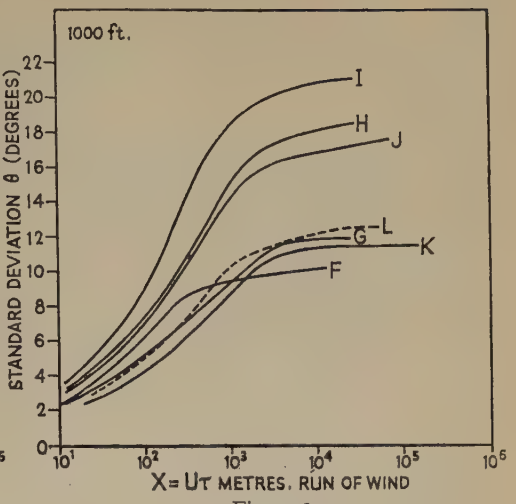

Figure 2.

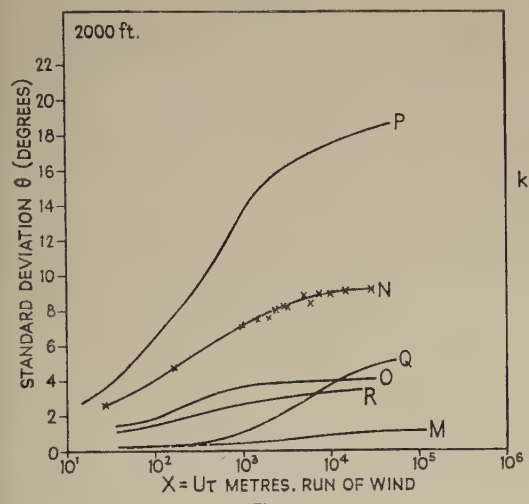

Figure 3.

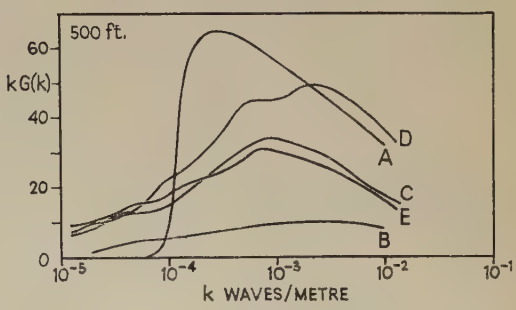

Figure 4.

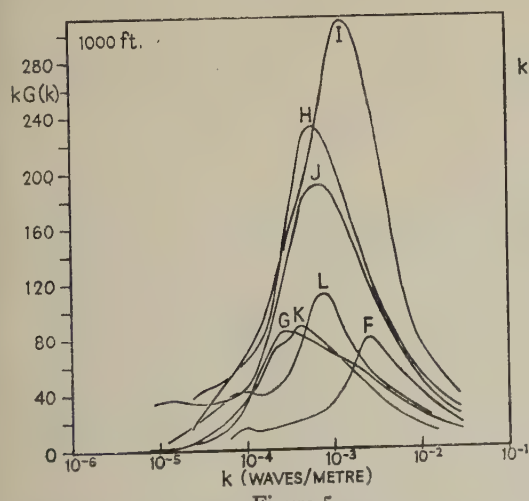

Figure 5.

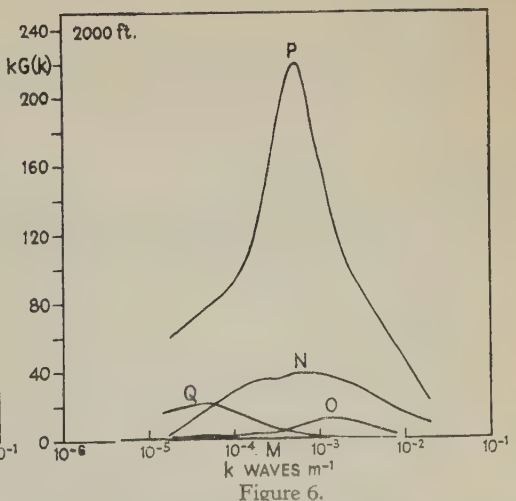

Figure 6.

Figures 1, 2, 3: Curves of r.m.s. fluctuations as a function of run-of-wind at 500 ft, 1,000 ft and 2,000 ft respectively. Figures 4, 5, 6: Corresponding spectra to Figs. 1, 2, 3. (Reference letters correspond to column 1, Table 1).

TABLE 1. TABLE OF F

1 Height and period Letter (ft)	2 Date 1959	3 Period (GMT)	4 No. of mins	5 U (m sec^{-1})	6 Θ_∞°	7 Θ_l°	8 l_Θ (m)	9 waves m^{-1} k max	10 l_s (m)	11 t_E (sec)
500 A	6 May	1340-1440	60	5·0	10·9	6·6	220	2·8 × 10^{-4}	830*	166
500 B	26 May	1020-1150	90	6·1	5·0	3·1	102	2·5 × 10^{-3}	94	15·4
500 C	27 May	0901-1050	109	6·6	8·9	5·4	270	7 × 10^{-4}	330	50
500 D	27 May	1119-1308	109	6·5	10·7	6·6	164	2·15 × 10^{-3}	110	16·7
500 E	5 June	0908-1059	111	5·5	8·9	5·4	290	9 × 10^{-4}	260	47
1,000 F	28 May	1430-1630	120	1·76	10·4	6·3	100	2·6 × 10^{-3}	90	51
1,000 G	29 May	0931-1120	109	3·1	12·0	7·3	330	2·7 × 10^{-4}	860*	277
1,000 H	29 May	1120-1312	112	3·2	19·0	11·5	370	5·8 × 10^{-4}	400	125
1,000 I	29 May	1312-1502	110	2·7	21·3	12·9	240	1·25 × 10^{-3}	190	70
1,000 J	29 May	0931-1502	331	3·0	18·5	11·2	390	7 × 10^{-4}	330	110
1,000 K	2 June	0945-1606	381	6·2	11·5	7·0	425	4·2 × 10^{-4}	555	90
1,000 L	3 June	1000-1300	180	4·9	12·6	7·6	350	7·8 × 10^{-4}	300	61
2,000 M	28 Jan.	1047-1405	198	9·5	1·1	0·67	4,500	3·9 × 10^{-5}	6,000	630
2,000 N	7 May	0929-1101	92	5·5	9·25	5·6	310	6 × 10^{-4}	390	71
2,000 O	26 May	1525-1638	73	7·6	4·25	2·5	230	1·4 × 10^{-3}	170	22
2,000 P	24 Sept.	1200-1400	120	3·2	21·0	12·8	800	5·5 × 10^{-4}	425	133
2,000 Q	1 Oct.	1030-1200	90	7·5	5·5	3·3	7,000	4·8 × 10^{-5}	4,900	654
2,000 R	1 Oct.	1300-1348	48	7·7	3·5	2·0	300	–	–	–

* both spectra were rather flat-topped, suggesting the presence of 2 peaks fairly close together. l_s probably overestimated.
† insufficient part of range obtained.

KEY

COLUMN

5 Average wind speed in m sec^{-1}
6 Standard deviation in degrees – asymptotic value for large run of wind
7 On the assumption of exponential correlogram, $\Theta_l = 0{\cdot}6065\ \Theta_\infty$
8 Length scale determined on this basis (m)
9 Frequency at peak of $kG(k)$ spectrum (waves m^{-1})
10 On the assumption of exponential correlogram, $l_s = 0{\cdot}2336/k$ max (m); $l_s = l_\theta$ only when correlogram exponential
11 Time scale $t_E = l_s/U$ (sec)
12 Intensity of turbulence $i = \pi\ \Theta_\infty/180$ (radians)
13 If locally $G(k) \propto k^{-p}$ then $p \simeq 1 + \log\left[\frac{\Theta_{30}^2}{\Theta_5^2} - 1\right] \Big/ \log 6$ in the range 5/6-5-30 sec. In the inertial sub-range $p = 5/3$
14 As for 13. Here, $p = 1 + \log\left[\frac{\Theta_{180}^2 - \Theta_{30}^2}{\Theta_{30}^2 - \Theta_5^2}\right] \Big/ \log 6$ in the range 5-30-180 sec
15 p determined from graph of $kG(k)$ against k on log-log paper for the high wave-number part of the spectrum
16 The r.m.s. vertical velocity w determined approximately by $w = iU$

Y-ANALYSED TRACES

14	15	16	17	18	19	20	21	22	23	24
180-30-5	p graph	w (m sec^{-1})	Range / Θ_∞	Cloud	Stability‡	Symmetry§	X_p (km)	X_{m_1} (km)	X_{m_3} (km)	Remarks
1·23	†	0·950	4·31	1	SU	A	0·94	2·40	2·77	Slightly suspect–variability in sensitivity from 2 per cent to − 10 per cent.
1·01	†	0·531	4·00	5–6	NS	S	2·77	7·95	13·20	Slight interference from wind pulses on L.F. trace
1·20	†	1·023	4·68	5	U	A	1·27	3·49	4·17	–
1·06	†	1·215	4·62	5	U	A	1·06	2·84	2·86	–
1·27	†	0·852	5·94	–	SU	A	1·31	3·41	4·17	–
1·50	$\frac{3}{4}\rightarrow\frac{4}{5}\rightarrow 2$	0·320	5·32	5	SU	S	1·80	5·52	3·02	Low wind speed. Slight non-stationary trend
1·47	–	0·651	5·42	8	U	A	0·80	2·00	2·27	As convective activity increased from period to period, i increased but l decreased
1·62	–	1·062	4·02	8	U	A	0·49	1·17	0·91	
1·58	–	1·004	3·90	8	U	A	0·43	1·09	0·72	
1·65	$\frac{4}{5}$	0·969	4·66	8	U	A	0·54	1·33	0·96	–
1·54	$\frac{4}{5}$	1·240	5·04	1	U	A	0·80	1·93	2·50	–
1·57	$\frac{4}{5}\rightarrow\frac{4}{5}\rightarrow\frac{4}{5}$	1·078	5·08	1	U	S	0·75	1·75	2·07	–
1·51	–	0·180	4·55	–	S	S	9·13	23·65	277·0	Very little (if any) dynamic turbulence
1·36	$\frac{4}{5}$	0·891	4·26	–	NS	S	1·08	2·75	3·82	–
1·28	–	0·562	4·00	5	NS	S	4·60	14·25	18·25	Θ_∞ only approximate
1·59	$\frac{4}{5}\rightarrow 2$	1·174	4·24	–	U	A	0·50	1·14	0·75	Slight non-stationary trend, Θ_∞ only approximate.
2·94	$\frac{4}{5}\rightarrow 3$	0·720	4·13	–	NS	S	1·54	3·71	10·85	Very little dynamic turbulence, Θ_∞ only approximate
–	–	0·470	4·44	8	NS	S	–	–	26·90	Part of a 3-hr period. Non-stationary. No spectrum attempted

‡ S – stable; SS – slightly stable; NS – neutrally stable; SU – slightly unstable; U – unstable.

§ A – asymmetric; S – symmetric

KEY

COLUMN

17 If from the low-pass trace for the period analysed, the two extreme peak values are rejected, a range is obtained from the next highest peaks. On average Range/$\Theta_\infty = 4{\cdot}60 \pm 0{\cdot}54$ (s.d)

18 Classification of low cloud : 1 small cumulus, 2 large cumulus, 5 stratocumulus, 6 stratus, 8 cumulus with stratocumulus, – no cloud

19 Stability, estimated from lapse rate from ground to appropriate height. Cardington vertical temperature gradients used whenever available

20 Symmetry. A classification of type of low-pass trace. Symmetric (S) trace looks similar whichever way up it is held. Asymmetric (A) trace suggests convection

21 The distance (km) at which particles first begin to reach the ground from continuous source at 300 m above ground (cone = 1/10 max. w.r.t. ht.)

22 The distance (km) at which the crosswind-integrated ground concentration is a maximum from a continuous source at 300 m above ground ($\sigma = 300$ m)

23 The distance (km) at which the ground concentration is a maximum from puff released at 300 m neglecting any vertical motion of centre of puff. $X_{m_3} = 300/3i^2$. Note $X_{m_3} < X_{m_1}$ for $X < 1$; $X_{m_3} \simeq X_{m_1}$ for $2 < X < 5$, $X_{m_3} > X_{m_1}$ for $X > 5$; the latter being anomalous (see text).

24 Remarks, containing comments on quality of traces and any noteworthy behaviour.

These values of Θ_τ have been plotted against run of wind ($x = U\tau$ metres) in Fig. 1 (500 ft records), Fig. 2 (1,000 ft records) and Fig. 3 (2,000 ft records). Distance, rather than time, was used because, in most problems of diffusion, interest is centred on conditions at *distances* from the source. These curves, which are the simplest and most elementary representation of the data, provide a basis for determining spectra, correlograms and properties of diffusion.

In most cases the length of the trace analysed proved sufficiently long for the standard deviation either to have reached its maximum asymptotic value or for this value to be confidently estimated within the bounds of accuracy required. The magnitude of this value, Θ_∞ (in degrees), is tabulated in column 6, Table 1. Given this value it is possible to estimate the length-scale l of the longitudinal correlogram by assuming that the correlogram is approximately exponential in form : $f(r) = e^{-r/l}$ (r denotes separation).

Then, any value of Θ_x is given by

$$\Theta_x^2 = \Theta_\infty^2 \left[1 - \frac{l}{x}(1 - e^{-x/l})\right]$$

so that when $x = l$

$$\Theta_l = e^{-\frac{1}{2}}\, \Theta_\infty$$

Values of $l = l_\theta$ calculated by this method are tabulated in column 8, Table 1. Apart from two stable situations on 28 January and 1 October when l is very large, the length-scale does not vary very significantly with height and is of the order of one or two hundreds of metres in magnitude.

5. The spectra

The autocorrelogram provided by fluctuations of wind inclination is of *lateral* type, and leads to the one-dimensional lateral spectrum $G(k)$,where k is in waves m^{-1}. These two functions are Fourier transforms of each other, and from this fact it follows that the total energy is

$$\Theta_\infty^2 = \int_0^\infty G(k)\, dk = \int_{-\infty}^\infty k\, G(k)\, d(\log_e k)$$

The variance for finite sampling times (i.e., for finite $x = U\tau$) is given by multiplying the spectrum by a weighting factor W

$$W(xk) = \left(1 - \frac{\sin^2 \pi kx}{(\pi kx)^2}\right)$$

which represents the reduction of contributions from the low frequencies (Ogura 1957), so that

$$\Theta_x^2 = \int_{-\infty}^\infty k\, G(k) \left(1 - \frac{\sin^2 \pi kx}{(\pi kx)^2}\right) d(\log_e k)$$

The factor is zero at $k = 0$, one for large k and $\frac{1}{2}$ when $kx = 0{\cdot}445$. The difference of two such Θ_x^2 for runs of wind x_1 and x_2 is therefore an estimate of the energy contained between wave numbers $0{\cdot}445\, x_1^{-1}$ and $0{\cdot}445\, x_2^{-1}$. This estimate will be at its best when the function $k\, G(k)$ is fairly flat. When this estimate is divided by the width of the wave-number band, $\log x_1/x_2$, and plotted at the mid-point $k = 0{\cdot}445\, (x_1\, x_2)^{-\frac{1}{2}}$ it yields, in conjunction with other such points, a spectrum which, on account of the process used, is in general a smoothed version of the true spectrum. Nevertheless, it should still retain the following features :

(i) the position of any peaks will be unchanged;

(ii) if the true spectrum conforms to a certain power of the wave-number over a fairly wide band of wave-numbers then the approximate spectrum will follow the same power.

The results of the analysis are shown in Fig. 4 (500 ft), Fig. 5 (1,000 ft) and Fig. 6 (2,000 ft). In all cases the major peak is clearly shown and a considerable part of the curve on both sides included, the extreme range of wave-numbers being from 1 wave every 33 m ($k = 0{\cdot}03\ \mathrm{m}^{-1}$) to 1 wave every 200 km ($k = 5 \times 10^{-6}\ \mathrm{m}^{-1}$).

Non-stationary trends in the level of turbulence manifest themselves on these curves most clearly as plateaux at the low wave-number end. Several curves show two peaks, the one at the higher wave-number usually being dominant. Inspection of the wave-numbers at these peaks suggests that the higher wave-number peak is due to dynamically generated, or thermally generated, turbulence, whilst the other reflects some disturbance on the macroscopic scale.

The forms of the curves at the high wave-number end of the spectra have been investigated to see whether they conform to the $-5/3$ power ($G(k) \propto k^{-5/3}$) predicted by dimensional arguments, valid for the inertial sub-range of turbulence. One way is to use actually determined values of $\Theta(\tau)$. If W is the weighting function defined above:

$$\Theta^2(a\,\tau_1) - \Theta^2(a\,\tau_2)) = \int_0^\infty k\,G(k)\,[W(a\,\tau_1\,Uk) - W(a\,\tau_2\,Uk)]\,d(\log k)$$

$$= \int_0^\infty \frac{k}{a}\,G\left(\frac{k}{a}\right)\,[W(\tau_1\,Uk) - W\ (\tau_2\,Uk)]\ \ d(\log k)$$

where a is some constant. In the wave-number band for which the difference in the two values of W is significantly non-zero, suppose that $G(k) \propto k^{-p}$. The constant a can then be taken outside the integral to give the identity

$$a^{p-1} = \frac{\Theta^2(a\tau_1) - \Theta^2(a\tau_2)}{\Theta^2(\tau_1) - \Theta^2(\tau_2)}$$

Choosing $\tau_1 = a\tau_2$, the value of p is determined from three values of $\Theta(\tau)$. Taking $\tau_1 = 5$ sec, $a = 6$ and neglecting the values of Θ^2 for $\tau = 5/6$ sec:

$$p = 1 + \left\{\log\left[\frac{\Theta_{30}{}^2}{\Theta_5{}^2} - 1\right] \Big/ \log 6\right\}$$

in the range of wave-number corresponding to $5/6 - 5 - 30$ sec. These values of p are given in column 13, Table 1. Also values of Θ appropriate to 180, 30 and 5 sec can be used to give p in a lower waveband as

$$p = 1 + \left\{\log\left[\frac{\Theta_{180}{}^2 - \Theta_{30}{}^2}{\Theta_{30}{}^2 - \Theta_5{}^2}\right] \Big/ \log 6\right\}$$

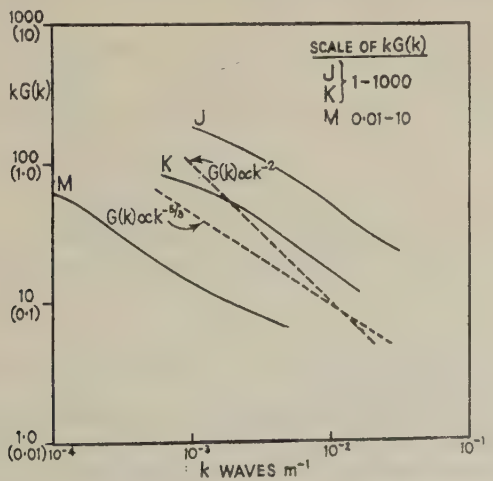

Figure 7. Power form of the high-frequency end of three spectra.

These values are tabulated in column 14. Generally the former values of p are nearer 5/3 than the latter, indicating that the peak of the spectrum may often be too close for an inertial sub-range to exist in the lower band of wave-numbers.

Values of p may also be obtained from the spectra by plotting $\log_{10}(kG(k))$ against $\log_{10} k$ (e.g., as in Fig. 7), and measuring the gradient of the best-fitting straight line to the curve at the high wave-number end. These values, where they could be obtained satisfactorily, are given in column 15. The following generalizations are indicated :

(i) the value of p is nearer to 5/3 the larger the length-scale, provided the intensity of turbulence is not too low. The results indicate that the inertial sub-range may exist at wave-numbers greater than about twice that of the peak of the $kG(k)$ curve,

(ii) the value of p is nearer to 5/3 the greater the intensity i ($i = \Theta_\infty$ expressed in radians).

As Gifford (1959) pointed out, where a value of p near 5/3 is found, it is implied that the form of the spectrum is consistent with an inertial sub-range without logically proving its existence.

Another estimate of the length-scale $l = l_s$ may be obtained from the wave-number at which $kG(k)$ is a maximum. Again this depends on assuming that the appropriate longitudinal correlogram is exponential in form. The corresponding spectrum is

$$kG(k) = \overline{\Theta_\infty^2}\,\frac{r(1+3r^2)}{4\pi(1+r^2)^2}$$

where $r = 2\pi kl$.

The maximum occurs at $kl = 0{\cdot}2336$. Such estimates, given in column 10, Table 1, differ somewhat from the estimates in column 8, implying that the present correlograms are not exactly exponential. Probably the spectral estimates of l are preferable because they do not depend very critically upon the energy at low wave-numbers and therefore upon non-stationary trends in the level of turbulence. Taking into account the limited amount of data and the range of conditions to which they refer, there is no striking variation of length-scale with height and in fully turbulent conditions it is of the order of 300 m (corresponding to a maximum in the $kG(k)$ spectrum at a wavelength of about 1,200 m). This is broadly consistent with the conclusions of Panofsky and McCormick (1960) regarding the spectra at heights greater than 250 m.

In theory, no more information is lost by the present method of analysis, based on the variation of standard deviation with sampling duration, than by the more conventional approach of determining lag-covariances : there is, however, a considerable saving in labour. The theoretical equivalence of the two methods is indicated below by the inter-relationship equivalent to that given by Charnock and Robinson (1957, Eq. (9)). The effect of finite-time sampling on the variance is (see, for example, Ogura (1959))

$$\overline{\Theta_\tau^2} = \overline{\Theta_\infty^2}\left[1 - \frac{2}{\tau^2}\int_0^\tau (\tau - \zeta)\,R(\zeta)\,d\zeta\right]$$

Solving for $R(s)$ where $s = \log\zeta$ and putting $Z = 1 - \overline{\Theta_\tau^2}/\overline{\Theta_\infty^2}$, the required inter-relationship is :

$$R(s) = Z + \tfrac{3}{2}\frac{d}{ds}Z + \tfrac{1}{2}\frac{d^2}{ds^2}Z$$

The correlogram could therefore be derived from the $\Theta - U\tau$ curve but in practice this is inevitably inaccurate as it involves the determination of both first and second derivatives of the curve.

6. Estimates of the total intensity of turbulence

The full standard deviations Θ_∞, converted to radians, give the intensities i, presented in column 12. A six-fold variation from 0·061 to 0·372 is manifested as a marked fall-off of intensity with increasing wind speed. Since nearer the ground no such general trend has been indicated, it was necessary to consider whether this variation is genuine or a result

of limited data. 60 other periods, taken at heights varying from 200 ft to 5,000 ft, were therefore analysed in less detail, the intensity being estimated from the width of the low-frequency trace (see § 2). These extra results confirmed the trend and also indicated that it became more clear-cut at the greater heights. All 78 points are marked on Fig. 8 where the thick sloping line represents the mean variation and the dotted lines represent the boundaries of the points. To relate this variation with stability a rather subjective division of these points has been made according to whether the low-frequency trace was symmetric (in the sense that to invert the trace did not produce a radically different appearance, suggesting non-convective conditions), or asymmetric (suggesting convection). This division is indicated on the figure; the asymmetric cases are associated with high intensity and are concentrated at lower wind speeds than most of the symmetric cases. This variation with stability is rather more objectively confirmed by associating with each point the stability deduced from observations of temperature gradient in the vertical, made as near as possible to the time of record. This stability is not a ' local ' stability measured at the height of the vane but is dependent on the overall lapse rate from the ground up to the vane. Estimated in this way, no entirely satisfactory method was available of introducing the effect of wind shear, as in a Richardson number. Indeed, in conditions markedly different from neutral, there is little theoretical reason for so doing, and Fig. 8 indicates that the use of lapse rate alone provides a useful division within the band of points. Each point was classified either as unstable, slightly unstable, neutral, slightly stable or stable. Although there is some overlapping of these stability bands, Fig. 8 shows that, superimposed upon the variation of intensity with wind speed, the intensity increases with instability, whilst within any stability range the variation with wind speed is much reduced.

As noted in § 2, the data are restricted to situations without appreciable precipitation. This may be a source of bias in so far as deep convection, associated with cold-front instability and with high values of both wind speed and intensity, may be excluded. Furthermore, it is probable that other cases with lower values of intensity, below the limit of accuracy of the present measurements, were omitted at all wind speeds. It is doubtful, however, whether such values would represent turbulence in any diffusive sense. Inspection of the behaviour of turbulence at any fixed level on occasions when the stability is

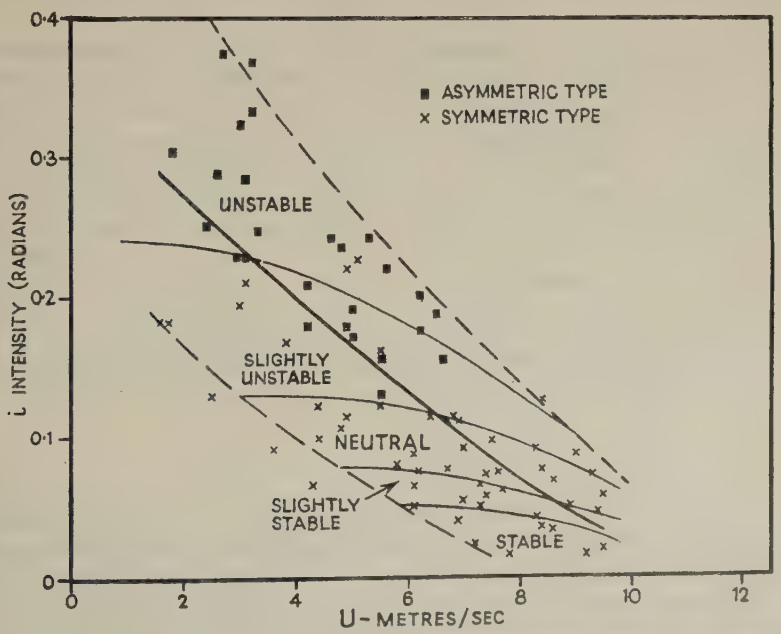

Figure 8. Distribution of points (78 periods), intensity against wind speed.

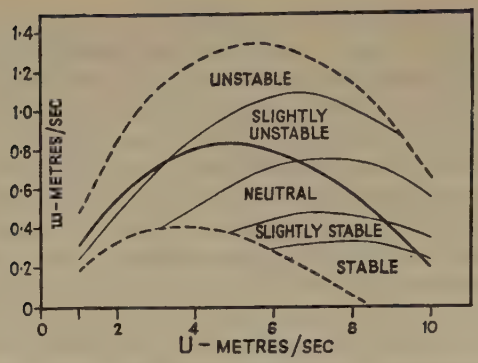

Figure 9. Variation of r.m.s. vertical velocity fluctuation w as a function of wind speed U and stability.

destroyed by the successive build-up of turbulence from below, suggests that the transition from very small intensity to fully-developed turbulence is quite rapid and therefore points lying between the omitted low-intensity points and the quoted points must be relatively uncommon.

Sometimes, w, the r.m.s. vertical velocity, is required. Assuming the fluctuations from the mean wind speed U to be small compared with U, or alternatively, no correlation between vertical and horizontal fluctuations, then $w = iU$. It is seen from Fig. 9, showing the range of w equivalent to Fig. 8, that for wind speeds less than about 4 m sec^{-1}, or 6 m sec^{-1} if restricted to a particular stability, the value of w increases with wind speed. Beyond these speeds w is either independent, or falls, with increasing U; the fall within a given stability range is only slight and may not be genuine. Stability also affects w, so that it can be as large as 1·3 m sec^{-1} in dry convective conditions but only about half as much in neutral or stable conditions.

Both this variation of w and the related variation of intensity i with wind speed may be a result of change in the relative proportions of energy of mechanical origin and of thermal origin. As Panofsky and McCormick (1960) have noted, under certain assumptions, w is of the form

$$w = A\,[z\,(\epsilon_1 + \delta\,\epsilon_2)]^{\frac{1}{3}}$$

where A and δ are dimensionless constants; ϵ_1 is the rate at which mechanical energy is added, $u_*^2\,dU/dz$; ϵ_2 is the energy added by convection $gH/c_p\rho T$ (H is the vertical heat flux). At a fixed height z, ϵ_1 is roughly proportional to U^3 whereas ϵ_2 is governed by H, and H must decrease with increasing U in some unknown way because of the dissipative action of mechanical turbulence on convective elements. The implied effect on w depends on the degree of stability, represented in the formula by $\delta\,\epsilon_2$. Thus w should be proportional to U for neutral or stable conditions but nearly constant for unstable conditions. Whilst the present results, indicated in Figs. 8 and 9, do not conform to this picture in all aspects, the following agreements may be noted :

(i) at any value of U, the value of w increases with increasing instability;

(ii) for unstable conditions, the intensity rapidly falls with increasing U;

(iii) the number of unstable cases decreases with increasing U.

7. Applications to diffusion

Results of the present nature have important application in several fields, notable among which are the effect of gustiness on aircraft and the problems of atmospheric diffusion. Considering only the latter, recent papers by Hay and Pasquill (1959) on the time-average width of a continuous-source plume and by Smith and Hay (1961) on the width of a puff from an instantaneous source both express their formulae in terms of parameters of the kind presented in this paper.

For the spread (standard deviation) of a continuous-source plume sampled over a period τ, at a distance x downwind of the source in a wind U, Hay and Pasquill give a relation which for the case of vertical diffusion can be written as

$$\sigma_\tau^2(x) = \frac{x^2}{(57{\cdot}3)^2}\left[\Theta_\tau^2 - \Theta^2_{x/\beta U}\right]$$

where the 57·3 is included to convert Θ in degrees to radians. The formula was originally determined for horizontal diffusion but can reasonably be applied here to vertical diffusion in the absence of marked changes in the turbulence along the vertical. The parameter β, which is the ratio of the Lagrangian and Eulerian time-scales, was originally estimated from data on lateral diffusion, to average about 4. A similar magnitude has been confirmed by data on the diffusion of a cluster of particles over vertical distances up to about 1,000 m. This approximate result, valid provided τ is several times larger than $x/4U$, has been applied to all the 17 fully-analysed periods, taking τ as 1 hour, and to several taking τ as 5 min. A typical example of the expansion curves obtained is presented in Fig. 10. The results are subject to two related provisos :

(1) the effect of vertical inhomogeneity in the turbulence may introduce errors at large x, and (2) the ground limits the downward diffusion (Fig. 10 gives σ up to values of x at which the cloud reaches the ground).

The previous section indicated that, within the conditions specified, the intensity is related to wind speed. It follows that, in so far as the $\Theta - U\tau$ curves are similar in shape whilst having different asymptotic values, the wind speed should give an indication of the spread of a plume. Consider a continuous source 300 m above ground (e.g., a power-station chimney whose virtual height is several times the actual stack height). Assuming that the distribution of concentration within the plume is Gaussian, and that perfect reflection takes place at the ground, the crosswind-integrated concentration takes the form $B/\sigma \exp\left[-h^2/2\sigma^2\right]$ where h is the height of the source. Two distances at ground-level are particularly relevant; the distance X_p at which particles first start to reach the ground (concentration 1/10, say, of maximum in plume at that distance) and the distance X_{m_1} at which the maximum ground-level crosswind-integrated concentration occurs. This latter distance is that at which the standard deviation is equal to the height (i.e., 300 m). These two distances have been evaluated for the 18 cases (see columns 21 and 22, Table 1) and plotted as a function of the intensity i. The scatter being small, only the mean curves are presented in Fig. 11, and it is seen that, generally, the maximum occurs at about 2·5 times the distance of first arrival. These curves can be used in conjunction with Fig. 9 to give the required distances in terms of the prevailing wind speed and stability.

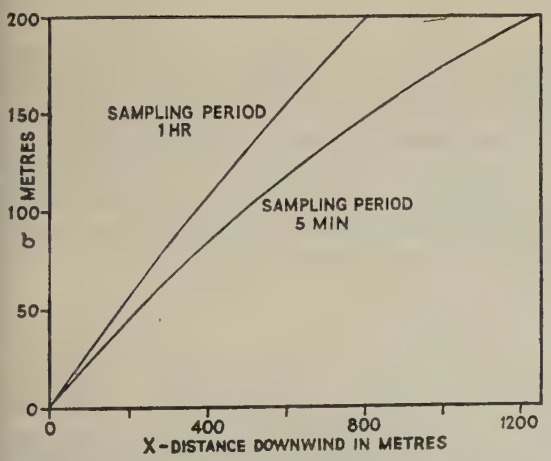

Figure 10. The vertical standard deviation of a continuous-source plume from vane fluctuations, observation *J*, at 1,000 ft.

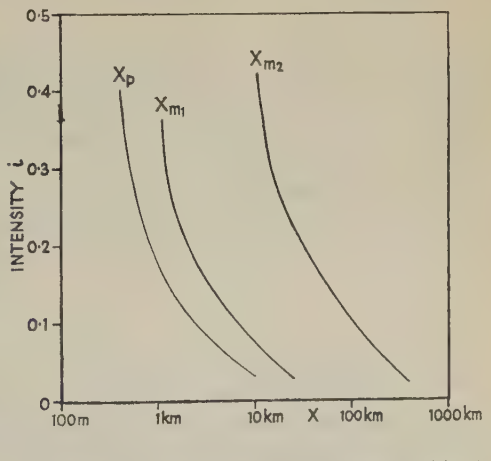

Figure 11. Variations of X_p, X_{m_1} (see Table 1) and X_{m_2} with intensity of turbulence.

A third curve is given in Fig. 11 which indicates the distance downwind at which crosswind-integrated concentration would be a maximum at a level 5,000 ft above the source, with homogeneous turbulence. This is relevant, for example, to rain-making experiments in which ' cloud-seeding ' agents have been released from a line-source at ground level with the hope that they will diffuse in sufficient quantity into the clouds. Since heights of at least 5,000 ft will often be of interest here, this curve provides some indication of the minimum distance at which the particles could be effective. The curve suggests that in non-convective situations this distance could be well over 100 miles.

The complementary problem of the determination of the expansion of a cluster is somewhat more complex. Smith and Hay gave two formulae, one an ' exact ' relation expressing the rate of growth as an integral of the spectrum weighted by a function V dependent on cluster size (see below), the other, a simple approximate formula based on the assumption of an exponential correlogram :

$$\frac{d\sigma}{dx} = 3\,i^2$$

where σ is the standard deviation of the particle distribution. Data of the present type enable a comparison to be made between the two formulae, and the example given below is based on the 500 ft trace (1119-1308 Z) on 27 May. The asymptotic value of Θ was taken as 10·7°. The simple formula thus gives :

$$\frac{d\sigma}{dx} = 0{\cdot}105$$

valid when σ is of the order of the length-scale of turbulence l.

The ' exact ' formula, dependent on the spectrum (Fig. 4), is

$$\frac{d\sigma}{dx} = 12\,\pi \int_{-\infty}^{\infty} kG\,(k)\,V\,(2\pi\sigma k)\,d\,(\log_e k)$$

where $V(s) = \frac{1}{s^2}\int_0^s r^2\,(2 - r^2)\,e^{-r^2}\,dr$ is given by Smith and Hay (1961, Fig. 2). The integrand was calculated for $\sigma = 1{,}000/2\,\pi \simeq 160$ m (by reference to Table 1, the same order as l and therefore comparable with the ' simple ' result) and gave :

$$\frac{d\sigma}{dx} = 0{\cdot}117$$

This satisfactory agreement, whilst not conclusive, provides some assurance that the simple formula is an adequate approximation. Column 23, Table 1, lists for comparison with column 22, the distances X_{m_8} at which the standard deviation of a puff would reach 300 m. Strictly, the values in column 23 should always be smaller than those in column 22 since the average size of a puff can never be greater than that of a plume. This is usually so, and the difference is particularly clear in conditions of low intensity. Cases of the reverse order, associated with either small length-scale or high intensity, indicate that the puff has grown beyond the limit of validity of the approximate formula.

Acknowledgements

I would like to express my thanks to all at C.D.E.E., Porton Down and B.D.E., Cardington, who were involved in obtaining the wind-traces, to Mr. J. W. Prince, a student of Magdalene College, Cambridge, who during a vacation appointment at C.D.E.E. carried out part of the analysis, and to the Director-General, Meteorological Office, for permission to publish this paper.

References

Charnock, H. and Robinson, G. D.	1957	*Air Ministry, Met. Res. Cttee., M.R.P.* No. 1062.
Gifford, F.	1959	*J. Met.*, **16**, p. 344.
Hay, J. S. and Pasquill, F.	1959	*Advances in Geophysics*, Atmos. Diff. and Air Poll., **6**, Academic Press.
Jones, J. I. P. and Butler, H. E.	1958	*Quart. J. R. Met. Soc.*, **84**, p. 17.
Jones, J. I. P. and Pasquill, F.	1959	*Ibid.*, **85**, p. 225.
Jones, R. A.	1957	*Air Ministry Met. Res. Cttee., M.R.P.* No. 1044.
	1958	Unpublished Ministry of Supply Paper.
Ogura, Y.	1957	*J. Met.*, **14**, p. 176.
	1959	*Advances in Geophysics*, Atmos. Diff. and Air Poll., **6**, Academic Press.
Panofsky, H. A. and Deland, R. J.	1959	*Ibid.*
Panofsky, H. A. and McCormick, R. A.	1960	*Quart. J. R. Met. Soc.*, **86**, p. 495.
Smith, F. B. and Hay, J. S.	1961	*Ibid.*, **87**, p. 82.
Townsend, A. A.	1950	*Proc. Camb. Phil. Soc.*, **47**, Pt. 2, p. 375.
Tukey, J. W.	1950	Symposium, 'Applications of autocorrelation analysis to physical problems,' O.N.R. Washington, NAVEXOS.

The spectrum of horizontal gustiness near the ground in high winds

By A. G. DAVENPORT*
Dept. of Civil Engineering, University of Bristol

(Manuscript received 22 March 1960; in revised form 27 October 1960. Communicated by Professor P. A. Sheppard)

Summary

Results of a study of about 70 spectra of the horizontal components of gustiness in strong winds are described. From these and other published data the following expression for the spectrum of gustiness for strong winds in the lower layers is suggested :

$$S_z(n) \cdot dn = 4{\cdot}0\, \kappa\, \overline{V}_1^2 \frac{x}{(1+x^2)^{4/3}}\, dx$$

$S_z(n)$ – power spectrum at height z
n – frequency
$\overline{V}_1$ – velocity at standard reference height of 10 m
κ – drag coefficient referred to mean velocity at 10 m
x – 1200 $n/\overline{V}_1$ where $n/\overline{V}_1$ is in cycles per metre.

Cross-spectra and cross-correlations of velocity between pairs of stations on a mast are given. From this it appears that the cross-spectra can be expressed as a simple function of the ratio of the vertical separation to the wavelength, no dependence on height being detectable.

1. Introduction

It is now recognized that in the design of nearly all above-ground structures, it is necessary to make some allowance for possible wind pressures. In the case of extremely exposed structures, such as tall antennae masts, long span bridges, radio telescopes, skyscrapers etc., this may be a major consideration, governing both the cost and the inherent safety of the structure.

A particularly difficult aspect of the problem has been to assess the transient and localized effect of gusts. Traditionally, structures were designed on the assumption that wind loads could be thought of as quasi-static and determined from simple wind tunnel tests in a steady airstream. The questions of what effective steady wind velocity should be used and, in particular, what allowance should be made for gusts do not appear, so far, to have been answered entirely satisfactorily.

It is now felt that this problem might usefully be discussed using the concepts of stationary time series, which have already been applied to the gust loading of aircraft. In this approach it has to be assumed that although gusts occur in a purely random sequence their statistical properties over a suitable period can be regarded as constant and independent of the origin of time. For this, a period between five minutes and an hour appears generally to be satisfactory. An important requirement of any solution along these lines is a knowledge of the spectrum of the gustiness. This defines the frequency-wise distribution of turbulent energy in the wind. The purpose of the investigations was to consider this question.

Spectra of the horizontal components of gustiness below 500 ft for a number of occasions of strong wind were computed. From these and other spectra previously published, an attempt was made to assess the possible changes in the spectrum due to variations in mean wind velocity, ground roughness and height above ground. These variations are reflected in an empirical expression suggested for the spectrum of horizontal gustiness in high winds which may be suitable for such practical problems as the wind loading of structures.

* At present with Faculty of Engineering Science, University of Western Ontario.

Some of the wind records consisted of simultaneous measurements at different heights on a vertical mast. For these data the cross-correlation coefficients between the velocities at pairs of stations were also computed and estimates made of the co-spectrum and quadrature spectrum.

2. Observations

Measurements of wind velocity made in winds faster than 9 m sec^{-1} (20 mi hr^{-1}) were available from three sources. General descriptions of the measurements, the recording gear and the sites at which they were made are as follows :

(1). Sale, Victoria, Australia (38° 06′S; 147° 04′E).

A number of high-speed, synchronized records of wind speed at three heights, obtained during an earlier investigation by Deacon (1955), were kindly made available. The measurements were made using cup anemometers with Sheppard-type rotors which were mounted at 12·2 m (40 ft), 64 m (210 ft), and 153 m (503 ft) on a radio mast. The site is described as open grassland with few trees. The resolving power of the recording equipment enabled the mean velocity to be evaluated accurately at two-second intervals. Further details of the installation are supplied in the paper by Deacon (1955).

Of the 31 successful observations which were made, 20 were chosen for spectral analysis (see Table 1 (a)) either because their duration was considered sufficient ($>$ 8 min) to provide reliable spectral estimates, or, in the case of observation No. 7, because of the high wind speeds (up to 71 mi hr^{-1}).

TABLE 1 (a). Results from Deacon's observations of wind velocity at Sale, Victoria

Obsn. No.	Date 1952	Time	Durn. (min.)	Mean velocities m sec^{-1} $\overline{V}_{12}$	$\overline{V}_{64}$	$\overline{V}_{153}$	$\overline{V}_{64}/\overline{V}_{12}$	$\overline{V}_{153}/\overline{V}_{12}$
	September							
2	2	1917	8·9	12·3	16·5	20·7	1·34	1·70
4	14	1634	8·6	13·7	17·3	21·1	1·25	1·54
5	16	1615	8·5	13·7	17·9	21·6	1·30	1·58
6	16	1715	5·8	11·0	14·0	17·1	1·27	1·55
7	16	1821	4·9	18·3	24·1	27·6	1·32	1·51
8	16	1828	8·4	14·0	18·6	24·8	1·33	1·78
9	16	1920	7·8	12·6	16·8	19·6	1·33	1·55
10	17	1327	9·0	14·5	18·4	21·7	1·18	1·39
12	17	1925	9·4	9·4	13·0	16·8	1·37	1·77
14	17	2155	13·4	9·1	12·6	16·2	1·30	1·68
16	19	0940	10·3	11·9	14·3	16·3	1·19	1·37
18	20	1000	8·5	12·0	15·2	18·3	1·26	1·53
22	20	1443	9·1	12·1	13·7	15·3	1·14	1·26
23	15	2148	13·2	10·7	13·9	17·1	1·34	1·58
24	15	2248	15·2	12·4	16·6	21·7	1·35	1·76
28	17	1420	8·8	9·7	11·6	13·5	1·20	1·40
34	28	1450	8·0	10·9	13·6	15·4	1·25	1·40
36	2	1420	8·3	11·2	13·8	15·7	1·23	1·40
37	10	1720	12·2*	11·5	15·1	17·6	1·32	1·54
38	19	1330	10·2	16·5	20·7	25·0	1·31	1·59
	Geometrical mean		9·2		Mean		1·279	1·544
					Standard deviation		0·063	0·141

* Not included in mean value owing to falling of mean velocity throughout run

TABLE 1 (b). VALUES OF NORMALIZED LOGARITHMIC SPECTRA FROM SALE OBSERVATIONS

Height	Values of $n \cdot S(n)/V^2 \times 10^2$												Intensity $\sigma(v)/V$		
	12·2 m (40 ft)				64 m (210 ft)				153 m (503 ft)				12·2 m (40 ft)	64 m (210 ft)	153 m (503 ft)
n/V (cycles/km^{-1})	1·54	3·12	7·80	15·4	1·27	2·40	6·00	12·7	1·00	2·00	5·00	10·0			
Obs'n No.															
2	0·35	0·41	0·40	0·26	0·30	0·39	0·24	0·10	–	–	–	–	·122	·109	·154
4	0·50	0·56	0·39	0·17	0·46	0·40	0·19	0·10	0·09	0·10	0·04	0·03	·150	·130	·063
5	0·84	0·84	0·50	0·23	0·44	0·48	0·31	0·15	0·25	0·22	0·08	0·05	·179	·126	·088
6	0·70	0·65	0·49	0·29	0·51	0·49	0·23	0·10	0·20	0·17	0·13	0·08	·239	·113	·082
7	1·10	0·89	0·50	0·30	0·41	0·32	0·14	0·18	0·16	0·15	0·10	0·04	·175	·104	·076
8	0·89	0·88	0·50	0·30	0·41	0·41	0·23	0·13	0·28	0·25	0·14	0·11	·174	·118	·098
9	0·74	0·77	0·54	0·30	0·47	0·44	0·23	0·16	0·38	0·35	0·11	0·07	·165	·129	·115
10	0·88	0·76	0·36	0·22	0·38	0·35	0·17	0·10	0·28	0·26	0·10	0·05	·167	·121	·099
12	0·86	0·95	0·82	0·43	0·51	0·56	0·39	0·22	0·28	0·31	0·26	0·11	·193	·137	·113
14	0·60	0·82	0·71	0·45	0·36	0·40	0·28	0·18	0·34	0·33	0·17	0·09	·171	·119	·112
16	0·52	0·60	0·37	0·22	0·37	0·37	0·20	0·12	0·16	0·16	0·12	0·10	·131	·113	·080
18	0·90	0·78	0·52	0·27	0·35	0·39	0·29	0·09	0·25	0·24	0·10	0·05	·165	·120	·100
22	0·52	0·62	0·45	0·25	0·44	0·52	0·40	0·16	0·35	0·40	0·24	0·12	·153	·141	·123
23	1·15	1·10	0·64	0·35	0·52	0·57	0·28	0·14	0·56	0·51	0·25	0·14	·204	·142	·131
24	0·78	0·84	0·56	0·31	0·43	0·58	0·27	0·15	0·32	0·29	0·15	0·07	·167	·132	·103
28	0·48	0·62	0·87	0·30	0·45	0·57	0·27	0·17	0·30	0·33	0·20	0·10	·145	·125	·100
34	0·94	1·00	0·66	0·40	0·43	0·44	0·25	0·13	0·32	0·31	0·17	0·10	·185	·127	·106
36	0·69	0·70	0·43	0·25	0·40	0·40	0·23	0·14	0·12	0·14	0·08	0·04	·162	·125	·070
37		2·10*	0·55*	0·27		0·88*	0·23*	0·16*		0·37*	0·17*	0·10*	·338*	·260*	·197*
38	0·92	0·91	0·33	0·22	0·41	0·44	0·21	0·09	0·54	0·40	0·14	0·08	·173	·126	·129
Mean	0·76	0·77	0·53	0·29	0·42	0·45	0·25	0·14	0·29	0·27	0·14	0·08	·170	·124	·098
Standard deviation	0·19	0·16	0·15	0·07	0·05	0·06	0·07	0·05	0·12	0·07	0·06	0·03	·021	0·010	0·036

* Values not used in determination of mean and standard deviation owing to decreasing velocity trend throughout run

(2). Cardington, Bedfordshire, England (52° 07'N; 0° 25'W).

These records were obtained from data published by Giblett and co-workers (1932) in their report covering their investigations into wind structure at the Royal Airship Works. The exposure at this site in the direction of the prevailing W'ly wind was probably similar to that at Sale, being open farmland broken only by a few trees and hedgerows. Four synchronized anemometers were mounted at a height of 50 ft (15·3 m) at the vertices of a 700 ft (214 m) equilateral triangle and at the mid-point of one side. Speed and direction were recorded separately using the Dines pressure-tube wind-speed recorder and the Baxendell direction recorder. The apparatus was considered sensitive enough to provide reliable estimates of five-second mean velocities and directions, and these have been tabulated in the original report. Seven runs (see Table 2) of approximately 10 min duration were selected for analysis because of their high mean velocities (up to 19·6 m sec^{-1} (44 mi hr^{-1})). Further details of the site and instruments are given in the original report (Giblett 1932).

TABLE 2. VALUES OF NORMALIZED LOGARITHMIC SPECTRA FROM CARDINGTON (computed from Giblett's observations)

Run No.	Approx. duration (min)	Mean velocity (m sec^{-1})	Values* of $n \cdot S(n)/V^2 \times 10^2$ n/V in cycles m^{-1} 0·001	0·002	0·005
314	10	10·1	0·68 (0·56)	0·80 (0·62)	0·62 (0·37)
357	9	12·6	0·46 (0·38)	0·56 (0·40)	0·35 (0·22)
360	9	17·9	0·89 (0·66)	0·86 (0·54)	0·54 (0·35)
361	10	19·6	1·00 (0·70)	0·82 (0·52)	0·56 (0·30)
371	10	12·7	0·43 (0·34)	0·54 (0·37)	0·35 (0·22)
391	10	15·4	0·58 (0·43)	0·64 (0·41)	0·49 (0·27)
393	9	12·2	1·30 (0·83)	1·18 (0·78)	0·61 (0·43)
		Mean	0·76 (0·56)	0·77 (0·52)	0·50 (0·31)
		Standard deviation	0·30 (0·17)	0·21 (0·14)	0·10 (0·07)

* Average values from simultaneous observations at four stations

Unbracketed values = total horizontal components of turbulence

Bracketed values = longitudinal component only

Height of observations = 50 ft (15·2 m)

(3). Cranfield, Bedfordshire, England (52° 04'N; 0° 37'W).

A record of a strong wind measured at the Windmill Research Station was made available through the co-operation of the Electrical Research Association. Although at this site the ground upwind of the anemometer is open for a distance of half a mile across a corner of an airfield, neighbouring land is broken by small hedged fields and it might be supposed that the terrain is generally rather rougher than either Sale or Cardington. Records were made using the Electrical Research Association gust anemometer described by Wax (1956). This instrument, which records the horizontal velocity in the mean wind direction, in principle records the drag of a small light perforated sphere. It can respond to changes of wind speed within 0·1 sec and hence has a frequency response which is rather higher than either of the other instruments referred to. From the continuous record, readings of the mean velocity at quarter-second intervals were made.

3. CALCULATION OF SPECTRA

All measurements of wind velocity were given in a digital form consisting of successive readings of the mean velocity at equal intervals throughout each record. The spectra were calculated from these data using Tukey's method which has been fully described by Panofsky and McCormick (1954) and is now more or less a standard procedure.

In this the spectra are determined from the autocorrelation coefficients rather than by a direct Fourier analysis of the original record. Computation of the autocorrelation coefficients and of the spectra from these were carried out on a Deuce electronic computer using a standard programme. Spectral estimates were made using various numbers of autocorrelation coefficients (denoted by m) in order to increase the statistical reliability on the one hand and low-frequency resolution on the other (see Figs. 1, 2 and 3). These spectral estimates were smoothed by a weighted 3-term moving average. However, instead of the weights (·23 : ·54 : ·23) originally suggested by Tukey, the modified values he suggested (·25 : ·50 : ·25) were used for computational convenience, except for the initial

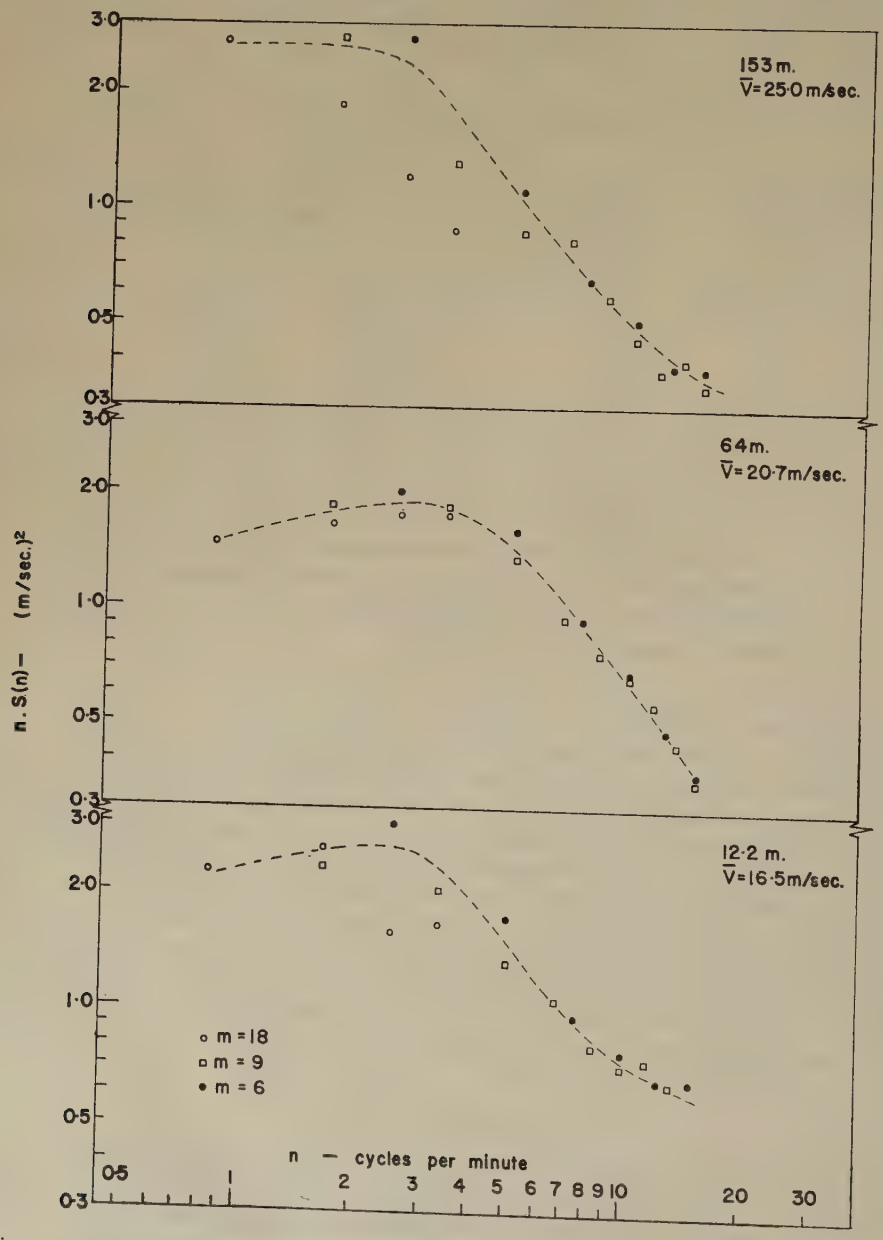

Figure 1. Spectrum of horizontal gustiness at three levels of observation Sale observation No. 38).

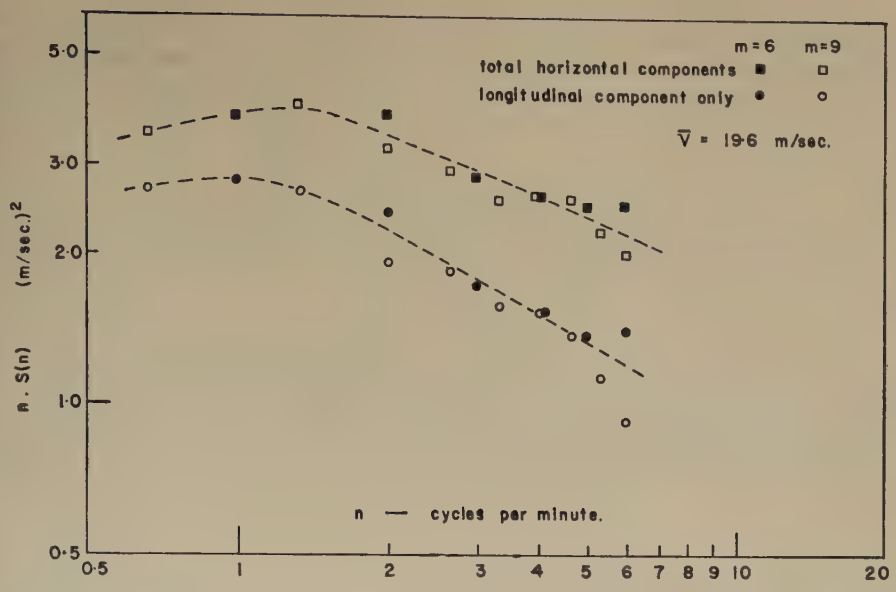

Figure 2. Spectrum of horizontal gustiness at 15·3 m height. (Cardington observation No. 361).

and final estimates of each sequence where weights of (·50 : ·50) were used instead of (·54 : ·46). Each smoothed spectral estimate was then multiplied by the variance of the data, giving the actual spectral density in units of (velocity)^2 per unit frequency.

Sample spectra computed from the Sale, Cardington and Cranfield records are shown in Figs. 1, 2 and 3. The three-level spectra from Sale observation No. 38 (Fig. 1) is from one of the longer and also higher-speed records, part of which has been reproduced in the paper by Deacon (1955). Fig. 2 shows the average spectrum obtained from the simultaneous observations at the four Cardington stations during run 361, one of the fastest. The spectrum obtained from the Cranfield record made with the sensitive gust anemometer, appears in Fig. 3.

It will be noticed that the Sale and Cardington spectra (Figs. 1 and 2) have been given in terms of the product of frequency n, and spectral density $S(n)$. This is known as the logarithmic spectrum and has units of (velocity)^2. This conventional representation is convenient because when represented graphically on a logarithmic frequency scale (as is often appropriate) the area under it still gives a true measure of the energy.

To enable comparisons between spectra to be made, two further modifications seemed appropriate as first steps. Firstly, the logarithmic spectra were normalized by dividing by the square of the mean velocity (proportional to the surface-shear stress) at the height of observation giving $n \, . \, S(n)/\bar{V}^2$, a dimensionless quantity. Secondly, the frequency scale was transformed into one of wave number $n/\bar{V}$ (or inverse wavelength). The reasons for preferring the latter was because it was believed that spatial pattern of the turbulence was invariant with wind speed and depended only on the height. The effect of increasing the wind speed would be to increase the intensity of the fluctuations and to sweep the spatial pattern past a point on the ground faster, but without actually altering the pattern. (These concepts are implicit in the original assumption by Taylor (1938) of the equivalence of the time and space spectra, which have been at least partially verified by Panofsky *et al.* (1958)). It should be pointed out, however, that the results were, in themselves, probably too scattered to favour either a wave-number or a frequency approach.

The resulting so-called normalized logarithmic spectra were plotted and 'best-fitting' lines were drawn in by eye, as in Figs. 1 and 2. From these lines representative estimates of the spectra were made at several wave numbers. These appear in Tables 1 (b) and 2.

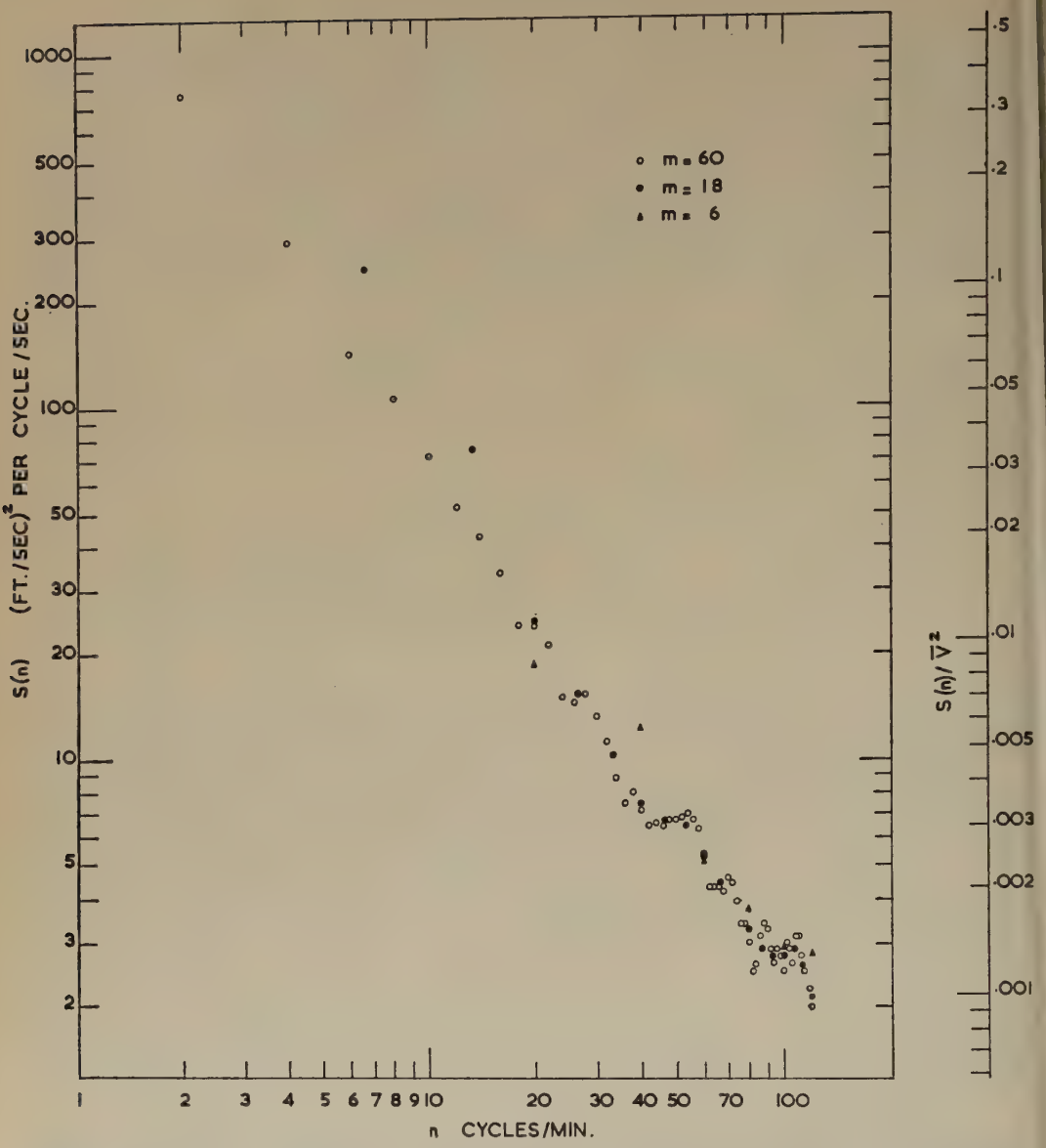

Figure 3. Spectrum of horizontal wind velocity from a record obtained at Cranfield, Bedfordshire using the Electrical Research Association gust anemometer.

Date : 23 December 1955 1655 GMT Duration of record : 10 min
Mean wind velocity : $V = 46{\cdot}0$ ft/sec Elevation : 50 ft above ground.

4. Discussion of results

Although turbulence in the atmosphere is generally both convective and mechanical in origin, in high winds, convective turbulence plays a relatively minor role. The reason for this is that whereas mechanical turbulence rapidly increases in intensity with wind speed, convective turbulence, if anything, tends to be damped out by the powerful mixing action caused by the mechanical turbulence; the latter prevents the necessary thermal instabilities from arising and tends to reduce the atmosphere to a state of neutral stability. This last process takes place even more rapidly if, as is frequently the case, cloud cover blankets incoming and outgoing radiation.

This almost complete predominance of mechanical turbulence suggests that in high winds the intensity of the turbulence nearer the ground will only vary significantly with the mechanical drag forces between the air and the ground and the height. The influence of both these factors is now discussed.

(a) *The influence of the surface drag*

The drag or shear force near the ground surface, denoted by τ, is given by the familiar expression

$$\tau = \kappa \rho \bar{V}_1^2 \quad . \quad . \quad . \quad . \quad . \quad (1)$$

where $\bar{V}_1$ is a reference mean velocity near the ground, ρ is the air density, and κ is a drag coefficient dependent on the roughness of the surface. Although for some natural surfaces the value of κ shows some slight dependence on wind velocity (due in part at least to the surface itself changing, as in the bending of grass stalks to the wind) it is probably, for all practical purposes, constant.

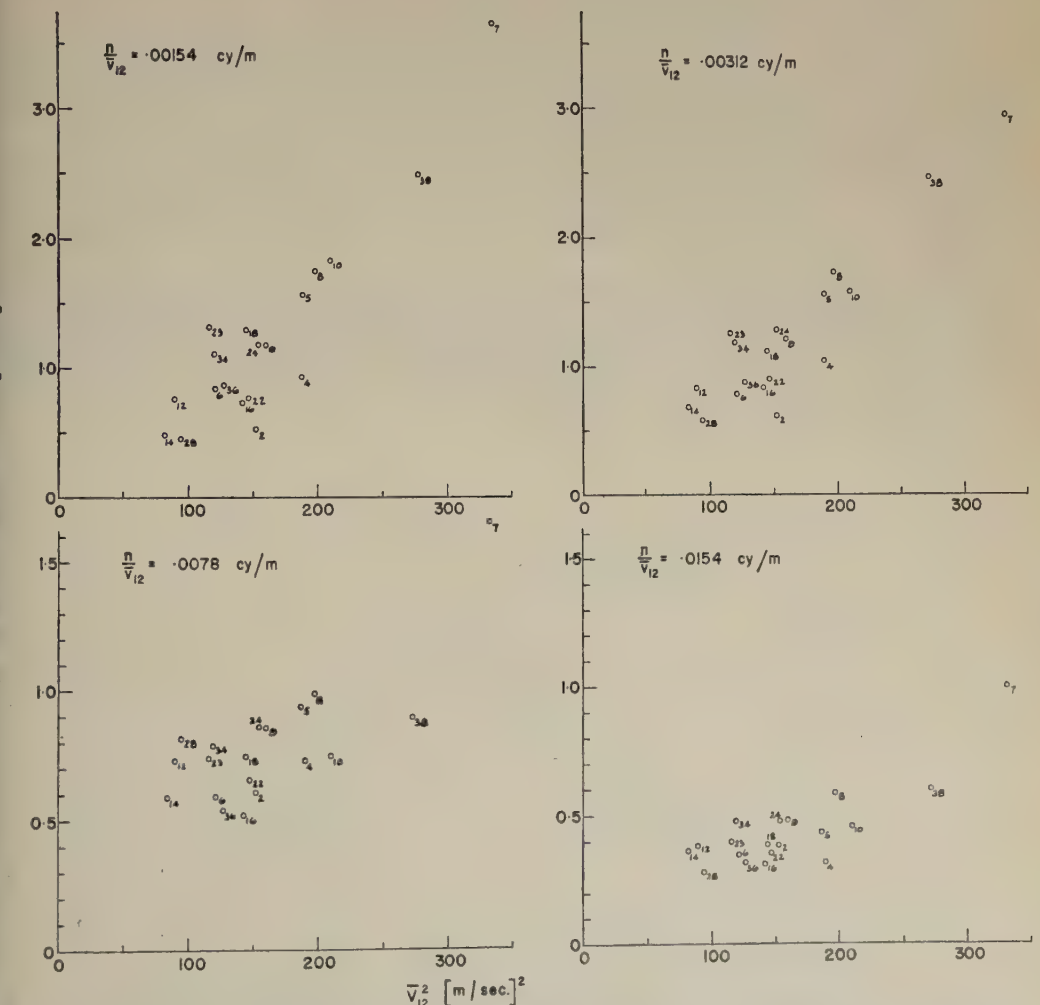

Figure 4. Logarithmic spectrum of horizontal gustiness at various wave-numbers as function of square of mean wind speed (from Sale observations at 12·2 m height).

It is natural to suppose that the energy of the eddy component should be direct proportional to the surface drag. This implies, because of Eq. (1), a proportionality $\overline{V}^2$. Fig. 4, showing the 12 m Sale data, and Table 2, listing the Cardington result show this to be at least approximately true, even at the longer wavelengths. Panofsk and McCormick (1954) came to much the same conclusion from observations made the same height range at the very much rougher Brookhaven site (scrub trees 10 m high It seems, therefore, that in high winds and over the frequency range considered, there some justification in assuming that for any given height, wavelength, and type of surfa $n \,.\, S\,(n)/\overline{V}^2$ is constant. The proportionality of the spectral density to κ, however, canno be verified until the variation of spectral density with height is first established. This now considered.

(*b*) *Variation of spectrum with height*

Fig. 5 shows the average results for all the normalized logarithmic spectra at all thre observation heights at Sale. To make comparisons easier the mean velocity at 12 r (rather than the mean velocity at the observation height) has been used both for normali ing the spectral estimates and deriving the wave number.

It appears that although the form of the logarithmic spectrum is more or less the sam at all three heights, there may be a slight falling-off of energy with height. This is furthe indicated by the ratios of the total variance to the square of the mean velocity at 12 r which for all the periods average 0·289, 0·255, 0·229, at the 12 m, 64 m, 153 m height respectively. This decrease in energy is more apparent at higher wave numbers (abou 100 m wavelengths) than at lower wave numbers (500 m wavelengths). In the latte case, the differences appear to be less than 10 per cent over the entire height range an probably not very significant considering the poorer statistical reliability of thes estimates.

At the higher wave numbers the energy appears to fall off almost exactly in invers ratio to the increasing mean velocity. Whether this is accidental or not is not understoo It does seem possible, however, that when the energy generated at or near the groun by the stress is translated to greater heights the energy density per unit volume may ten to change inversely as the wind speed, in the same way as the concentration of smok from a chimney depends on the wind speed.

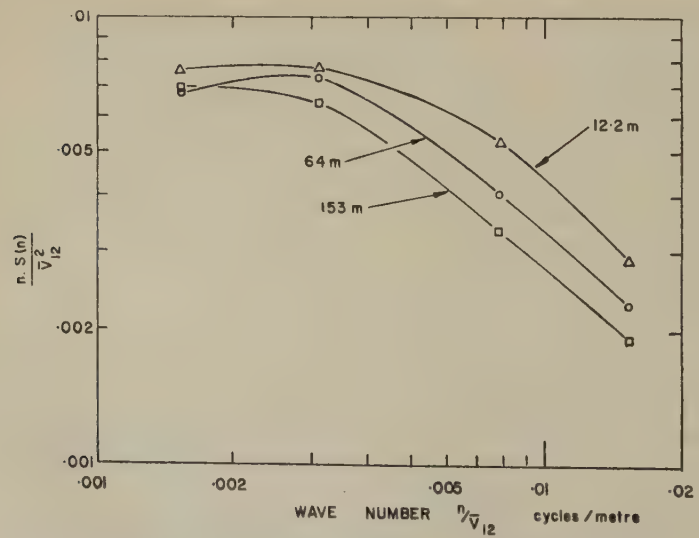

Figure 5. Average horizontal spectra at 12·2 m, 64 m and 153 m heights (from observations at Sale Victoria).

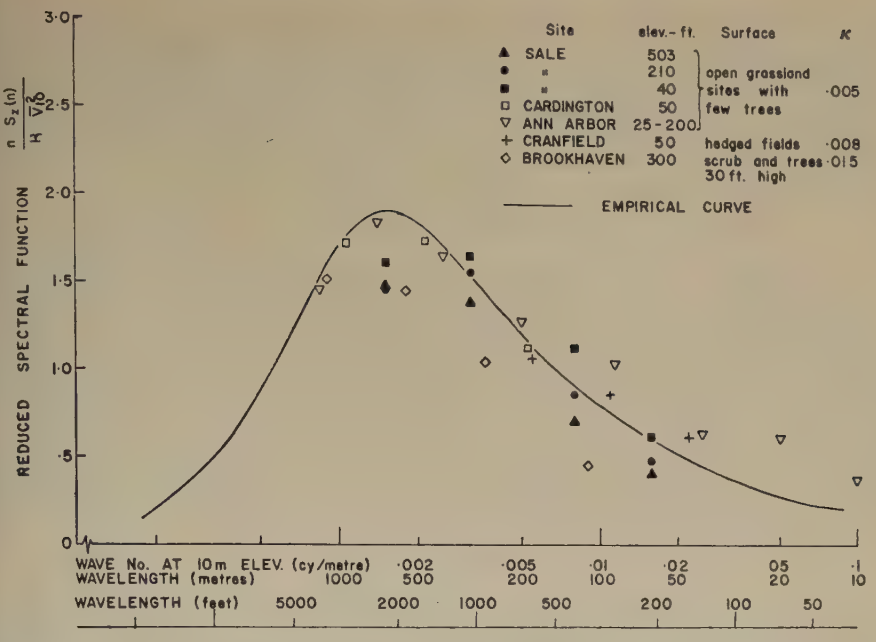

Figure 6. Spectrum of horizontal gustiness in high winds.

$n \cdot S_z(n)$ – proportion of energy per unit fractional increase of frequency (n) at height z.

$\overline{V}_{10}$ – mean wind velocity at reference height, 10 m (33 ft).

κ – frictional drag coefficient of surface (referred to velocity at 10 m).

This speculation is not, however, supported by all the evidence, and Smith and Singer (1956), for example, have noted a maximum of energy at about 46 m above ground at the rougher Brookhaven site (scrub trees about 10 m high). (See Fig. 7).

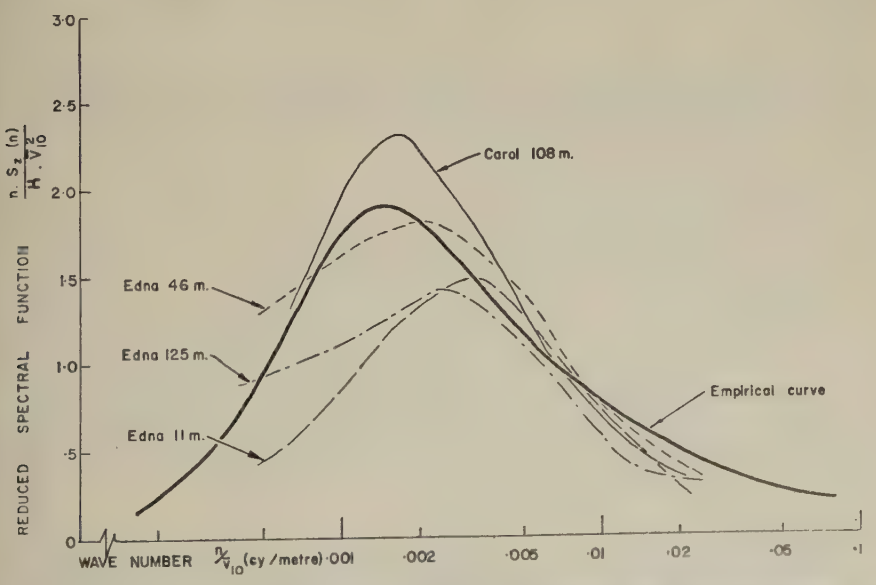

Figure 7. General expression for horizontal gust spectrum compared with individual spectra obtained in hurricane winds at Brookhaven (Long Island, U.S.A.).

Assumed value of $\kappa = \cdot 017$.

These apparent variations in the energy with height are not very large, however, and may in any case, be of the same order as the errors in its estimation. The simplest assumption to adopt for the present, therefore, seems to be that the spectrum is invariant with height. If we combine this assumption with the earlier assertion concerning the proportionality to the surface shear stress, we may write for the logarithmic spectrum at height z

$$\frac{n \,.\, S_z(n)}{\kappa \overline{V}_1^2} = F\left(\frac{n}{\overline{V}_1} L\right) \quad . \quad . \quad . \quad . \quad (2)$$

where $\overline{V}_1$ is a reference velocity near the ground and L is some characteristic length.

It will be apparent later in the discussion that there is no evidence to show that this characteristic length L for the horizontal components of gustiness depends either on the height above ground or the roughness length for the surface. The same feature has been noted by Townsend (1957) in the constant stress layer of the wind-tunnel. It will therefore be taken as constant, so that the above expression for the spectrum can be considered simply as a function of the wave number at the reference height. The reference velocity has, in this paper, been taken as the velocity at the standard 10 m reference height. Where this is not known it can be estimated according to the power law profile :

$$\overline{V}_z \propto z^{\alpha} \quad . \quad . \quad . \quad . \quad . \quad (3)$$

in which values of the exponent α have been established by actual measurement.

Eq. (2) can now be used to compare other results (including those from Cranfield and Cardington) obtained at different observational heights and over surfaces of different roughness (see Fig. 6).

For the Sale results the average value of the exponent α from the observations (see Table 1 (a)) is 0·16 (Deacon 1955). Using this in conjunction with the average results of Table 1 (b), and assuming a drag coefficient of 0·005 characteristic of this type of surface (see Deacon 1955), leads to the following values :

$n/\overline{V}_1 \times 10^3$ cycles m^{-1}		1·59	3·18	7·95	15·9
$\frac{n \,.\, S_z(n)}{\kappa \overline{V}_1^2}$	$z = 153$ m	1·48	1·38	0·71	0·41
	$z = 64$ m	1·46	1·57	0·87	0·49
	$z = 12{\cdot}2$ m	1·62	1·65	1·13	0·62

For the Cardington site the power law exponent measured by Frost (1947) is 0·17. Again using a drag coefficient of 0·005 appropriate to this open grassland site we obtain the following values from Table 2.

Observation height : 15·2 m (50 ft)

$n/\overline{V}_1 \times 10^3$ cycles m^{-1}	1·06	2·12	5·3
$\frac{n \,.\, S_z(n)}{\kappa \overline{V}_1^2}$	1·71	1·73	1·12

For the Cranfield site no information on the variation of wind velocity with height is available. However, since the surface is slightly rougher than the previous two sites (but less rough than the Brookhaven site discussed below), a power law exponent of 0·20 with a drag coefficient of 0·008 is assumed. Using these quantities the following results are derived from Fig. 3.

Observation height : 15·2 m (50 ft)

$n/\overline{V}_1 \times 10^3$ cycles m^{-1}	5·5	11·0	22·0
$\frac{n \,.\, S_z(n)}{\kappa \overline{V}_1^2}$	1·06	0·87	0·62

Some comparative high quality spectra of the horizontal components of gustiness in strong winds are also available for the Brookhaven site on Long Island. Spectral estimates were made from six published spectra on occasions when the wind velocity at 91 m exceeded 9 m sec^{-1} : these include periods F, H, K, L, P (Van der Hoven and Panofsky 1954) and Hurricane *Connie* (Van der Hoven 1957). These results are listed in Table 3. From the ratios of the mean velocity at 91 m to that at 11 m a power law with an exponent of 0·27 would seem appropriate. Using this result in conjunction with the drag coefficient of 0·015 calculated from the measured shear stress at 91 m (quoted by Deacon 1955) leads to the following :

Observation height : 91 m (300 ft)

$n/\overline{V}_1 \times 10^3$ cycles m^{-1}	0·90	1·80	3·60	9·0
$\frac{n \,.\, S_z(n)}{\kappa \overline{V}_1^2}$	1·51	1·45	1·05	0·45

The average peak frequency occurs at $n/\overline{V}_1 = 0{\cdot}00144$ cycles m^{-1}.

TABLE 3. VALUES OF NORMALIZED LOGARITHMIC SPECTRA FROM BROOKHAVEN
(from results by Panofsky and Van der Hoven)

Period	Mean velocity $\overline{V}_{91}$ m sec^{-1}	$\overline{V}_{91}/\overline{V}_{11}$	Values of $n \,.\, S(n)/\overline{V}^2 \times 10^2$ $n/\overline{V}$ in cycles m^{-1} 0·0005	0·001	0·002	0·005	Peak value $n \,.\, S(n)/\overline{V}^2$	$n/\overline{V}$ cycles m^{-1}
F	9·8	1·85	1·01	0·72	0·39	0·19	1·10	0·0003
H	15·3	1·80	0·35	0·51	0·50	0·22	0·52	0·0009
K	9·9	1·57	0·76	0·70	0·52	0·23	0·76	0·0007
L	12·8	2·00	0·31	0·40	0·39	0·18	0·46	0·0016
P	9·1	1·69	1·06	0·90	0·54	0·18	1·20	0·0007
Connie	20·0	–	0·65	0·65	0·41	0·21	0·80	0·0007
	Mean	1·78	0·68	0·65	0·47	0·20	–	0·0008

Another set of results for an open grassland site is available from the spectral analysis of Sherlock's Ann Arbor observations carried out by Bushnell and Huss (1958). In this case spectral estimates were made by a more approximate method. This involved computing the variance of the data when various numbers of consecutive quarter-second readings were grouped together and then averaged. The energy in the frequency band $n_1 : n_2$ was then found from the increment in the variance when the $1/2n_1$ and then $1/2n_2$ consecutive terms were grouped. The average spectral density for this frequency band was found and the result applied to the mid-frequency. In these calculations, results from all eight levels of observation (25 to 200 ft) were grouped together. Using the wind velocity profile for this storm given by Sherlock (1953) and the drag coefficient of 0·005 the following results are obtained :

$n/\overline{V}_1 \times 10^3$ cycles m^{-1}	0·833	1·40	2·50	5·00	11·66	25·0	50·0	100
$\frac{n \,.\, S_z(n)}{\kappa \overline{V}_1^2}$	1·45	1·84	1·65	1·28	1·04	0·646	0·602	0·37

All the results quoted are shown together in Fig. 6. As can be seen they are reasonably consistent with one another and suggest that over the range of wave numbers considered, the spectrum has a general ' cocked-hat ' shape. This general shape of the spectrum is defined in more detail in the following section which describes certain other physical requirements that a generalized spectrum must, it seems, satisfy.

(c) *General form of the logarithmic spectrum*

At high wind speed, the logarithmic spectrum of turbulence in the micrometeorological range of frequencies would appear to be characterized by three features :

(1) A spectral gap at wave numbers in the vicinity of 0·0001 cycles m^{-1} (10 km wavelength).

(2) A spectral peak at a wave number of about 0·001 cycles m^{-1} (1 km wavelength).

(3) A spectral pattern characteristic of the inertial subrange of frequencies at wavelengths less than the height of observation.

Although the existence of the spectral gap appears to have been established by Van der Hoven (1957) for a number of different weather conditions and locations it seems possible that under extremely unstable conditions at lower wind speeds, this gap might be less apparent. In extremely high winds, however, it is felt that the shorter wavelength mechanical turbulence, tending to increase with the square of the wind-speed, will dominate the long wavelength convective turbulence to such an extent that the contribution to the energy by convective turbulence, even if large absolutely, will be comparatively insignificant. At present the evidence appears to be in favour of such a gap being present in most conditions of strong wind*. From the viewpoint of predicting gust-loads on structures this gap is of great significance since it enables these predictions to be linked quite simply with climatological wind records which, in the main, consist of hourly mean velocities.

At high mean wind speeds, the spectral peak appears to exist at wave numbers (referred to the 10 m reference velocity) between 0·001 and 0·002 cycles m^{-1}. The average wave number of the peaks of the six Brookhaven spectra was 0·00144 cycles m^{-1}. The Sale results also indicate a peak in this neighbourhood. There is no evidence to suggest that the peak wavelength is affected by the type of surface. This point was also observed by Deland and Panofsky (1957).

At the high-frequency end of the spectrum (wavelengths less than observation height) the eddies appear to belong to the inertial subrange of frequencies. These eddies acquire energy only by the decay of larger eddies and lose energy only by transfer to smaller eddies : the viscous forces are insignificant and the average properties are determined solely by the average rate of dissipation of energy per unit mass of the fluid.

There is still some uncertainty as to whether the time spectra of the velocity components in this region should vary with the wave number, $n/\overline{V}$ as $(n/\overline{V})^{-5/3}$ or $(n/\overline{V})^{-2}$ although the balance of experimental evidence is now in support of the former, as required by theory. At the high-frequency end the Sale results would also appear to support the former (see Fig. 5). The Cranfield and Ann Arbor data indicated a power even less than $-5/3$.

It seemed desirable to try to determine an empirical algebraic expression which fitted the observed values and also satisfied all the above conditions. An expression quoted by Panofsky and McCormick (1954) for the vertical components of gustiness, of the form

$$S(x)\,dx = \frac{10}{9} \cdot \frac{x}{(1+x)^{8/3}}\,dx \qquad . \qquad . \qquad . \qquad (4)$$

has the right ' cocked-hat ' shape, but when, as in the present case, there is only a small contribution from convective turbulence the peak of this formula is somewhat too broad.

* Some recent measurements of $n \cdot S(n)/\overline{V}^2$ from records of three anemometers of a strong wind ($\overline{V}$ = 25-30 m sec^{-1}) at the railway bridge across the Severn estuary at Sharpness tend to confirm this. In the frequency range 3-60 cycles hr^{-1} (i.e., $n/\overline{V} \approx$ 0·00005-0·008 cycles m^{-1}) the value of $nS(n)/\overline{V}^2$ was never greater than 0·002, and, over the range $n/\overline{V} \approx$ 0·0001-0·0008, averaged about 0·0005. These values are seen to be much less than the higher-frequency Sale values given in Fig. 5, for which site the roughness is probably of the same order. To this extent there was apparently a gap in the spectrum. This gap, however, should still be regarded as speculative, particularly at lower wind speeds.

An alternative expression which is more peaked is

$$S(x) \,.\, dx = \frac{3}{2} \cdot \frac{x}{(1 + x^2)^{4/3}}\, dx.$$

By trial it was found that a satisfactory fit to the points appearing on Fig. 6 was given by the curve

$$\frac{n \,.\, S_z(n)}{\kappa \overline{V}_1^2} = 4{\cdot}0\, \frac{x^2}{(1 + x^2)^{4/3}} \quad . \quad . \quad . \quad . \quad (5)$$

in which $x = 1200\ n/\overline{V}_1$ ($n/\overline{V}_1$ in cycles m^{-1}). This curve is shown in Fig. 6.

In Fig. 7 this proposed expression for the spectrum is compared with individual spectra for the 1954 hurricanes, *Carol* and *Edna*, obtained at Brookhaven by Smith and Singer (1956). (The spectra shown have been obtained by drawing smooth lines through the original data). The 108 m wind speed in *Carol* was 28·8 m sec^{-1} and the 125 m wind speed in *Edna* was 25·9 m sec^{-1}. The power-law exponent for the two storms was 0·31 and 0·29 respectively – somewhat larger than the average value of 0·27 for other storms at this locality. This implies a relatively greater shear stress; consequently a slightly larger value of κ had been used.

The suitability of this empirical curve can also be tested by comparing the total variance it gives with the observed values. The contribution to the total variance $\sigma_z^2(V)$ in the frequency band $n_1 : n_2$ is given by the integral of $S_z(n)$ between these limits. It follows from Eq. (5) that the total variance at height Z

$$\sigma_z^2(V) = \int_0^\infty S_z(n) \,.\, dn$$

$$= 6{\cdot}0\, \kappa \overline{V}_1^2 \quad . \quad . \quad . \quad . \quad . \quad (6)$$

The corresponding intensity of turbulence at height z denoted by I_z (and defined by the following) is

$$I_z = \frac{\sigma_z(V)}{\overline{V}_z} = 2{\cdot}46\, \kappa^{\frac{1}{2}} \left(\frac{\overline{V}_1}{\overline{V}_z}\right)$$

$$= 2{\cdot}46\, \kappa^{\frac{1}{2}} \left(\frac{z}{10}\right)^{-\alpha} \quad . \quad . \quad . \quad . \quad (7)$$

assuming the power-law profile of mean wind speed.

In applying this formula to the observations, however, some additional allowance must be made for what is, in effect, a high-frequency 'cut-off' which is imposed by the averaging of readings over finite-time intervals. In the case of the Sale data this averaging interval (Δt) is two seconds and the 'cut-off' frequency is therefore approximately $(1/2\Delta T)$ ·25 cycles sec^{-1}. At the wind speeds considered (10 m sec^{-1}) the corresponding wave number is about 0·25 cycle m^{-1}.

The contribution to the variance under the theoretical curve of Fig. 6 made by wave numbers less than this 'cut-off' value is in fact 90 per cent of the total variance given by Eq. (6). Accordingly the apparent intensity of turbulence will be about 5 per unit less than that given by Eq. (7). For the Sale site these results lead to $I_{12{\cdot}2} = 0{\cdot}168$ (0·170); $I_{64} = 0{\cdot}120$ (0·124); $I_{153} = 0{\cdot}111$ (0·098). The values in parenthesis are the average values from the observations, given in Table 1 (b). These results are also shown in Fig. 6. This reasonable agreement with observation does help to confirm the form of the empirical expression used to represent the spectrum.

In order to apply this spectrum to practical problems all that is required is a knowledge of the surface-drag coefficient κ. Suggested values of these (and of α, the power law index) are given below :

Type of surface	κ	α
Open unobstructed country (e.g., prairie-type grassland, arctic tundra, desert)	·005	·15
Country broken by low clustered obstructions such as trees and houses (below 10 m high)	·015-·020	·27-·31
Heavily built-up urban centres with tall buildings	·050	·43

The first of these categories conforms to terrain exemplified by that at Sale and Cardington for which results are available. The values in the second category were based largely on the Brookhaven data. The values of κ in the third category were estimated from the roughness length which observations by Jensen (1958) in the centre of Copenhagen, and by Shiotani and Yamamoto (1950) in the suburbs of Tokyo, suggest is about 3 m* (one-tenth of a typical building height). This suggests a drag coefficient between three and four times that at Brookhaven where the roughness length, calculated from the velocity profile, is about 1 m. (The latter calculations are based on the Prandtl formula for the velocity profile near the ground in a neutrally stable atmosphere).

Values of α agree with those suggested by Davenport (1960).

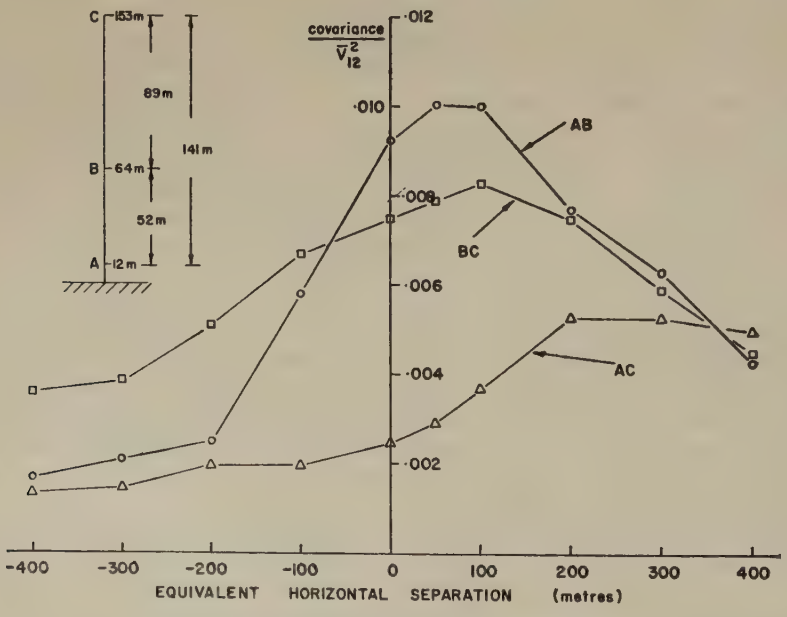

Figure 8. Normalized covariance between horizontal wind speeds at stations on a vertical mast for different equivalent horizontal separations.

Equivalent horizontal separation = time interval between velocity readings × mean velocity at 12 m (positive when upper station leading).

* This estimate is made from the observations and does not quite agree with the values *deduced* by the authors which do not always appear to be appropriate. Jensen has used the upper two (of three) measurements made at heights where the logarithmic profile probably no longer holds. The lower two measurements were thought more appropriate.

5. Cross-correlation and co-spectra

In addition to the auto-correlation coefficients of the Sale runs, cross-correlation coefficients of the velocity readings at pairs of stations for various time lags were calculated. From these the co-variance diagrams (for various time lags) were obtained and normalized (by dividing by the square of the 12 m velocity) and then averaged using a spatial instead of the original time separation or lag. This last step was carried out by multiplying the time-lag interval by the mean 12 m velocity. Results are shown in Fig. 8. (The average cross-correlation coefficients can be found by dividing the co-variances by the product of the intensities at the two stations).

The maximum correlation between pairs of stations is seen to occur, not simultaneously but at a separation when the upper station leads by an amount approximately equal to the vertical distance between the stations. A similar result has also been obtained by Favre, Gaviglio and Dumas (1957, 1958) in the boundary layer of a wind tunnel. (Some of the possible implications of this have been discussed by Townsend (1957)).

From this normalized co-variance diagram the complex cross-spectrum was obtained. This measures the contributions by the different frequencies to the co-variance between two stations just as the spectrum measures the contributions by the different frequencies to the variance at a single station. The cross-spectrum consists of two parts termed the co-spectrum and the quadrature-spectrum. These measure respectively the in-phase correlation and the correlation when the two readings are one-quarter of a period out of phase.

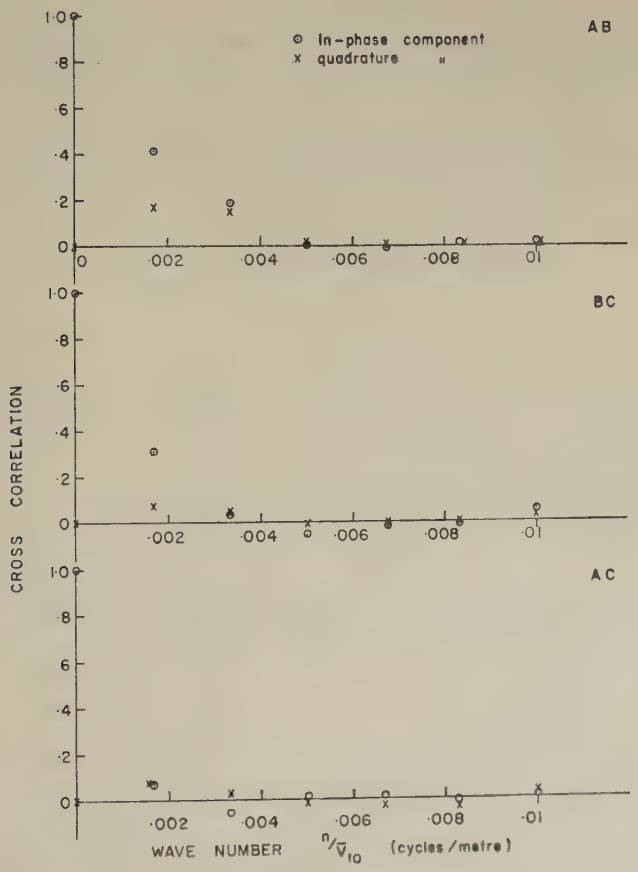

Figure 9. Cross-correlation spectra for stations on a vertical mast.

Of possible greater interest than the cross-spectrum itself is the cross-correlation spectrum (also complex) which can be defined as follows :

$$R_{12}(n) = \frac{Co_{12}(n) + i\, Qu_{12}(n)}{\sqrt{S_1(n) \,.\, S_2(n)}} \qquad . \quad . \quad . \quad . \quad . \quad (8)$$

in which

$R_{12}(n)$ = cross-correlation between velocity fluctuations of frequency n at stations 1 and 2.

$Co_{12}(n)$ and $Qu_{12}(n)$ = co-spectrum and quadrature spectrum of velocity fluctuations of frequency n between stations 1 and 2.

$S_1(n)$ and $S_2(n)$ = spectra at stations 1 and 2 respectively.

The three sets of cross-correlation spectra are shown in Fig. 9. In each case it is seen that the in-phase cross-correlation (initially unity for zero-wave number) falls off roughly as a heavily damped cosine wave. The cross-correlation coefficient in quadrature (initially zero) dies away almost as a damped sine wave.

As might be expected the cross-correlation is higher when the vertical distance separating the stations is less. In fact it might be expected that this correlation will be suitably expressed as a ratio of the vertical separation to the wavelength. To test this the *coherence* between velocities at each pair of stations was expressed as a function of the vertical separation to wavelength ratio (denoted by $\Delta z \,.\, n/\overline{V}_1$). The coherence (see Panofsky and McCormick – 1954) is defined as the absolute square of the cross-correlation spectrum given in Eq. 8. The square root of this quantity, which gives the modulus of the cross-correlation spectrum is plotted as a function of $\Delta z \,.\, n/\overline{V}_1$ in Fig. 10 for all three pairs of stations.

From this it is seen that readings from all three stations are fairly well in agreement and certainly no great height-variation in the coherence is apparent. Over the significant part of the curve the points can be closely approximated by a curve of the type

$$|R_{12}(n)| = e^{-k\frac{\Delta z \,.\, n}{\overline{V}_1}}$$

in which $k \approx 7{\cdot}7$.

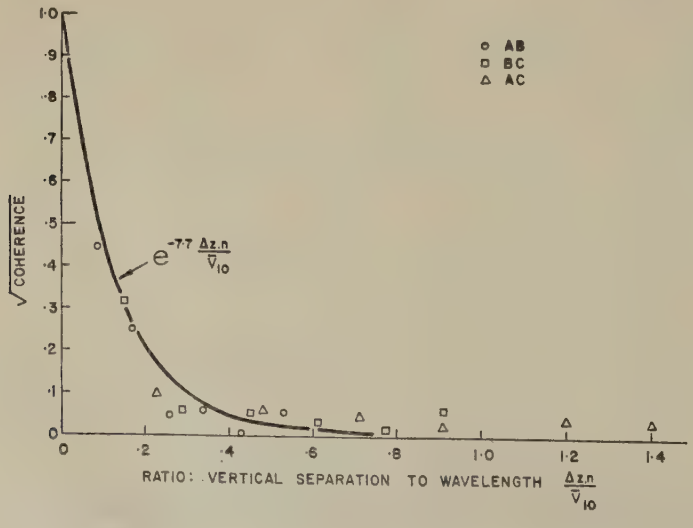

Figure 10. Square root of coherence as function of vertical separation to wavelength ratio ($\Delta z \,.\, n/\overline{V}_{10}$).

In fact this curve is probably more accurately represented by a curve with a series of rapidly diminishing humps. It appears from Figs. 9 and 10 that the coherence approaches zero for the first time when

$$\frac{\Delta z \cdot n}{V_1} \approx \cdot 5$$

This indicates that there is negligible correlation when the height separation is about half the wavelength, and that the eddies are therefore on the average roughly as long as they are high.

Acknowledgments

The writer wishes to record his gratitude to a number of people who helped in this research. In particular, Mr. E. L. Deacon of the Division of Meteorological Physics, Commonwealth Scientific and Industrial Research Organization (Australia) who not only generously provided the Sale records but also gave the writer the benefit of his ideas on the subject; Mr. G. Gimpel of the Electrical Research Association who provided the interesting Cranfield record; Mr. V. Bell, who did the extensive Deuce computations; Miss Watkins who undertook the remaining hand computations; and finally, to Professor Sir Alfred Pugsley, O.B.E., F.R.S., who offered much helpful guidance, discussion, and kindly encouragement and under whose general supervision the work was undertaken.

References

Bushnell, R. H. and Huss, P. O.	1958	*J. Met.*, **15**, p. 180.
Davenport, A. G.	1960	*J. Str. Div., Proc. of Am. Soc. Civ. Engr.*, May, p. 39.
Deacon, E. L.	1955	*Quart. J. R. Met. Soc.*, **81**, p. 562.
Deland, R. J. and Panofsky, H. A.	1957	Penn. State Univ. Div. Met. Phys. Sci. Rep. No. 2.
Favre, A. J., Gaviglio, J. J. and Dumas, R.	1957	*J. Fluid Mech.*, **2**, p. 313-42
	1958	*Ibid.*, **3**, p. 344.
Frost, R.	1947	*Met. Mag.*, London, **76**, p. 14.
Giblett, M. A.	1932	*Geophys. Mem.*, No. 54, Met. Office, London.
Jensen, M.	1958	*Ingenioren Inter.*, **2**, p. 121.
Panofsky, H. A. and McCormick, R. A.	1954	*Quart. J. R. Met. Soc.*, **80**, p. 546.
Panofsky, H. A., Cramer, H. E. and Rao, V. R. K.	1958	*Ibid.*, **84**, p. 270.
Sherlock, R. H.	1953	*Am. Soc. Civ. Eng.* (Trans.) paper, **118**.
Shiotani, M. and Yamamoto, G.	1950	*Geophys. Mag.*, Tokyo, **21**, p. 134.
Smith, M. E. and Singer, I. A.	1956	'*Hurricane winds at Brookhaven National Laboratory*,' Brookhaven (mimeographed report).
Sutton, O. G.	1953	*Micrometeorology*, McGraw-Hill.
Taylor, G. I.	1938	*Proc. Roy. Soc.*, A, **164**, p. 476.
Townsend, A. A.	1957	*IUTAM symposium on boundary-layer research*, Springer 1958 – p. 7.
Van der Hoven, I. and Panofsky, H. A.	1954	Phys. *Final Report*. Div. Met., Pennsylvania State Univ.
Van der Hoven, I.	1957	*J. Met.*, **14**, p. 160.
Wax, M. P.	1956	*Tech. Rep.*, C/T 114, Brit. Elec. and Allied Ind. Res. Assn.

551.511 : 551.558.1 : 551.576.11

Calculations of the ascent of a saturated buoyant parcel with mixing

By B. J. MASON* and R. EMIG
Department of Meteorology, University of California, Los Angeles

(Manuscript received 2 August 1960; in revised form 8 November 1960)

Summary

Numerical computations are made to show how the vertical velocity, temperature, humidity-mixing ratio and liquid-water content of a cloudy parcel will vary with height and time as it ascends from the condensation level, rises through, and mixes with, the surrounding environment whose temperature and humidity distributions are specified. The rate at which the parcel is diluted by mixing is formulated in two different ways which lead to essentially the same conclusions. This treatment does not attempt a detailed description of the mixing processes but arrives at rather critical values for a single parameter used to represent the rate of mixing. If this is sufficiently large to prevent the vertical motion undergoing large oscillations (such as are experienced by a closed parcel), the first-formed cloud is small – usually only a few hundred metres deep over land and perhaps less than 100 m deep over the oceans. This implies that large clouds must evolve by successive thermals rising through air which has been warmed and moistened by their predecessors. Computations are made to demonstrate this stage-by-stage growth. The formation and growth of the first visible cloud appears to depend rather critically upon the excess temperature and velocity with which the thermal reaches the condensation level. These conclusions, and also the computed vertical profiles of temperature, updraught speed and liquid-water in these small clouds, appear to be consistent with observations.

1. Introduction

The object of this work was to compute how the vertical velocity, temperature, humidity-mixing ratio and liquid-water content of a cloudy parcel varies with height and time as it ascends from the condensation level, rises through, and mixes with, its surroundings. The idea was to develop a simple model of cumulus growth which would subsequently provide a dynamical framework for a computation of the growth of a population of cloud droplets. In this model the micro-physical processes of droplet growth, the thermodynamical and dynamical development of the cloud shall be internally consistent and so improve on earlier treatments in which the droplets were considered to grow in an adiabatically-cooled, closed parcel rising with an *arbitrarily assigned* vertical velocity.

Although we are very conscious of the limitations of the following treatment in which the thermal is assumed to possess horizontal homogeneity and the complex mixing process to be represented by only a single parameter, a number of features emerge which appear to be relevant to the *first stages* of cumulus development and which are consistent with observation.

When these calculations were started the only known attempts to compute the properties of a rising cloudy air mass, allowing for entrainment of the environmental air, were those of Stommel (1947, 1951) and of Houghton and Cramer (1951). Later, however, there appeared a more detailed treatment by Haltiner (1959) whose formulation is similar, in some respects, to our own. However, our much more extensive calculations, covering a much wider range of conditions, differ in some important aspects and lead to a number of interesting conclusions which are not apparent in Haltiner's work.

2. Equations for the growth of a saturated parcel with mixing

We now consider the growth of a cloudy parcel, in which the properties are assumed to be uniform in the horizontal plane, as it rises above the condensation level. We realize that horizontal homogeneity is not likely to be achieved in practice and that the relatively undiluted parts of a thermal will grow above the levels predicted for the uniformly mixed parcel, although these will be subject to rapid erosion on emerging from the protection

* Now returned to Imperial College, London.

of the surrounding thermal. While recognizing the complexity of the mixing process, which may be appreciably influenced by such factors as the rate of evaporation of the cloud margins, the stability and humidity of the environment, and may differ for upward and downward motions, these are matters for further research and beyond the scope of this paper. Here we use a single parameter as a portmanteau for the complex physics of the mixing process in the belief that even such a simple model may provide a useful guide to the development of the first cloudy thermals before the stability and other environmental properties have become seriously modified by the convection.

The equations governing the ascent above the condensation level of the first cloudy thermal are as follows :

(*a*) *The equation of motion* of the parcel equates its rate-of-change of momentum to the algebraic sum of the buoyancy and ' drag ' forces. The buoyancy force per unit mass is $((T - T_e)/T_e - w)\,g$ where $(T - T_e)$ is the excess virtual temperature of the thermal over that of its environment at the same level, and w is the liquid-water content in grammes per gramme of air. The latter term, which makes a significant contribution to the buoyancy, was omitted by Haltiner. We assume that, in addition to a net transfer of mass between the environment and the thermal due to entrainment, there is also a turbulent interchange of both heat and momentum which gives rise to a ' drag ' force in the manner described by Priestley (1953, 1954). We make the further simplification that the exchange coefficients are the same for heat and momentum.

The equation of motion then reads :

$$\frac{d}{dt}(MU) = M\left(\frac{T - T_e}{T_e} - w\right)g - MkU,$$

or

$$\frac{dU}{dt} = \left(\frac{T - T_e}{T_e} - w\right)g - \left(k + \frac{1}{M}\frac{dM}{dt}\right)U, \qquad . \quad . \quad (1)$$

where U is the vertical velocity of the thermal, M its mass, and T_e is the environmental temperature. Vertical motions in the environment have been neglected. Compensating downward motions in the environment would effectively reduce the acceleration of the parcel, but, in practice, they may be partially compensated by the large-scale convergence of air into the convective region. In any case, a reliable assessment of their magnitude must await the computation of the three-dimensional flow around a rising thermal.

(*b*) *Thermodynamic equations.* The cloudy air is assumed to remain just saturated with respect to liquid water and so the rate-of-change of humidity-mixing ratio, $dx/dt \doteq d/dt\,(\epsilon e/p)$ is, according to the Clausius-Clapeyron and hydrostatic equations :

$$\frac{1}{x}\frac{dx}{dt} = \left(\frac{gU}{RT} + \frac{\epsilon L}{RT^2}\frac{dT}{dt}\right), \qquad . \quad . \quad . \quad . \quad (2)$$

where ϵ is the density of water vapour relative to that of dry air, L the latent heat of condensation, R the gas constant for dry air and T the temperature of the parcel.

The rate-of-change of temperature of the thermal may be evaluated by equating the heat released by condensation $(-MLdx)$, to that required to saturate the entrained environmental air and to warm it from T_e to T, $[L(x - x_e)\,dM + C_p(T - T_e)\,dM]$, plus the heat lost by diffusion to the environment, $Mkdt\,[C_p(T - T_e) + L(x - x_e)]$, plus the energy absorbed by the gas in expanding from pressure p to $p - dp$ $[M(C_p\,dT - RT\,dp/p)]$.

This, together with Eq. (2) and the hydrostatic equation yields

$$\frac{dT}{dt} = \frac{-\frac{gU}{C_p}\left[1 + \frac{Lx}{RT}\right] - \left(k + \frac{1}{M}\frac{dM}{dt}\right)(T - T_e) - \frac{L}{C_p}\left[\left(k + \frac{1}{M}\frac{dM}{dt}\right)(x - x_e)\right]}{\left[1 + \frac{L^2\epsilon x}{C_p RT^2}\right]} \quad . \quad (3)$$

Conditions in the environment are represented by

$$\frac{dT_e}{dt} = U\frac{dT_e}{dz}, \quad x_e = H\epsilon\frac{e_s(T_e)}{p},$$

where H is the humidity.

It will be seen that if $(k + 1/M\, dM/dt) = 0$, Eq. (3) reduces to the usual expression for the saturated adiabatic lapse rate.

The rate-of-change of liquid-water content is

$$\frac{dw}{dt} = -\frac{dx}{dt} - \left(k + \frac{1}{M}\frac{dM}{dt}\right)(x - x_e + w) \quad . \quad . \quad (4)$$

If now k and $1/M\, dM/dt$ are specified, Eqs. (1) to (4) may be integrated numerically to evaluate U, T, $(T - T_e)$, x and w as functions of height z and t.

Evaluation of both k and $1/M\, dM/dt$, as functions of U, z or t, require much more knowledge of the air motion in and around the thermal than we now possess. Priestley defines k, the exchange coefficient, by $k = K/r^2$, where K is the transfer coefficient for dominant eddies of radius r. If we assume $K \approx 4 \times 10^4$ cm^2 sec^{-1}, and imagine the transfer to be due mainly to eddies of 20 to 50 m radius, the corresponding values of k lie between 10^{-3} and 10^{-2} sec^{-1}.

In the simplest case, we shall assume that the 'damping factor,' $k' = (k + 1/M\, dM/dt)$ remains constant during the evolution. We therefore integrate Eqs. (1) to (4) with k' constant for any one computation, but vary k' between 0 and 6×10^{-3} sec^{-1} to investigate the effect of this on the cloud development.

More generally, we may expect k' to depend upon $\Delta T/T_e$, the vertical velocity U and the radius R of the parcel and, accordingly, we write

$$k' = \beta\frac{\Delta T}{T_e}\frac{U}{R},$$

where β is a constant. This formulation is consistent with the thermal expanding along a cone as observed in the model experiments of Woodward (1959). We have no reliable theoretical basis for evaluating β, but again, we may integrate Eqs. (1) to (4) with (Eq. 1) now taking the form

$$\frac{dU}{dt} = \left(\frac{T - T_e}{T_e} - w\right)g - \frac{\beta}{R}\frac{\Delta T}{T_e}U^2 \quad . \quad . \quad . \quad (5)$$

for various values of β/R and determine whether the cloud development is critically dependent upon the adopted value of β/R.

TABLE 1. VALUES OF PARAMETERS USED IN THE COMPUTATIONS

k'	$0,\ 10^{-3},\ 2 \times 10^{-3},\ 4 \times 10^{-3},\ 6 \times 10^{-3}$ sec^{-1}
β/R	$2 \times 10^{-3},\ 4 \times 10^{-3},\ 6 \times 10^{-3},\ 8 \times 10^{-3}$ cm^{-1}
$\alpha = -\frac{dT_e}{dz}$	6, 6·5, 7·0, 8·0, 9·0°C km^{-1}; in some cases the lapse rate was reduced to 6·5°C km^{-1} above 700 mb.
Environmental humidity	60, 70, 80, 90 per cent.
Initial excess temperature of thermal, ΔT_0	0, 0·1, 0·5, 0·6, 0·8, 1·0°C.
Initial velocity of thermal U_0	0, 25, 50, 100 cm sec^{-1}
Cloud base	$T_0 = 10$°C, $p_0 = 900$ mb (temperate clouds)
	$T_0 = 20$°C, $p_0 = 950$ mb (trade-wind cumuli)

The equations were integrated numerically in time steps of usually 5 or 10 sec (checks for computational stability were made by using time steps of 1 sec) on the IBM 709 high-speed computer, values of U, T, $(T - T_e)$, x, w, z and the pressure p being printed usually once every minute. Computations were made for various values of environmental humidity and lapse rate, of the mixing parameters k' or β/R, and of the initial velocity and excess temperature of the thermal on arriving at the condensation level. The values chosen for these parameters are shown in Table 1; in all, computations representing the growth of several hundreds of different clouds were made.

3. The formation of proto-clouds over land

The outstanding feature of the computations for an adiabatically-cooled, closed parcel in which there is no entrainment nor mixing with the environment, i.e., $k' = 0$, is that the vertical motion of the parcel is violently oscillatory as shown in Fig. 1. Very strong updraughts, in excess of 10 m sec^{-1}, are followed within a few minutes by even stronger downward motions. The magnitudes of these vertical motions, which are rather sensitive to the value of the environmental lapse rate, are much higher than those normally observed except in very vigorous, mature thunderstorms. The difference in temperature between the draughts and the environment at the same level may reach several degrees Centigrade and the liquid-water content exceed 8 g kg^{-1}. All these characteristics of the adiabatic model, together with the fact that the cloud development is, in this case, independent of the environmental humidity, appear strongly at variance with observed behaviour of cumuli.

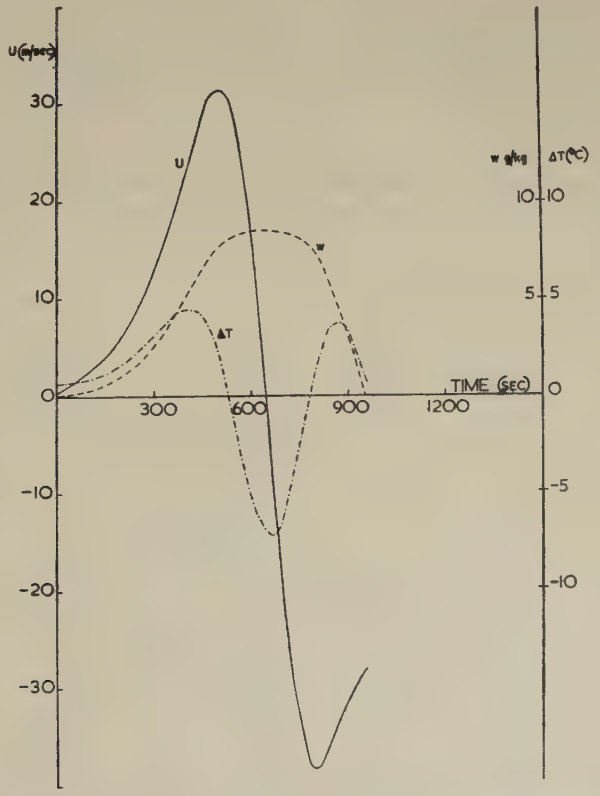

Figure 1. Updraught velocity U, liquid-water content w, and excess temperature ΔT of a closed parcel as functions of time of ascent above the condensation level. Cloud-base temperature $T_0 = 10$°C, pressure $p_0 = 900$ mb, lapse rate $\alpha = 7$°C km^{-1}, $\Delta T_0 = 0$°C, $U_0 = 50$ cm sec^{-1}, $k' = 0$.

The next set of computations, in which k' was assumed to be constant during the development of any one parcel, showed that oscillatory motion is strongly damped only if k' exceeds about 4×10^{-3} sec^{-1}. The influence of k' on the vertical motion and the other cloud parameters is illustrated in Table 2.

TABLE 2. INFLUENCE OF $k' = \left(k + \frac{1}{M}\frac{dM}{dt}\right)$ = CONST. ON CLOUD DEVELOPMENT

($T_0 = 283°K$, $p_0 = 900$ mb; $\alpha = 7°C\,km^{-1}$; $H = 80$ per cent, $\Delta T_0 = 0{\cdot}8°C$, $U_0 = 100$ cm sec^{-1})

	U^+_{max}			$U = 0$		U^-_{max}			w_{max} (g kg^{-1})			ΔT_{max}	
k'	U (cm sec^{-1})	t (sec)	z (m)	t	z	U	t	z	w	t	z	+	−
0·001	2,039	480	4,732	660	7,049	1,714	840	4,776	5·71	540	5,902	3·04	3·26
0·002	972	480	2,634	780	4,540	577	1,020	3,485	3·11	600	3,761	1·62	0·73
0·004	204	120	213	300	440	8	305	440*	0·09	180	327	0·80	0·53
0·006	No visible cloud formed												

* cloud has completely evaporated at this stage.

If the value of k' is sufficiently large to damp the oscillations of vertical velocity the growth of the first cloudy parcel or *proto-cloud* is severely restricted and, as seen in Table 3, does not exceed a depth of a few hundred metres unless the environment lapse rate and humidity are exceptionally high and the thermal arrives at the condensation level with an excess temperature of more than 0·5°C. The influences of the environmental lapse rate and humidity, and of the initial excess temperature and initial velocity of the parcel on its subsequent growth are shown in Table 3.

TABLE 3. EFFECT OF INITIAL EXCESS TEMPERATURE, INITIAL VERTICAL VELOCITY, LAPSE RATE AND HUMIDITY ON CUMULUS GROWTH (MODEL 1)

α	H per cent	ΔT_0	U_0 (cm sec^{-1})	U_{max}	z_{max} (m)	t (sec)	w_{max} (g kg^{-1})	
7	80	0·8	100	206	440	300	0·09	Effect of α
8	80	0·8	100	245	913	530	0·25	
9	80	0·8	100	1,173	4,483	780	1·90	
7	70	0·8	100		No condensation			Effect of H
7	80	0·8	100	206	440	300	0·09	
7	90	0·8	100	297	1,572	780	0·71	
8	80	0·1	100		No condensation			Effect of ΔT_0
8	80	0·5	100		No condensation			
8	80	0·6	100	172	358	240	0·03	
8	80	0·7	100	204	584	395	0·11	
*8	80	0·8	100	245	913	530	0·25	
8	80	0·8	25		No condensation			Effect of U_0
8	80	0·8	50	186	465	315	0·05	
8	80	0·8	100	245	913	530	0·25	
7	90	0·8	25	223	927	600	0·43	
7	90	0·8	50	247	1,127	660	0·52	
7	90	0·8	100	297	1,570	750	0·71	

($T_0 = 283°K$, $p_0 = 900$ mb, $k' = 4 \times 10^{-3}$ sec^{-1}, $\alpha = 6{\cdot}5°C\,km^{-1}$ above 700 mb)

According to these calculations, the effect of increasing the environmental lapse rate from 7 to 8°C km^{-1} is relatively small, but an increase from 8 to 9°C km^{-1} produces a large increase in the maximum values of vertical velocity, cloud depth and liquid-water content.

The inhibiting effect of a dry environment is clear. For example, an increase in humidity from 70 to 90 per cent may make the difference between no cloud being formed at all and the development, under otherwise similar conditions, of a proto-cloud more than 1½ km deep. The calculations suggest that no cloud would develop in an atmosphere of 70 per cent humidity and having a lapse rate as high as 9°C km^{-1} unless the parcel possessed an excess temperature of more than 1°C and an initial vertical velocity in excess of 1 m sec^{-1}.

The most critical parameter determining the growth of an initial cloud appears to be the excess temperature which it possesses on arriving at the condensation level. Table 3 shows that whereas no cloud may form for $\Delta T_0 = 0{\cdot}5$°C, an increase to only 0·6°C, under otherwise similar conditions may produce a cloud about 450 m deep, while an increase to 0·8°C would produce a cloud of twice this depth.

There is very little observational evidence as to whether thermals do, in fact, arrive at cloud base with excess temperatures of 0·5 — 1·0°C, but the Meteorological Research Flight have measured, with a high-speed resistance thermometer, temperature fluctuations in clear air of up to 2°C over horizontal distances of order 100 m, at heights of a few thousand feet above the ground.

The calculations suggest that two parcels arriving at the condensation level with temperatures differing by only 0·1°C may experience considerable differences in vertical development. Over land, such temperature differences may readily be attributed to differences in the surface temperatures of the ground sites from which the thermals originate. It would appear that the wide range of sizes exhibited by small cumulus growing over land may be explained in terms of these temperature differences reinforced by spatial differences in humidity caused by the evaporation of pre-existing clouds. This latter aspect will be discussed in more detail in § 5.

The cloud growth is not quite so sensitive to the initial velocity U_0 of the parcel although, in marginal circumstances, as Table 3 indicates, an increase from ¼ to ½ m sec^{-1} may make the difference between the appearance of a small cloud and no cloud at all.

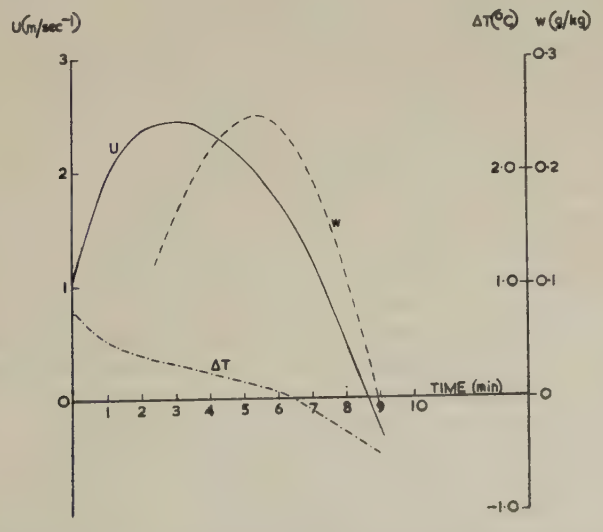

Figure 2. U, w and ΔT as functions of time of ascent above condensation level for a parcel mixing with its surroundings according to Model I with $k' = 4 \times 10^{-3}$ sec^{-1}. ($T_0 = 10$°C, $p_0 = 900$ mb, $\alpha = 8$°C km^{-1}, $H = 80$ per cent, $\Delta T_0 = 0{\cdot}8$°C, $U_0 = 100$ cm sec^{-1}).

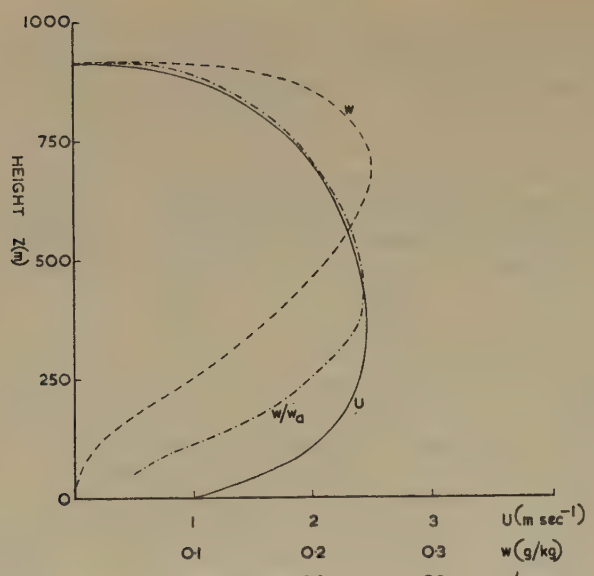

Figure 3. The parameters of Fig. 2 plotted as functions of height above the condensation level.

The cloud marked with an asterisk in Table 3 is thought to represent rather well the first stage of cumulus development in a moderately unstable atmosphere. The detailed variations of U, w and ΔT with time and height for this cloud are shown in Figs. 2 and 3. In Fig. 3 we also show how the ratio w/w_a varies with height, w_a representing the value of the liquid-water content computed on the basis of adiabatic ascent. This ratio reaches a maximum value of 0·25 about half-way up; this agrees rather well with measured vertical profiles of liquid water in small cumulus.

We re-emphasize the main conclusions of these computations that, if the cloud motion is critically damped by mixing with the environment, the first-formed cloud is small and the initial properties (ΔT_0, U_0) of the parcel at the condensation level are of critical importance in determining its subsequent development. If, however, the drag forces are small enough to allow large vertical oscillations of the cloudy thermal, strong vertical motions may develop for very small values of ΔT_0 and U_0; this development is not greatly affected if the values of these parameters are substantially increased but is now more sensitive to the environmental lapse rate and humidity. Rather similar conclusions were reached by Morton (1957) concerning the behaviour of clouds formed in buoyant plumes penetrating a moist atmosphere. Herein lies the reason for the apparent contradictory conclusions reached by Haltiner and ourselves. Haltiner was led to conclude that the initial temperature and velocity of the parcel were unimportant for its growth compared with the lapse rate and environmental humidity because he considered only cases for which his computations, had they been carried further, would have shown the vertical motion to be strongly oscillatory. We do not wish to attach too much significance to the computed value of k' at which, according to our simple model, the vertical motion becomes critically damped. The computations do, however, illustrate how the cloud behaviour may be modified by mixing and suggest that if, in fact, the vertical motion is not violently oscillatory, it is determined by the acceleration, buoyancy and rate of mixing of the parcel in such a way that the latter may lie between rather narrow limits.

Turning now to the model in which we assume the drag forces to be proportional to the square of the vertical velocity, we find that if the factor β/R of Eq. (5) is less than 4×10^{-3} cm^{-1}, the vertical motion of the cloudy parcel becomes strongly oscillatory for the initial conditions of Table 1, although the maximum velocities are not so large as those attained in Model I. If, on the other hand, β/R exceeds 6×10^{-3} cm^{-1}, no clouds are

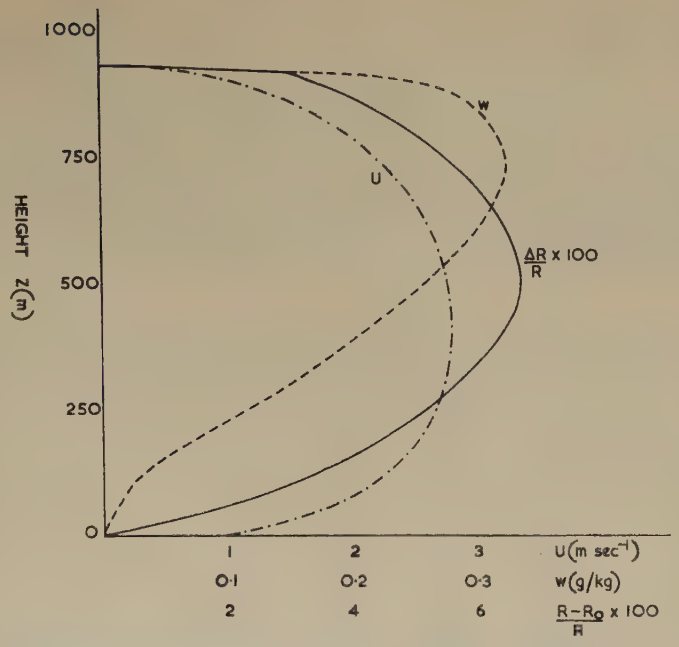

Figure 4. U, w and the radius R of the thermal as functions of height according to Model II with $\beta/R = 4 \times 10^{-3}$ cm^{-1}, $T_0 = 10°$C, $p_0 = 900$ mb, $\alpha = 7°$C km^{-1}, $H = 80$ per cent, $\Delta T_0 = 0{\cdot}8°$C, $U_0 = 100$ cm sec^{-1}

formed unless the environmental humidity reaches 90 per cent. Thus, according to this formulation of the problem, β/R must usually lie between 4×10^{-3} and 6×10^{-3} cm^{-1} if non-oscillatory, proto-clouds are to form.* Some typical results of computations made with $\beta/R = 4 \times 10^{-3}$ cm^{-1} are shown in Table 4. They show very similar characteristics to those of Table 3 indicating that, if the drag forces are large enough to damp vertical oscillations of the thermal, the computed development of the proto-cloud is not greatly affected by choosing a linear or a quadratic form of the damping term. The latter formulation has the attraction that the rate of dilution is inversely proportional to the radius of the thermal which is in line with observational experience that small clouds tend to be eroded more rapidly than larger ones. The vertical profiles of velocity, water content and w/w_a for a cloud achieving a thickness of about 1 km on this second model are shown in Fig. 4 and are, in fact, very similar in shape to those of Fig. 3.

If, on this model, we put the exchange coefficient $k = 0$ and write

$$k' = \frac{1}{M}\frac{dM}{dt} = \frac{\beta}{R} \cdot \frac{\Delta T}{T} \cdot U, \qquad (6)$$

or

$$\frac{1}{M}\frac{dM}{dz} = \frac{\beta}{R}\frac{\Delta T}{T},$$

we may now calculate how the radius of the thermal will change with height for a given constant value of β/R.

Thus :

$$\frac{1}{M}\frac{dM}{dz} = \frac{3}{R}\frac{\partial R}{\partial z} + \frac{1}{\rho}\frac{\partial \rho}{\partial z} = \frac{\beta}{R}\frac{\Delta T}{T} \qquad (7)$$

For the cloud represented in Fig. 4 and indicated by an asterisk in Table 4, $\beta/R = 4 \times 10^{-3}$ cm^{-1}, and $1/\rho\ \partial\rho/\partial z$ may be neglected compared with $\beta/R\ \Delta T/T$.

* Values for this parameter lying between 10^{-3} and 10^{-2} cm^{-1} may be deduced from measurements on the deceleration of cumulus towers by Malkus and Scorer (1955).

Integrating Eq. (7) we have

$$\ln R/R_0 = \frac{4 \times 10^{-3}}{3} \int_0^z \frac{\Delta T}{T} \cdot dz \quad . \quad . \quad . \quad (8)$$

The percentage increase in the radius of the thermal is plotted as a function of height in Fig. 4. In this particular example, the thermal expands as it rises, achieving a maximum of 107 per cent of its initial radius about half way up and thereafter contracting to 103 per cent at the cloud summit.

TABLE 4. EFFECT OF ΔT_0, U_0, α and H ON CUMULUS GROWTH (MODEL II)

α	H per cent	ΔT_0	U_0 (cm sec^{-1})	U_{max}	z_{max} (m)	t (sec)	w_{max} (g kg^{-1})	
7	88	0·8	50	222	606	385	0·14	Effect of α
8	80	0·8	50	381	2,727	900	0·74	
9	80	0·8	50	459	3,317	960	0·97	
7	70	0·8	50		No condensation			Effect of H
7	80	0·8	50	222	606	385	0·14	
7	90	0·8	50	374	2,637	960	0·99	
8	80	0·1	50		No condensation			Effect of ΔT_0
8	80	0·5	50		No condensation			
8	80	0·6	50	179	526	400	0·03	
8	80	0·7	50	251	1,460	780	0·32	
8	80	0·8	50	381	2,727	900	0·74	
7	80	0·8	25	189	464	345	0·05	Effect of U_0
7	80	0·8	50	222	606	385	0·14	
7	80	0·8	100	278	923	480	0·32	

($T_0 = 283$°K, $p_0 = 900$ mb, $\beta/R = 4 \times 10^{-3}$ cm^{-1})

4. CUMULUS FORMATION OVER THE SEA

Over the sea, because of the small air-sea surface-temperature differences and the uniformity of the sea-surface temperature, it is unlikely that the parcels reaching the condensation level will be appreciably warmer than the environment. In what follows we shall assume that parcels reaching the condensation level are unlikely to possess excess temperatures of more than 0·1°C but that some may possess vertical velocities of up to 1 m sec^{-1} in consequence of their random eddying motions in the sub-cloud layer.

In an attempt to investigate the initial growth stages of maritime trade-wind cumulus we have made similar computations to those in § 3 but with the condensation level at 20°C, 950 mb, and for constant environmental lapse rates of either 6, 7 or 8°C km^{-1} up to the level of the trade-wind inversion at 800 mb.

Under these conditions, with an exchange coefficient $k' = 4 \times 10^{-3}$ sec^{-1}, cloud formation is very unlikely. Even with maximal values of $\alpha = 8$°C km^{-1}, $\Delta T_0 = 0{\cdot}1$°C, $U_0 = 100$ cm sec^{-1} and $H = 90$ per cent, clouds only 120 m deep and containing only 0·02 g kg^{-1} of liquid water would form. In order to produce clouds of this same depth with U_0 only 50 cm sec^{-1}, k' would have to be reduced to 2×10^{-3} sec^{-1}, and if ΔT_0 were zero instead of 0·1°C, the corresponding cloud would be only 50 m deep. Further reduction of U_0 to 25 cm sec^{-1} would require k' to be reduced to 1×10^{-3} sec^{-1} in order to produce a visible cloud. The implication is that the mixing parameter k' must be smaller over the oceans than over the land.

The computations, some typical results being shown in Table 5, indicate that proto-clouds deeper than 100 m will be formed in only rather exceptional circumstances. The small puffs of cloud which mark the beginning of cumulus formation over the trade-wind oceans are probably not much larger than this. The computations suggest that mixing causes their rapid deceleration and that they will usually last for less than 5 min. Because the very small initial buoyancy of the cloud element is rapidly destroyed by mixing, the humidity of the surrounding air is rather critical ; the calculations suggest that unless this exceeds 85 per cent and unless the parcels arrive at the condensation level with vertical speeds in excess of $\frac{1}{2}$ m sec^{-1}, formation of even small clouds will be very unlikely.

TABLE 5. GROWTH OF CUMULUS OVER THE OCEANS

k (sec^{-1})	α	H per cent	ΔT_0	U_0 (cm sec^{-1})	U_{max}	z_{max} (m)	t (sec)	w_{max} (g kg^{-1})	
1×10^{-3}	7	90	0	50	50	146	420	0.125	Effect of k'
2×10^{-3}	7	90	0	50	50	47	150	0	
4×10^{-3}	7	90	0	50		No condensation			
2×10^{-3}	6	90	0	50	50	44	140		Effect of α
2×10^{-3}	7	90	0	50	50	47	150		
2×10^{-3}	8	90	0	50	50	57	180		
2×10^{-3}	7	85	0	100	100	119	190	0·049	Effect of H
2×10^{-3}	7	90	0	100	100	199	320	0·143	
2×10^{-3}	7	90	0	50	50	47	150		Effect of ΔT_0
2×10^{-3}	7	90	0·1	50	58	118	270	0·043	
2×10^{-3}	6	85	0	100	100	106	170	0·045	
2×10^{-3}	6	85	0·1	100	102	170	240	0·090	
2×10^{-3}	7	90	0	25		No condensation			Effect of U_0
2×10^{-3}	7	90	0	50	50	47	150		
2×10^{-3}	7	90	0	100	100	199	320	0·143	

($T_0 = 293$°K, $p_0 = 950$ mb)

5. THE FURTHER GROWTH OF CUMULUS

The computations described above suggest that the growth of the proto-cloud will usually be severely restricted by mixing with the drier environmental air. Typically, they will attain depths of a few hundreds of metres over land and perhaps only 100 m over the trade-wind oceans. It appears that further growth occurs by successive stages in which new thermals rise up through the pre-existing cloud.

A theoretical investigation of the development of a second parcel rising through an *active* proto-cloud is very difficult because the velocity fields of the two parcels will interact. To simplify the problem, we assume that when the second parcel arrives at the condensation level the proto-cloud is quiescent, has assumed the environmental temperature at each level, and has merely created a damp patch in which the relative humidity is 100 per cent. The growth of the new thermal, rising through this damp patch, may then be calculated as before, with all the parameters remaining the same except that the humidity is now taken as 100 per cent between the condensation level and the summit level of the proto-cloud, but reverts to the environmental value at greater heights. Such a computation is likely to underestimate the growth of the second parcel in that the proto-cloud is now assumed to possess zero buoyancy, liquid water, and vertical velocity. On the other hand the assumption that mixing now occurs only with the air in the damp patch and not at all with the drier air outside, will obviously tend to overestimate the growth.

However, the results of the specimen calculation, given in Table 6, do illustrate that a cumulus may grow quite rapidly in stages as successive parcels rise through the residues of their predecessors.

TABLE 6. GROWTH OF NEW THERMAL RISING THROUGH PROTO-CLOUD

Characteristics of a proto-cloud (Environmental humidity = 80 per cent)			
U_{max} (cm sec^{-1})	z_{max} (m)	t (sec)	w_{max} (g kg^{-1})
188	494	375	0·053
Growth of second thermal (H = 100 per cent up to 494 m ; 80 per cent above)			
U_{max}	z (m)	t (sec)	w_{max}
1,094	4,333	720	2·12

$T_0 = 283°K$, $p_0 = 900$ mb, $\alpha = 8°C\,km^{-1}$ up to 700 mb, $6·5°C\,km^{-1}$ above.
$\Delta T_0 = 0·8°C$, $U_0 = 50$ cm sec^{-1}, $k' = 4 \times 10^{-3}$ sec^{-1}.

Thus we see that, whereas the proto-cloud attained a maximum height of only 494 m, a maximum water content of only 0·05 g kg^{-1}, and a maximum vertical velocity of 1·88 m sec^{-1}, the corresponding values for the second thermal are 4,333 m, 2·12 g kg^{-1} and 10·94 m sec^{-1}.

6. Conclusions

This study, which does not attempt a detailed description of the mechanisms by which a cloudy thermal grows and mixes with its surroundings but arrives empirically at rather critical values for a single parameter used to represent the rate of mixing, indicates the manner in which the growth and other properties of the rising thermal will be influenced by its initial properties and those of the environment.

The rate at which the parcel is diluted by mixing with the environment is formulated in two different ways which lead to essentially the same conclusions. If the rate of mixing acts as a sufficiently large brake on the vertical motion to prevent it from becoming oscillatory, the first-formed cloud is small – a few hundred metres deep over land and perhaps less than 100 m deep over the oceans. In such circumstances large clouds must evolve by successive thermals rising through air which has been warmed and moistened by their predecessors.

The formation and growth of the first visible cloud appears to depend rather critically upon the excess temperature and velocity with which the thermal reaches the condensation level. These conclusions, and also the computed vertical profiles of temperature, updraught speed and liquid water in these small clouds, appear to be consistent with observations.

Acknowledgments

This work was carried out whilst one of us (B.J.M.) was on leave as Visiting Professor of Meteorology at the University of California, Los Angeles, and was partly sponsored under the National Science Foundation Contract G-5095.

The authors wish to gratefully acknowledge the use, without charge, of the IBM 709 computer and the other facilities of the Western Data Processing Center of the University of California, Los Angeles.

References

Haltiner, G. J. 1959 *Tellus*, **11**, p. 4.
Houghton, H. G. and Cramer, H. E. 1951 *J. Met.*, **8**, p. 95.
Morton, B. R. 1957 *J. Fluid Mech.*, **2**, p. 127.
Malkus, J. and Scorer, R. S. 1955 *J. Met.*, **12**, p. 43.
Priestley, C. H. B. 1953 *Aust. J. Phys.*, **6**, p, 279.
1954 *Met. Mag.*, **83**, p. 107.
Stommel, H. 1947 *J. Met.*, **4**, p. 91.
1951 *Ibid.*, **8**, p. 127.
Woodward, B. 1959 *Quart. J. R. Met. Soc.*, **85**, p. 144.

551.501.81 : 551.574.13 : 551.578.71

Calculations of Mie back-scattering of microwaves from ice spheres

By B. M. HERMAN and L. J. BATTAN
Institute of Atmospheric Physics, University of Arizona, Tucson

(Manuscript received 23 May 1960; in revised form 17 October 1960. Communicated by D. Atlas)

Summary

Thunderstorms containing hail have been found to have extremely large radar reflectivities. Experimental work by Atlas, Harper, Ludlam and Macklin (1960) has shown that hailstones may have unexpectedly large back-scattering cross-sections. In order to shed additional light on this problem, the normalized back-scattering cross-sections (σ_b) of spherical ice particles with complex index of refraction $N = 1{\cdot}78 - 0{\cdot}0024i$ ($N = m - mki$ where m is the ordinary index of refraction, and mk is the Mie absorption coefficient) were calculated from the complete Mie equations. Small intervals of $\alpha\ (= 2\pi a/\lambda$, where a is the radius of the scattering particle and λ is the wavelength of incident radiation) were taken up to a value of 30. The back-scattering from large ice spheres is shown to be considerably higher than that from water spheres of the same size. In general, the differences between the reflectivities of ice and water spheres increase with increasing α up to an α of about 60.

Calculations of σ_b were made for various values of the complex index of refraction in order to better understand the properties of the back-scattering equations.

1. Introduction

It is well known that when an electromagnetic wave encounters a particle in the free atmosphere, a certain amount of power is intercepted. The particle absorbs a fraction of the power in the form of heat and re-radiates the remainder in various directions. That part of the power scattered back towards the source of the wave is referred to as ' back-scattered ' and represents a quantity of primary interest in all radar applications. The remainder of the power, namely that absorbed and that scattered in other directions, is also of importance in some microwave problems because it is related to attenuation of the wave.

It has been found that when the particle diameter is of the order of magnitude of the wave length involved, the scattering properties of the particles are complex functions of the particle diameters and the complex index of refraction. Studies of this problem were made in the late 1800's by Lord Rayleigh who considered particles much smaller than the wavelength. Mie (1908) published the first exact theoretical treatment of the scattering by spherical particles. Since that time, a substantial amount of research has been done on various aspects of the problem. (See Stratton (1941) for detailed discussion of a concise treatment of the theory involved).

2. Back-scattering cross-section

The back-scattering cross-section, σ, has been defined as the area which, when multiplied by the incident power intensity, gives the total power radiated by an isotropic source which radiates the same power in the backward direction as the scatterer. Thus, one can write

$$\sigma = 4\pi r^2 \frac{P_s}{P_i} \quad . \quad . \quad . \quad . \quad . \quad (1)$$

where P_i is the power density (power per unit area) in the incident plane wave at the position of the scatterer, and P_s is the power density of the scattered field at a distance r from the scatterer in the direction of the source.

Quite evidently σ has the units of length squared. It is common to express the back-scattering cross-section of a particle of radius, a, as a non-dimensional quantity by dividing σ by the area of the particle. This leads to

$$\sigma_b = \frac{4r^2}{a^2}\frac{P_s}{P_i} \quad . \quad . \quad . \quad . \quad . \quad . \quad (2)$$

a quantity referred to as the normalized back-scattering cross-section.

As shown by Aden (1951) and others, when spherical particles and linearly polarized electromagnetic waves are involved

$$\sigma_b = \frac{1}{\alpha^2}\left|\sum_{n=1}^{\infty}(2n+1)(-1)^n(a_n^s - b_n^s)\right|^2 \quad . \quad . \quad . \quad (3)$$

where α is $2\pi a/\lambda$ and λ is the wave length. The terms a_n^s and b_n^s are referred to as scattering coefficients and involve spherical Bessel and Hankel functions. The quantity n refers to the term of the expansion of the coefficients.

It can be shown that the scattering coefficients are given by

$$\begin{aligned} a_n^s &= -\left[\frac{J_n(\alpha)}{H_n(\alpha)}\right]\cdot\left[\frac{\sigma_n(\alpha) - N\sigma_n(N\alpha)}{P_n(\alpha) - N\sigma_n(N\alpha)}\right] \\ b_n^s &= -\left[\frac{J_n(\alpha)}{H_n(\alpha)}\right]\cdot\left[\frac{\sigma_n(N\alpha) - N\sigma_n(\alpha)}{P_n(N\alpha) - NP_n(\alpha)}\right] \end{aligned} \quad . \quad . \quad . \quad (4)$$

where $J_n(\alpha)$ is the spherical Bessel function and $H_n(\alpha)$ is a Hankel function of the second kind. The quantity N is the complex index of refraction of the scattering medium expressed in the form $N = m - mki$ where the imaginary part is referred to as the absorption coefficient. The quantities σ_n and P_n depend on appropriate Bessel and Hankel functions respectively, and are given by the following expressions :

$$\sigma_n(\alpha) = \frac{J_{n-1}(\alpha)}{J_n(\alpha)} - \frac{n}{\alpha}$$

$$P_n(\alpha) = \frac{H_{n-1}(\alpha)}{H_n(\alpha)} - \frac{n}{\alpha}$$

Calculations of σ_b for ice were made by Ryde (1946) up to an α of 4, but other studies of the back-scattering of ice have been only for the Rayleigh region. Tables of scattering coefficients for various values of N have been published by Lowan (1949), Penndorf (1956), and Haugen (1953). Aden (1951) has presented a detailed investigation of water particles of dielectric constant $\epsilon = 81 - 7{\cdot}8\,i$ (where $\epsilon = N^2$) and $\lambda = 16{\cdot}230$ cm. He demonstrated that up to $\alpha = 6{\cdot}0$, experimental values of σ_b correspond very closely to theoretical values calculated from Eq. (3).

All of the published back-scattering functions have referred to water particles or to particles having diameters such that values of α have been smaller than about 6. Water particles in the atmosphere are usually of such sizes that α is less than 6. Ice particles, and particularly hail, reach sizes which lead to large values of α over the wave length band commonly used with weather radar. This study has been entirely concerned with the scattering of ice particles and has involved values of α spanning the range likely to be encountered in nature.

Calculations of a_n^s and b_n^s were made with an electronic computer (IBM-650) and were combined to obtain values of normalized back-scattering cross-sections. The complex index of refraction of the ice particles was taken as $N = 1{\cdot}78\text{-}0{\cdot}0024\,i$, a typical value for ice at a temperature of 0°C over the radar wave lengths (1-10 cm) commonly

TABLE 1. CALCULATED VALUES OF σ_b FOR ICE SPHERES OF $m = 1{\cdot}78$, $k = 0{\cdot}00135$

α	σ_b	α	σ_b	α	σ_b	α	σ_b	α	σ_b	α	σ_b	α	σ_b
0·1	7×10^{-5}	2·6	1·4646	7·2	6·7028	12·2	10·2694	17·2	22·9722	22·2	22·6530	27·2	20·0157
0·2	$1{\cdot}1 \times 10^{-3}$	2·7	1·7704	7·4	10·3707	12·4	22·0480	17·4	18·5164	22·4	14·5250	27·4	31·9916
0·3	$5{\cdot}6 \times 10^{-3}$	2·8	2·2135	7·6	6·5771	12·6	21·1806	17·6	15·8850	22·6	22·6408	27·6	26·9828
0·4	$1{\cdot}72 \times 10^{-2}$	2·9	3·1091	7·8	4·7213	12·8	12·3596	17·8	26·8321	22·8	24·5290	27·8	17·1326
0·5	$4{\cdot}08 \times 10^{-2}$	3·0	3·8304	8·0	10·9309	13·0	8·8786	18·0	26·2438	23·0	19·8164	28·0	26·6273
0·6	$8{\cdot}10 \times 10^{-2}$	3·2	2·4544	8·2	4·2887	13·2	17·0460	18·2	14·0078	23·2	26·3726	28·2	32·2838
0·7	0·1412	3·4	2·7091	8·4	6·2415	13·4	21·0595	18·4	16·6284	23·4	21·3766	28·4	23·5485
0·8	0·2205	3·6	6·4172	8·6	3·0834	13·6	9·7223	18·6	29·5433	23·6	19·1324	28·6	25·0345
0·9	0·3106	3·8	8·8841	8·8	5·1995	13·8	14·2656	18·8	22·5677	23·8	23·1163	28·8	24·5703
1·0	0·3928	4·0	4·6144	9·0	9·5341	14·0	14·9815	19·0	14·3629	24·0	33·3929	29·0	25·0680
1·1	0·4384	4·2	3·8994	9·2	6·2737	14·2	12·3239	19·2	25·3810	24·2	23·5812	29·2	24·9565
1·2	0·4168	4·4	13·9184	9·4	5·1482	14·4	17·5082	19·4	28·9221	24·4	17·9974	29·4	31·8320
1·3	0·3131	4·6	11·6072	9·6	7·4351	14·6	10·5048	19·6	18·8585	24·6	33·6263	29·6	25·5204
1·4	0·1580	4·8	6·0102	9·8	13·2813	14·8	11·7126	19·8	21·7305	24·8	34·7672	29·8	20·8244
1·5	0·0598	5·0	12·3088	10·0	10·0378	15·0	10·4418	20·0	22·0843	25·0	21·0351	30·0	35·8092
1·6	0·1530	5·2	11·3175	10·2	7·1086	15·2	16·0916	20·2	19·9911	25·2	23·0087		
1·7	0·3827	5·4	11·0038	10·4	13·9627	15·4	16·5382	20·4	16·2073	25·4	33·1696		
1·8	0·5564	5·6	7·2166	10·6	16·2087	15·6	7·9470	20·6	23·8476	25·6	27·1167		
1·9	0·6316	5·8	9·6191	10·8	11·4612	15·8	17·1191	20·8	21·8578	25·8	22·5253		
2·0	0·6655	6·0	12·0030	11·0	12·5049	16·0	14·2622	21·0	14·0746	26·0	30·5862		
2·1	0·6839	6·2	5·5433	11·2	18·0036	16·2	12·3911	21·2	24·5234	26·2	27·8026		
2·2	0·6579	6·4	11·9571	11·4	13·7645	16·4	14·0905	21·4	22·9111	26·4	21·9221		
2·3	0·6259	6·6	9·2789	11·6	12·3802	16·6	16·9274	21·6	15·5188	26·6	32·3319		
2·4	0·7869	6·8	5·1204	11·8	22·5442	16·8	17·3167	21·8	17·2873	26·8	32·0174		
2·5	1·1241	7·0	11·0214	12·0	16·3903	17·0	16·5161	22·0	21·7763	27·0	19·8481		

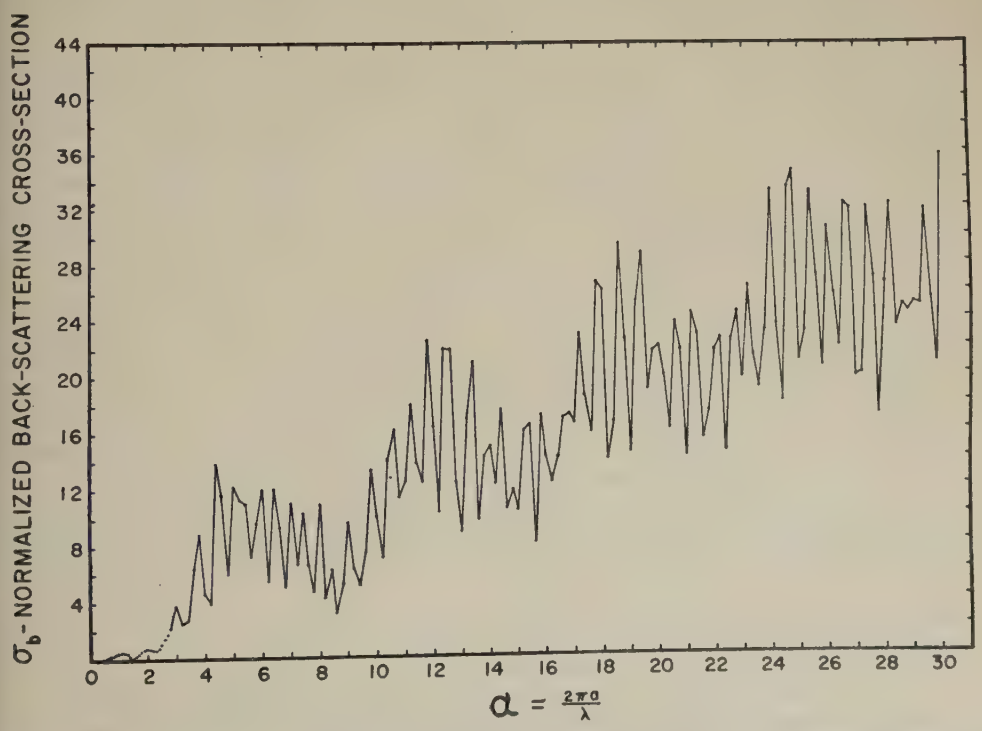

Figure 1. Calculated values of σ_b as a function of α for ice spheres of $m = 1{\cdot}78$ and $k = 0{\cdot}00135$. Intervals of α of 0·1 were used over the dotted portion of the curve; intervals of 0·2 were used elsewhere.

employed for weather observations. At lower temperatures the real part of N remains constant while the imaginary part decreases somewhat (Gunn and East 1954). However, this should not appreciably change the values of σ_b because the imaginary term remains a very small value. The results were quite different from those expected (see Table 1 and Fig. 1).

Fig. 2 shows the normalized back-scattering cross-sections of both ice and water with complex indices of refraction appropriate for a wave length, λ, of 3·21 cm. It can be seen that the oscillations of σ_b for water become quickly damped as α increases, and by the time an α of 10 is reached, the deviations from the limiting value of σ_b for a flat water surface, 0·63, are quite small. The values of σ_b for ice, on the other hand, show no tendency to approach the limiting value of 0·078, but rather continue to increase in an irregular manner up to a value of $\alpha = 30$, the limit to which the original calculations were carried. It is quite probable that, were smaller increments of α employed, the oscillations would be even more irregular than those presented in Fig. 1.

It should be pointed out here that it is not at all obvious from the definition of σ_b that, as the radius of the scatterer approaches ∞, i.e., a flat surface, it should approach the value of the reflectivity from a flat surface of the material in question. However, a proof of this rather peculiar property of σ_b has been worked out by Dr. J. E. McDonald and will be published in the future.

Since the value of σ_b for ice must eventually start decreasing towards its limiting value for a flat surface, additional calculations were made at various values of α ranging up to $\alpha = 500$ (see Table 2 and Fig. 3). It is evident that σ_b reaches a maximum in the vicinity of $\alpha = 60$ and then begins to decrease. At $\alpha = 500$, it has a value of about 0·3.

Almost 15 years ago, Ryde (1946) published the results of calculations of σ_b of ice particles with α as large as 4. However, since he gave few details and no one had duplicated his work, there has been some doubt as to the validity of his results. Over the range of Ryde's calculations, shown in Fig. 2, his calculations are in perfect agreement with the new ones.

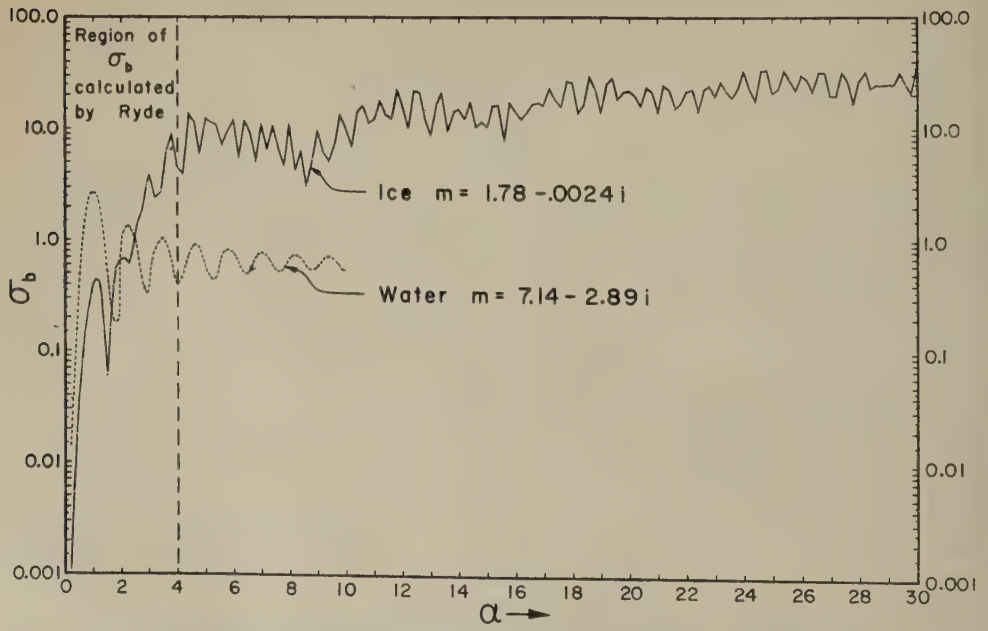

Figure 2. Calculated values of σ_b as a function of α for ice and water spheres. Ryde (1946) published values of σ_b for values of α up to 4·0.

TABLE 2. CALCULATED VALUES OF σ_b FOR ICE SPHERES $m = 1{\cdot}78$, $k = 0{\cdot}00135$ AT SOME VERY LARGE VALUES OF α.

α	σ_b	α	σ_b
40	24·9543	90	15·5643
50	31·0070	100	13·5398
60	38·5239	150	11·0306
70	24·3862	200	7·4799
80	18·8127	500	0·2957

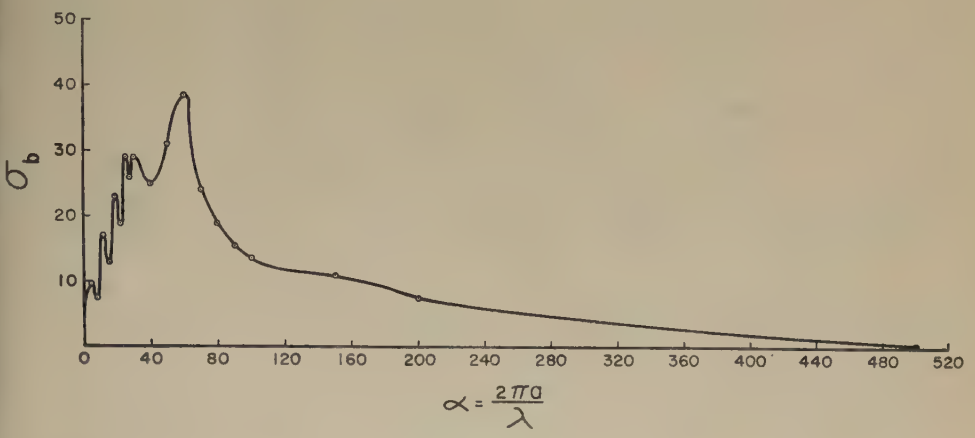

Figure 3. Smoothed curve of σ_b as a function of α for spheres of $m = 1{\cdot}78$ and $k = 0{\cdot}00135$.

The calculations show that over a large range of particle sizes, the back-scattering from large hailstones exceeds that from water drops of the same size. Quite obviously, all-water particles having diameters of several centimeters will not be encountered in the atmosphere, but it is reasonable to expect that a large hailstone may develop a layer of water on its surface when it starts melting. Also, Ludlam (1950) has pointed out that a hailstone may accumulate a film of supercooled water if it sweeps up excessive amounts of supercooled water by collision with smaller cloud and raindrops. Calculations of σ_b for melting hailstones are currently being made and results will be presented in a future paper.

It is important at this point to ask whether or not the equations can be accepted as applicable over the assumed conditions. Fortunately, some experimental data are available with which to compare the theoretical results. Atlas, Harper, Ludlam and Macklin (1960) have been carrying out measurements of the back-scattering cross-section of ice spheres over a range of α from about 0·4 to 10. They have reported excellent agreement between their experimental results and the theoretical findings discussed here.

The result that an ice sphere has a higher radar reflectivity than a water sphere over a large range of particle sizes was unexpected because with particles much smaller than the wave length, the reverse is true. When $\alpha \ll 1$, that is, when Rayleigh scattering prevails, the normalized back-scattering of a single spherical particle is given by

$$\sigma_b = 4\,\alpha^4 \left| \frac{N^2 - 1}{N^2 + 2} \right|^2 \qquad (4)$$

The term inside the brackets has values of about 0·93 and about 0·19 for water and ice respectively. The ratio of about 5 : 1 in favour of water has long been known. The calculations show that outside the Rayleigh region, the ratio of back-scattering of ice and water spheres is a highly variable quantity and cannot be generalized in a simple equation.

This is clearly demonstrated in Table 3 which shows the back-scattering cross-sections of water and ice spheres of various sizes. The results are applicable to 3·21-cm radiation. This Table also shows that a single large hailstone may have a reflectivity some 8 orders of magnitude higher than a typical raindrop.

The conclusion that large hailstones have much larger radar reflectivities than previously assumed has important meteorological significance. Extreme echo intensities of the kind reported by Donaldson (1959) now seem to be more reasonable. Also, rapid changes of echo intensity of the type reported by Battan (1953) need re-examination in the light of this new information.

TABLE 3. BACK-SCATTERING CROSS-SECTIONS OF WATER AND ICE SPHERES IN CM^2 (λ = 3·21 cm)

Diameter cm	α	σ (Water)	σ (Ice)	Ratio
0·1	0·098	$(2{\cdot}67 \times 10^{-6})$	$(0{\cdot}51 \times 10^{-6})$	0·2
3·0	2·93	2·4	24	10·0
6·0	5·86	22·6	291	12·9
10·0	9·78	44·7	1,005	22·5

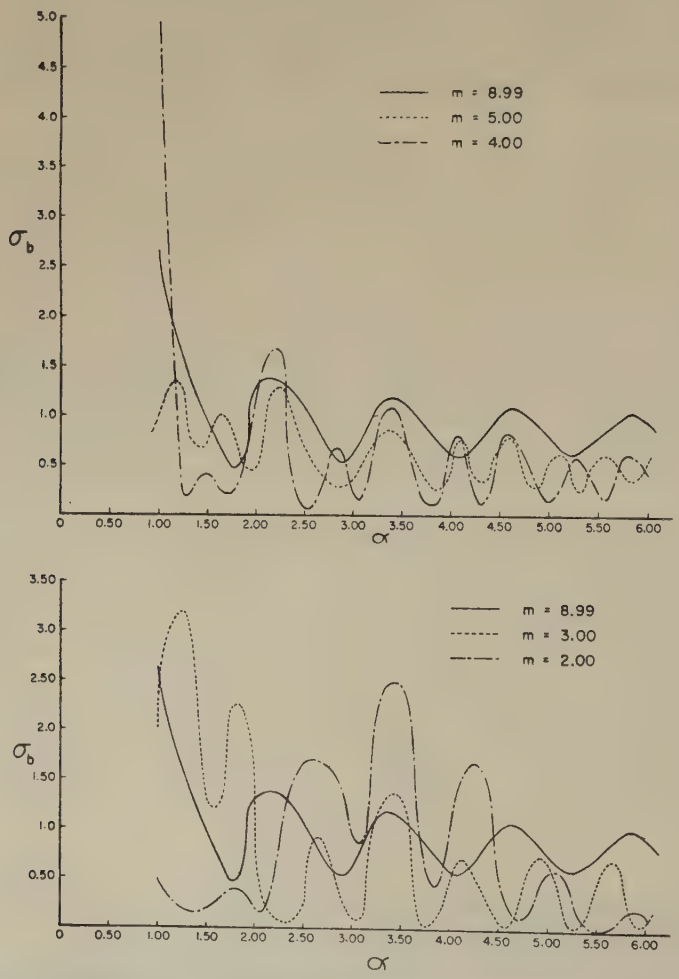

Figure 4. Calculations of σ_b for spheres of $k = 0{\cdot}048$ and various values of m. Here $k = mk$ as explained in text.

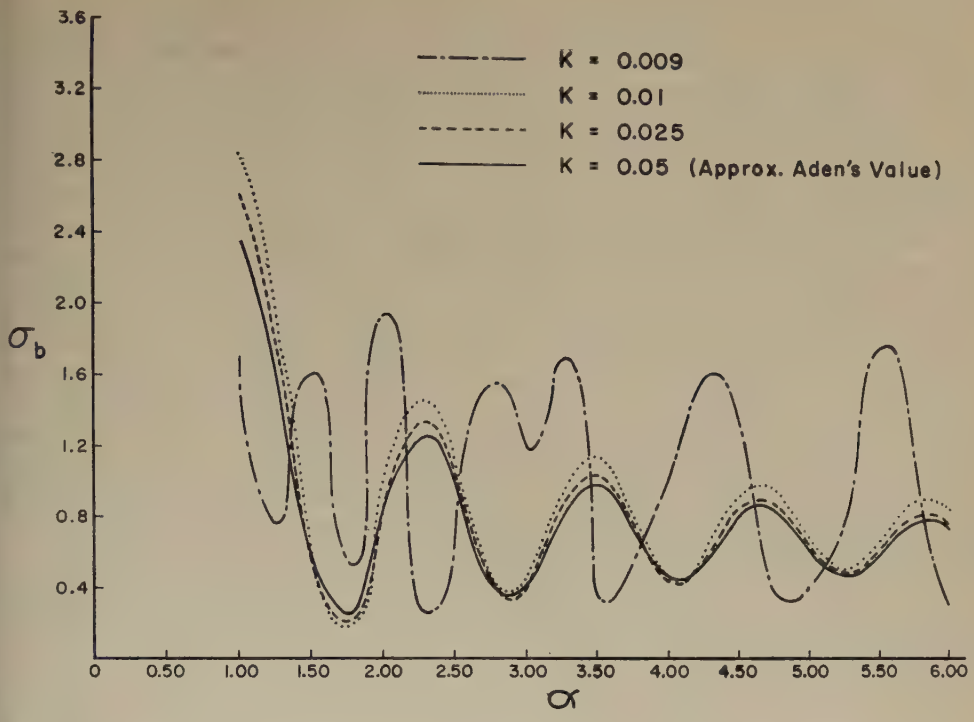

Figure 5. Calculations of σ_b for spheres of $m = 8{\cdot}99$ and various values of k.

3. Calculations of σ_b for various values of N and k

Since the properties of the Mie equations are poorly known, unusual results should probably have been expected. In order to learn more about the equations various additional calculations have been made.

Because of the large differences in the magnitudes of σ_b for water and ice, it was decided to examine the effects of changing the real and imaginary parts of the complex index of refraction over a range between that of water and that of ice. The results of the calculations are shown in Figs. 4 and 5. In Fig. 4 the value of the imaginary part of the complex index of refraction, $mk = k$, was fixed at a value of 0·048, the value used by Aden, while the value of the real part was reduced from 8·99 to 2·0. The values of of σ_b, for the most part, are of the same order of magnitude and the oscillations are damped as larger values of α are approached. It can be seen that at large values of α the curves approach magnitudes of σ_b which decrease as m decreases. This result is quite reasonable, as can easily be shown in the limit, by considering a flat surface.

The curves shown in Fig. 5 are of greater interest because they throw some light on the question of the differences in the back-scattering of water and ice. For these calculations the real part of the refractive index was fixed at 8·99 while the absorption coefficient was changed. It can be seen that over the range from 0·05 to 0·01, the shape of the curves and the magnitudes of σ_b are quite close to one another. However, when the coefficient is reduced from 0·01 to 0·009, the curve suddenly undergoes a substantial change. The phase of the oscillations is very much different than those of the other curves, the amplitudes are larger, and there is little sign that the amplitudes are decreasing with increasing α. On the basis of Fig. 1, it might be expected that further increases of α would result in increases of σ_b.

With an absorption coefficient of 0·005, the frequency of the oscillations as well as the magnitudes is even greater than those shown for $k = 0{\cdot}009$. For example, at α values of 3·75 and 5·5, σ_b has magnitudes of 3·3 and 2·8 respectively.

On the basis of the calculations, it appears that the main factor in causing ice spheres to have such large back-scattering coefficients is the small absorption coefficient. Furthermore, the results show that there is a sudden transition from a scattering regime where the back-scattering decreases fairly rapidly with increasing sphere diameter to one where it oscillates between very large and small values, and where it may increase over a very large range of sphere sizes.

Atlas, Harper, Ludlam and Macklin (1960) have suggested that with a water sphere, the back-scattering is essentially a surface phenomenon as with a metal sphere. However, when the absorption of the medium composing the sphere is extremely low, as is the case with ice, the sphere may act like a lens which focuses the incoming wave on the back side from which it may be reflected backwards in a concentrated beam. This is recognized as a crude description, but, for the time being, it at least permits visualization of a physical process which may have some reality. If, in fact, this is close to the actual mechanism, the calculations shown in Fig. 5 would lead one to conclude that back-scattering from the front side of the sphere is predominant when the absorption coefficients are greater than some critical value. It might be further speculated that until this value is reached, the quantity of energy penetrating the drop and being focused is virtually zero. When the absorption drops below the critical value, there is a marked increase of the fraction of the incoming energy which is focused and back-scattered.

The most obvious conclusion regarding the physical processes involved is that at this point we know very little with certainty. Further research is in progress and will be reported in subsequent papers.

Acknowledgments

The authors are grateful to General S. R. Browning of the Numerical Analysis Laboratory of The University of Arizona for his contributions to this research.

This work has been mainly supported by the Office of Naval Research under Contract NR-082-164. The National Science Foundation under Grant No. G-8216 also con-contributed partial support.

References

Aden, A. L. 1951 'Electromagnetic scattering from spheres comparable to the wave length,' *J. Appl. Phys.*, **22**, pp. 601-605.

Atlas, D., Harper, W. G. Ludlam, F. H. and Macklin, W. C. 1960 'Radar scatter by large hail,' *Quart. J. R. Met. Soc.*, **86**, p. 468

Battan, L. J. 1953 'Observations on the formation and spread of precipitation in convective clouds,' *J. Met.*, **10**, pp. 311-324.

Donaldson, R. J. 1959 'Analysis of severe convective storms observed by radar,' *J. Met.*, **16**, pp. 281-287.

Gunn, K. L. S. and East, T. W. R. 1954 'The microwave properties of precipitation particles,' *Quart. J. R. Met. Soc.*, **80**, pp. 522-45.

Haugen, D. A. 1953 'On the scattering of light by spherical absorbers,' M.S. Thesis (unpub.), Mass. Inst. Tech.

Lowan, A. N. 1949 *Tables of scattering functions for spherical particles, Appl. Math. Series*, **4**, Nat. Bur. Standards, Washington.

Ludlam, F. H. 1950 'The composition of coagulation elements in cumulonimbus,' *Quart. J. R. Met. Soc.*, **76**, pp. 52-58.

Mie, G. 1908 'Beitrage zur optik trüeber medien,' *Ann. Physik.*, **25**, p. 377.

Penndorf, R. B. 1956 'New tables of Mie-scattering functions for spherical particles,' *Geophys. Res. Pap. No. 45*, Air Force Cambridge Research Center.

Ryde, J. W. 1946 'The attenuation and radar echoes produced at centimetre wavelengths by various meteorological phenomena,' *Met. factors in radiowave propagation.* (Phys. Soc., London).

Stratton, J. 1941 '*Electromagnetic theory*,' (McGraw-Hill, New York), Chapt. IX, § 9.25, 9.26. and 9.27.

551.507.362.2 : 551.521

Heat-balance measurements from an earth satellite – an analysis of some possibilities

By K. J. BIGNELL
Imperial College, London

(Manuscript received 3 August 1960; in revised form 7 December 1960)

Summary

A detailed discussion of the basic ' black ' and ' white ' sphere experiment designed by Suomi, and successfully launched in more elaborate form in Explorer VII in October 1959, is presented. It is concluded that this experiment is in almost every respect well suited for making heat-balance measurements from a simple unstabilized satellite, but that it suffers from the serious disadvantage of any such system that the sampling rate is inadequate for giving the daily or short-term heat balance of any region of the earth. Other main conclusions are : the magnitude of the possible error incurred by employing a spherical detector to measure the vertical intensity of a diffuse, anisotropic radiation stream is estimated to be a few per cent only; corrections for heat transfer by conduction and radiation to the spheres from the main body of the satellite can be reduced to negligible proportions, but heating due to high velocity impacts with gas molecules may be considerable for low orbits (0·16 cal cm^{-2} min^{-1} at 200 km); the time constant of the detector is shown to be not less than about two minutes; the sensitivity is of the order of 1°K per 0·01 cal cm^{-2} min^{-1}; the prospects of checking the calibration of the equipment in flight seem reasonable.

1. Introduction

The importance of heat-balance measurements has been discussed in a paper by Suomi (1958) in which he describes apparatus for making the necessary observations from an earth satellite. Up to the date of writing, this appears to be the only satellite experiment proposed for heat-balance studies, although several writers mention the opportunities afforded by earth satellites (Kelly 1955; Widger and Touart 1957; Wexler 1960). The temperature variation of a satellite vehicle as a function of the radiative field is discussed by Gast (1956).

The instrumentation of a simple satellite must fulfil some very important requirements; the following are essential : simplicity, robustness, low weight and low power consumption. If the satellite is not attitude-controlled, a further very desirable property of a radiation instrument is that it should give the same response for all orientations and should not be influenced by spinning motions. The apparatus described by Suomi satisfies all of the above requirements. It consists essentially of two spherical detectors whose surfaces have different relative absorptivities in the visible and infra-red wavebands. By measuring the temperatures of the spheres it is possible to deduce the intensities of the long and short-wave radiation streams at the satellite, so that information on the heat balance of the earth-atmosphere system can be inferred. A recent article (National Academy of Sciences, Washington; I.G.Y. Bulletin No. 29) refers to a more elaborate array of sensing elements mounted on Explorer VII, consisting of four spheres and two hemispheres, but the principles of operation are not given.

The present study shows that while the technique described by Suomi is admirably adapted to an unstabilized satellite, there are certain difficulties in sampling and in the interpretation of the data. These difficulties are discussed in the following sections and summarized in § 7.

The following symbols are used :

A	$\frac{R}{R+h}$
B	$2\left(\frac{1-\sqrt{1-A^2}}{A^2}\right)$
$B(\lambda, T)$	Planck function
C_L	long-wave anisotropy factor
C_s	short-wave anisotropy factor
e_L	long-wave absorptivity of a surface ($\lambda > 4\ \mu$)
e_L'	total hemispherical emissivity of a surface
e_s	short-wave absorptivity of a surface ($\lambda < 4\ \mu$)
F_L	outward vertical flux per unit area of long wave radiation from earth and atmosphere
F_N	outward vertical flux per unit area of net radiation
F_s	outward vertical flux per unit area of direct solar radiation, i.e., F_s is negative
F_{ss}	outward vertical flux per unit area of scattered solar radiation from earth and atmosphere
h	height of satellite above earth's surface
H	thermal capacity of sphere
i	inclination of satellite orbit to the earth's equator
k	$\frac{e_L}{e_s}$ $\quad k' = \frac{e_L'}{e_s}$
R	radius of earth
$r(p)$	water vapour mixing ratio as function of pressure
S	solar constant at the outer limit of the earth's atmosphere (2 cal cm^{-2} min^{-1})
$T(p)$	temperature of atmosphere as function of pressure
x	$BC_s F_{ss} + S$
y	$BC_L F_L$
Z	solar zenith angle
α	semi-angle subtended by earth at the satellite $= \sin^{-1} A$
σ	Stefan's constant $= 5{\cdot}73 \times 10^{-5}$ erg cm^{-2} sec^{-1} $°K^{-4}$
ψ, θ	directional coordinates (see Fig. 1)

Other symbols are defined where they occur.

2. Specification of the radiation streams

Let us now specify the radiation streams at a point P height h above O on the earth's surface (Fig. 1). The area visible from P is indicated by the closed curve; the radius r of this area (semi-angle at P $= \alpha$) as a function of h is given in Table 1, together with the radii $r_{0{\cdot}5}$ and $r_{0{\cdot}75}$ of those areas subtending 50 per cent and 75 per cent respectively of the total solid angle subtended by the earth at P.

TABLE 1. RADII OF VISIBLE AREA AND AREAS SUBTENDING 0·5 AND 0·75 OF TOTAL SOLID ANGLE

h (km)	200	300	400	500	600	700	800	900	1,000
r (km)	1,591	1,912	2,190	2,450	2,670	2,860	3,040	3,200	3,360
$r_{0\cdot5}$ (km)	258	366	465	555	640	723	795	870	930
$r_{0\cdot75}$ (km)	450	615	770	905	1,030	1,135	1,255	1,360	1,457
B	1·608	1·541	1·495	1·458	1·419	1·397	1·371	1·349	1·329

The radiation streams at P are:

(i) Direct solar radiation denoted by F_s; very nearly all of this is confined to wavelengths shorter than 4 μ

(ii) Diffuse scattered solar radiation from the earth and atmosphere, denoted by F_{ss}; like F_s, this is confined to wavelengths shorter than 4 μ

(iii) Diffuse 'thermal' radiation from the earth and atmosphere, denoted by F_L; very nearly all of this is confined to wavelengths longer than 4 μ.

In general (ii) and (iii) will be anisotropic, so it is necessary to specify their intensities as functions of direction. In a system of cylindrical coordinates, let the intensities of (ii) and (iii) in a direction QP be $I_s(\theta, \psi)$ and $I_L(\theta, \psi)$ respectively, where

$$I_s(\theta, \psi) = \int_0^{4\mu} I_\lambda(\theta, \psi)\, d\lambda \qquad I_L(\theta, \psi) = \int_{4\mu}^{\infty} I_\lambda(\theta, \psi)\, d\lambda$$

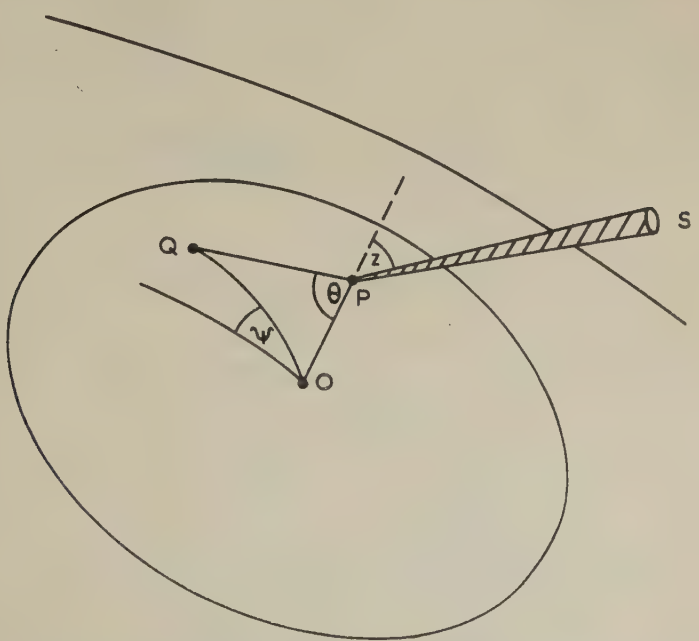

Figure 1. The area visible from the satellite at P is indicated by the closed curve. Solar radiation is incident along SP. O is vertically beneath P and the direction PQ is specified by θ, ψ.

The outward vertical fluxes of radiation per unit area for each radiation stream are then given by :

$$\left.\begin{aligned} &\text{(i)}\quad F_s = -S\cos Z \\ &\text{(ii)}\quad F_{ss} = \int_{\psi=0}^{\psi=2\pi}\int_{\theta=0}^{\theta=\alpha} I_s(\theta,\psi)\sin\theta\cos\theta\,d\theta\,d\psi = 2\pi\int_0^{\alpha} I_s(\theta)\sin\theta\cos\theta\,d\theta \\ &\text{(iii)}\quad F_L = \int_{\psi=0}^{\psi=2\pi}\int_{\theta=0}^{\theta=\alpha} I_L(\theta,\psi)\sin\theta\cos\theta\,d\theta\,d\psi = 2\pi\int_0^{\alpha} I_L(\theta)\sin\theta\cos\theta\,d\theta \end{aligned}\right\} \quad (1)$$

where $I_s(\theta)$ and $I_L(\theta)$ are the mean intensities around a strip with constant θ.

3. Measurement of the radiative fluxes

(a) *Introduction*

In general, the only direct way of measuring the flux of a diffuse radiation stream across unit area in a given direction is to employ a plane-sensing element placed normal to this direction. But this, for satellite use, would involve the difficult task of satellite stabilization in a terrestrial frame, and the use of an omnidirectional sensor is therefore suggested. It is shown in § 3 (*b*) that it is then necessary to know the functions $I_s(\theta)$ and $I_L(\theta)$ in order to obtain a correct result. The only truly omnidirectional sensor is an isolated sphere.

(b) *Theory of the spherical sensor*

Consider a sphere, radius a, situated at P (Fig. 1). We want to find the relation between the flux f incident on the sphere (this determines its temperature, which is to be the measured quantity) and the outward vertical flux per unit area, F, of any radiation stream at P. We have

$$f = \pi a^2 \int_0^{\alpha} I(\theta)\,2\pi\sin\theta\,d\theta$$

which with Eq. (1) gives

$$F = \frac{1}{\pi a^2}\frac{\int_0^{\alpha} I(\theta)\sin\theta\cos\theta\,d\theta}{\int_0^{\alpha} I(\theta)\sin\theta\,d\theta}$$

It is convenient to rearrange this by multiplying and dividing by

$$B = \frac{\int_0^{\alpha}\sin\theta\,d\theta}{\int_0^{\alpha}\sin\theta\cos\theta\,d\theta} = 2\frac{1-\sqrt{1-A^2}}{A^2}$$

Then

$$F = \frac{1}{\pi a^2\,CB}f \quad (2)$$

where

$$C = \frac{\int_0^{\alpha}\sin\theta\cos\theta\,d\theta\int_0^{\alpha} I(\theta)\sin\theta\,d\theta}{\int_0^{\alpha} I(\theta)\sin\theta\cos\theta\,d\theta\int_0^{\alpha}\sin\theta\,d\theta} \quad (3)$$

For numerical values of B as a function of h, see Table 1.

(c) *Effects of anisotropic radiation*

For isotropic radiation, $I(\theta)$ = constant and $C = 1$ from Eq. (3). For all other cases C will be different from unity because a spherical sensor gives equal weight to radiation from all directions, whereas the vertical flux per unit area, F, is a sum over all elements of solid angle weighted by cos θ. So if $I(\theta)$ is a decreasing function of θ (limb darkened), C will be less than unity to offset the effect of the added weight given to the darker limb regions. Similarly, if the limb is brighter than the central regions, C will be greater than unity.

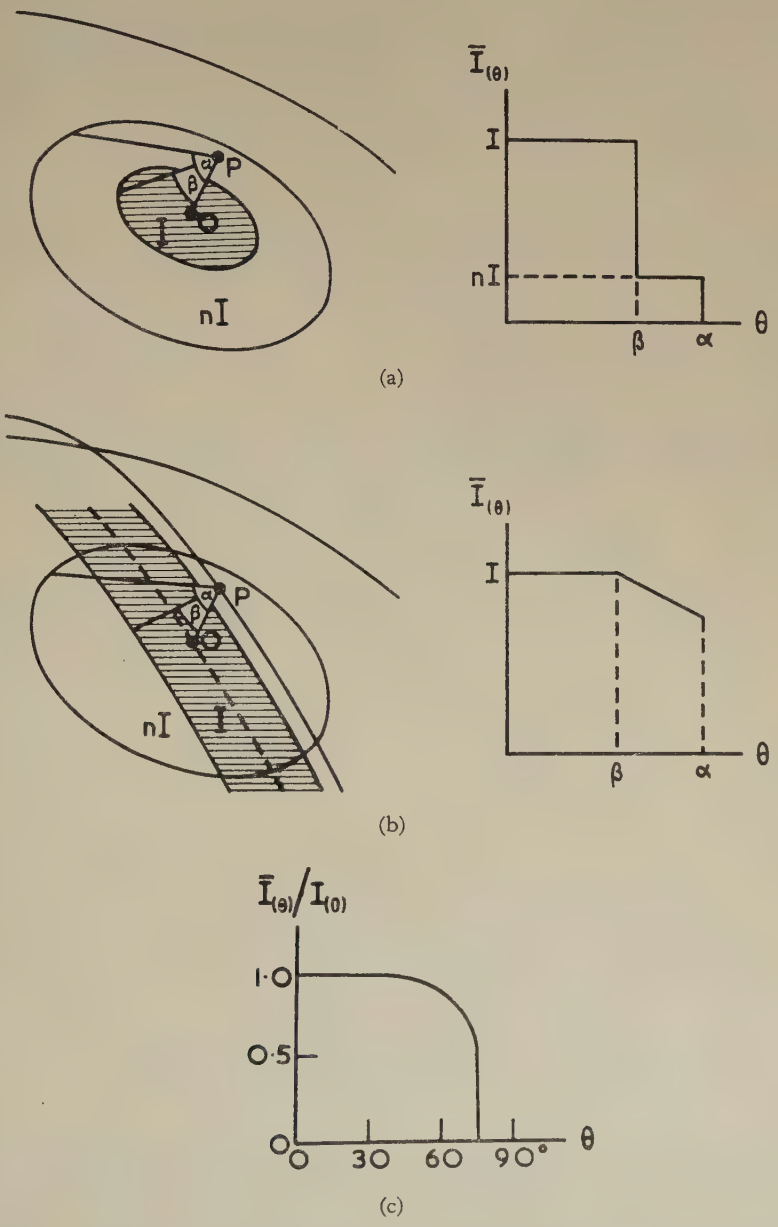

Figure 2 (a) (b) (c). Fields of anisotropic radiation : (a) for instantaneous response; (b) for slow response. The figures on the left in (a) and (b) show the bright (unshaded) and dark (shaded) areas corresponding to the figures on the right. Typical limb darkening in the infra-red is shown in (c) for h = 200 km.

It is of interest to know the limits between which C must lie. The derivation of the function $I(\theta)$ giving a stationary value to C is difficult, but a simple approximation which is particularly appropriate here is a step function, since bright and dark regions will often be separated by sharp boundaries, such as the edges of cloud systems. With this simplification the departure of C from unity will be a maximum (see Fig. 2 (a)) when

$$\left.\begin{aligned} I(\theta) &= \text{constant } (= I) \quad \text{for} \quad 0 < \theta < \beta \\ I(\theta) &= \text{constant } (= nI) \quad \text{for} \quad \beta < \theta < \alpha \end{aligned}\right\} \tag{4}$$

where n is a constant and β is to be determined.

The value to be taken for n is the ratio of the maximum and minimum intensities likely to occur over the area visible from the satellite. For long-wave terrestrial radiation n is about 2 or 3, corresponding to the ratio of the total black body intensities at around 280°K and 220°K. For reflected solar radiation n can be as high as 10, corresponding to the albedo ratio of snow or cloud and the oceans. The stationary value C_0 of C is easily determined by inserting Eq. (4) into Eq. (3) and eliminating β by using the condition $(\partial C/\partial\beta)_{C=C_0} = 0$. The result is

$$C_0 = \frac{A^2}{2(1-\sqrt{1-A^2})} \frac{1+\sqrt{n}}{(1+\sqrt{n}\sqrt{1-A^2})} \tag{5}$$

Inspection of Eq. (5) yields the following :

(i) For isotropic radiation $n = 1$ and $C_0 = 1$ for all h

(ii) As $A \to 0$ (i.e., $h \to \infty$) $C_0 \to 1$ for all n

(iii) As $A \to 1$ (i.e., $h \to 0$) $C_0 \to (1+\sqrt{n})/2$

Values of C_0 for $n = 2$, 10, $\frac{1}{2}$ and $\frac{1}{10}$ as a function of h are given in Table 2.

TABLE 2. VALUES OF C_0 AS A FUNCTION OF HEIGHT AND n

h (km)	200	300	400	500	600	700	800	900	1,000
$n = 10$	1·46	1·40	1·35	1·31	1·29	1·27	1·25	1·24	1·22
2	1·12	1·10	1·09	1·08	1·08	1·07	1·07	1·06	1·06
$\frac{1}{2}$	0·905	0·916	0·921	0·926	0·935	0·937	0·940	0·943	0·948
$\frac{1}{10}$	0·761	0·779	0·794	0·807	0·823	0·828	0·837	0·845	0·855

We see that $(1 - C_0)$ decreases with increasing h, i.e., uncertainties due to anisotropy are smaller for high orbits. It should be emphasized that these values of C_0 correspond to the most unfavourable distributions of radiating matter below the satellite, and would be encountered very rarely. They take the form of a circular bright (or dark) area centred under the satellite surrounded by a dark (or bright) region (see Fig. 2 (*a*)). For long-wave radiation, with $\frac{1}{2} < n < 2$, we obtain $0{\cdot}9 < C_L < 1{\cdot}1$ and for short-wave radiation, with $\frac{1}{10} < n < 10$, we obtain $0{\cdot}76 < C_s < 1{\cdot}46$ at a height of 200 km, which is the lowest height at which a satellite has a useful lifetime. These are instantaneous values, and, as the satellite traverses such regions, the form of $I(\theta)$ changes rapidly such that C returns towards unity. Since the time constant of a practicable detector is likely to be of order one minute (see § 3 (*g*)) we are more interested in the possible extremes in the mean value $\bar{C}$ over about five minutes than in the instantaneous value. If in this time the satellite travels a distance comparable with the instantaneous diameter of its field of view the variation in intensity in the direction of motion is smoothed out and the only contrasts of importance are those perpendicular to the path. From Table 1 we see that this is a fair approximation for low orbits (speed $\simeq 8$ km sec^{-1}). The configuration of radiating surfaces

giving an extreme value to $\overline{C}$ for this case is a bright (or dark) lane placed centrally under the satellite's orbit in a dark (or bright) region (see Fig. 2 (b)). Approximate calculations show that, for the above values of n, we now have $0{\cdot}98 < \overline{C}_L < 1{\cdot}02$ and $0{\cdot}9 < \overline{C}_s < 1{\cdot}1$ at a height of 200 km. Thus the smoothing effect of the slow detector is such that we may enter Table 2 with $0{\cdot}8 < n < 1{\cdot}2$ for long-wave radiation and $0{\cdot}5 < n < 2$ for short-wave radiation.

A further cause of anisotropy, in the case of long-wave radiation, is the 'natural' limb darkening due to obliquity of view of an atmosphere in which temperature and composition are height-dependent. Approximate calculations for a typical atmosphere (e.g., Elsasser 1942, p. 27) were made using the Elsasser radiation chart, giving the result shown in Fig. 2 (c) for a height of 200 km. For this distribution we find that $1{\cdot}01 > C_L > 1{\cdot}005$ for 200 km $< h <$ 1,000 km.

Summarizing the above discussion, we can state that in all cases

$$0{\cdot}98 < \overline{C}_L < 1{\cdot}02$$

$$0{\cdot}9 \ < \overline{C}_s < 1{\cdot}1$$

Since the special configurations of cloud giving rise to these limiting values will be very rare and the pattern of intensity contrasts will not often be highly organized, $\overline{C}$ will in general be much closer to unity than these limits.

(*d*) *Equilibrium temperature of the sphere as a function of the radiation field*

Initially we neglect any heat transfer by conduction and radiation from the main body of the satellite and by conduction to the very tenuous atmosphere. From Eq. (2) the long and short-wave fluxes absorbed by the sphere are

$$\left.\begin{aligned} f_L &= \pi a^2 \, BC_L \, F_L \, e_L \\ f_s &= \pi a^2 \, (BC_s \, F_{ss} + S) \, e_s \end{aligned}\right\} \tag{6}$$

where e_L and e_s are the respective absorptivities of the surface defined by

$$e_L = \frac{\int_{4\mu}^{\infty} e_\lambda \, I_\lambda \, d\lambda}{\int_{4\mu}^{\infty} I_\lambda \, d\lambda} \qquad e_s = \frac{\int_{0}^{4\mu} e_\lambda \, I_\lambda \, d\lambda}{\int_{0}^{4\mu} I_\lambda^{*} d\lambda}$$

where e_λ is the hemispherical spectral emissivity of the surface and I_λ is the spectral distribution of the incident radiation stream.

If the effective equilibrium temperature of the sphere is T, then

$$f_L + f_s = 4\pi a^2 \, \sigma T^4 \, e_L' \tag{7}$$

where

$$e_L' = \frac{\int_{4\mu}^{\infty} e_\lambda \, B_{(\lambda,T)} \, d\lambda}{\int_{4\mu}^{\infty} B_{(\lambda,T)} \, d\lambda}$$

In fact there will be some variation of temperature over the surface of the sphere, depending on the orientation of the spin axis relative to the incident radiation. In the worst case of solar radiation incident along the spin axis the temperature difference between the poles is proportional to $a^2 \, e_s / Kd$ where K is the thermal conductivity of the shell and d its thickness. For a black painted aluminium sphere 1 cm in diameter and 0·1 mm thick the temperature difference is of the order of 1°C, assuming the paint to be a good conductor.

Eqs. (6) and (7) give

$$B(C_L F_L k + C_s F_{ss}) + S = 4\sigma k' T^4 \tag{8}$$

where

$$k = \frac{e_L}{e_s} \qquad k' = \frac{e_L'}{e_s}$$

For the ideal surface material e_λ would be constant out to at least 20 μ. Then $e_L = e_L'$ and $k = k'$ to a very close approximation. In practice, e_λ would not be constant, but the difference between e_L and e_L' should not be more than a few per cent since the weighting functions $B_{(\lambda,T)}$ and I_λ are broadly similar, the main difference being that I_λ is relatively large in the 8-13 μ window region.

(*e*) *Measurement of* F_N

The quantity of greatest interest to the meteorologist is the net flux of radiation F_N from the earth-atmosphere system; the earth satellite provides an opportunity of making world-wide measurements for the first time. We now discuss the determination of F_N at the position of the satellite. We have $F_N = F_L + F_{ss} - S\cos Z$, considered as positive in the outward direction. This can be written, using Eq. (8), as

$$F_N = \frac{4\sigma k' T^4}{B} - S\left(\frac{1}{B} + \cos Z\right) + (1-k)\overline{C}_L F_L - \left(1 - \frac{1}{\overline{C}_L}\right)\overline{C}_L F_L - \left(1 - \frac{1}{\overline{C}_s}\right)\overline{C}_s F_{ss} \quad . \tag{9}$$

In this form we separate those terms which can in principle be determined experimentally from those which can not. Since the product $\overline{C}_L F_L$ can be determined (§ 3 (*f*)), while $\overline{C}_L$ and $\overline{C}_s$ are both unknown, only the last two terms on the right-hand side of Eq. (9) cannot be evaluated, though some indication of their values might be available from synoptic charts of cloud cover. The upper limits of these terms are estimated to be 0·01 and 0·1 cos Z cal cm^{-2} min^{-1} respectively, since $F_L < 0{\cdot}5$ and $F_s < \cos Z$ cal cm^{-2} min^{-1} under the conditions giving rise to extreme values of $\overline{C}_L$ and $\overline{C}_s$.

In most cases these terms will be much smaller than the values given above so that their neglect would not lead to serious error in F_N when F_N is greater than 0·1 $S\cos Z$.

A special case of Eq. (9) should be noted : if we choose $k = 1$ and neglect the last two terms, the expression for F_N reduces to

$$F_N \doteq \frac{4\sigma k' T^4}{B} - S\left(\frac{1}{B} + \cos Z\right)$$

So a single sphere can give all the information necessary for measuring F_N (S is to be assumed) without determining the component fluxes separately. However, it may not be possible to obtain a surface with $k = 1$ in which case it would be necessary to determine $\overline{C}_L F_L$ in order to evaluate the third term in Eq. (9); this problem is dealt with in the next section.

(*f*) *Discrimination between and determination of the fluxes*

Even if it were possible to obtain F_N without measuring the long and short-wave fluxes separately, it would still be of great interest to measure the latter fluxes. In particular, a measure of F_{ss} would give the albedo of the underlying surface, which in turn is a measure of the cloud amount.

A simple special case arises when the satellite is in the earth's shadow. Eq. (8) then reduces to

$$BC_L F_L = 4\sigma T^4 \frac{k'}{k} = 4\sigma T^4 \frac{e_L'}{e_L} \tag{10}$$

We see that $C_L F_L$ can be determined on the night side of the earth by measuring T only. Further, since $k'/k \doteq 1\ (= e_L'/e_L)$ to a very good approximation for all surfaces [see § 3 (*d*)], T will depend only slightly on the coating material of the sphere, especially as $T \propto (k/k')^{\frac{1}{4}}$.

On the sunlit side of the earth we must employ two spheres whose surfaces have different values for k (k_1 and k_2). We then obtain two equations of the form of Eq. (8) which are solved to give

$$BC_L F_L = 4\sigma \frac{k_1' T_1^4 - k_2' T_2^4}{k_1 - k_2} = y \tag{11}$$

$$BC_s F_{ss} + S = 4\sigma \frac{k_1 k_2}{k_2 - k_2} \left(\frac{k_1'}{k_1} T_1^4 - \frac{k_2'}{k_2} T_2^4 \right) = x \tag{12}$$

The relation between the incident fluxes and the equilibrium temperature of a sphere is shown in Fig. 3 for $k_1 = k_1' = 20$ (' white ' sphere) and $k_2 = k_2' = 1$ (' black ' sphere), ' black ' and ' white ' referring to properties in the visible. The sensitivity $\Delta T/\Delta F$ is readily assessed from this diagram, which clearly illustrates the decrease of sensitivity with increase of sphere temperature. Typical values of $\Delta T/\Delta F_L$, with $B = 1{\cdot}5$, are 0·14°K and 0·04°K per 0·001 cal cm^{-2} min^{-1} at $T = 200$°K, 300°K respectively.

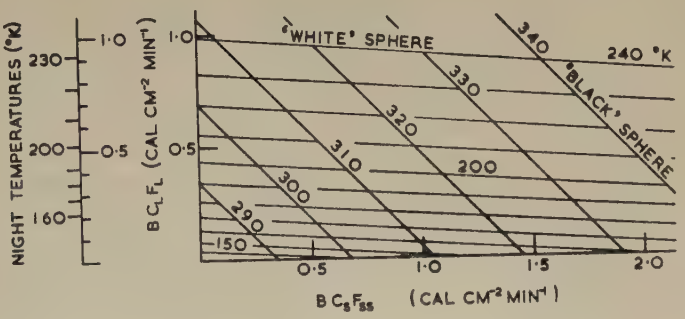

Figure 3. Relation between the incident fluxes and the equilibrium temperatures of black ($k_2 = k_2' = 1$) and white ($k_1 = k_1' = 20$) spheres ($S = 2$ cal cm^{-2} min^{-1}). Over the night side of the earth both spheres have the same temperature.

A discussion of the errors of the determination of x and y from Eqs. (11) and (12) is given in § 6. It is shown there that the error in x is considerably larger than that in y. This is particularly unfortunate from the point of view of estimating albedo since the relevant part of x (i.e., $BC_s F_{ss}$) is often – with low sun – only a small fraction of S. The consequence is that F_{ss} can be measured only to moderate or poor relative accuracy, especially when it is small, i.e., when the solar zenith angle is large; under these conditions we can estimate the albedo only roughly.

Suomi (1958) refers to an alternative method of measuring F_{ss} over areas where the sun is low. He employs two additional spheres of low long-wave emissivity (Tabor coating, $k = 0{\cdot}11$) and shielded from sunlight. It is difficult to assess the likely improvement in the precision of the measurement without a knowledge of the geometry of the shields and the effects of obscuration of the scattered radiation and their own long-wave emission, and possible incomplete shielding from the sun as the spin axis of the satellite precesses.

(g) *Effect of time constant and local sources of heat*

The incident flux of radiation will be a varying quantity, and the time constant of the sphere will lead to a lagging response. The effect on sphere temperature of the heat transfer by radiation and conduction from the main body of the satellite and from the residual atmosphere is also to be considered.

The time constant of a spherical shell of thickness d, density ρ_s at temperature T is $\tau = d\rho_s C/4\sigma T^3 e_L'$ where C is the specific heat of the material. This is the lower limit for τ since the conductivity of the shell and coating has been assumed infinite. For a magnesium shell 0·1 mm thick we find $\tau = 60$ sec at $T = 200°$K and 20 sec at $T = 300°$K. Although it would seem desirable to have a faster response, the advantage is probably rather doubtful since the time averages $\overline{C}_L$ and $\overline{C}_s$ are more uncertain for shorter intervals (see § (3 *c*)). It is to be noted that in an interval of about 5 minutes the satellite traverses a distance of the same order as its instantaneous diameter of vision on the earth.

The heat transfer to the sphere by conduction and radiation from the main satellite body can be reduced to negligible proportions by separating these bodies sufficiently. Since only very slender supports are required there is in principle no difficulty in obtaining the required separation and the ideal conditions so far considered may almost be realised in practice.

The energy dissipation due to collisions with gas molecules is given by $\frac{1}{2}\pi a^2 \rho V^3$ where ρ is the air density and V is the satellite velocity (large compared with molecular thermal velocities). Assuming this energy to be used in heating the sphere, putting $V = 8$ km sec^{-1} and using recent satellite data for ρ (King-Hele 1960), we find that this source of heat is equivalent to an increase of 0·15 cal cm^{-2} min^{-1} in the incident radiation stream at $h = 200$ km ($\rho = 4 \times 10^{-13}$ gm cm^{-3}) and 0·002 cal cm^{-2} min^{-1} at $h = 400$ km ($\rho = 6 \times 10^{-15}$ gm cm^{-3}). Thus, provided perigee height is greater than about 400 km, the effect is negligible.

(*h*) *Reduction of the observations to a standard level*

In general, the satellite's orbit will be elliptical and the flux measurements will be made from different heights at different points in the orbit. It is desirable, indeed essential for integral studies, to reduce the observations to a standard level, at height h_0, say. The flux per unit area at h_0 can be written :

$$F_{h_0} = K\left(\frac{R+h}{R+h_0}\right)^2 F_h$$

where K is a constant at any instant. When the region visible from the satellite is horizontally homogeneous the radiation field below the satellite is radial and $K = 1$, but in all other cases it will differ from unity by an amount depending on the location and intensity of inhomogeneities. It becomes progressively more difficult to estimate K as $h_0 \to 0$, where the field can be appreciably non-radial, so that it is probably not profitable to reduce the observations to a level lower than perigee height. As an example, in the reduction of an observation made at $h = 1{,}000$ km to $h_0 = 500$ km, we find $0{\cdot}5 < K < 2$ for $n = 10$ and $0{\cdot}8 < K < 1{\cdot}2$ for $n = 2$.

4. Choice of k

For a two-sphere system we must choose k_1 and k_2 so that the effect of errors in the measured values of T_1, T_2, k_1 and k_2 is a minimum. A statistical analysis shows that the errors are minimized by making $k_1 - k_2$ as large as possible, i.e., the surfaces should have the largest possible difference in relative emissivities in the long and short wavebands.

There is a major disadvantage in employing a surface with $k < 1$ since this can only be achieved by making $e_L < 1$ and so increasing the time constant, which at best is already long (> 1 minute). Further, diminishing e_L could lead to undesirably high temperatures, at which conventional thermistor materials cannot be used, e.g., a Tabor coated sphere with $k = 0{\cdot}11$ attains a temperature of 500°K to 600°K on the day side of the earth.

The practicable upper limit of k depends on how highly reflecting a surface can be made in the solar waveband. Suomi quotes a value of $k = 19$ for lead carbonate white paint for which $e_L = 0{\cdot}95$ and $e_s = 0{\cdot}05$; other figures quoted are for black paint ($e_L = e_s = 0{\cdot}95$) and for the Tabor coating ($e_L = 0{\cdot}10$, $e_s = 0{\cdot}90$).

We conclude that the choice of k is mainly determined by technical restrictions, with $k_1 \simeq 20$, $k_2 \simeq 1$.

5. In-flight calibration

(a) *Introduction*

Ideally, once the satellite leaves the laboratory the instrumentation should maintain its calibration, i.e., the k's and the temperature calibrations (temperature *vs* signal parameter) should not change. There is the possibility that both of these conditions could fail, the first owing to surface erosion by micrometeorites or radiation damage (Lagow 1957) and the second owing to the development of minor faults in the electronics, including the temperature measuring elements. There are ways of detecting the occurrence of these defects from the observations and it might be possible to correct for them to a fair degree of accuracy.

(b) *Check on temperature calibration*

We have already seen from Eq. (10) that both spheres must have nearly the same temperature when on the dark side of the earth. If the observations indicate an abnormal systematic difference of temperature, then a fault must be inferred in the temperature calibration of at least one sphere, which may be located in either measuring element or in a part of the electronic circuits not common to both elements. In the event of a serious change of calibration it would be possible to recalibrate approximately by reversing the sense of the experiment on suitable occasions, *e.g.*, when the satellite is known to be over a substantial area of reasonably homogeneous surface and atmosphere of known constitution ($T(p)$ and $r(p)$ from radiosonde data). It would then be possible to compute F_L from radiation charts to fair accuracy ($\pm$ 10 per cent) and thence determine the temperature of the spheres to $\pm$ 5°K (from Eq. (10) $\Delta T/T = \frac{1}{4}\,\Delta F_L/F_L$). This provides a single check to $\pm$ 5°K at one point on the temperature calibration. By making repeated checks of this kind over different regions of the earth, the accuracy could be improved and the range covered would be about 160°K to 200°K.

(c) *Check on surface emissivities*

The cooling and warming curves as the satellite enters or leaves the earth's shadow might allow estimates of the emissivities of the surface to be made. At these times there is a large known change ($\pm S$) in the incident radiation and the slope of dT/dt against T^4 is then proportional to e_L' provided that the fluxes arriving from the earth are not also changing. The magnitude of the latter changes is, however, relatively small. With similar reservations, the value of e_s can be inferred directly from the change in the value of dT/dt at the instant of sunrise or sunset. Although the precision of an individual check of this kind is unlikely to be high, it will be possible to perform them about 30 times per day.

It should also be noted that the combination $k_1 k_2/k_1 - k_2$ could be estimated from observations taken when the satellite is in sunshine over the twilight region of the earth, for Eq. (12) then provides, as $F_{ss} \to 0$,

$$S = 4\sigma \frac{k_1 k_2}{k_1 - k_2}\left(\frac{k_1'}{k_1} T_1^4 - \frac{k_2'}{k_2} T_2^4\right)$$

in which [see § 3 (d)] k_1'/k_1, $k_2'/k_2 \simeq 1$. Thus the precision in measuring F_{ss} is aided (see, also, § 6 below). This check can be made about 15 times daily, just before entry into the shadow (observations taken just after exit from the shadow will be subject to large lag corrections as the temperatures are then changing rapidly).

6. Errors

Errors in the flux determinations due to uncertainties in k_1 and k_2 will be systematic, while those due to uncertainties in T_1 and T_2 will be partly random. For this reason these sources of error are considered separately. Table 3 gives estimated errors in the derived fluxes for uncertainties of $\pm$ 5 per cent in k_1 and k_2 ($k_1 = 20$, $k_2 = 1$) and $\pm$ 1°K in T_1 and T_2.

It has been assumed for the purpose of this analysis that k_1 and k_2 are known only from laboratory measurements to $\pm$ 5 per cent. The resulting relative error in $k_1 k_2/k_1 - k_2$ is about 10 per cent. As explained in § 5 (*c*) this factor can be determined from in-flight data. If T_1 and T_2 are measured to $\pm$ 1°K then it is determined to about $\pm$ 3 per cent, which may be better than the accuracy obtainable from laboratory measurements, giving improved precision in the measurement of F_{ss}.

TABLE 3. Summary of errors due to stated uncertainties in k and T (units are cal cm^{-2} min^{-1})

Quantity		From error in T $\pm$ 1°K (Partly random)	From error in k ($\pm$ 5 per cent) (Systematic)	Anisotropy error	Range of quantity
$BC_s F_{ss}$		·04 to ·08	0 to 0·2	0	0 to 2
$BC_L F_L$	Day	·003 to ·018	0 to 0·2	0	0·2 to 1·0
	Night	·003 to ·018	0	0	0·2 to 0·5
F_N	Day	0 to 0·02	0 to 0·1	0·1 cos Z	0·1 to − 1·5
	Night	0 to 0·02	0	0·01	0·2 to 0·3

7. Sampling

We now examine the sampling obtainable by a satellite. Figure 4 shows the disposition of the satellite's orbit with respect to the earth's equator and orbit in the most general case. The terminator is the great circle dividing the day and night sides of the earth;

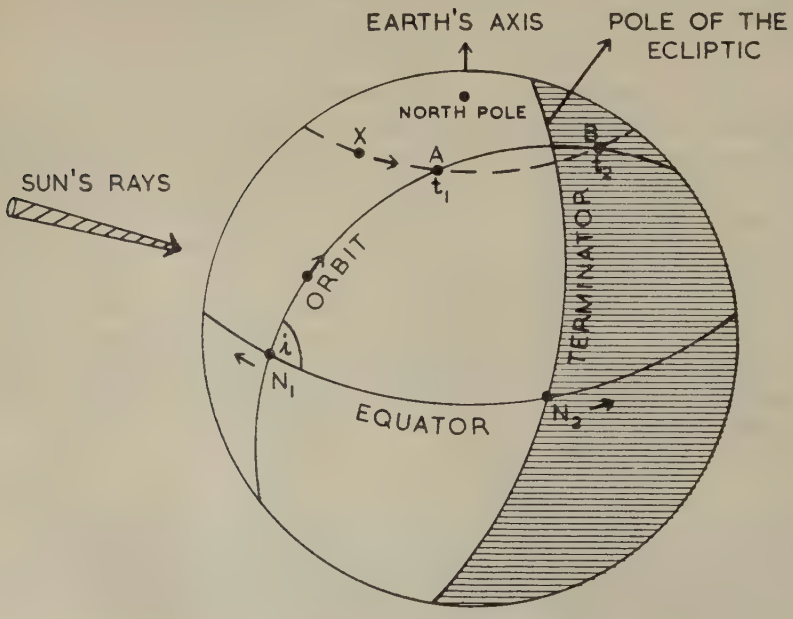

Figure 4. Geometry of a satellite orbit

it rotates slowly in space (at about 1° per day) about the pole of the ecliptic, which is the normal to the plane of the earth's orbit, so that its intersection N_2 with the equator moves in the direction indicated. The satellite's orbit precesses about the earth's axis in the direction shown at a rate of approximately 9 cos i degrees per day (for a low, nearly circular orbit; King-Hele 1960), its inclination i remaining constant. Consider a point X situated on the earth at latitude ϕ ($< i$). Since the rotation of the earth carries X under the orbit twice a day it follows that the satellite, unless otherwise controlled in flight, will, in general, pass close to X only twice daily, when X is near A and B. It is convenient to specify A and B by their local solar times t_1 and t_2. It is apparent that all places with latitude ϕ will be observed by the satellite at about the same two local times t_1 and t_2. The effect of the earth's angular motion around the sun and the precession of the satellite's orbit is to cause a slow change in t_1 and t_2 given by

$$\frac{\partial t_1}{\partial t} = \frac{\partial t_2}{\partial t} \simeq -4\,(1 + 9\cos i) \text{ min day}^{-1} \text{ (for a low, nearly circular orbit)}$$

So the satellite will cross a given latitude circle about 22 min earlier (in local time) each day for $i \simeq 60°$. For the special case of $i = 96{\cdot}5°$ the orbital precession cancels the earth's angular motion and the satellite always crosses a given latitude circle at the same local times.

Since the orbital period is 1½ to 2 hours, we should obtain 12-16 observations around each latitude circle in the course of a day at each of two nearly fixed local times determined initially by the time of launch. Since the useful area observed by the satellite is of order 1,000 km across, a good sample of observations will be provided in longitude, L.

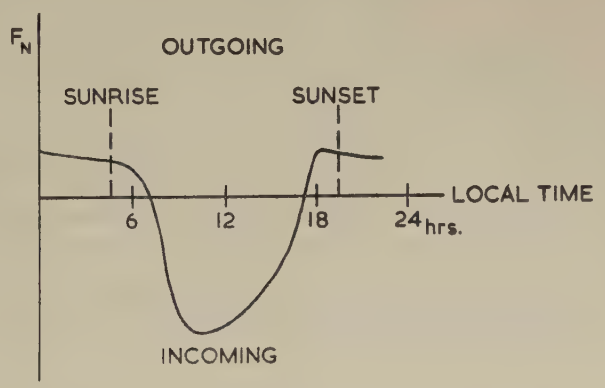

Figure 5. Qualitative nature of the diurnal variation of F_N neglecting diurnal variation of cloud amount.

The problem now arises of how to obtain values of the heat balance as a function of latitude and longitude. A desirable aim is to arrive at a world-wide picture of the net radiation $Q(\phi, L)$ where $Q = \int F_N\,dt$ taken over a period of a day or at most a few days. Now there is a large diurnal variation in F_N, shown qualitatively in Fig. 5 in which the diurnal variation of cloud is neglected. Clearly, observations of F_N at two points only of this curve, at practically the same local times in all longitudes, do not allow construction of the whole curve. Observations over a week would moreover only cover two sections of the curve each about 2½ hr wide ($i \simeq 60°$), making use of the precession of the orbit. Wexler (1960) remarks that a solution to the sampling problem could involve the launching of a number of satellites into 'stationary' orbits of inclination 96·5° so that they are suitably spaced in local time about the earth.

If a high satellite orbit were used, say $h = 3{,}000$ km, then each place on the earth within the orbital zone would be observable over about 6 hours per day, but at the expense, in the two-sphere experiment, of large spatial smoothing. A high orbit recommends itself,

however, for a restricted-aperture radiometer giving spatial resolution of order say 100 km, but this requires an advanced, altitude-controlled satellite and it would then be necessary to assume (or measure) the form of the angular distribution of intensity of radiation leaving each area in order to obtain fluxes.

8. Conclusions

We state first the conclusions which are relevant to all satellite measurements of total radiation, no matter how they are made.

(1) Satellite measurements can only give the flux at the position of the satellite, i.e., at a height of 200 km or more. The flux at a lower level can only be inferred with precision under ideal conditions (visible area homogeneous).

(2) The sampling of data obtainable with a single satellite is inadequate for the purposes of world-wide heat balance studies because observations of F_N at a point are made at only two times during the day. Since all points around a given latitude circle are observed at the same two local times the data will be sufficient to give a zonal mean of the net flux at these two times.

The following conclusions relate to the two-sphere experiment described.

(1) The use of an omnidirectional sensing element gives rise to an uncertainty in the determination of the vertical fluxes at the satellite. It is shown that this uncertainty is acceptably small (< 2 per cent for long wave flux and < 10 per cent for short-wave flux) in most situations. The difficulty can only be avoided by using a plane sensing element maintained parallel to the earth's surface at all times.

(2) The experiment described is simple, and the apparatus required could be made very small and light, with small power requirements.

(3) The sensitivity is shown to be sufficient and the errors in the flux determinations are tolerably small in most cases. In the event of the occurrence of a minor defect not causing a complete breakdown of the experiment it should be possible to recalibrate the equipment in flight sufficiently well to make good use of continued observations.

(4) Conduction and radiation errors from the satellite itself can be made acceptably small. Heating by collision with gas molecules cannot be avoided and may be appreciable for low orbits (< 300 km), but is negligible above 400 km.

Acknowledgments

I am indebted to Professor P. A. Sheppard for many helpful suggestions and discussions, to the Royal Society for a research grant, and to Miss M. Street for preparing the diagrams.

References

Elsasser, W. M.	1942	Harvard Met. Studies, No. 6.
Gast, P. R.	1956	*Scientific uses of earth satellites*, p. 73 (Chapman and Hall, London).
Kelly, J. J.	1955	*Weatherwise*, **8**, p. 121.
King-Hele, D.	1960	*Satellites and scientific research*, p. 19 (Routledge and Kegan Paul, London).
Lagow, H. E.	1956	*Scientific uses of earth satellites*, p. 68 (Chapman and Hall, London).
Suomi, V. E.	1958	*I.G.Y. Annals*, **6**, pp. 331-340.
Wexler, H.	1960	*W.M.O. Bulletin*, **9**, p. 2.
Widger, W. K. Jr. and Touart, C. N.	1957	*Bull. Amer. Met. Soc.*, **38**, p. 521.

SHORTER CONTRIBUTION

551.511.13 : 551.521 : 551.508.72

The energy balance of an evaporation pan and the measurement of the reflectivity of its bottom

By L. WARTENA and A. J. W. BORGHORST

Research Division, Nederlandsche Heidemaatschappij, Arnhem

Physics Laboratory, Agricultural University, Wageningen

(Manuscript received 11 May 1960; in revised form 7 November 1960)

Summary

A U.S. Weather Bureau Class A evaporation pan was used for micro-meteorological measurements in Iraq. Because it seemed doubtful if the method of the U.S. Weather Bureau could be used for working up the data in the desert climate of Iraq, the energy balance of the pan was studied, and details are published elsewhere. The considered items are summed up in this contribution and the results are given in Table 1. The problem of the albedo for sunlight of the shallow water in the pan was studied in the laboratory. Measurements were taken with a filtered lightbeam and a silicon photo-cell. In a zinc pan filled with 0·175 m water, 8 per cent of the direct and diffuse sunlight with wavelengths $< 1\ \mu$ which has penetrated through the water surface is reflected.

1. The energy balance of a Class A evaporation pan

An evaporation pan is used widely for evaporation measurements. The evaporation of a moist surface can be found by multiplying by a pan factor. Different pans have different factors for the same surface (Lake Hefner Studies 1954). Well known is the U.S. Weather Bureau Class A evaporation pan.

The energy transfer of an evaporation pan is very different from a natural surface, e.g., a lake surface or a crop. Therefore Kohler, Nordenson and Fox (1955) made a study of the 'Class A' pan and derived a partly empirical method which could give a more general application of the pan-evaporation figures. However, his proof of the utility of the nomogram does not seem to be tenable, because he employed for this purpose the same data with which he constructed the graphs.

It seems doubtful whether it is possible to use Kohler's method in very different climates, viz., Iraq, and there were some indications that the evaporation from pans depended upon the soil temperature and on the cloudiness. These were the reasons that led one of the authors (Wartena 1959) to make a study of the different items of the energy balance of the Class A pan.

The figures were derived for conditions in Iraq, and the energy budget of the Class A pan in the desert near Samarra (approx. 200 km NW Baghdad) can be found in Table 1.

The following items are considered (+ sign was used for energy supply to the water of the pan). All values are the amounts absorbed by the water or the pan wall.

(a) *Short-wave radiation* ($\lambda < 3\ \mu$)

Symbol :	Energy-flux densities of :
${}^{w}H_{sh}$	radiation on the water ($\lambda < 1\ \mu$, see note)
${}^{pa}H_{sh}^{di}$	direct radiation from the sun on the wall of evaporation pan
${}^{pa}H_{sh}^{df}$	diffuse radiation on the wall of pan
${}^{pa}H_{sh}^{so}$	radiation reflected from the soil on to the wall of pan

(b) *Long wave radiation* ($\lambda > 3\ \mu$)

${}^{w}H_{lo}^{ne}$	net radiation from the air on the water ($\lambda > 1\ \mu$, see note)
${}^{pa}H_{lo}^{ai}$	radiation from the air on the wall
${}^{pa}H_{lo}^{so}$	radiation from the soil on the wall
H_{lo}^{pa}	radiation from the wall

TABLE 1. THE ENERGY BALANCE OF THE CLASS A PAN IN THE DESERT IN 10^3 JOULES (24 HR)$^{-1}$

	1957									1958		
	March	April	May	June	July	Aug.	Sept.	Oct.	Nov.	Dec.	Jan.	Feb.
${}^{w}H_{sh}\ (<1\ \mu)$	9,733	12,731	14,295	17,001	16,150	14,428	12,228	8,705	—	5,019	4,692	9,107
${}^{w}H_{lo}^{ne} + H_{sh}\ (>1\ \mu)$	− 1	957	2,081	3,745	4,298	3,677	2,207	− 942	—	− 4,201	− 5,464	− 2,268
${}^{w}H_{se}$	159	− 858	1,050	11,258	12,680	13,769	12,220	6,006	—	511	− 837	3,105
${}^{pa}H_{se}$	92	502	615	6,570	7,407	8,035	7,135	3,507	—	297	− 490	1,812
${}^{pa}H_{co}$	33	− 155	251	2,093	2,465	2,871	2,716	1,469	—	154	− 218	624
${}^{pa}H_{sh}^{di}$	2,461	2,645	2,557	3,126	3,407	3,419	3,578	2,796	—	2,695	1,875	3,222
${}^{pa}H_{sh}^{df}$	1,055	1,214	1,339	498	485	435	381	682	—	636	870	883
${}^{pa}H_{sh}^{so}$	1,130	1,456	1,607	1,862	1,820	1,637	1,431	1,025	—	732	653	1,105
${}^{pa}H_{lo}^{ai}$	11,053	11,015	11,772	13,852	13,999	14,233	13,635	12,568	—	11,082	9,759	10,567
${}^{pa}H_{lo}^{so}$	10,881	8,516	12,074	12,534	12,869	12,869	12,074	10,881	—	8,433	8,224	9,416
H_{lo}^{pa}	− 17,996	− 17,012	− 18,184	− 21,218	− 21,176	− 21,302	− 20,804	− 19,515	—	− 17,150	− 17,096	− 16,732
H_{ev}	− 17,159	− 25,110	− 35,154	− 73,028	− 69,889	− 68,634	− 47,709	− 30,676	—	− 5,817	− 5,524	− 12,136
H_{sp}	− 1,441	4,099	5,697	21,707	15,485	14,563	908	3,494	—	− 2,391	3,556	− 8,705

(c) *Sensible heat*

${}^{w}H_{se}^{ai}$	sensible-heat transfer from the air to the water
${}^{pa}H_{se}^{ai}$	sensible heat transfer from the air to the wall
${}^{pa}H_{co}$	conduction of heat from the rim of the pan above the water to the wall

(d) *Evaporation*

H_{ev}	latent heat used for evaporation

(e) *Surplus*

H_{sp}	surplus (−) or deficit (+) of heat in order to get the sum of 1 to 12 to equal zero.

The calculation gave many difficulties. One was the estimation of the absorption by water of short-wave radiation (item 1).

The reflection of water of relatively great depth was studied by different authors, Albrecht (1940), Budyko (1958), U.S. Govt., Lake Hefner Studies (1954), U.S. Govt., Lake Mead Studies (1958) and were used and discussed by Wartena (1959). The water in the evaporation pan gave extra difficulties. These were partly overcome theoretically by Wartena (1959) (influence of the rim).

Because the water depth in the Class A pan varies only between 0·15 m and 0·20 m, short-wave radiation is reflected on the bottom of the pan. The reflection of the water of the evaporation pan will be higher than that of a water surface with greater depth. An experimental study of the reflection of the water of the evaporation pan was therefore made and is reported in the present note.

2. Apparatus

A used zinc drum is taken as a model of an evaporation pan. It has a diameter of 0·4 m, with the walls partly covered inside with black paper, and filled with 0·175 m water. This is the mean water height for the Class A pan.

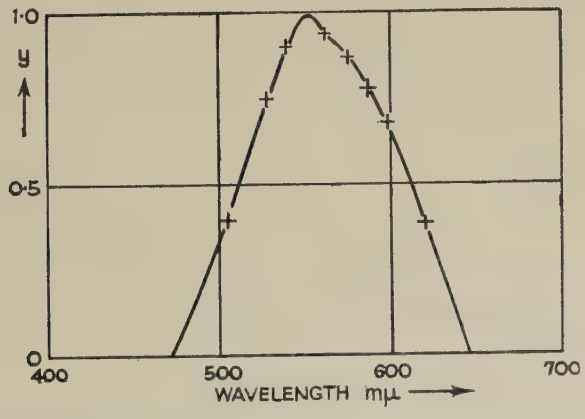

Figure 1. Spectral responsivity of silicon photo-cell with filter BG 18 2 mm and wolfram incandescent lamp $\theta = 2710$ °K.

(Note) Zuidhof and De Vries (1940) found that in a water layer of a depth of 0·10 m, 30 per cent of the solar radiation ($\lambda < 3\ \mu$) was absorbed. Water has an absorption peak at approximately 0·960 μ and $\lambda \geq 1\ \mu$ includes 35 per cent of the solar energy in mean conditions. The path length in water in the pan is always $\geq$ 0·30 m, so for item 1 only 65 per cent of the solar radiation is dealt with (roughly $\lambda \geq 1\ \mu$). On the other hand, 35 per cent of the solar radiation is dealt with as long-wave radiation for item 5 ($\lambda > 1\ \mu$).

A small light beam of constant intensity falls perpendicularly on the water surface, about 0·12 m from the edge of the pan. This beam is excentrically placed so that it has a sufficiently long measuring path. The energy of the outgoing light, after reflection at the bottom of the pan, is measured with a photo-cell moving just above the water. As water has no appreciable spectral absorption in the short wave part of the solar spectrum, and absorbs nearly all radiation at wavelengths greater than 1 μ, measurements are made with filtered light and a silicon photo-cell, which gave the spectral responsivity represented in Fig. 1. The silicon cell used for the measurements has many advantages over other cells. It has a high electrical output and is not affected by changes of temperature. The current delivered by the cell is proportional to the light energy at constant spectral composition, if the resistance of the measuring device is not altered and the tension is held below 0·1 volt. From our measurements we could establish that the cell follows the cosine law, i.e., it actually measures the energy coming to the surface of the cell, irrespective of the angle of incidence.

3. Measurements

The energy measured with the photo-cell, diameter d, at distance r from the light beam, is representative for a ring area $2\pi rd$. Multiplying the cell output with $2\pi rd \div \pi d^2/4 = 8r/d$ and dividing by d gives the energy per cm ring (Fig. 2). By integrating the curve in Fig. 2 we arrive at the total reflected energy of 3·15 C watt. The light beam gives 40·2 C watt. The reflection of the perpendicular light beam on the water surface can be calculated at 2 per cent. The reflection coefficient of the bottom of the pan when covered with water is then 8·0 per cent. The constant C during our measurements amounts to about $6 \cdot 10^{-5}$ W per μA.

A second measurement gave 8·2 per cent reflection. Measurements in their spectral regions with yellow and red filters gave the same results as with the green filter BG 18. Thus it is justified to use the results from our experiments for the total solar radiation with wavelength $< 1\ \mu$.

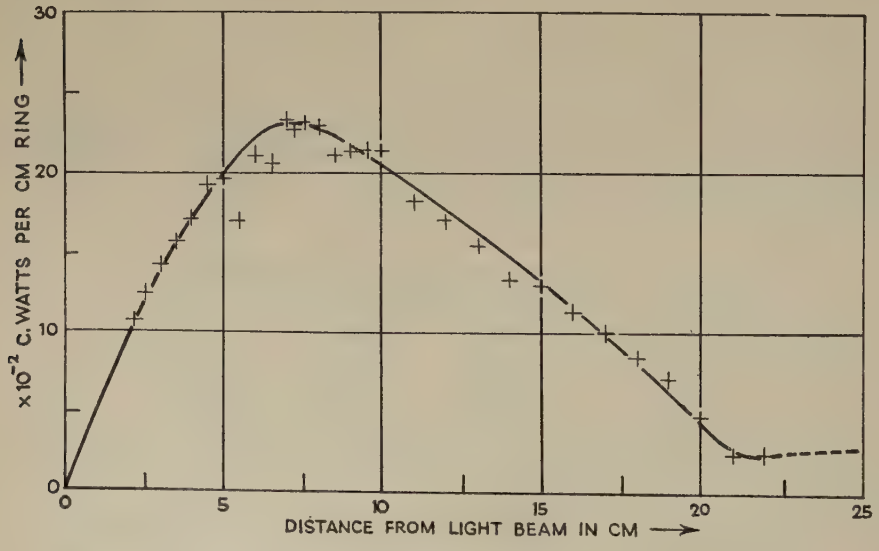

Figure 2. Energy distribution at the water surface in concentric rings of 1 cm width.

4. Conclusions from the measurements

In a zinc pan filled with 0·175 m water, 8 per cent of the shortwave radiation which has penetrated through the water surface is reflected when the light beam is perpendicular to the water surface. From measurements we found that the bottom reflects the short-wave radiation nearly diffusely. For this reason the reflection is independent of the angle of incidence. Moreover, the angle of incidence at the bottom does not change as much as the sun height. Therefore, the value of 8 per cent can be used for all short-wave radiation ($\lambda < 1\ \mu$).

References

Albrecht, F. 1940 'Untersuchungen über den Wärmehaushalt der Erdoberfläche in verscheidenen Klimagebieten,' *Wissenschaftliche Abhandlungen*, Bd VIII, **2**, Reichsamt für Wetterdienst (Julius Springer, Berlin).

Budyko, N. J. 1958 *The heat balance of the earth's surface*, U.S. Weather Bureau, Washington.

Dogniaux, R. 1954 'Etude des climats de la radiation en Belge,' *Bijdragen*, **18**, K.M.I. Uccle.

Kohler, M. A., Nordenson, T. J. and Fox, W. E. 1955 'Evaporation from pans and lakes,' *Res. Pap.*, **38**, U.S. Weather Bureau, Washington.

Lake Hefner Studies 1954 'Water loss investigations,' *U.S. Geol. Surv. Prof. Pap.* 269, U.S. Govt. Print Off. Washington.

Lake Mead Studies 1958 'Water loss investigations,' *U.S. Geol. Surv. Prof. Pap.* 298. U.S. Govt. Print Off. Washington.

Wartena, L. 1959 'Het klimaat en de verdamping van een meer in Centraal Irak,' *Meded. Landbouwhogeschool*, Wageningen 59, **9**, pp. 1–90.

Zuidhof, G. and De Vries, D. A. 1940 'Stralingsmetingen te Wageningen, 1930–1940,' *Meded. Landbouwhogeschool*, Wageningen 44 (4).

NOTICE

551.5 : 025.45

Note on Universal Decimal Classification

By G. A. BULL

Meteorological Office, Harrow

The January 1958 *Quarterly Journal* contained a general note on the subject classification of literature in libraries with special mention of the Universal Decimal Classification which has long been applied to the classification of papers in this journal. Also included were the major changes in this classification which were effective from 1 January 1957.

At its second session in November 1957 the former Commission for Bibliography and Publications of the World Meteorological Organization again agreed on a number of revisions of 551.5 which were later agreed by the Executive Committee and the International Federation for Documentation.

The complete revised classification was published in 1959 by the W.M.O. in *Technical Regulations* with the object of its introduction from 1 January 1961, or earlier dates according to the desires of individual users. All papers in *Quarterly Journal* are classified according to the revised classification from and including the issue of October 1960.

References

Bull, G. A. 1958 'Note on Universal Decimal Classification,' *Quart. J. R. Met. Soc.*, **84**, p. 78.

World Meteorological Organization, Geneva 1959 *Technical Regulations*. **1**–General, 2nd Ed., Appendix G., W.M.O., No. 49. Bd. 2/3.

British Standards Institution London 1943 *Universal Decimal Classification*, English Standard British Standard, 1000 **2**, Pt. 3, Geology (including Meteorology).

1957 *Ibid.*, Abridged English Edition, (revised, enlarged with detailed alphabetical index), British Standard 1000A.

International Federation for Documentation (F.I.D.), The Hague *Extensions and corrections to the U.D.C.* Issued half-yearly cumulative.

551.510.53 : 551.521.31 : 551.571.7 : 535.8

Spectroscopic observations of the water-vapour content of the stratosphere

By J. T. HOUGHTON and J. S. SEELEY

(Read 19 October 1960. Presented by Dr. Seeley. See *Q.J.*, **86**, p. 358)

Dr. J. M. Stagg (*President*) : I am still puzzled about the consistency of the results presented in these two papers.* I can understand that a water-vapour mixing ratio of 37 mg kg^{-1} at 27 km is not incompatible with a spectroscopic measurement at 15 km which gives an integrated mixing ratio for the whole column above that height of only 3 mg kg^{-1}. But in the last column of Table 2 of their paper Drs. Houghton and Seeley have given us measures of mixing ratio derived from observations at three levels on each of the three days, 10 December 1957, 21 January and 12 June 1958. If their results were consistent with the direct measures at 27 km obtained from the cooled-vapour trap (or the other way round), I would expect to see some indication of a systematic change in the ratio as the spectroscope was taken higher into the atmosphere. Perhaps the answer is that at the lowest of the three levels, on one or more of those three days, the aircraft was still in the troposphere ?

Mr. N. D. P. Hughes : In the course of making a detailed analysis of the whole of Houghton and Seeley's spectra from 1 to 6·5 μ I have found that there is an absorption line in group D which is due to hydrogen in the solar atmosphere. This line which occurs at 3808 cm^{-1} is the second member of the Brackett series, transition 4-6, and blends with the water line 3806·7 cm^{-1}. I have made calculations which show that the hydrogen line, with an estimated strength of 0·3 cm^{-1} (integrated absorption), would give the observed distortion to the profile of the short wavelength edge of group D. It is apparent that less water vapour is required to give the absorption observed in group D of the solar spectrum than in the laboratory measurements.

Dr. R. S. Scorer (*communicated*) : There is an argument which should at least be put on record concerning the temperature of mother-of-pearl clouds. There have never been any measurements of temperature close to them, unfortunately, but extrapolation of radiosonde ascents suggests a temperature of about — 80°C; but this extrapolation is unreliable because near that altitude there is often a rapid increase with height. When compared with other wave clouds they often look as if they are composed of water droplets, and two other features support the conclusion. First the intense iridescence characteristic of uniform spherical particles, and second, the trails of ice crystals streaming from the leeward edge at which the main body of the cloud evaporates. These both suggest that often the main cloud is a water cloud. If we can assume that at those pressures water droplets would freeze almost instantaneoulsy at temperatures below — 40°C and that ice spheres would not evaporate any more readily than crystals at lower temperatures, one must conclude that the temperature of the clouds is higher than — 40°C.

It would be interesting to have this argument demolished, if it can be, or to know whether it is discounted simply because the experts cannot at present believe that there could ever be enough water vapour at 25 km to produce clouds at — 35°C.

In considering this it should be borne in mind that these clouds are not common, but this may only be because the conditions for waves at those heights are not common and not because the mechanism for getting the water there is rare.

Dr. J. T. Houghton (*in reply*) : We thank Mr. Hughes for his observation. If we made allowance for the hydrogen line, the resulting correction to our results would be small, as is demonstrated by the fact that measurements involving Group D do not give consistently higher values of water content. In reply to Dr. Stagg, we would like to emphasize that our observations give an integrated value of the product of (pressure $\times$ water-vapour path-length) for the path between the aircraft and the sun. Thus, as well as being consistent with a uniform mixing-ratio throughout the atmosphere above 150 mb of about 3×10^{-6}, they would also be consistent, for instance, with a mixing ratio of 2×10^{-6} for the region 150 mb to 31 mb and 40×10^{-6} above 31 mb. Our observations are thus not inconsistent with the existence of a layer of higher water-vapour concentration in the upper stratosphere.

Dr. J. M. Stagg (*President*) : In congratulating the authors of the two papers* on their work, I look forward to seeing more results from both methods of measurement, particularly if made on sets of consecutive days so that the changes in mixing ratio can be related to the circulation at those levels.

* See following discussion of the paper, ' A direct measurement of the humidity in the stratosphere using a cooled-vapour trap.'

551.508.71 : 551.510.53 : 551.571.7

A direct measurement of the humidity in the stratosphere using a cooled-vapour trap

By F. R. BARCLAY, M. J. W. ELLIOTT, P. GOLDSMITH and J. V. JELLEY

(Read 19 October 1960. Presented by Mr. Goldsmith. See *Q.J.*, **86**, p. 259)

Prof. P. A. Sheppard : Can the authors assure us that diffusion of water vapour through the skin of the balloon, from the relatively water-vapour-rich mixture within, did not lead to too-large mixing ratios ?

Dr. A. W. Brewer : I am very interested in these papers,* and very concerned at the apparent disagreement between the two measurements. In so far as they conflict, I find Mr. Goldsmith's measurements from a balloon more difficult to accept. If there were high humidity-mixing ratios in the stratosphere, then we ought to find the moist air descending somewhere to levels where we can find it by humidity measurements from aircraft. This happens with ozone which is created at levels of 25-30 km. but is found quite easily in the lower polar stratosphere.

The evidence of mother-of-pearl clouds has not yet been fully exploited, though a treatment similar to that given by Dr. Ludlam for the noctilucent clouds, would appear fairly straightforward to give an order-of-magnitude estimate of the humidity-mixing ratios involved. Unfortunately I do not know of any temperature measurement on an occasion of mother-of-pearl clouds, but they are only seen at a season when stratosphere temperatures are sometimes very low.

Dr. W. T. Roach : It seems to me that the results obtained by Drs. Seeley and Houghton may not be inconsistent with the results obtained by Barclay *et al.* since the absorption measured above 45,000 ft will be very insensitive to the mixing ratio at 90,000 ft, owing to the heavy weighting of water-vapour amount towards the lower level. A constant mixing ratio of 0·003 g kg^{-1} implies 4-5 μ of water vapour above 45,000 ft, whereas a mixing ratio of 0·03 g kg^{-1} between 80,000 and 90,000 ft (implied by Barclay *et al.*) would amount to about 2 μ. Since absorption is proportional to $\sqrt{pm}$, the absorption produced by this layer would only be about one-quarter of that observed by Seeley and Houghton above 45,000 ft and comparable with their quoted experimental error.

Mr. F. Singleton (*communicated*) : With regard to Dr. Brewer's question concerning the temperature at which mother-of-pearl clouds form, Hesstvedt (1959), from an analysis of radiosonde observations up to heights of 25 km, during occasions when these phenomena were observed, gives values of − 75°C to − 80°C. Assuming mixing ratios to be the same as those given by M R.F. for the tropopause and lower stratosphere, he then explains the formation of the clouds as partly orographic lifting and partly mass uplift due to lifting of stratospheric air as it overruns tropospheric frontal cyclones. Should the values of mixing ratio given by Barclay *et al.* be correct, then the clouds could be more plausibly explained, purely in terms of orographic effects.

Reference

Hesstvedt, E. 1959 *Geofys. Pub.*, Oslo, **20**, 10.

Dr. H. L. Penman : The data give totals of carbon dioxide and water. How unreasonable is it to suggest that a constant frost-point temperature might be assumed, and the data used to estimate the variation of carbon-dioxide concentration with height ?

Mr. E. Gold (*Honorary Member*) : May I ask if there has been any attempt to ascertain the track of the air in which the measurements of the water-vapour have been made ? There might well be a difference between the water-vapour content of air which has come more or less direct from the equator and air which has been for an appreciable time over the polar regions. A synoptician might be able to estimate the recent history of the air with sufficient accuracy to enable a comparison to be made.

Mr. P. Goldsmith (*in reply*) : In reply to Professor Sheppard, we were, of course, very much aware of the possibility of the balloon being a source of water vapour and, during a continuation of this work in 1959, the distance from balloon to sampler was varied between 150 and 400 ft without affecting the measured mixing ratio significantly. In 1960, a very elegant method of

* The paper ' Spectroscopic observations of the water-vapour content of the stratosphere ' by J. T. Houghton and J. S. Seeley, was also read.

testing this possibility was carried out by Dr. F. Brown and co-workers of A.W.R.E. Heavy water (D_2O) was introduced into the balloon hydrogen before launch and the D/H ratio of the collected water subsequently measured. The results of these investigations showed no increase in the D/H ratio which indicates that no water was picked up from the balloon.

I think the remarks of Dr. Brewer pin-point the difficulties of reconciling the presence of moist layers and mother-of-pearl clouds to our present ideas on stratospheric conditions. But as Dr. Roach points out, the infra-red results are not necessarily contrary to their presence in the upper stratosphere.

As regards Dr. Penman's suggestion, I would refer to recent extensive measurements by Hagemann *et al.* (*Science*, **130**, p. 542, 1959) at altitudes between 15 and 30 km and latitudes between 45°N and 23°S which show that the concentration of carbon dioxide is 311 ppm (± 2 per cent) by volume.

In answer to Mr. Gold, I think the information required for this type of analysis is not yet available, since the height of these flights is somewhat greater than the average burst height of the standard radiosonde balloon.

As I mentioned during the course of this discussion, the work described in our paper has been continued by one of us (P.G.) in conjunction with Dr. F. Brown and co-workers of A.W.R.E. and it is hoped to publish these new results in the near future.

551.594.11 : 551.594.13 : 623.454.8

Some recent changes in atmospheric electricity and their cause

By K. H. STEWART

(Read 16 November 1960. See *Q.J.*, **86**, p. 399)

Dr. T. W. Wormell : This interesting paper brings the story of a disturbance of the atmospheric electric field by artificial means to a satisfactory conclusion and seems, if we omit the anomalous behaviour at Kew Observatory, to tie up the loose ends successfully. Dr. Stewart makes various suggestions as to why an increase of ionization near the ground has been accompanied at Kew by an increase of air-earth current rather than by a decrease of vertical electric field, but he would hardly claim, I think, to have established a quantitative explanation. The anomaly may be entirely due to the effect of increased motor traffic (one of his suggestions); some exhaust fumes carry considerable positive charge and affect the electric field in the neighbourhood appreciably.

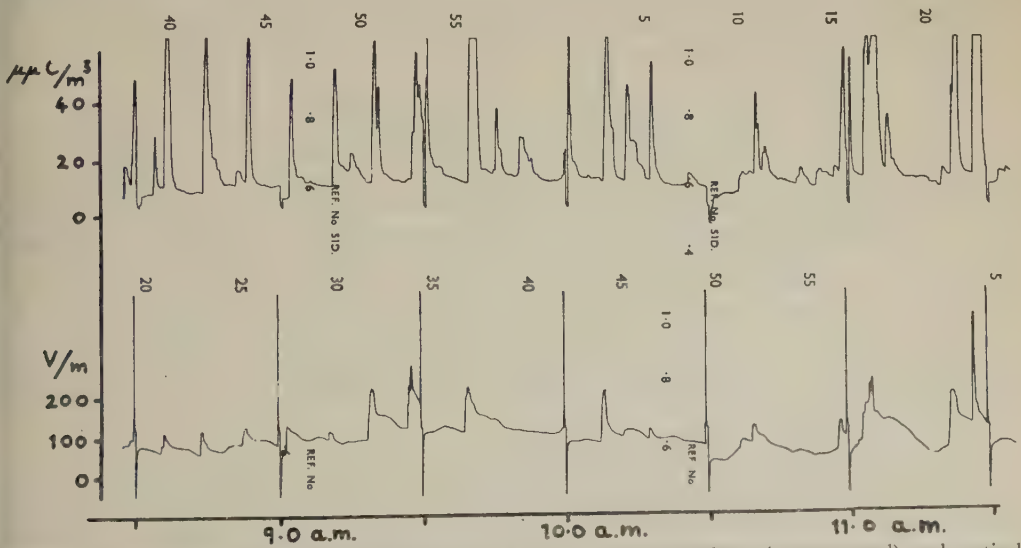

Figure 1. Simultaneous records of net positive space charge in the atmosphere (upper record) and vertical potential gradient near the ground (lower record).

Mr. J. Law : The two records shown in Fig. 1 are of the space charge in the atmosphere and of the vertical potential gradient near the ground. They were obtained in a field beyond the built-up area to the west of Cambridge, about 30 m south of a fairly busy main road running east to west and in a N'ly wind. They are typical of records obtained at this site under such conditions. Bursts of positive charge, apparently originating in the smoky exhausts of a relatively small proportion of the passing vehicles, drift across the site and cause temporary increases in the positive potential gradient, in some cases by as much as 100 per cent. (Apart from the time-marks at half-hourly intervals the spikes on the records represent the effects of passing vehicles).

Most vehicles appear to give little or no charge to the air; the background level of both space charge and potential gradient, at this site, are only slightly greater in N'ly winds than when the exhaust fumes are blown away from the recording instruments.

551.511.6 : 551.551.8 : 551.554

The diabatic wind profile

By H. A. PANOFSKY, A. K. BLACKADAR and G. E. McVEHIL

(Read 16 November 1960. Presented by Professor Panofsky. See *Q.J.*, **86**, p. 390)

Dr. T. H. Ellison : The curve which bears my name in Fig. 1 of the paper follows from the interpolation formula which I suggested in 1957 only if one makes the assumption that K_h/K_m is constant ; but the main object of my paper was to put forward a theory predicting that K_h/K_m would be a strong function of the flux Richardson number Rf especially in stable conditions where it would fall to zero as Rf approached a critical value Rf_{crit}. The general character of this variation has since been confirmed by laboratory experiments.

The constant (which Professor Panofsky has called γ) in the interpolation formula for K_m* cannot be chosen independently of Rf_{crit}, but must equal $1/Rf_{\text{crit}}$ if the formula is to behave correctly in the limit of very stable conditions.

For any value of Rf_{crit} (and the best guess is probably slightly lower than the value 0·15 which I put forward in 1957) it is easy to calculate the correct form which the curve on Panofsky's Fig. 1 would have according to my theory. It turns out to lie between those marked $\alpha = 0{\cdot}6$ and $\alpha = 4{\cdot}5$.

Dr. G. D. Robinson : There has been some discussion of the constancy or inconstancy of the ratio of the eddy diffusivity for momentum K_M, and for heat K_h.

We have by definition

$$\text{Flux of heat} = \rho\, C_p\, K_H\, \partial\theta/\partial z$$

$$\text{Flux of momentum} = \rho\, K_M\, \partial u/\partial z$$

We are told the fluxes are sufficiently constant over the height ranges with which we are concerned, at least for most of the time. We have innumerable measurements of the gradient of potential temperature and wind near the ground. If the ratio of the gradients is constant with height then the ratio of the coefficients is constant with height. Do we need a more subtle approach ?

Prof. P. A. Sheppard : The measurements of the gradients of potential temperatures and wind speed near the ground may, as Dr. Robinson says, be innumerable but they have not been taken, according to my and some others' diagnosis, with sufficient precision to provide a clear-cut answer to his question, particularly at the greater heights or larger values of whatever stability parameter is favoured.

My colleagues and I are currently attempting to make more satisfactory observations of the ratios of the gradients and I hope shortly to present evidence on the question. It is, however, desirable to classify results according to the stability and we find that the gravity term in this is not adequately expressed (over water) through the temperature gradient or heat flux. The potential density gradient or flux of buoyancy are the basic quantities and these appear to derive as much from water vapour as from temperature.

Dr. R. S. Scorer : Can Professor Panofsky give a physical justification in terms of the mechanism he imagines to be operating, for the assumption that K_m/K_h is a constant ? Is it not surely reasonable to expect it to vary according to the way in which the stirring motion is produced (mechanically or thermally). A recent estimate for its value when this motion is primarily produced by buoyancy forces, made by one of my students, suggests that the ratio can be as low as 0·1. I would not regard experimental evidence of a rather restricted kind as being appropriate here : what we need is an understanding of the mechanism, and until this is clearer, observations under special conditions will scarcely settle the matter.

Dr. H. A. Panofsky (*in reply*) : Replying to Dr. Ellison, a relation beteeen Rf_{crit} and γ exists only when the same value of γ is to be valid for stable and unstable cases. As stated, the theory is not expected to be valid under stable conditions at all so that Rf_{crit} does not influence the value of γ in unstable air.

As to the dependence of K_h/K_m on Richardson number, the observations here summarized suggest that it must be rather weak. Even for ' free convection ' a value of K_h/K_m of only 1·3 seems indicated by the Australian and the O'Neill observations. This same ratio can be used for the whole range of observations in unstable air, although the picture would not be altered significantly if the ratio dropped to unity under neutral conditions.

In reply to Dr. Scorer, as pointed out before, the observations here summarized show that K_h and K_m are nearly the same. A simple explanation would be that, in unstable air, a displaced parcel will be in foreign surroundings long enough to have equal opportunity to rid itself of its excess momentum and heat, and share both equally with the surrounding air.

551.511.32 : 551.513.1

A problem in baroclinic stability

By J. S. A. GREEN

(Read 18 January 1961. See *Q.J.*, **86**, p. 237)

Dr. A. W. Brewer : Mr. Green has referred to the interchangeable nature of effects of stretching and the effects of the variation of the Coriolis parameter in their effects on the vorticity to determine the resulting motions. Variations in the depth of the fluid can play a similar part. This is well known and used, for example, in model experiments. I would like to ask Mr. Green if the effects of the spatial variations of the height of the tropopause are likely to be significant in the atmosphere.

Mr. J. S. A. Green (*in reply*) : The variation of average tropopause height with latitude is so small that significant vortex stretching effects are not expected. Tropopause breaks are associated with jets and the appropriate perturbation analysis would have to be based on a two-dimensional wind field $U(y, Z)$, as distinct from the one-dimensional $U(Z)$ analysis of my paper. The effect would not be simply superposable, but connected energetically with the geometry of the isentropic surfaces in relation to the tropopause, whereas the stretching mentioned by Dr. Brewer would be a pseudo-β effect.

Proceedings at meetings of the Society

Ordinary Meeting, 14 December 1960

The following candidates were declared to have been elected that day by the Council:

Fellows

Acharya, Sqdn. Ldr. Udipi Raghavendra, M.A., Air Force Station, Agra, India.
Brock, Andrew, M.A., University College of Rhodesia and Nyasaland, Private Bag 167H, Salisbury, Southern Rhodesia (*transfer from Student Membership*).
Bryant, Peter Buckland, 47 Castle Drive, Horley, Surrey.
Chadwick, Instr. Lt. Cdr. Andrew Charles, B.A., R.N., 10 Bruce Road, Southsea, Hants.
Coates, Richard Martin, 78 Wood Berry Avenue, North Harrow, Middx. (*transfer from Student Membership*).
Dave, Jitendra Vishvanath, M.Sc., Ph.D., Department of Meteorology, Imperial College, Exhibition Road, London, S.W.7.
Flavell, Raymond George, 141 Clyfford Road, Ruislip, Middx.
Griggs, Peter Derek George, M.I.N., P.O. Box 30163, Nairobi, Kenya.
Grimmer, Michael, B.Sc., Meteorological Office (M.O.12), Dunstable, Beds.
Lakin, William Kenneth Houghton, B.Sc., 6 Martin Crescent, Rumney, Cardiff (*reinstatement*; *elected 1945, resigned December 1953*).
Manterfield, David, 29 Beauchief Rise, Sheffield 8, Yorks.
Perks, Philip Henry, A.C.P., (A.I.Hsq.), 'Wyndley,' Rising Lane, Lapworth, Solihull, Warwicks.
Perry, John David, B.Sc., Officers' Mess, Armament Practice Station, Royal Air force SYLT, B.F.P.O.46.
Russell, Rodney, 14 Lansdowne Lane, Charlton, London, S.E.7.
Rodda, John Carrol, B.Sc., Dip. Ed., 3 St. Peter's Street, Wallingford, Berks.
Townsend, Christopher Francis, 1 Station Crescent, Wembley, Middx.
Ward, Graham Frederick Adams, B.Sc., Beit Hall, Imperial College, Exhibition Road, London, S.W.7.
Watkins, Leonard Henry, B.Sc., 203 Rochester Avenue, Feltham, Middx.

Foreign Members

Battan, Louis Joseph, B.S., M.S., Ph.D., Institute of Atmospheric Physics, University of Arizona, Tucson, Arizona, U.S.A.
Dunlap, Donald Vern, B.S., 1610 Evans Avenue, Prospect Park, Pennsylvania, U.S.A.
Hiergesell, Valentine, H.B. Instrument Company, American & Bristol Sts., Philadelphia, 40, Pa., U.S.A. (*reinstatement*; *elected 1950, resigned February 1958*).
Strachan, Ronald, 2405 Oakmont Avenue, Orange, California, U.S.A.
Szeicz, Geza, Dip. Met., Physics Department, Rothamsted Experimental Station, Harpenden, Herts.

Student Members

Atkinson, Bruce Wilson, East View, Bottoms, Holmfirth, Huddersfield, Yorks.
Baker, Keith Godfrey, 31 Salisbury Road, Seaford, Sussex.
Brereton, Miss Barbara Mary, 72 Dobcroft Road, Millhouses, Sheffield 7, Yorks.
Carter, Allan Stewart, 34 South Vale, Sudbury Hill, Harrow, Middx.
Dodds, Ian, 11 Mansfield Road, Eston, Middlesborough, Yorks.
Fitzgerald, Brian Patrick, 25 Dors Close, London, N.W.9.
Goodger, John David, 70 Kedleston Road, Leicester.
Harker, Alan, 12 North View, Aspatria, Carlisle, Cumberland.
Hazlewood, John Charles, 48 St. Mungo's Park, Aspatria, Carlisle, Cumberland.
Hennessy, Michael Wallace, 7 Markham Avenue, Weymouth, Dorset.
Paren, Julian Gerald, 21 The Birches, Winchmore Hill, London, N.21.
Rosenberg, Harris, 10 Breeze Mount, Prestwich, Lancs.
Ryall, Roderick Arthur, 109 Weston Lane, Otley, Yorks.
Williams, Michael Charles, 48 Rough Common Road, Canterbury, Kent.
Wilson, Michael, 17 Westward Way, Kenton, Harrow, Middx.

Corporate Member

Negretti & Zambra Limited, 122 Regent Street, London, W.1. (*Nominee*: L. B. Lambert).

The meeting took the form of a Discussion, commencing at 2.30 p.m., when the Society was pleased to welcome members of the Commission of Climatology of the World Meteorological Organization.

Mr. A. L. Maidens introduced the subject ' Automatic methods of handling meteorological data,' and the speakers included Mr. C. V. Else, who spoke on ' Automatic methods of observing recording and transmitting meteorological data and the basis of the systems involved,'; Mr. E. J. Sumner who spoke on ' Computers ' and Mr. J. M. Craddock, who spoke on ' The mathematical functions performable by computers.' After the tea interval the second discussion period followed and contributions were made by delegates from the Commission of Climatology of the World Meteorological Organization.

A full account of the meeting appeared in the March issue of *Weather*.

Evening Discourse, 4 January 1961

Council regrets that it was necessary to cancel the Evening Discourse at short notice owing to the indisposition of Dr. F. H. Ludlam who was to have spoken on ' Giant hail.' It is hoped that the Discourse will take place during the 1961/1962 Session.

Ordinary Meeting, 18 January 1961

The following papers were read and discussed :

1. ' A problem of baroclinic stability ' by J. S. A. Green (*Q.J.*, **86**, p. 237).
2. ' Some computations of the variation of vertical velocity with pressure on a synoptic scale ' by E. Knighting (*Q.J.*, **86**, p. 318).

Ordinary Meeting 15 February 1961

The following candidates were declared to have been elected that day by the Council :

FELLOWS

CHENG, Tin Tai Peter, B.Sc., 192 Lockhart Road, 2nd Floor, Hong Kong.
CHILDS, John Harry Frederick, 11 Hill View, Crowd Hill, Fair Oak, Eastleigh, Hants.
DIXON, Roy, B.Sc., 119 Bullbrook Drive, Bracknell, Berks.
FROUDE, Geoffrey, 66 Glebe Road, Cambridge.
GRANT, Hugh Duncan, Metropolitan Club, 1 E. 60th Street, New York 22, U.S.A.
JACKSON, Graham Douglas, 157 Eccles Old Road, Salford 6, Lancs.
JONES, Thomas William Vernon, Rest Harrow, Frog Lane, Bracknell, Berks. (*reinstatement; elected 1928; resigned 1934; reinstated 1938; resigned 1947*).
KRISHNAMURTI, T.N., M. S., Department of Meteorology, University of California, Los Angeles 24, California, U.S.A.
MACKLIN, William Charles, M.Sc., Dip.Ed., Ph.D., Department of Physics, University of Western Australia, Nedlands, W. Australia (*transfer from Student Membership*).
NIELSON, Adrian William, 33 Spen Road, West Park, Leeds 16 (*transfer from Student Membership*).
PADDON, Thomas Northey, 14 Cresthill Road, Plymouth, Devon.
SIMPSON, John Egerton, M.A., 50 Stanhope Road, Reading, Berks.
SMITH, Brian Maurice, 1 Waterloo Place, Cranbrook, Kent (*transfer from Student Membership*).
STEWART, John Brampton, B.Sc., D.I.C., 8 Cope Place, London, W.8 (*transfer from Student Membership*).
TELLING, Frederick Daniel M.I.P.R.E., ' Fontana,' Church Street, Crowthorne, Berks.
WATSON, Neil Rae, B.Sc., D.I.C., 88 Homestead Crescent, Manchester 19, Lancs. (*transfer from Student Membership*).
WILLIAMSON, Kenneth, F.R.S.E., M.B.O.U., 53 Upper Road, Kennington, Oxford.

Foreign Members

Eberly, Donald Lee, B.Sc., 75 Crescent Court, Novato, California, U.S.A.
Lunn, George William, B.A., 24 Chilton Avenue, San Carlos, California, U.S.A.
Prophet, David Tindle, B.Sc., 1395 Golden Gate Avenue, San Francisco 15, California, U.S.A.
Riegel, Christopher Albert, B.A., 10422 Tabor Street, Los Angeles 34, California, U S.A.
Silva, Hector, B.S., M.S., The Institute of Arizona, Tucson, Arizona, U.S.A.

Student Members

Babalola, Joshua Makanjuola, 218 Walm Lane, London, N.W.2.
Bean, David Wilfred, 1 School Road, Neatishead, Norwich, Norfolk.
Hale, John Christopher Charles, 103 Oakwood Park Road, Southgate, London, N.14.
Wilson, Anthony Walford, Clarendon Laboratory, Parks Road, Oxford.

Canadian Members

Fellows

Million, Capt. Herbert Arthur, B.S., M.Sc., 2775 McCarthy Street, Montreal, Quebec.
Rioux, J. A. Raymond, B.Sc., M.A., Main Meteorological Office, Terminal Building, Montreal International Airport, Dorval, Quebec.
Steiner, Capt, Harold Austin, B.S., 1401 Canora Road, Montreal 16, Quebec.
Tabata, Susumu, B.A., M.A., Pacific Oceanographic Group, Biological Station, Nanaimo, British Columbia.

Student Member

Kurdyla, John, 3647 Colonial Avenue, Montreal 18, Quebec.

A Discussion was then held on ' The meteorological implications of the distribution of radioactive fall-out.' The opening speaker was Professor P. A. Sheppard, followed by Mr. D. H. Pierson of the United Kingdom Atomic Energy Authority, Harwell, whose subject was ' Observations of large-scale distribution of radioactive fall-out,' and Dr. L. Facy of Météorologie Nationàle, Paris, who spoke on ' Wash-out and scavenging.'

An account of this meeting will appear in a future issue of *Weather*.

Canadian Branch, Royal Meteorological Society to hold Congress in Montreal, 6-7 June 1961

The Canadian Branch of the Royal Meteorological Society is planning to hold its second Congress at Montreal on 6 and 7 June 1961. Of the four sessions, three will be at the University of Montreal (where visitors can also be accommodated) and one at the newly founded Department of Meteorology of McGill University. The programme will include some twenty papers on a variety of subjects, notable among which will be hail, and the arctic stratosphere. About one-half of the contributions will be formal presentation of work recently published; the remainder will deal with current work.

The primary purpose of the Congress – as of its predecessor at Kingston last June – is to bring together Canadian meteorologists who rarely have a chance of meeting, and to present and debate a programme which should be a cross-section through the activities in our science. Meteorologists from abroad, and especially Fellows of the Royal Meteorological Society, will be most welcome, whether or not they contribute papers. Advance notice of the intention to attend will be greatly appreciated, as it will give the organizing committee a chance to mail out news on the programme and other information. The Committee is under the chairmanship of Dr. Walter Hitschfeld, Department of Meteorology, McGill University, Montreal 2, Canada.

Reviews

The atmosphere and the sea in motion (Scientific contributions to the Rossby memorial volume). Ed. by B. Bolin. New York (Rockefeller Institute Press in association with Oxford University Press), 1960. Pp. 509. 105s.

Memorial volumes to great scientists do not always attain the scholarly standard which the occasion deserves or the editors intend, for the invited authors may be distinguished rather than active or for many a good reason unable at the time to match scientific inspiration to their respect for the master. Perhaps it is on this account that such volumes are few on our scientific shelves and, indeed, if one were to say that the best memorial to a great scientist is his own published work, it would be very true of Rossby. But any fear there may be that this volume will, after a brief *succès d'estime*, rest undisturbed in our libraries may be at once dispelled. Much has been written about Carl-Gustaf Rossby whose untimely and sudden death in Stockholm in 1957 sent a shock of dismay and grief through the world of meteorologists. To anyone who came under his influence respect for his intellect and admiration for his shining enthusiasm were immediate; but to these quite soon were added a growing affection for a warm-hearted host or companion. It was natural, then, that a group of his admirers should plan a volume as a 60th birthday present, most of the authors being men at the height of their creative work, and so it was that, with the tragic change of circumstances, a memorial volume meant little more than a change of title.

It is a good collection of some 36 papers, the majority from the United States where Rossby had spent the greater part of his working life, a number from his native Scandinavia, with some other European countries represented by single papers. In most cases, perhaps in all, the authors had worked for a time with Rossby, in America or in Europe. All are known for previous work of quality and evidently a special effort was made to provide contributions worthy of the company and the occasion.

The first paper is an English translation from a survey published by Rossby himself in 1956 ' Current problems in meteorology,' characteristically far-sighted and stimulating. Here he says " the main task for meteorology is, of course, to describe the general circulation of the atmosphere, its variations and superimposed secondary systems of motion in accordance with the basic principles of hydrodynamics and thermodynamics," a statement which, especially with its naïve " of course," indicates not only Rossby's own attitude but equally succinctly the scope of this memorial volume. Almost consistently, the work maintains the attack on the atmosphere (and in a few papers also the ocean) by the quantitative methods of fluid mechanics, mathematical and in principle exact, and it cannot be overlooked by anyone interested in the theory of world weather and climate.

To pick out individual papers for special mention may betray a bias in judgement or a superficial study, and one cannot at a first acquaintance recognise all that is important in 500 pages of thoughtful new work, but some of the papers seem certain to take their place in the select bibliography which defines the main highway of progress. Amongst these one might venture to place Charney's computations with a model of the general circulation; Fjørtoft's discussion of global energy transformations, although this is difficult reading, perhaps more difficult than it need be; Palmén's paper on the maintenance of kinetic energy, brief, clear and cogent comment; Eliassen's contribution to the dynamics of fronts, a curiously neglected subject. There must also be many others which will become important references but I shall mention only one, a work of a different kind, an historical and critical survey of weather analysis and forecasting by Rossby's contemporary and compatriot, Bergeron. There is a hint that Rossby's feeling of exclusion from the great Bergen school of meteorology might have driven him emotionally to ignore both its discoveries and its methods and so to see the problems of weather in a fresher light. Perhaps, indeed, a measure of wilful blindness is not incompatible with genius – we have our Nelson story – but however it may have been with Rossby it is good to see Professor Bergeron, the great exponent of the earlier synoptic school, acknowledging with scholarly grace the significance of the more recent dynamical work with which Rossby's name will always be associated.

R.C.S.

Physics of the upper atmosphere. Edited by J. A. Ratcliffe. London (Academic Press), 1960. Pp. xi, 586. 169 Figures; 71 Tables. $14.50.

This volume of twelve monographs by eleven authors is concerned with that part of the atmosphere above about 50 km. Each monograph provides, in the editor's words, ' a detailed authoritative account, well supported by references (complete up to December 1959) ' of one branch of the subject. Inevitably there is overlapping, but surprisingly little inconsistency, between the various authors. Misprints are few and usually trivial (e.g., in Table V, p. 32), but occasionally more serious (e.g., in Table III, p. 27, where the variation of ozone concentration is given as 10^{-7} to 10^{-8} instead of, presumably, 10^{-7} to 10^{-5}). The index is disappointing. Many of the references are trivial yet, for example, there is no reference in the index to a three-page discussion (pp. 208-210) on the concentration of molecular oxygen in the atmosphere. Also disappointing is the use of mm Hg as a pressure unit, instead of dynes/cm^2.

In the opening chapter, Chapman, after a short outline of the temperature structure and constitution of the earth's atmosphere at lower levels, tells us what it is like at the boundary between the earth's atmosphere and the solar corona. It seems that at this boundary, which may be at a ' height ' of 100,000 km (' a considerable fraction of the distance to the moon ') the ' temperature ' is likely to be at least 50,000°K and the density of the atmosphere (mostly, at this level, ionised hydrogen) perhaps 500 particles per cc (there are some 10^{19} particles per cc at ground level). In chapter 2, Nicolet discusses the downward flow of heat through the atmosphere from this hot outer fringe, and examines the structure of an atmosphere consisting of a mixture of several gases in diffusive equilibrium under gravity. Nicolet, like Chapman, begins with a description

of the lower atmosphere but, unlike Chapman's, Nicolet's description is not entirely correct. In the table on p. 27, for example, Nicolet states, of water vapour, that the ratio by volume is ' variable, particularly in the troposphere. Decrease in the stratosphere.' The ratio, in fact, although it certainly is variable in the troposphere, decreases on the average more or less uniformly throughout the troposphere and, in these latitudes, the lower stratosphere. What measurements there are in the higher stratosphere suggest that the ratio has *increased* considerably by the time a height of 30 km is reached. One would also like to know what evidence there is for the statement that ' One of the essential characters of the troposphere is that the geographic equator is, to a certain extent, a ' barrier ' differentiating and separating the northern and southern hemispheres.'

Chapter 3, on ' The upper atmosphere studied by rockets and satellites,' is written by H. E. Newell, of the National Aeronautics and Space Administration, Washington. Newell sketches the several methods for the determination of atmospheric structure from rockets (pressure gauges, spectrographs, grenades, falling spheres, etc.) and presents some results – including those from three ozone soundings at White Sands. There is a brief section on atmospheric contamination experiments (e.g., ' seeding ' with sodium vapour) but Newell appears to regard these as no more than chemical experiments. In fact, by tracking the glow clouds which are produced, winds can be measured; and it is hoped that it will turn out to be possible to measure temperatures at these levels (above 85 km) by measuring the Doppler broadening of the spectral lines. In this chapter there are also brief sections on night air-glow (some of which, it seems originates from as low as 50 km); aurora, cosmic rays, and micro-meteorites – all of which are treated extensively in other chapters. Newell concludes : ' A fairly complete picture of the high atmosphere up to 200 km is beginning to take form – and it should be possible to fit the structure and winds observed together into a reasonable theoretical picture of the general circulation of the atmosphere, showing the seasonal effects.' Referring to regions somewhat higher Newell says : ' The exciting challenge of the moment is to obtain the full story of the hitherto hidden portion of the ionospheric charge density curve (and) to trace it out to the distance of the moon if possible.'

Chapter 4 is on ' The sun's ionising radiation,' by H. Friedman. This is followed by ' The airglow,' ' The general character of aurora ' and ' The auroral spectrum and its interpretation ' all by D. R. Bates; ' Radar studies of the aurora ' by H. G. Booker; ' The ionosphere ' by J. A. Ratcliffe and K. Weekes; and ' The upper atmosphere and geomagnetism ' by E. H. Vestine. The authors are primarily concerned with electrical and photo-chemical processes in the atmosphere brought about by solar ultra-violet and X-radiation (the formation and destruction of ozone is not treated) but much of the fascination of these chapters lies in the realisation which they bring of the wide variety of tools and techniques now available to the meteorologist in his study on the dynamics and physical structure of the atmosphere at levels above 60 km or so. Measurements of the absorption of ultra-violet and X-radiation are used to determine atmospheric constitution and density – Friedman presents graphs of atmospheric densities measured in this way. Winds (of some sort) may be measured by tracking the movement of recognisable irregularities in the aurora and in the ionosphere. It is shown in this way that there are regular horizontal movements, or drifts, with marked seasonal, diurnal and semi-diurnal variations, superimposed on which are random (' turbulent ') fluctuations of up to 50 m sec^{-1}. These are all movements, or drifts, of ions, and since, at these levels, there are something like one million un-ionised air molecules to every ion, it does not immediately follow that these movements correspond to ' real ' winds. Ratcliffe and Weeks suggest that up to at least 150 km (about 500,000 ft) the ' ionospheric wind ' is probably the same as the ' true ' wind. On the other hand, Booker speaks of measurements of auroral drifts of up to 1,000 m sec^{-1}. Such speeds are far greater than any possible ' real ' wind; they are presumed to be caused by an auroral electric field.

J. S. Greenhow and A. C. B. Lovell write on ' The upper atmosphere and meteors.' Observation of meteors not only enables estimates to be made of the influx of meteoric particles of various sizes into the earth's atmosphere, but it enables measurements to be made of winds and turbulence at levels between about 85 and 110 km. As the authors point out, ' with radio echo techniques a large number of meteors can be detected each hour and diurnal and seasonal variations of winds can be investigated in considerable detail.' Many results are quoted. It is interesting to note that there is evidence of great turbulence even in this region, notwithstanding the great static stability which prevails.

Enough has been said to indicate the value of this book to meteorologists. The primary purpose is not to present new results but rather to indicate where these new results can be found and to provide the physical background against which to view them. It is a book which will convince the meteorologist that the atmosphere does not stop at 120,000 ft.

R.F.

The scientific papers of Sir Geoffrey Ingram Taylor. Vol. 2 : Meteorology, Oceanography and Turbulent Flow. Ed. G. K. Batchelor, (Cambridge University Press), 1960. Pp. x., 515; Figures; Tables; Plates. 75s.

What a delightful and exceptional book this is. So much of science, as commonly presented, wears an over-serious, even forbidding, aspect – like morality – but Sir Geoffrey Taylor's papers have a quite different look. Their subjects and their handling are as professional as the ' best,' but the author is there on nearly every page saying what fun science is and that to be thus unsophisticated – a quite inadequate word but the only alternative I know is ' Taylorish ' – is to have the secret of charm as well as of power. Impersonality may be at the heart of science but her cloak can be as coloured and individual as any art's.

This book, or rather the four-volume series of which the second has now appeared, is, I suppose, the

first to be written by Taylor and for the pleasure afforded we have also to thank Dr. Batchelor, as editor. Few of us, probably, have thought of collected papers as highlights in the history of scientific literature – admirable for institutional shelves, for reference from time to time, but hardly for the most accessible row or for personal shelves. This volume, however, should, for meteorologists and fluid dynamicists, quite reverse that attitude where it exists.

Of 45 papers presented, the first is the classical 1915 *Philosophical Transaction*, 'Eddy motion in the atmosphere,' the paper in which Taylor initiated the theoretical study of turbulent transfer in the atmosphere. Here Taylor was able to test and interpret his theory against observations he had taken at sea only a year or so earlier from the ice-scout ship *Scotia*. The last paper, published in 1958, 'Flow induced by jets,' contains some of the results of the author's last-war studies of F.I.D.O. (fog dispersal by heated jets). Those papers between deal with two broad fields : the turbulent motion of fluids, in the atmosphere, the oceans and the laboratory; and gravity waves in fluids; the former being dominant. Turbulence has evidently exercised Taylor's mind more or less continuously throughout his career but it is of great interest that a relatively quiet period – in regard to very new ideas at least – came on the heels of the epoch-making 1921 paper 'Diffusion by continuous movements' in which some statistical properties of a turbulent field were first formally related. Then in 1935 came the great burst, growing out of the 1921 paper, of the 'Statistical theory of turbulence, Parts I to V' and Taylor himself ascribes this break-through to the development of experimental techniques, the hot-wire anemometer and associated circuitry in particular, which made the measurement of the statistical properties of turbulent fields and the test of theory therefrom possible. Thus, as in 1915, and indeed in almost all his work, Taylor advances theory by being continuously aware of the advances in and potentialities of observational techniques. And, so great is his power, he has been ever ready to undertake experimental research himself when theory needed prompting or testing and the required observations were not to hand. I believe there is an important lesson here for the theoretical meteorologist to take and digest, even though much atmospheric turbulence is of so large a scale as to be beyond a single observer's eyes to encompass directly. It is also of interest that Taylor has never shown any disposition to think that the study of turbulent flow would be much advanced by the use of perturbation methods on the linearised Navier-Stokes equations. Rossby, I believe, had come round to the same viewpoint in his later years in regard to large-scale atmospheric turbulence.

There are three papers on gravity waves in the atmosphere, those of 1929, 1932 and 1936. In the first of these Taylor showed that the velocity of propagation of the pressure wave from the Krakatoa eruption did not imply a 12-hour resonance period for the atmosphere, as was suggested by the semi-diurnal variation of pressure. Moreover, he had not, by 1936, been able to resolve this discrepancy, though he then showed that the atmosphere might have a number of natural periods and had even suggested in 1932 (to our Society) that these might arise from the complex thermal structure of the upper atmosphere. Later, of course, Pekeris, and then Weekes and Wilkes, showed indeed that a 12-hour period was thus obtainable but the problem of the semi-diurnal variation of pressure is not thereby closed. It might moreover be helpful to its further elucidation to make a much more comprehensive analysis of the observed behaviour, so as again to give wider scope to the test of theory.

It is feasible that this volume will make its greatest appeal to those workers who, by experience and maturity of outlook, are most able to appreciate Taylor's strategy and dexterity but who feel themselves to be past their most productive phase. To them the fact that Taylor, by his attitude and methods, goes on seemingly forever, producing work of high originality should, however, be a stimulus as well as a great source of enjoyment. But, let us hope, the volume will be carefully read and digested by many younger workers also, not only or even mainly as a record of research, but essentially to gain insight as to how such a remarkable record has been and can perhaps again be achieved.

P.A.S.

Atlantic hurricanes. By G. E. Dunn and B. I. Miller. (Louisiana State University Press), 1960. Pp. 326; 87 Figures; 31 Tables. $10.

The authors are uniquely qualified to write on Atlantic hurricanes; Dunn is Chief Meteorologist, and Miller is Research Meteorologist at the United States Weather Bureau's National Hurricane Center in Miami, Florida. In 1959 Dunn was awarded the Department of Commerce Gold Medal for Exceptional Service in developing and maintaining the hurricane-warning organization. Both authors have made significant contributions to the study of hurricanes.

Atlantic hurricanes is a successful attempt at the very difficult task of producing a book which can be read with profit by layman and professional alike. For the general reader there is a lively style which conveys the enthusiasm of the authors for their subject, a variation in the level of treatment which will satisfy a wide range of readers and a useful glossary. For the professional meteorologist there is much useful background information and a comprehensive (up to 1958) bibliography running into six pages. Dunn and Miller may well have produced the successor to Tannehill's twenty-two years old classic, *Hurricanes, their nature and history*.

This is not a text-book on hurricanes nor is it likely that it was the authors' intention that it should be. The professional meteorologist will turn to the appropriate journals for his information. Its value is greatest for those concerned with organizing, maintaining and operating hurricane warning systems. Dunn and Miller have shown the effectiveness of this organization in the United States, which is largely the result of effort by the United States Weather Bureau, and in this book provide the material which is needed for a proper appreciation by a non-meteorologist of the technical problems of hurricane forecasting.

In concentrating on the North American reader, Dunn and Miller have perhaps under-emphasized the effect of Atlantic hurricanes outside the continent of the United States and have said too little about the close international co-operation which is a feature of the Atlantic hurricane season, and which does produce a real contribution to the function of the United States Weather Bureau's hurricane forecasting centres. This is a matter of space rather than intention as both authors are familiar visitors and persuasive ambassadors to forecast centres throughout the area affected by Atlantic hurricanes.

I.J.W.P.

Proceedings of the International Clean Air Conference; National Society for Clean Air, London 1960. Pp. 290; Figures; Tables. 30s.

To celebrate its Diamond Jubilee the National Society for Clean Air organized an International Clean Air Conference which was held in London in October 1959. The conference was attended by more than 1,000 delegates of whom 180 came from 30 countries overseas. This volume of proceedings contains 78 papers presented for discussion, in sessional order, followed by the reviews of the rapporteurs, discussions, and authors' replies, also in sessional order. There can be no doubt that the publication is an important addition to the ever-increasing literature on air pollution.

The address at the opening session by Sir Graham Sutton, C.B.E., F.R.S., senior Vice-President of the Society, in which he reviewed the theoretical work on pollution problems, is of particular interest to meteorologists but all will agree with his conclusion that ' the cure for pollution is simple – don't put nasty substances into the air ! '

Papers from session II relate to national air pollution problems, legislation, education, etc., and hardly concern the meteorologist (except as a citizen) and few of the papers from session III although all of a technical nature contain meteorological considerations. But several of the papers from session IV concerning observations, investigations and measurement of air pollution and from session V concerning research and international co-operation are of special meteorologist interest. To give examples, P. J. Meade's contribution on inversions and air pollution is of particular importance, whilst R. S. Scorer's paper on the photography of air pollution gives a lucid exposition of the uses of the camera in air pollution observations and investigations and illustrates with the aid of some excellent photographs the limitations and possibilities of error associated with such work; the paper by G. Spurr on the penetration of inversions by hot plumes shows that it is possible to calculate the heat required in a chimney to ensure penetration of an inversion of known height and intensity and it is not surprising that one conclusion is that high chimneys are essential and that another conclusion is that there is a need for more information on inversions ! Indeed, to say that the meteorologist has an important contribution to make to the solution of pollution problems cannot be disputed and he who is interested in this particular aspect of applied meteorology should certainly find much thought-provoking material in this excellently produced publication.

R.G.V.

Theorie der meereswellen. By W. W. Schulejkin. Berlin (Akademie-Verlag) 1st German Edition, 1960. Pp. vi, 158; 49 Figures; 3 Tables. 26DM.

This is a translation by Dr. Erich Bruns of the book by Schulejkin originally published in 1956. The German edition is considerably better produced than the original Russian edition which I have also seen. The book deals with many aspects of wave phenomena. The mathematical treatment is rather geometrical in character and is based on the shape of the trochoid and its related curves. The theoretical results are checked experimentally in a ' storm basin ' which appears to be a large testing tank where water waves up to 20 metres in length can be produced by winds of speed ranging up to over 20 m/sec^{-1}.

The chapters on the breaking and distortion of waves in shallow water are particularly interesting and are probably the most valuable in the book. A value for the distance a wave can travel in shallow water before breaking was found in 1924 by Jeffreys on the assumption that a wave broke when the amplitude of the second harmonic (produced by distortion) becomes equal to that of the fundamental. This seemed to be a plausible assumption but led to the result that waves would also break eventually in deep water. Schulejkin assumes that a wave is about to break when its profile is such that there is a sheer vertical slope at the steepest point. This shape is worked out for a wave which was originally sinusoidal in deep water and for one which was trochoidal, and the distance of travel before breaking is calculated. This leads to a more realistic result which, it is claimed, has been checked experimentally in the storm basin.

The action of wind in deforming and breaking waves is considered in another chapter. The drift current formed by the wind is considered to be the effective factor.

Several chapters are devoted to the generation of waves by wind in both deep and shallow waters, the analysis being always applied to trochoidal or modified trochoidal waves and wave frequency and directional spectra are not considered. An empirical formula is obtained in the storm basin for the power transmitted by the wind to the waves. It is $W_v = Aa\,(V - c)^2$ where A is a constant, V the wind speed, c the wave velocity, and a the wave amplitude. Attempts are made to explain this theoretically with the aid of experiments over ' solid waves ' in a wind tunnel. A pressure profile is produced which shows the pressure minimum to be at the crest of the wave and is slightly unsymmetrical with an increased pressure on the windward side. This profile is not used in the calculation, however, but solid waves, of the same shape as those of water waves observed in the basin, are used in a wind tunnel and the pressure differences between two corresponding

points one on each side of the crest are measured directly for 17 pairs of points for 5 successive waves. The results derived agree with the empirical relationship for wind speeds up to 8 m sec^{-1} but not with higher wind speeds. This discrepancy is explained by the effect of small wavelets riding on the crests of the larger waves. This is confirmed by placing a small wooden wavelet of triangular section on the crest. The effect is to increase the wave-making force six times in some cases.

The increase in wavelength under the action of wind is considered by taking into account angular momentum as well as energy relationships. The result found was that :

$$h/\lambda \propto t^{-n} \qquad \text{where} \qquad -0{\cdot}5 < n < -0{\cdot}2$$

$$\text{and also} \qquad h/\lambda = 0{\cdot}04 + 0{\cdot}103\,(\lambda_0/\lambda)^{2/3}$$

where λ_0 is the length of the wave initially formed by the wind. This shows a variation in steepness from the maximum possible value of 1/7 to one of 1/25 which, it is claimed, is satisfied by ' saturated ' ocean waves.

These results are somewhat at variance with those found by us as the steepness of saturated waves appears on the whole, according to our observations, to increase with the wind speed although 1/25 is of the right order of magnitude. The first equation is also different from a result found recently for the North Sea where it can be shown that $h/\lambda^{3/2}$ is independent of fetch and time, but there is still a lot to learn about this effect.

The effect of an eddy or turbulent viscocity is also considered and it is shown that it causes a given wind speed in the storm area to produce a constant wavelength in the decay area which is different from the wavelength in the storm area. These wavelengths are calculated for a range of wind speeds but they do not agree with our observations.

The effect of opposing winds is also considered.

Finally, reference is made to previous observations by other workers indicating that the limiting height in the ocean is proportional to the square of the wind speed and this is compared with the theoretical result that this should vary as $(V - c)^2$ and accordingly it is deduced that the limiting value of c is between 0·75 and 0·85 V. This is in agreement with Vaughan Cornish's result but it is lower than that indicated by our observations which place the ratio nearer unity.

The work is extended to shallow water where the effect of loss of energy due to breaking is taken into account.

To sum up, the treatment in the book is very consistent but most of the ideas are quite familiar to workers of other nations although some of them are no longer in great favour. Frequency and directional spectra of wind waves are not considered at all and this is a very serious limitation. I know, however, that a good deal of recent Russian work has been dealing with these.

J.D.

Quellentexte zur Witterungsgeschichte Europas von der Zeitwende bis zum Jahre 1850. By Curt Weikinn, (Akademie-Verlag, Berlin). (*Quellensammlung zur Hydrographie und Meteorologie*, Band I). Hydrographie, Teil 1 (1958) Zeitwende-1500 pp. viii, 531. DM 64. Teil 2 (1960) 1501-1600. Pp. vi, 485. DM 76.

The two volumes under notice are the first of a series under the auspices of the Institut für Physikalische Hydrographie der Deutschen Akademie der Wissenschaften zu Berlin. Four further volumes are projected in which hydrographical source-material will be published covering the period up to 1850. The first two volumes provide a very large compilation of original source-material in the form of extracts from a very wide range of early chronicles, printed or in manuscript, relating to the behaviour of the rivers, lakes and adjacent seas over a great part of Central Europe. The collection begins with an extract from Dio Cassius referring to the flooding of the Tiber in B.C. 27; and there are 24 entries referring to years before A.D. 500. 80 pages cover the events of the thirteenth century, and the subsequent scale of the work can be judged by the fact that the second volume, each year throughout the sixteenth century is given an average of four large octavo pages of extracts. Choosing at random the year 1552, a year in which river floods seem to have been very widespread in January, followed by storm floods along the Dutch coast, some scattered summer floods in Central Germany and a severe December when the lake of Constance was frozen, 56 extracts are given from places ranging between Hamburg, Zürich, Antwerp and the Erzgebirge. They are given in the original; many in regional German, some in old Dutch, Danish or mediaeval French, rarely in contemporary English, frequently in Latin. To the Latin extracts only, there is a German translation appended. Authorities are cited in full and there is a quite overwhelming bibliography; more than 700 references in the first volume alone.

Entries with regard to the effects of the weather on the rivers are many. Some of them are striking; such as the fact that in 1435 the Rhine was frozen from Basle to Dordrecht, an entry that begs many questions among those who have watched the Rhine from its Alsatian bank.

Without doubt the compilation will be found useful by many who are interested in past vicissitudes. Some indication of scope may be given; in the index to the first volume there is one entry only referring to Scotland and one to Ireland, four to Denmark and two to Sweden; but 13 to Poland, 72 to England and upwards of 120 to the Low Countries. There are 80 references to the river Rhine and 34 to the Seine. The assemblage appears to be less exhaustive as we move further from Germany; and, for example, C. E. Britton is not named among the references. At the same time these volumes are concerned primarily with the hydrography, so that their utility for those seeking meteorological material relating to surrounding countries is limited.

For meteorological events in general, beyond those recorded by the waters, we must await the appearance of future volumes. The high standards of scholarly production in the volumes under notice will ensure that meteorologists interested in past events will eagerly look forward to further works in this series.

G.M.

The Green Flash and other low sun phenomena. By D. J. K. O'Connell, S.J., Amsterdam (North Holland Publishing Co.), 1958. Pp. 192; Figures; Tables; 80 Colour Plates. 45s.

This book is essentially a collection of photographs of the low sun, mostly taken at sunset from the Vatican Observatory at Castel Gandolfo. All were taken through one or other of the Observatory's telescopes, the favourite one being a refractor with a focal length of 6 m. The primary object was to obtain photographs of the Green Flash, but inevitably effects due to scintillation and distortions due to the stratification of the atmosphere were also photographed and are given a fair share of the author's attention. The total number of photographs is about 300, of which 80 are in colour.

It is a magnificent and fascinating collection. Most of the coloured photographs show very clearly the green upper rim of the sun, and in some cases they have caught the instant when only this green rim remained visible – often magnified, or even detached from the horizon, by the effects of abnormal refraction. The author claims by implication that these photographs are proof of the objectivity of the Green Flash, but one may doubt whether the case is sound. Nobody doubted that the upper rim of a heavenly body near the horizon was green – this can be seen on any clear evening with a small telescope. What the opponents of the objective theory said was that the green fringe was too narrow to be perceptible to the naked eye, and certainly too narrow to cause a striking flash, and it is hard to counter this argument with photographs taken through powerful telescopes. Fortunately, as the text of this book makes clear, there was already overwhelming evidence for the objectivity of the Green Flash.

Fantastic distortions of the sun's disc are shown in almost every photograph and there are a number of series of photographs in black and white, taken at intervals of a few seconds which show the rapidity with which its appearance varies. That the distortion is mostly due to refractions in the upper air is demonstrated by some very dramatic photographs which show a ship in silhouette against the setting sun. The sun is much distorted and constantly changing in form while the ship (50 miles away !) is so clear and sharp in outline that we readily accept the assurance that, on the original photograph, its rigging could be seen. The book reproduces radiosonde ascents and synoptic charts for some such occasions and, as it were, invites the reader to interpret the sun's appearance in terms of meteorological conditions : but the author does not attempt to do so himself.

There is, indeed, little discussion of the photographs. The main body of the text runs to only 29 pages (very pleasantly written pages, though it may be felt that the trick of quoting all authorities in their original language is outmoded). Into this small space are packed a history of the Green Flash, an account in almost popular terms of the theories of its cause and of the factors which presumably influence its intensity, and a description of the experimental and photographic methods used by the author and his collaborator (C. Treusch, S.J.). There are snippets of commentary, mostly purely factual, accompanying each group of photographs, and an appendix describes some neat laboratory experiments by which most of the observed optical effects were reproduced – with considerable fidelity, as photographs prove. There is not a line of mathematics in the whole work.

Obviously, this is not research in the grand manner. But we get quite enough grimly laborious scientific literature, and it is a pleasant change to have a book which is easy and entertaining to read, which suggests in a casual, throw-away fashion many stimulating thoughts and which is above all a delight to look at.

The volume is very well and clearly printed on good paper. The blue cloth binding is perhaps not quite robust enough, and marks rather easily, for a book which is likely to get a lot of handling. The colouring of the plates makes little claim to realism, but successfully brings out the important colour phenomena. There is an adequate index and a bibliography of about 300 papers. Alas, not one of them appeared in the *Quarterly Journal*, and few in any meteorological periodical. Perhaps this book may persuade meteorologists that there is still meat on the carcass of meteorological optics.

B.C.V.O.

Cumulus dynamics. Proceedings of the first conference on cumulus convection. (Pergamon Press), 1960. Pp. ix, 211. 70s.

In this volume there is a good deal of observational material, much of which is very interesting, but in general it seems to be too incomplete, or too inaccurate to serve as even the beginning of any thorough dynamical theory of atmospheric convection. Of course, this is hardly the fault of the people who organized or contributed to the symposium, which doubtless served the valuable purpose of enabling workers in the field to exchange ideas and enthusiasms. One can wonder, however, if it is justifiable to publish the conference proceedings in such an expensive volume with such an imposing title.

Among the better contributions are those from Miss Betsy Woodward on convection in thermals, and Dr. Joanne Malkus on cumulonimbus. Other well-known meteorologists, for example, Squires, Newton, Glaser and Fujita, do little more than briefly recall and comment upon good work which they have published in more detail elsewhere.

F.H.L.

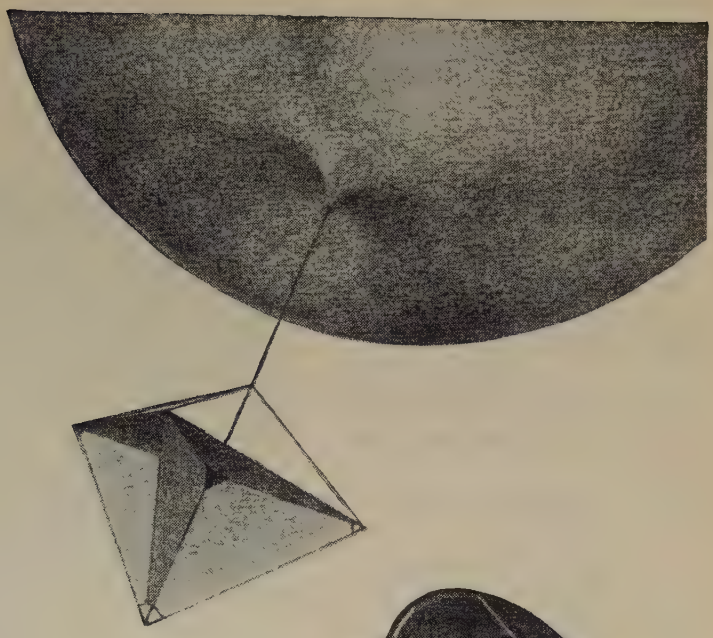

DECCA PRIMARY RADAR

the most economical windfinding system

An outstanding feature of the new Decca WF2 Windfinding Radar is its high performance coupled with low daily operating cost. A new high power transmitter increases the possible maximum slant range to some 200,000 metres, and enables a smaller and cheaper target to be used for shorter ranges. The equipment is so designed that it can be operated by one man and is capable of providing wind speed and direction up to an altitude of 100,000 feet in all parts of the world.

WF2—the most advanced windfinding radar in the world

DECCA RADAR

DECCA RADAR LIMITED · LONDON · ENGLAND

DR151

HMSO

Scientific Papers

A new series designed to replace the present series of *Meteorological Reports* and *Professional Notes*. Giving the results of investigations made in the Meteorological Office, it will include monographs both on pure meteorological research and on the application of meteorology to transport and industry. The format has been enlarged to enable the diagrams, always an important feature of meteorological publications, to be larger and clearer. Titles available are listed below :

No. 1. **Airborne measurements of the Latitudinal Variation of Frost-Point, Temperature and Wind.** By N. C. Helliwell. **3s. 6d.** (*post* 4*d.*)

No. 2. **Rainfall of Malta.** By B. F. Bulmer and K. Stormonth. **3s.** (*post* 4*d.*)

No. 4. **Pressure Variation over Malaya and the Resonance Theory.** By R. Frost. **2s. 6d.** (*post* 2*d.*)

No. 6. **Seasonal Variation of the Sea Surface Temperatures in Coastal Waters of the British Isles.** By F. E. Lumb. **3s.** (*post* 4*d.*)

Further titles are in preparation

Upper Winds over the World

PARTS I AND II

by H. Heastie and P. M. Stephenson

Published together as *Geophysical Memoirs No. 103*, the first two parts of this monograph occupy a small portion only of this volume, the greater part of which is devoted to detailed charts and diagrams and to data in tabular form. Part I deals with the average height of isobaric surfaces and Part II with average winds in the upper air. A third part, to be published later, will describe and present the charts of standard vector deviation. **30s.** (*post* 1*s.* 1*d.*)

From the Government Bookshops

or through any bookseller

HMSO

THE FINEST SOUNDING AND PILOT BALLOONS AVAILABLE

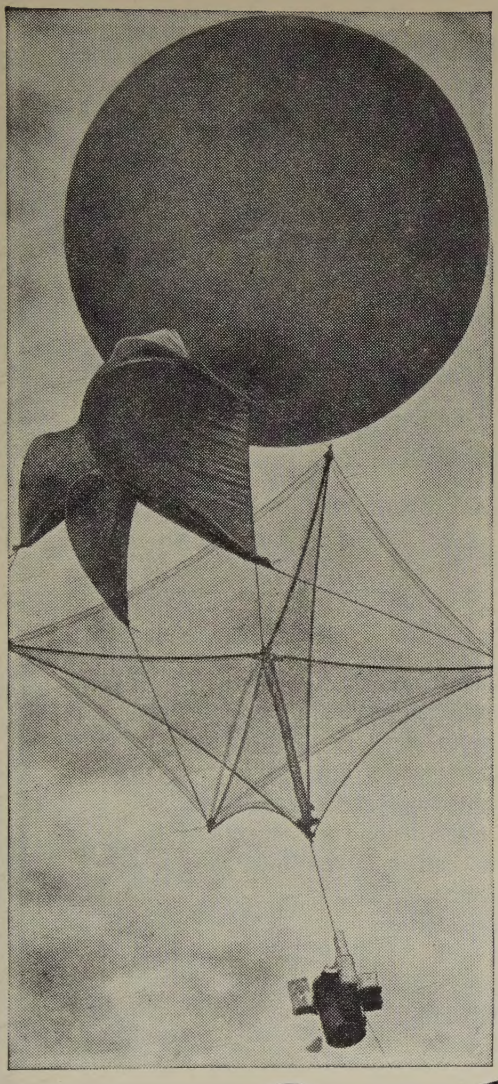

Manufactured by the Guide Bridge Rubber Company of Vulcan Mill, Bury, these balloons are in use throughout the world.

OVERSEAS SALES

Phillips Patents Limited
250 Western Avenue, Acton, London, W.3

HOME SALES

Guide Bridge Rubber Co. Ltd, Vulcan Mill, Butcher Lane, Bury, Lancs

Beritex SEAMLESS REGD.

Mufax

THROUGHOUT THE WORLD

II

ARCTIC

RESOLUTE IN NORTHERN CANADA

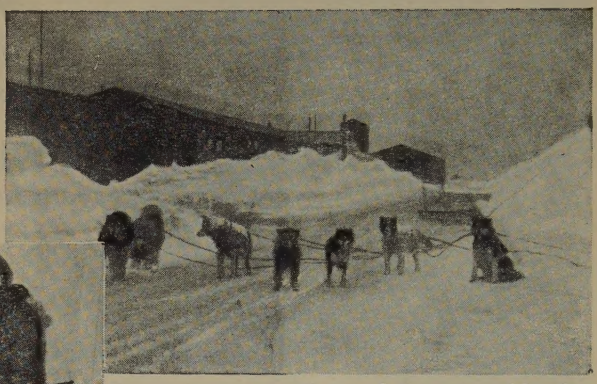

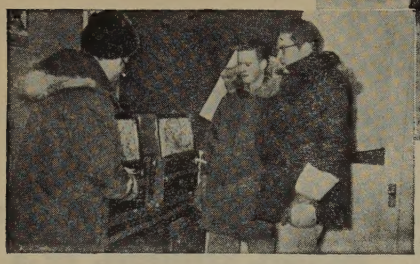

Photographs by courtesy of Canadian Department of Transport.

Resolute is 500 miles inside the Arctic Circle and is the most northerly station in the vast weather chart facsimile network operated by the Canadian Department of Transport.
For their weather briefing, the Canadian and U.S. pilots at Resolute depend almost entirely on radio facsimile weather charts—none are drawn at the station.
The weather chart recorders—seen in the lower photograph—are of the Mufax D-649-G/AR type, which have been specially designed for automatic radio working.

MUIRHEAD

MUIRHEAD & CO. LIMITED, Beckenham, Kent, England
Tel: Beckenham 4888

MUIRHEAD INSTRUMENTS LIMITED, Stratford, Ontario, Canada
Tel: 271-3880

MUIRHEAD INSTRUMENTS INC., 441 Lexington Avenue, New York 17, N.Y., U.S.A.
Tel: Murray Hill 2-8131

HORSTMANN

CHART CLOCK

The robustly constructed movements and high quality jewelled lever escapements of Horstmann Chart Clocks ensure the extremely accurate timekeeping necessary in meteorological equipment. The clocks, which are used extensively by the Air Ministry Meteorological Office, are available in two types – one to drive chart drums revolving once every 24 hours and the other for 7 day rotation.

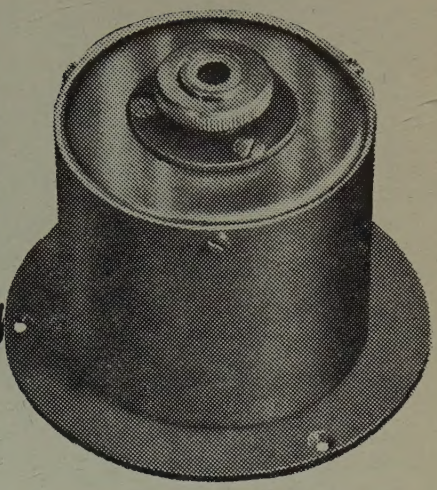

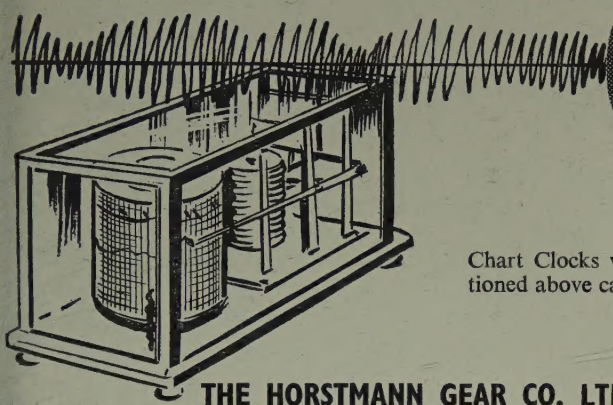

Chart Clocks with speeds other than those mentioned above can also be supplied to special order.

THE HORSTMANN GEAR CO. LTD.
NEWBRIDGE WORKS · BATH · Tel. : Bath 7241

NEWBRIDGE WORKS BATH
REGISTERED TRADE MARK

RUDOLF GEIGER

Das Klima der bodennahen Luftschicht

Ein Lehrbuch der Mikroklimatologie

Von Prof. Dr. RUDOLF GEIGER, München.
4., vollkommen neubearbeitete und erweiterte Auflage. XII, 648 Seiten mit 281 Abbildungen. Halbleinen DM 54, – – (*In deutscher Sprache*)

Die gewaltige Entwicklung seit 1950, insbesondere die erstaunliche Ausweitung der praktischen Anwendung der Mikroklimatologie, machte es notwendig, das Buch neu zu schreiben. Die Abrundung unseres Wissens erlaubte auch eine noch klarere Gliederung des Stoffes. (*Aus dem Vorwort zur 4. Auflage*)

Inhaltsverziechnis : Das Mikroklima und seine Erforschung – Der Wärmehaushalt der Erdoberfläche als Grundlage der Mikroklimatologie – Die bodennahe Luftschicht über ebenem und unbewachsenem Boden – Der Einfluss der Unterlage auf die bodennahe Luftschicht – Zahlenmässige Erfassung der Wärmehaushaltsgrössen – Die bodennahe Luftschicht bei pflanzenbedecktem Boden – Forstmeteorologische Klimafragen – Einfluss der Geländegestaltung auf das Mikroklima – Die Beziehung von Mensch und Tier zum Mikroklima – Messtechnische Hinweise für mikroklimatologische und mikrometeorologische Untersuchungen – Literaturverzeichnis.

Sonderprospekt auf Anforderung.

FRIEDR. VIEWEG & SOHN · BRAUNSCHWEIG (GERMANY)
Post Box 185

Plessey

TELECOMMUNICATIONS

speed weather forecasting

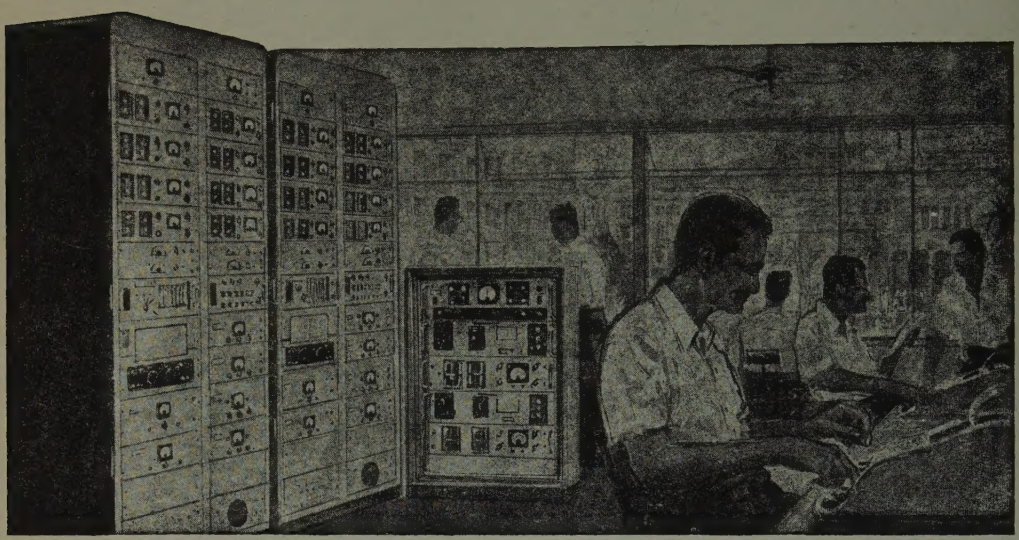

Plessey is everywhere, you'll find . . . in the Middle and Far East for example, where minute by minute plotting and data transmission are the only key to effective warning of adverse weather conditions.

The ubiquity of Plessey Radio Teleprinter Equipment is as complete in world meteorology, press and consular services, as Plessey Telecommunications is in the total telecommunications field. A vital amenity for any civilised community, the accurate dissemination of weather data is essential to airways, to planned agriculture, and in many localities to the very preservation of life itself. It is a field of service in which Plessey is proud to be making a major contribution.

Behind this achievement are the extensive prototype and quantity manufacturing resources of the Telecommunications Division, inspired by the work of a unique research and development organisation. The Company recognises the need to segregate advanced thinking from the hustle and distraction of the factory. Accordingly, in addition to the Group Research Laboratories at Roke Manor and other specialised research centres already existing in the U.K., extremely well equipped laboratories have recently been established at West Leigh for advanced telecommunications studies. In these establishments, the next generation of telecommunications equipment is already taking shape.

In close support at all times are the complete resources of the Plessey Group of Companies which include unrivalled tool making and machining facilities, a full range of environmental testing and production laboratories, and the services of the materials laboratories at Caswell.

TELECOMMUNICATIONS DIVISION • ELECTRONIC & EQUIPMENT GROUP
THE PLESSEY COMPANY LIMITED • ILFORD • ESSEX • Telephone: ILFORD 3040
Overseas Sales Organisation: Plessey International Limited • Ilford • Essex • England

TD6A

Printed in Great Britain in Horley Series by The Salisbury Press Ltd., Publicity House, Wilton Road, Salisbury, Wilts. (26704)